Alma Mater Studiorum · Università di Bologna

School of Science
Department of Physics and Astronomy
Master Degree in Physics

ARS Leptogenesis in Scalar Extensions of the Standard Model

Supervisor:
Prof. Silvia Pascoli

Co-supervisor:
Dott. Alessandro Granelli

Submitted by:
Margherita Pulga

Academic Year 2024/2025

Abstract

One of the open problems of the Standard Model (SM) is the dominance of matter over anti-matter. Among the proposed explanations, Leptogenesis stands out as one of the most compelling mechanisms. This framework is particularly interesting since it can naturally take place in seesaw models, namely extensions of the SM which can explain both the generation of neutrino masses and their smallness.

The simplest realization, thermal leptogenesis, extends the SM with three right-handed neutrinos (RHNs) and the lepton asymmetry arises from their out-of-equilibrium decay. Although extensively studied, this scenario requires very large Majorana masses for the RHNs ($> 10^9$ GeV), which are challenging to test experimentally. For this reason, models involving RHNs at the GeV-scale have emerged as promising alternatives. Among them, the Akhmedov-Rubakov-Smirnov (ARS) mechanism generates the lepton asymmetry via RHNs oscilations in a freeze-in scenario. However, this model does not address the origin of RHNs masses, leaving open the question about the generation of these masses and if it could be tied to early universe dynamics.

In this thesis, we investigate the possibility of dynamically generating the RHN masses in the context of ARS leptogenesis. Specifically, we extend the type-I seesaw model with two RHNs by introducing a complex scalar singlet Φ and a global $U(1)_{B-L}$ symmetry under which Φ carries charge $+2$ and the RHNs charge -1. After the spontaneous symmetry breaking (SSB) of $U(1)_{B-L}$, the real part of Φ acquires a non-vanishing vacuum expectation value, and its coupling to N generates a Majorana massive term for the RHNs. This construction naturally explain the origin of the heavy neutral leptons masses. However, after SSB, two real scalar degrees of freedom remain, ϕ and θ (the Majoron), which interact with the RHNs via the Yukawa coupling y_N. These additional interactions may modify the RHNs number density, potentially bringing them into thermal equilibrium before the electroweak phase transition. To take into account this new interaction we first identify the leading contributions, then we modify the Quantum Kinetic Equations to study their effects on the final baryon asymmetry of the universe (BAU). Finally, we perform a parameter scan to explore how the parameter space of viable leptogenesis is modified in this new theoretical framework.

Contents

Introduction

The Standard Model (SM) of particle physics is the current theoretical framework describing nature at the smallest scales. Over the past decades, it has proven to be extremely successful, both in explaining a wide range of phenomena and in predicting experimental observations with remarkable precision. The biggest success of the SM is the prediction of the Higgs boson, which has been detected in 2012 [1, 2]. Other SM successes include the prediction of the anomalous magnetic dipole moment of the electron, that matches the experimentally measured value to twelve digit precision [3], the prediction of the W and Z bosons and their masses, which agree with experimental data [4]. Despite its history of successes the SM is not a complete theory, as there are still some loose ends which the SM is unable to connect. For instance the nature of Dark Matter (DM), the generation of neutrino masses (see Chapt. 2), and the observed asymmetry between matter and anti-matter (see Chapt. 3) are the most relevant phenomenological evidence that cannot be explained within the SM framework.

In this thesis, we will focus on two of these open problems, namely the generation of neutrino masses and the generation of the Baryon Asymmetry of the Universe (BAU), which are strictly correlated.

The discovery of neutrino masses is related to the experimental evidence of neutrino flavour oscillations [5]. Neutrinos come in three generations as all the other SM particles. In 1962, L. M. Lederman, M. Schwartz and J. Steinberger discovered the existence of two different neutrinos, ν_e and ν_μ [6]. The third type of neutrinos, the one associated with the τ lepton, was discovered in 2000 by the DONUT experiment [7]. The discovery of neutrino families opened the question whether there could be neutrino mixing.

Neutrino oscillations were observed both in atmospheric neutrino, i.e. the ones produced when cosmic rays interact with nuclei in the atmosphere, and solar neutrinos, i.e. the ones originating form nuclear fusion in the Sun's core. Oscillations in atmospheric neutrinos were first discovered in 1998 by the Super-Kamiokande experiment [8], showing that the muon neutrino depletion is L/E dependent in agreement with an oscillatory behaviour. In 2001, the SNO experiment was able to demonstrate that ν_e constitutes only roughly a third of the overall solar neutrino flux and that the observed total flux is in good agreement with the theoretical predictions [5].

Another important feature of neutrinos is that they are neutral, implying that they could be indistinguishable from their antiparticles. This idea was due to Majorana in 1937 [9]. This question turns out to be intrinsically linked to the conservation or not of lepton number and to the nature of neutrino masses (see Sec. 2.3).

Observations also indicates that in the Universe there is more matter than anti-matter. The existence of antimatter was first predicted by Paul Dirac [10] and then discovered by Carl Anderson [11]. In principle, there is nothing that prevents antimatter to form the same complex structures that we observe in the Universe, such as stars, galaxies and clusters. However, there is evidence that there is an overabundance of matter over antimatter. First of all, our Earth and the other planets of the Solar Sys-

tem are made of matter, as we were able to reach them with spacecraft without annihilating. Moreover, the particles composing the solar wind do not annihilate with the objects in the Solar System, otherwise we will detect the γ-rays generated by this annihilation. The amount of antiprotons and positrons in cosmic rays can be explained by their secondary origin in cosmic particle collisions or high energetic astrophysical processes (see Sec. 3.1). Another evidence of the absence antimatter domination in other galaxies can be seen to be the absence of annihilation radiation $p\bar{p} \to \pi^0 \to \gamma\gamma$ that should be generated in the interface between matter dominated and antimatter dominated region. Another possibility is that the Universe consists of a patchwork of regions that are strongly dominated by either matter or antimatter. This scenario has been investigated [12], but it can be excluded due to the absence of distortions in the cosmic microwave background (CMB), which would otherwise arise from annihilations at the boundaries of these regions at CMB times.

A theory framework that addresses these two open questions simultaneously is the extension of the SM with at least two right-handed (or sterile) neutrinos (RHNs). The introduction of these neutrinos (which are Majorana fermions) can explain the masses of active neutrinos through the so-called seesaw mechanism [13–16]. Moreover, in seesaw models a mechanism which could account for the BAU is naturally embedded. This mechanism is called Leptogenesis [17–20]. In fact, a baryon asymmetry can be generated if the Sakharov conditions (see Sec. 3.1.1) are satisfied. This conditions are: the violation of baryon number, C and CP violation and departure from thermal equilibrium [21]. The basic idea of Leptogenesis is that a lepton asymmetry is created in the Early Universe (EU) and this is then converted into a baryon asymmetry via sphaleron effects [22] (see Sec. 3.3). A seesaw type I model can satisfy these conditions. However, the seesaw mechanism on its own does not give any explanation on the origin of the RHNs as they are put by hand. Also, another problem of the seesaw mechanism by itself is that it does not imply any specific scale for the RHNs masses. One may wonder if the answer can come from leptogenesis. And indeed, the specific patterns of Majorana masses of RHNs single out different scales. For example, if the spectrum of RHNs is hierarchical, i.e. $M_I \ll M_J$, a lower bound of 10^9 GeV was found for the mass of the lightest RHN [23], well beyond the reach of current or planned experiments (see Sec. 4.3.3). The mechanism leading to BAU in this case is called *thermal leptogenesis* [18]. If instead the spectrum is nearly degenerate, i.e. there is a pair of RHNs such that $\Delta M \ll M$, the leptogenesis may take place for M as small as $\mathcal{O}(100)$ GeV [24]. The corresponding leptogenesis mechanism is called *resonant leptogenesis* [25, 26] (see Sec. 4.5). Another interesting model is *baryogenesis via oscillations*, or *ARS leptogenesis* [27–29] (see Chapt. 5) , which can be successful for heavy Majorana neutrino mass scales as low as 100 MeV, thus being accessible to low-energy searches of heavy neutral leptons [30, 31].

In thermal leptogenesis the deviation from thermal equilibrium takes place during the decay of the RHNs, when the decay rate becomes smaller than the Hubble parameter, i.e. it happens during freeze-out of RHNs. The lepton asymmetry comes from the interference between tree and one loop processes like $N \to LH$, see Chapt. 4 for details. This decay asymmetry is further enhanced if the two RHNs are degenerate in masses, as in the case of resonant leptogenesis.

In baryogenesis via neutrino oscillations, the deviation from thermal equilibrium happens during freeze-in. In this model RHNs masses are at the 100 MeV $-$ 1 GeV scale and, as a result of the seesaw mechanism, the Yukawa couplings of light RHNs must be tiny. Consequently, the interaction rate is much smaller than the Hubble parameter and the RHNs never reach thermal equilibrium. The asymmetry generated in the processes of the RHNs is further enhanced by their oscillations.

Therefore, there are two opportunities to generate the observed BAU. The first is during a period of freeze-in, while the first RHNs are being produced and they approach equilibrium. The second opportunity is when the Universe cools down to temperatures below the RHNs masses and the RHNs decay out-of-equilibrium simultaneously with a freeze-out of the SM lepton number, see Fig. 1.

In this thesis we will focus on the ARS mechanism, i.e. in the freeze-in scenario. In particular,

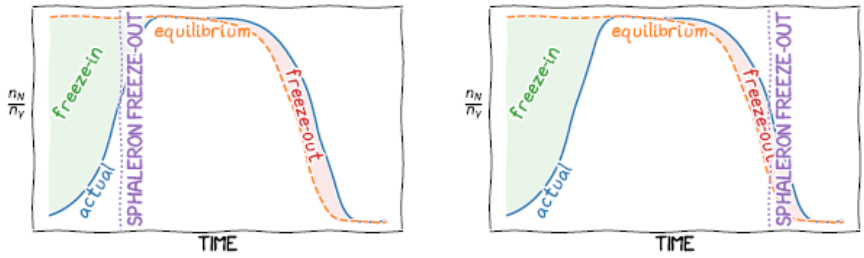

Figure 1: A sketch of the evolution of RHNs abundance in the Early Universe. Figure taken from Ref. [32].

we extend this model to take into account the origin of neutrino masses. In order to do that, we add to the SM particle content and symmetries not only two RHNs, but also a singlet complex scalar Φ, and a $U(1)_{B-L}$ global symmetry, under which the RHNs have charge $B - L = -1$ and the complex scalar has charge $+2$. Then we study the possibility of dynamically generating the masses for the RHNs through the spontaneous breaking of the $U(1)_{B-L}$ symmetry at some energy scale v_ϕ, above the electroweak scale. The generation of RHNs masses then automatically gives rise to the usual type I seesaw mechanism with consequent ARS leptogenesis.

The introduction of an additional scalar singlet has some consequences on the phenomenology of this model. In fact, new interactions between the scalar Φ and the RHNs change the dynamics of the RHNs in the EU. This would affect the efficiency of the ARS mechanism to produce the observed BAU, since in the freeze-in scenario it is assumed that RHNs remain out of equilibrium until the electroweak phase transition. This provides a very long time for RHNs production, scattering and oscillations needed to generate the lepton asymmetry. However, due to new interactions, the RHNs could enter in thermal equilibrium earlier, inhibiting the lepton asymmetry generation. The aim of this thesis is to explore how the introduction of new interactions modifies the parameter space of this leptogenesis model.

Extensions of the minimal sterile-neutrino framework and their effect on ARS leptogenesis have been discussed in earlier works. In particular, Ref. [33] considered a gauged $U(1)_{B-L}$ model and derived conservative bounds on the hidden sector parameters by requiring sufficient baryon asymmetry assuming that the evolution starts from a state of thermal equilibrium, i.e. in the freeze-out scenario. Similarly, Ref. [34] examined the effects of RHNs equilibration due to interactions with gauge bosons and scalars in a gauged $U(1)_{B-L}$ model with three singlet neutrinos, finding that it was possible to obtain freeze-in sterile neutrino DM without spoiling ARS leptogenesis. Finally, Ref. [35] investigated ARS leptogenesis in the context of a singlet Majoron model.

This thesis is organized as follows. In Chapt. 1, we present a brief review of the SM of Particle Physics by introducing its particle content and its fundamental symmetries, then we explain the Spontaneous Symmetry Breaking mechanism (Sec. 1.2) and we conclude by giving a brief review of dark sectors as a possible source of physics beyond the SM. Chapt. 2 focuses on neutrino oscillations (Sec. 2.2.1) and the problem of neutrino masses from a theoretical point of view (Sec. 2.3) and its possible solution via seesaw mechanism with a focus on the type I seesaw (Sec. 2.4). In Chapt. 3 we introduce the problem of baryon asymmetry, describing its experimental evidence and why we need physics beyond the SM to explain it. In Chapt. 4 we start by reviewing the thermal leptogenesis model and its basic ingredients such as the CP asymmetry factor and Boltzmann Equations. First we consider the single flavour regime, then we also take into account flavour effects (Sec. 4.4); finally we move to give a brief description of resonant leptogenesis (Sec. 4.5). In Chapt. 5 we describe the ARS leptogenesis mechanism, by deriving

the Quantum Kinetic Equations. In Sec. 5.2 we introduce the additional scalar singlet to this mechanism. First we study the symmetry breaking pattern of the theory in order to generate the RHNs masses. Then we study the new interactions generated by the introduction of an additional particle to the standard ARS model (Sec. 5.2.1) and we compute the analytical contributions to the Boltzmann Equations due to the scalar decay in Sec. 5.2.2. Finally, we perform a numerical analysis to study how the presence of the new scalar degree of freedom in the theory can influence the parameter space of ARS leptogenesis.

Chapter 1

The Standard Model

In this Chapter, which is mainly based on Refs. [36–38], we will provide an overview on the Standard Model of Particle Physics. We start by introducing the SM particle content and the SM symmetry group. Then we will focus on the Spontaneous Symmetry Breaking in Sec. 1.2 and the Higgs mechanism, see Subsec. 1.2.2. Finally, we will introduce the open questions of the SM (Sec. 1.3) with a brief description of Dark Sectors as a possible solution (Sec. 1.4).

1.1 The particle content

The Standard Model (SM) of Particle Physics is the theory describing elementary particles that constitute matter and three of the four known fundamental forces (electromagnetic, weak and strong interactions), i.e. how the elementary particles interact among themselves. It is a renormalizable quantum field theory whose gauge symmetry groups are:

$$\mathcal{G}_{\rm SM} = SU(3)_c \times SU(2)_L \times U(1)_Y. \tag{1.1}$$

In gauge theories interactions are identified with gauge groups: the strong interaction is described by the $SU(3)_C$ gauge group, the weak interaction by $SU(2)_L$ and the hypercharge interaction is described by $U(1)_Y$. The theoretical formulation of the the standard model relies on the principle of gauge invariance. Requiring that the Lagrangian is gauge invariant leads to the introduction of covariant derivatives, therefore it implies the existence of gauge bosons which are the mediators of the interactions. In order to have a complete description of the Standard Model we need two other ingredients: the particle content and the scalar sector. The particles involved are characterized by their spin, their mass, and the quantum numbers determining their interactions. These quantum numbers (charges) can be assigned to particles according to their transformation under the gauge group actions: the charge related to $SU(3)_C$ is called color, the one related to $SU(2)_L$ is the weak isospin and to $U(1)_Y$ is the hypercharge. Weak isospin and hypercharge can be related to the known electric charge Q through the so-called Gell-Mann-Nishijima relation: $Q = T^3 + Y/2 = (\sigma^3 + Y)/2$, where T^3 and Y are respectively, the generators of $SU(2)_L$ and $U(1)_Y$ groups.
Fermions (spin=1/2) in the standard model are divided into three generations with identical quantum numbers and different masses. Each fermion is associated to two so-called chiralities. Chirality, by definition, distinguishes the two irreducible representations of the Lorentz group that can be used to describe spin 1/2 particles. The four fermions in each family are distinguished by their charges under strong and electromagnetic interactions:

- **Quarks**. Quarks carry color and have both a weak and an electromagnetic charge. Quarks can be divided into $SU(2)_L$ doublets:

$$\begin{bmatrix} u \\ d \end{bmatrix}_L \qquad \begin{bmatrix} c \\ s \end{bmatrix}_L \qquad \begin{bmatrix} t \\ b \end{bmatrix}_L \tag{1.2}$$

  and singlets: u_R, d_R, c_R, s_R, t_R, b_R. All the quarks, both left and right-handed are in the fundamental representation of $SU(3)_C$, namely they are $SU(3)_C$ triplets.

- **Leptons**. The main difference between leptons and quarks is that leptons are not charged under the strong interaction. Leptons can be distinguished between left-handed and right-handed. Left chirality leptons, $L = (\nu_i, i)^T$ with $i = e, \mu, \tau$ are in the fundamental representation of $SU(2)_L$, i.e. they are $SU(2)_L$ doublets; while right-handed leptons: e_R, μ_R, τ_R are singlet under $SU(2)_L$ group. All leptons are $SU(3)_C$ singlets an the hypercharge of lepton doublets is $Y_L = -1$, while for right-handed leptons $Y_R = -2$. Notice that particles in the same doublet have the same hypercharge. It is worth to notice that there are no right-handed neutrinos ν_R in the lepton sector.

The SM Lagrangian is constructed as follows:

$$\mathcal{L}_{\rm SM} = \mathcal{L}_{kin} + \mathcal{L}_{gauge} + \mathcal{L}_{Higgs} + \mathcal{L}_{Yukawa}. \tag{1.3}$$

The gauge invariant kinetic terms for the gauge bosons are:

$$\mathcal{L}_{gauge} = -\frac{1}{4} G^a_{\mu\nu} G^{\mu\nu}_a - \frac{1}{4} W^a_{\mu\nu} W^{\mu\nu}_a - \frac{1}{4} B_{\mu\nu} B^{\mu\nu}, \tag{1.4}$$

where $F^a_{\mu\nu} = \partial_\mu F^a_\nu - \partial_\nu F^a_\mu - g_F f^{abc} F_{\mu,b} F_{\nu,c}$. g_F is the gauge coupling constant and f^{abc} are the structure constant of the gauge group defined by the commutator $[T^a, T^b] = i f^{abc} T^c$, where T^i are the generators of the group. The kinetic Lagrangian is responsible for the interactions between gauge bosons and fermions:

$$\mathcal{L}_{kin,fer} = \bar{\psi} i \gamma^\mu D_\mu \psi. \tag{1.5}$$

The covariant derivative, needed for gauge invariance, is $D_\mu = \partial_\mu - i g_S G^a_\mu \lambda_a - i g W^a_\mu \sigma_a - i g' Y B_\mu$, where λ_a and σ_a are, respectively, the generators of $SU(3)_C$ and $SU(2)_L$ and g_S, g, g' are the $SU(3)_C$, $SU(2)_L$, $U(1)_Y$ gauge couplings.

1.2 Spontaneous Symmetry Breaking

Spontaneous symmetry breaking (SSB) is one of the most important concepts in quantum field theory. The distinction between spontaneous and explicit symmetry breaking is that with spontaneous symmetry breaking the Lagrangian is invariant under the symmetry, but the ground state of the theory is not. Spontaneous symmetry breaking has different implications depending on the nature of the symmetry. The simplest symmetries are discrete and in this case SSB looks like explicit symmetry breaking. On the other hand, if the symmetry is a continuous global symmetry, the breaking of the symmetry implies the existence of long-range correlations and associated massless particles, thanks to the Goldstone theorem [37]:

The Goldstone Theorem: Spontaneous breaking of continuous global symmetries implies the existence of massless particles, that are called *Goldstone bosons*.

If the symmetry is gauged with an associated massless gauge field, then in the broken phase the gauge boson will acquire a mass. This is known as the Higgs mechanism. In this section, which is mainly based on Ref. [36] we will first focus on the SSB of a global $U(1)$ symmetry, since in our model we will consider the spontaneous breaking of a $U(1)_{B-L}$; then we will give a brief review on electroweak symmetry breaking and masses in the SM.

1.2.1 Spontaneous breaking of a continuous global symmetry

The simplest Lagrangian with a global $U(1)$ global symmetry can be written as:

$$\mathcal{L} = (\partial_\mu \phi)^\dagger (\partial^\mu \phi) - \mu^2 \phi^\dagger \phi - \lambda (\phi^\dagger \phi)^2, \tag{1.6}$$

where ϕ is a complex scalar field. This Lagrangian is invariant under a global $U(1)$ symmetry $\phi(x) \to e^{-i\alpha}\phi(x)$ for constant α. To find the ground state of the theory we need to minimize the potential: $V(\phi) = \mu^2|\phi|^2 + \lambda|\phi|^4$, namely we need to consider the first derivative, i.e. $\frac{\partial V(\phi)}{\partial \phi} = 0$. The shape of the potential and the structure of the ground state depends on the sign of the parameter μ^2.
For $\mu^2 > 0$, the potential has an unique minimum at $\phi = 0$, and the exact symmetry of the Lagrangian is preserved. The situation when $\mu^2 = -|\mu|^2 < 0$ is that of a spontaneously broken symmetry. In this case, the theory is unstable around $\phi = 0$ and the potential has a continuum of absolute minima, corresponding to a continuum of degenerate vacua, at $|\phi|^2 = \frac{-\mu^2}{2\lambda} \equiv \frac{v^2}{2}$. So now there are an infinite number of equivalent vacua $|\Omega_\theta\rangle$ with $\langle\Omega_\theta|\phi|\Omega_\theta\rangle = ve^{i\theta}$ and θ parametrized the position of ϕ in the circle with radius v of degenerate minima.
All the vacua are equivalent (by symmetry) so one can pick any convenient parametrization. It is conventional to pick $|\Omega\rangle$ such that $\langle\Omega|\phi|\Omega\rangle$ is real and equal to v, i.e. we can assume $\theta = 0$. Then, the physical degrees of freedom are represented by the oscillations around the true vacuum $|\Omega\rangle$. To find them we shift the fields in order to rewrite the Lagrangian in terms of displacements from the physical vacuum, which has been chosen such that $\langle\phi\rangle_0 = v/\sqrt{2}$. We then shift the field $\phi' = \phi - v$, which is conveniently parametrized in polar coordinates as $\phi(x) = \rho(x)e^{i\theta(x)/v}$, where $\rho(x) = \langle\rho\rangle_0 + \frac{\tilde{\rho}(x)}{\sqrt{2}}$ and $\theta(x) = \theta_0 + \tilde{\theta}(x)$. Since we have chosen $\langle\phi\rangle_0 = \frac{v}{\sqrt{2}}$, this implies that $\langle\rho\rangle_0 = v/\sqrt{2}$ and $\theta_0 = 0$, and we finally obtain

$$\phi(x) = \frac{v + \tilde{\rho}(x)}{\sqrt{2}} e^{i\tilde{\theta}(x)/v} \simeq \frac{v + \tilde{\rho} + i\tilde{\theta}}{\sqrt{2}}, \tag{1.7}$$

where $\theta(x)$ parametrized the "flat directions" along which the potential is constant. As $V(\phi)$ does not depend on $\theta(x)$, the corresponding real degree of freedom is massless and only has derivative interactions. They are the Golstone bosons. In fact, by substituting Eq. 1.7 in the potential we obtain

$$V(\phi) = \frac{\lambda v^2}{2}\tilde{\rho}(x)^2 + \frac{\lambda}{4}\tilde{\rho}(x)^4 + \frac{\lambda}{2}\tilde{\rho}(x)^2 v^2 + \lambda\tilde{\rho}(x)^3 v + \text{const.}\,. \tag{1.8}$$

Therefore, the physical degree of freedom $\tilde{\rho}(x)$ acquires a mass proportional to the symmetry breaking scale v and to its self-coupling, $m_\rho^2 = 2\lambda v^2$, while Goldstone bosons $\tilde{\theta}(x)$ have no massive term as expected. Goldstone bosons are also associated to shift symmetry, which forbid them to acquire a mass and it's related to the invariance of the Lagrangian under $\tilde{\theta} \to \tilde{\theta} + v\alpha$.
The discussion above can be generalized to the case of a generic continuous global symmetry group G and a generic scalar field content. Let us call H the subgroup of G that leaves the vacuum invariant. We can correspondingly divide the generators of G into two sets: the unbroken ones, which annihilate the vacuum, and the broken ones, the orthogonal set. According to the Goldstone theorem each broken

generator in G/H is associated to an independent massless scalar, carrying the same quantum number as the generators.

1.2.2 Higgs mechanism

So far we have considered only global symmetries. We now briefly discuss the spontaneous symmetry breaking of gauge invariance, i.e. we consider what happens if there is a gauge boson associated with the broken symmetry. The main feature of such phenomenon is that the gauge vector associated to each broken generators gets a longitudinal component and a mass. The additional longitudinal degree of freedom is provided by the Goldstone boson associated to the broken generator, which gets "eaten up" by the vector.
Let us now consider the complex scalar field again and promote the global $U(1)$ symmetry to a gauge symmetry, i.e. $\phi(x) \to e^{i\alpha(x)}\phi(x)$. To have a Lagrangian invariant under this symmetry we need to introduce a covariant derivative $D_\mu = \partial_\mu + igA_\mu$ and the Lagrangian becomes:

$$\mathcal{L}_{gauge} = -\frac{1}{4}F_{\mu\nu}F^{\mu\nu} + (D_\mu\phi)^\dagger(D^\mu\phi) - V(\phi^\dagger\phi) + \text{gauge fixing}. \tag{1.9}$$

Let us spontaneously break $U(1)$ by taking $\mu^2 < 0$. The complex field develops a vev $\langle\phi\rangle_0 = v/\sqrt{2}$ as before. Correspondingly a mass term $M^2 \propto g^2v^2$ is generated for the vector boson, as we can see by substituting the parametrization in Eq. 1.7 in the kinetic term of the Lagrangian in Eq. 1.9. In this way we obtain

$$(D_\mu\phi)^\dagger(D^\mu\phi) = (\partial_\mu\phi)^\dagger(\partial^\mu\phi) + \frac{g^2v^2}{2}\left(A_\mu - \frac{1}{gv}\partial_\mu\theta\right)\left(A^\mu - \frac{1}{gv}\partial^\mu\theta\right). \tag{1.10}$$

By noting that

$$\begin{cases}\phi(x) = \rho(x)e^{i\theta(x)/v} \\ A_\mu(x)\end{cases} \quad \text{is equivalent to} \quad \begin{cases}\phi(x) = \rho(x) \\ A_\mu(x) - \frac{1}{gv}\partial_\mu\theta(x)\end{cases}, \tag{1.11}$$

as the two configurations are related by a gauge transformation, we can see that the Goldstone boson becomes the longitudinal component of the gauge boson. In fact, we can choose a *unitary gauge* in which the field $\phi(x)$ is real, as on the right side of Eq. 1.11, and does not contain $\theta(x)$, which can be recognized as the longitudinal component of $A_\mu(x)$. In the general case the gauge vector associated to each broken generator gets a mass by absorbing the corresponding Goldstone boson. It is worth noticing that in the context of gauge theories, unlike the global symmetry case, the Goldstone boson do not correspond to physical scalar degrees of freedom. The scalar fields breaking spontaneously the gauge symmetry are called Higgs fields [38].

1.2.3 Scalar terms

At this point we can conclude the SM picture by taking in consideration the scalar terms. The Higgs field is a complex scalar field and a doublet under $SU(2)_L$, which can be represented as

$$H = \frac{1}{\sqrt{2}}\begin{bmatrix}G_1^+ + iG_2^+ \\ h^0 + iG_3^0\end{bmatrix} = \frac{e^{iG_a\tau^a}}{\sqrt{2}}\begin{bmatrix}0 \\ h\end{bmatrix}. \tag{1.12}$$

The Higgs Lagrangian reads

$$\mathcal{L}_{Higgs} = (D_\mu H)^\dagger(D^\mu H) - \mu^2 H^\dagger H + \lambda(H^\dagger H)^2. \tag{1.13}$$

When $\mu^2 < 0$ the Higgs field acquires a vacuum expectation value and breaks the electroweak group $SU(2)_L \times U(1)_Y \to U(1)_{EM}$. At this point, by expanding the Lagrangian around the true vacuum $\langle H \rangle = \begin{pmatrix} 0 & v/\sqrt{2} \end{pmatrix}^T$ we observe, in accordance with the Goldstone Theorem, that G_1, G_2 and G_3 are massless, whereas h is massive, with $m_H = 2\lambda v^2$. Then, we can fix the gauge by choosing the unitary gauge, realized through a rotation such that $H = (0 \;\; h/\sqrt{2})$. In this way Goldstone bosons become the longitudinal component of the gauge bosons, that become massive. In conclusion, we get three massive and one massless vector bosons, defined as [38]:

$$W_\mu^\pm = \frac{1}{\sqrt{2}}(W_\mu^1 \mp i W_\mu^2), \quad Z_\mu = c_W W_\mu^3 - s_W B_\mu, \quad A_\mu = c_W B_\mu + s_W W_\mu^3, \tag{1.14}$$

where $c_W = g/\sqrt{g^2 + g'^2}$, $g = e/s_W$, $g' = e/c_W$, and the masses of the gauge bosons are:

$$M_W = \frac{gv}{2}, \qquad M_Z = \sqrt{g^2 + g'^2}\frac{v}{2}, \qquad M_A = 0. \tag{1.15}$$

1.2.4 Yukawa terms

To conclude the particle content of the Standard Model, we must notice that the introduction of the scalar field H allows us to write additional terms invariant under the $\mathcal{G}_{\text{SM}}$: the Yukawa Terms.
All left-handed fermions are doublet under $SU(2)_L$, therefore we can write [37]:

$$\mathcal{L}_{Yukawa} = -Y_{ij}^e(\bar{L}^i H)e_R^j - Y_{ij}^u(\bar{Q}_L^i \tilde{H})u_R^j - Y_{ij}^d(\bar{Q}_L^i H)d_R^j + \text{h.c.}, \tag{1.16}$$

where $\tilde{H} \equiv i\sigma_2 H^*$ and we have included all three generations, indexed by i and j. Y_{ij} are the 3×3 Yukawa matrices. After SSB, these interaction terms give the charged leptons and quarks a Dirac mass term of the form $m\bar{\psi}\psi = m(\bar{\psi}_L\psi_R + \bar{\psi}_R\psi_L)$ with $m = yv/\sqrt{2}$ and $\psi_{L,R} = P_{L.R}\psi = \frac{1 \pm \gamma^5}{2}$.
In the quark sector, the Yukawa matrix is not diagonal and the different generations mix. Therefore, to work with mass eigenstates one has to switch to a flavor basis in which the mass terms are real and diagonal. These physical states are obtained by diagonalizing $Y^{u,d}$ by four unitary matrices $U_{L,R}^{u,d}$ as $Y_{diag}^f = U_L^f Y^f U_R^{f\dagger}(v/\sqrt{2})$, with $f = u, d$. As a result, the charged current $W^\pm$ interactions couple to the physical u_{Lj} and d_{Lk} quarks with coupling given by [39]:

$$\mathcal{L}_{\text{SM}} \supset -\frac{g}{\sqrt{2}}\bar{u}_{Li}\gamma^\mu W_\mu^+ V_{CKM} d_{Li} + \text{h.c.} \quad V_{CKM} = U_L^u U_L^{d\dagger}. \tag{1.17}$$

V_{CKM} is the so-called Cabibbo-Kobayashi-Maskawa (CKM) matrix and is a 3×3 matrix. It can be parametrized by three mixing angles and a complex phase that allows for CP-violation in the quark sector.

$$V_{CKM} = \begin{bmatrix} 1 & 0 & 0 \\ 0 & c_{23} & s_{23} \\ 0 & -s_{23} & c_{23} \end{bmatrix} \begin{bmatrix} c_{13} & 0 & s_{13}e^{-i\delta} \\ 0 & 1 & 0 \\ -s_{13} & 0 & c_{13} \end{bmatrix} \begin{bmatrix} c_{12} & s_{12} & 0 \\ -s_{12} & c_{12} & 0 \\ 0 & 0 & 1 \end{bmatrix}, \tag{1.18}$$

where $s_{ij} = \sin\theta_{ij}$, $c_{ij} = \cos\theta_{ij}$ and δ is the CP-violating phase, the so-called Dirac phase. It is worth noting that in the SM there is no mixing in the lepton sector. In fact, there is no right-handed neutrino particle ν_R and the Lagrangian for the lepton sector contains only the term $\mathcal{L}_{Yukawa} \supset -Y_{ij}^e(\bar{L}^i H)e_R^j$ and for this reason it is always possible to diagonalize the Yukawa matrices without flavor mixing. However, neutrino oscillations have been experimentally observed, implying that flavor mixing is present also in the lepton sector and neutrino are massive. Therefore, it is evident that the Standard Model is not a complete theory, but there are some open questions, as we shall see in the next section.

1.3 Open questions in the Standard Model

The Standard Model is phenomenally successful in describing the physics of familiar matter to high precision, it is also known to be incomplete in a wide variety of environments and over a large energy range. In this section we will outline the main limitations of the Standard Model and examine the questions it's not able to answer.

- *Neutrino masses*: The discovery of neutrino oscillations has revealed the incompleteness of the SM. In fact, neutrino oscillations imply that neutrinos are massive, in contradiction with the SM in which there are not right-handed neutrinos and a mass term involving only ν_L particles would violate gauge invariance.

- *Matter-Antimatter asymmetry*: The Standard Model is not able to explain the amount of asymmetry between the relic density of baryons and of antibaryons. This asymmetry has no clear origin in the Early Universe, where matter and antimatter were created in equal amounts.

- *Dark Matter*: Evidence for the existence of Dark Matter comes from the observation of individual spiral galaxies, of cluster of galaxies and of the Cosmic Microwave Background. From these observation we know that Dark Matter constitutes approximately the 25% of our universe [40].

It is worth noting that there are also other open problems in the Standard Model, such as the Hierarchy Problem, the strong CP problem and the flavour puzzle, which are not discussed here as they lie beyond the scope of this thesis.

1.4 Dark sectors

In the previous section we have seen that physics beyond the standard model is needed to solve the SM problems. One of the main direction in the search of new physics is the search for a dark sector [41–43], defined to be a collection of particles that are not charged directly under the SM strong, weak, or electromagnetic forces. Such particles may interact through several 'portal' interactions that are constrained by the SM symmetries. Dark sectors are particularly interesting for their power to explain the known gaps in the SM. For example, dark matter, whose only well established features are the lack of strong or electromagnetic interaction and its abundance, can be easily embedded in a dark sector model, producing the observed abundance through thermal freeze-in or freeze-out mechanisms. Likewise, a very simple dark sector such as sterile neutrinos could explain the origin of neutrino masses, as we will see in the next chapter. Also, the interactions of either sterile neutrinos or a more complex dark sector can readily introduce the ingredients (Sakharov conditions, see Sec. 3.1.1) needed to produce a matter-antimatter asymmetry and transmit it to the baryon sector.
Dark sectors typically include one or more mediator particles coupled to the SM via a portal. The portal relevant for dark sector-SM interactions depends on the mediator spin and parity. The gauge and Lorentz symmetries of the SM restrict the ways in which the mediator can couple to the SM. The dominant interactions between the SM and these mediators are the SM gauge singlet operators: The vector portal, mediated by a dark gauge boson usually referred to as dark photon; the scalar portal, mediated by a new scalar that mixes to the SM Higgs boson; the fermion portal, mediated by a heavy neutral lepton (HNL) interacting with one of the left-handed SM doublets and the Higgs boson; the

pseudoscalar portal, mediated by an axion (or axion-like particle)[42].

$$\mathcal{L} \supset \begin{cases} -\frac{\epsilon}{2\cos\theta_W} B_{\mu\nu} F'^{\mu\nu}, & \text{vector portal} \\ \lambda(H^\dagger H)|\Phi|^2, & \text{scalar portal} \\ y_\nu^\alpha (\bar{L}_\alpha \cdot \tilde{H}) N^c & \text{neutrino portal} \\ \frac{a}{f_a} F_{\mu\nu} \tilde{F}^{\mu\nu} & \text{axion portal} \end{cases} \tag{1.19}$$

In this thesis we will mainly focus on the neutrino and scalar portal. Indeed, the introduction of a right-handed heavy neutrino (RHN) is necessary to explain the origin of neutrino masses and can produce the Sakharov condition necessary to produce a baryon asymmetry. These RHNs must be massive in order to produce the light neutrino masses. To explain the origin of RHNs masses we will add a scalar singlet to the SM along with an additional $U(1)_{B-L}$ symmetry and the spontaneous breaking of this symmetry will generate the massive terms for the sterile neutrinos.

Chapter 2

Neutrino masses and oscillations

In this Chapter, which is mainly based on Refs. [44, 45], we will review the concept of leptonic mixing, which leads to neutrino oscillations. Then we will focus on the neutrino masses problem and its possible solutions.
Neutrinos are singlets of $SU(3)$, but belong to $SU(2)_L$ doublets together with the corresponding charged leptons. They have hypercharge $-1/2$ and do not carry electric charge, as from the Gell-MannNishijima formula: $Q = T_3 + Y$. In the SM, neutrinos are Weyl fermions with left chirality $\nu_{\alpha L} \equiv P_L \nu_\alpha$, $\alpha = e, \mu, \tau$. For massless neutrinos, chirality and helicity match as the chiral projectors and the projectors on helicity components are the same up to corrections of order m/E. Left-handed neutrinos are accompanied by right-handed antineutrinos as required by invariance under CPT theorem. Parity, which transforms left particles into right particles and, viceversa, is maximally violated in the SM as there are no right-handed neutrinos. Left-handed neutrinos interact via the weak force according to the charged current and neutral current terms in the SM Lagrangian:

$$\mathcal{L}_{\text{SM}} = -\frac{g}{\sqrt{2}} \sum_\alpha \bar{\nu}_{\alpha L} \gamma^\mu l_{\alpha L} W_\mu - \frac{g}{2\cos\theta_W} \sum_\alpha \bar{\nu}_{\alpha L} \gamma^\mu \nu_{\alpha L} Z_\mu + \text{h.c.} \tag{2.1}$$

where g is the $SU(2)_L$ coupling, θ_W is the Weinberg angle.

2.1 Leptonic mixing

The discovery of neutrinos oscillations shows that neutrinos have a mass. Hence, there are two basis that can be used to describe them:

- The flavour basis, ν_α, $\alpha = e, \mu, \tau$, in which each neutrino is associated to the corresponding charged lepton;
- The mass basis, ν_i, $i = 1, 2, 3$, in which each neutrino has a definite mass.

The two basis are related by a unitary matrix U, the so-called Pontecorvo-Maki-Nakagawa-Sakata (PMNS) matrix [46, 47]:

$$\nu_{\alpha L} = \sum_{i=1}^{3} U_{\alpha i} \nu_{iL}. \tag{2.2}$$

The PMNS matrix enters the CC Lagrangian when we express it in terms of mass fields, *i.e.* when we switch to a basis in which the mass terms are real and diagonal (mass eigenstates basis):

$$\mathcal{L}_{\rm SM} = -\frac{g}{\sqrt{2}} \sum_{\alpha,i} \bar{\nu}_i U^*_{\alpha i} \gamma^\mu P_L l_\alpha W_\mu + \text{h.c.}, \tag{2.3}$$

with $\alpha = e, \mu, \tau$ and $i = 1, 2, 3$. The flavor states are related to mass states as $|\nu_\alpha\rangle = \sum_i U^*_{\alpha i} |\nu_i\rangle$. In general a 3×3 unitary matrix can be parametrized in terms of 3 angles and 6 phases. Actually, several of phases are unphysical since we can eliminate three phases from the PMNS by performing a phase-rotation of the fields as $\psi \to e^{i\phi}\psi$. In this way the PMNS phases disappear from the Lagrangian as they do not affect kinetic terms, the NC one and the mass term for the leptons as far as both left and right-handed component undergo the same rephasing. If neutrinos are Dirac particles the same rephasing can be applied to them as well, eliminating two further phases. Therefore remains only a physical phase, δ, the so-called Dirac phase. If, instead, neutrinos are Majorana particles, there are three physical phases, two of which enter only in lepton number violating processes. Since for antineutrinos we need to use the conjugate of U, any physical phase represents a violation of the CP symmetry and will be called CP violating (CPV) phase. The PMNS matrix can be parametrized as [48]:

$$U_{\alpha i} = \begin{bmatrix} c_{12}c_{13} & s_{12}c_{13} & s_{13}e^{-i\delta} \\ -s_{12}c_{23} - c_{12}s_{23}s_{13}e^{i\delta} & c_{12}c_{23} - s_{12}s_{23}s_{13}e^{i\delta} & s_{23}c_{13} \\ s_{12}s_{23} - c_{12}c_{23}s_{13}e^{i\delta} & -c_{12}s_{23} - s_{12}c_{23}s_{13}e^{i\delta} & c_{23}c_{13} \end{bmatrix} \cdot \mathcal{P}, \tag{2.4}$$

where we define $c_{ij} \equiv \cos\theta_{ij}$ and $s_{ij} \equiv \sin\theta_{ij}$, with $\theta_{ij} \in [0, 90]$. δ is the Dirac CPV phase and $\mathcal{P}$ is a diagonal phase matrix $\mathcal{P} \equiv \text{diag}(1, e^{i\alpha_{21}/2}, e^{i\alpha_{31}/2})$ which embeds the two Majorana CPV phases α_{21}, α_{31}. The unitarity of U, which can be expressed as a combination of the normalization and orthogonality conditions

$$\sum_i U_{\alpha i} U^*_{\beta j} = \delta_{\alpha\beta}, \qquad \sum_\alpha U_{\alpha i} U^*_{\alpha j} = \delta_{ij}, \tag{2.5}$$

is the only constraint imposed by the SM itself. In particular, this constraint leads us to a unique rephasing-invariant measure of CP violation, the so-called Jarlskog invariant, defined through [49, 50]

$$\Im[U_{\alpha i} U_{\beta j} U^*_{\alpha j} U^*_{\beta i}] = J \sum_\gamma \epsilon_{\alpha\beta\gamma} \sum_k \epsilon_{ijk} \tag{2.6}$$

where $\epsilon_{\alpha\beta\gamma}$ and ϵ_{ijk} denote the three dimensional Levi-Civita symbols, where greek indices denote flavor and latin ones mass eigenstates. With the parametrization in Eq. 2.4 the Jarlskog invariant is given by

$$J = c_{12}s_{12}c_{23}s_{23}c^2_{13}s_{13}\sin\delta = \frac{1}{8}\sin 2\theta_{12}\sin 2\theta_{23}\sin 2\theta_{13}\cos\theta_{13}\sin\delta. \tag{2.7}$$

Therefore it is clear that Dirac CP violation is a 3-neutrino mixing effect whose physical impact depends on all of the three mixing angles.

2.2 Neutrino oscillations

In presence of leptonic mixing and non-degenerate neutrino masses, the phenomenon of neutrino oscillations take place. This is a beautiful manifestation of quantum mechanics on macroscopic distances. The oscillations are generated by the interference of different massive neutrinos, which are produced and detected coherently because of their very small mass differences. The coherence is a key condition which

needs to be satisfied to have neutrino oscillations and it is satisfied thanks to the uncertainty in the neutrino momentum at production. Indeed, we have a superposition of massive neutrinos if the energies and momenta of the particles which participate in neutrino production process are not measured with a degree of accuracy which would not allow the determination of the massive neutrino that is emitted. It is worth noting that if the momentum uncertainty is small compared to the mass differences, for instance if there exist a very heavy nearly-sterile neutrino, such coherence is lost and oscillations do not develop. At production in a specific event either the light states will be produced coherently or the heavy one. If coherence is satisfied the massive components of the initial state propagate over long distances with slightly different phases. This amounts to a change in the state over distance. It is then possible that at detection, when projecting the flavor components out, a different flavor is found compared to the initial one. In order for the oscillatory behaviour to hold, coherence is needed also during propagation, and this is possible because of the very weakly interacting nature of neutrinos.

2.2.1 Oscillation probability in vacuum

Here we limit the discussion to the commonly used plane-wave approximation. This approximation does not capture the momentum uncertainty necessary for coherence, hence we will assume by hand that the initial state is a coherent superposition of massive states with a definite spatial momentum $p \equiv |\mathbf{p}|$. Let's consider a ν_α produced at $t = 0$ in a charged current interaction. We describe the initial state as a superposition of mass eigenstates, which we take as plane waves with momentum p,

$$|\nu, t = 0\rangle = |\nu_\alpha\rangle = \sum_i U^*_{\alpha i} |\nu_i\rangle. \tag{2.8}$$

The mass states $|\nu_i\rangle$ are eigenstates of the free Hamiltonian $\hat{H}$ with eigenvalues $E_i = \sqrt{\mathbf{p}^2 + m_i^2}$. The evolution of the neutrino state can be obtained by solving the evolution equation and is expressed (in natural units) as

$$|\nu, t\rangle = \exp(-i\hat{H}t)|\nu_\alpha\rangle = \sum_i U^*_{\alpha i} \exp(-iE_i t)|\nu_i\rangle. \tag{2.9}$$

The probability of transition from ν_α to ν_β at time t is obtained projecting the state $|\nu, t\rangle$ in the ν_β direction as

$$P(\nu_\alpha \to \nu_\beta, t) = |\langle \nu_\beta | \nu, t\rangle|^2 = \left| \sum_i U_{\beta i} U^*_{\alpha i} \exp(-iE_i t) \right|^2, \tag{2.10}$$

where we have used the fact that we have a massive orthonormal states $\langle \nu_j | \nu_i \rangle = \delta_{ji}$. In all experimentally relevant situations, neutrinos are highly relativistic and one can approximate, for common momentum p,

$$E_i - E_j \simeq \frac{m_i^2 - m_j^2}{2p}, \tag{2.11}$$

and moreover one can take $L = t$. Finally, one obtains the general formula for neutrino oscillations in vacuum

$$P(\nu_\alpha \to \nu_\beta, t) = |\langle \nu_\beta | \nu, t\rangle|^2 = \left| \sum_i U_{\beta i} U^*_{\alpha i} \exp\left(- \frac{\Delta m^2_{i1} t}{2E} \right) \right|^2, \tag{2.12}$$

where $\Delta m^2_{i1} \equiv m_i^2 - m_1^2$ and we have approximated $E \simeq p$. From this formula it is clear that oscillations between one flavor and another are possible only if there is leptonic mixing, *i.e.* $U \neq 1$ and neutrinos have masses. We notice that neutrino oscillations conserve lepton number L, since if a neutrino is produced, the state will be continue being a neutrino, but does not respect leptonic flavor (L_α, $\alpha = e, \mu, \tau$) as the neutrino can change from one to the other over distances. We furthermore notice that Majorana phases do not enter in the oscillation formula as expected, and the overall mass scale does not play a role in it.

Experimental knowledge on neutrino oscillations

Neutrino oscillations have been observed in atmospheric, accelerator, solar, reactor neutrino experiments. And thanks to these experiments we have now a quite precise picture of neutrino properties, although some key questions remain unanswered. The information on the mass squared differences from neutrino oscillation experiments indicates that there are three massive neutrinos and that we can order them in two ways:

- normal ordering (NO): $m_1 < m_2 < m_3$, i.e. $\Delta m^2_{31} > 0$,
- inverted ordering (IO): $m_3 < m_1 < m_2$, i.e. $\Delta m^2_{32} < 0$.

For each ordering the three neutrino masses can be expressed in term of just one unknown parameter, the lightest neutrino mass $m_{\rm MIN}$. We have

$$m_1 = m_{\rm MIN}, \qquad m_2 = \sqrt{m^2_{\rm MIN} + \Delta m^2_{21}}, \qquad m_3 = \sqrt{m^2_{\rm MIN} + \Delta m^2_{31}}, \quad \text{for NO;} \tag{2.13}$$

$$m_3 = m_{\rm MIN}, \qquad m_1 = \sqrt{m^2_{\rm MIN} + |\Delta m^2_{32}| - \Delta m^2_{21}}, \qquad m_2 = \sqrt{m^2_{\rm MIN} + |\Delta m^2_{32}|}, \quad \text{for IO.} \tag{2.14}$$

The Δm^2_{21} mass squared splitting is determined to be $7.49^{+0.19}_{-0.19} \times 10^{-5}\text{eV}^2$ with a 3σ range of $6.92 - 8.05 \times 10^{-5}\text{eV}^2$ [51]. The sign of this mass squared difference is positive. Δm^2_{31} is known slightly less precisely and its sign is not known yet, leaving open two possibilities: normal (NO) and inverted (IO) ordering. The measured values slightly differ between the orderings due to subleading effects in the oscillation probabilities. For NO one has $\Delta m^2_{31} = 2.534^{+0.025}_{-0.023} \times 10^{-3}\text{eV}^2$ with a 3σ range of $2.463 - 2.606 \times 10^{-3}\text{eV}^2$ and similarly for IO $\Delta m^2_{32} = -2.510^{+0.024}_{-0.025}$ with a 3σ range of $-2.584 - 2.438 \times 10^{-3}\text{eV}^2$ [51]. There are three mixings angles and they control the flavour content of the three mass eigenstates, given by $|U_{\alpha i}|^2$. Their values are known with quite good accuracy:

$$\theta_{12} = 33.68^{+0.73}_{-0.70}(31.63 - 35.95) \quad \text{For both mass orderings,} \tag{2.15}$$

$$\theta_{23} = 48.5^{+0.7}_{-0.9}(41.0 - 50.5)\ \text{(NO)} \qquad \theta_{23} = 48.6^{+0.7}_{-0.9}(41.4 - 50.6)\ \text{(IO)}, \tag{2.16}$$

$$\theta_{13} = 8.52^{+0.11}_{-0.11}(8.18 - 8.87)\ \text{(NO)} \qquad \theta_{13} = 8.58^{+0.11}_{-0.11}(8.24 - 8.91)\ \text{(IO)}, \tag{2.17}$$

in degrees. Currently, there is a preference for large CP violation with $\delta = 217\ (135 - 366)$ (NO) and $\delta = 280\ (196 - 351)$ (IO), in degrees, altought at 3σ the CP-conserving values $\delta = 0, 180$ for NO are still allowed.

2.3 Neutrino masses

As we have seen in previous sections the discovery of neutrino oscillations implies that neutrinos are massive. So it is necessary to augment the SM Lagrangian in order to include the neutrino mass term and to explain the origin of these terms in a gauge invariant manner. The mass terms we can add to $\mathcal{L}_{\rm SM}$ are closely related to neutrinos' nature, in fact neutral fermions could be either Dirac or Majorana type. In the first case, the particles and antiparticles are different, while in the latter case there is no distinction between particles and antiparticles. Their nature is strictly related to the conservation of lepton number.

2.3.1 Dirac and Majorana mass terms

Being neutrinos Dirac or Majorana particles, different options are available to describe their masses.

- *Dirac masses.* The Lagrangian contains a mass term

$$-\mathcal{L}_{Dirac} = \bar{\nu} m_D \nu = \bar{\nu}_L m_D \nu_R + \text{h.c.} \tag{2.18}$$

This mass term requires both ν_L and ν_R and is analogous to the mass terms for the SM charged fermions. This term conserves lepton number as it is possible to give both chiral components the same lepton number, so that under a $U(1)_L$ transformation $\nu_{L,R} \to e^{i\eta}\nu_{L,R}$

$$\mathcal{L}_{Dirac} \xrightarrow{U(1)_L} e^{i\eta} e^{-i\eta} \mathcal{L}_{Dirac} = \mathcal{L}_{Dirac} \tag{2.19}$$

the mass term remains invariant. Generically there are several neutrinos and the mass term contains a mass matrix M_D. To find the masses, it is necessary to diagonalise the mass matrix via a biunitary transformation $V_{\nu L}^\dagger M_D V_{\nu R} = \text{diag}(m_i)$: the eigenvalues correspond to the neutrino masses and the mass states are related to the initial states as $\nu_{iL} = V_{\nu L}^\dagger \nu_L$. The matrix $V_{\nu L}$ will then enter the CC Lagrangian, together with one coming from the diagonalisation of the charged lepton mass matrix, and from there neutrino oscillations.

- *Majorana masses.* Using only one Weyl spinor ν_L it is still possible to construct a mass term using the fact that the charged conjugate field $(\nu_L)^c$ is a right-handed field (see App. A for details about charge conjugation). It reads

$$-\mathcal{L}_{Majorana} = \frac{1}{2}\bar{\nu^c} m_M \nu = -\frac{1}{2}\nu_L^T C^\dagger m_M \nu_L + \text{h.c.} \tag{2.20}$$

This term is Lorentz invariant as both ν and ν^c behave in the same way under a Lorentz transformation. This term breaks lepton number by two units

$$\mathcal{L}_{Majorana} \xrightarrow{U(1)_L} e^{2i\eta} \mathcal{L}_{Majorana}. \tag{2.21}$$

For several ν_L, the mass m_M becomes a matrix M_M which needs to be diagonalised. It can be shown that this matrix is symmetric, i.e. $M_M = M_M^T$, hence it can be diagonalised via a unitary transformation $V_\nu^T M_M V_\nu = m_{diag}$ and in this way m_{diag} contains the real and positive masses m_i as eigenvalues. The massive fields $\nu_{i,L}$ will be related to the initial states ν_L as $\nu_{iL} = V_\nu^\dagger \nu_L$. If one defines the Majorana fields as $\nu_i \equiv \nu_{i,L} + \nu_{i,L}^c$, this term can be rewritten as $-\mathcal{L}_{Majorana} = 1/2 m_i \bar{\nu}_i \nu_i$, showing that the resulting massive fields are of Majorana type.

- *Dirac plus Majorana masses.* In presence of both ν_L and ν_R fields, generically both Dirac and Majorana masses terms will be present

$$\mathcal{L}_{Dirac+Majorana} = -\bar{\nu}_L M_D \nu_R + \frac{1}{2}\nu_L^T C^\dagger M_{M,L} \nu_L + \frac{1}{2}\nu_R^T C^\dagger M_{M,R} \nu_R + \text{h.c.} \tag{2.22}$$

Defining the left-handed field $N_L \equiv (\nu_L \;\; \nu_R^c)^T$, one can write the Lagrangian terms as

$$\mathcal{L}_{Dirac+Majorana} = \frac{1}{2} N_L^T C^\dagger \mathcal{M} N_L + \text{h.c.}, \tag{2.23}$$

where the mass matrix $\mathcal{M}$ is given by

$$\mathcal{M} = \begin{bmatrix} M_{M,L} & M_D^* \\ M_D^\dagger & M_{M,R} \end{bmatrix}. \tag{2.24}$$

Upon diagonalisation of this mass matrix, the mass eigenvalues can be found and the mass eigenstates $\nu_{i,L} = V_{D+M}^{\dagger} \begin{bmatrix} \nu_L \\ \nu_R^c \end{bmatrix}$. The resulting fields are Majorana, as expected since this Lagrangian breaks lepton number.

These mass terms are forbidden in the SM as there are no right-handed neutrinos and a Dirac mass term cannot be included. A Majorana mass term can be constructed using the ν_L fields only, but breaks the SM gauge invariance. Consequently we need to extend the SM. Here we review the two main proposed models, i.e. the Dirac and Majorana ones.

2.3.2 Dirac masses beyond the SM

The simplest extension which can be made to the SM involves adding new SM gauge singlets, called sterile neutrinos ν_R. The Yukawa coupling allowed by the gauge symmetries is

$$-\mathcal{L}_y = \bar{L}_{y_\nu} \cdot \tilde{H} \nu_R + \text{h.c.}, \tag{2.25}$$

where $L \equiv (\nu_L^T, l^T)^T$ is the leptonic doublet, $\tilde{H} = i\sigma_2 H^*$ and H is the Higgs doublet $H^T = (H^+, H^0)$. Once the neutral component of the Higgs field acquires a vacuum expectation value $\langle \tilde{H} \rangle = (v_H/\sqrt{2}, 0)^T$, this term generates a Dirac mass for the light neutrinos

$$-\mathcal{L}_y \xrightarrow{\langle \tilde{H} \rangle \neq 0} -\mathcal{L}_{Dirac} = \frac{v_H}{\sqrt{2}} \nu_L y_\nu \nu_R + \text{h.c.} \,. \tag{2.26}$$

This Yukawa coupling and the resulting Dirac mass conserve lepton number. Indeed, as a Majorana mass term for ν_R is not forbidden by gauge invariance, its absence must be imposed by requiring lepton number conservation. In this case, this symmetry needs to be promoted from being an accidental symmetry of the SM to a fundamental ingredient of the theory of particles interaction. We can estimate the order of magnitude of the coupling y_ν. Working in a one generation case, taking $m_\nu = y_\nu v_H/\sqrt{2}$ to be sub-eV, we get that $y_\nu \sim 10^{-12}$. This is a very small number and in this minimal model there is no explanation for the strong hierarchy of masses between charged leptons and neutrinos.

2.3.3 Majorana masses and the Weinberg operator

Among all SM fermions, neutrinos are the only ones that can have a Majorana mass term. Noticing that the term $\bar{L} \cdot \tilde{H}$ is gauge invariant, it is possible to construct a singlet combination resulting in a dimensional-5 operator, the so-called Weinberg operator [52]:

$$\mathcal{L}_{M,BSM} = \frac{c_5}{\Lambda} L^T \cdot \tilde{H}^* C^\dagger \tilde{H}^\dagger \cdot L + \text{h.c.} \,, \tag{2.27}$$

where c_5 is the Wilson coefficient, i.e. the coupling constant of the EFT interaction and $C = i\gamma^2\gamma^0$ is the charge conjugation matrix (in Dirac representation of the γ^μ matrices). This term is called the Weinberg operator and is the only $D = 5$ operator admitted by the SM. Since it is five-dimensional it requires some mass scale Λ (to have a renormalizable theory), which represents the scale at which the EFT stops being valid, i.e. the scale of the underlying physics. Therefore, the presence of this operator suggests that there is a new theory at high scale Λ that is integrated out at low energies. Before discussing the possible UV completions of the Weinberg operator we shall notice that it breaks lepton number by two units and leads to a Majorana mass term once the Higgs boson gets a VEV, i.e. $\langle \tilde{H} \rangle = v_H/\sqrt{2}$:

$$\mathcal{L}_{M,BSM} \xrightarrow{\langle \tilde{H} \rangle \neq 0} \frac{\lambda v_H^2}{2\Lambda} \nu_L^T C^\dagger \nu_L + \text{h.c.} \,. \tag{2.28}$$

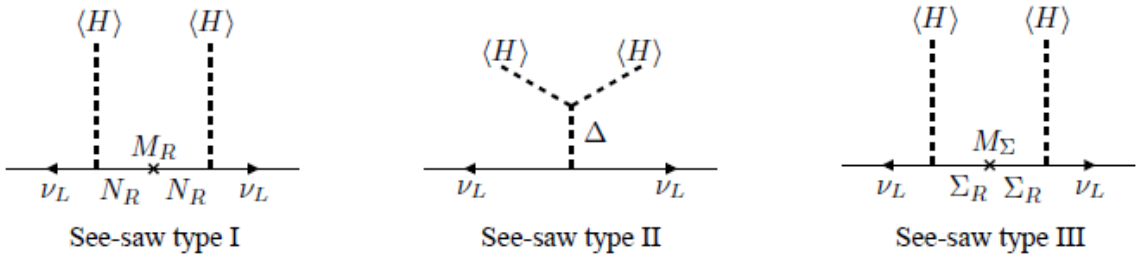

Figure 2.1: Diagrams contributing to light neutrino masses in the three seesaw cases. $\langle H \rangle$ indicates the vev of the neutral component of the Higgs field. Δ is a scalar triplet and Σ is the neutral component of a fermionic triplet, with mass M_Σ. Figure taken from Ref. [44].

We can conclude that if neutrinos are Majorana particles, a Majorana mass term can arise as the low energy realization of a higher energy theory.

2.4 Seesaw mechanism

To explain the physics responsible for the presence of the Weinberg operator one can consider the exchange of virtual massive particles at tree level. Their mass M corresponds to the scale Λ. There are three main options which have been classified according to the nature of the exchanged particle [13–16]:

- **Type I**: SM gauge singlet fermion;
- **Type II**: $SU(2)$ triplet scalar;
- **Type III**: $SU(2)$ triplet fermions.

In figure (2.1) we schematically show the contribution to neutrino masses in the three cases. Seesaw mechanisms are appealing because they provide a natural explanation of the smallness of the neutrino masses. Here we will focus on the Type I seesaw [53–55]. In this model we introduce two or more[1] sterile neutrinos $N_j, R\,(j\,1)$ (singlets under the SM gauge group) and the most general Lagrangian which respect the required symmetries is

$$\mathcal{L}_I = \mathcal{L}_{SM} - \sum_{j,\alpha} \overline{L_\alpha} Y_{\alpha j} \cdot \tilde{H} N_{j,R} + \sum_{j,k} \frac{1}{2} N_{j,R}^T C^+ M_{N,jk} N_{k,R} + h.c. \tag{2.29}$$

where Y is a $3 \times j$ complex matrix representing the Yukawa couplings and M_N is a $j \times j$ symmetric Majorana mass matrix which we assume to be diagonal. Once the H^0 component of the Higgs doublet gets a VEV, the Yukawa term will generate Dirac masses

$$m_D \equiv \frac{Yv}{\sqrt{2}}, \tag{2.30}$$

and we can rewrite the Lagrangian in this form, upon introducing a right handed doublet:

$$\mathcal{L} = \frac{1}{2} \begin{bmatrix} (\nu_L^c)^T & N_R^T \end{bmatrix} C^+ \begin{bmatrix} 0 & m_D \\ m_D^T & M_N \end{bmatrix} \begin{bmatrix} \nu_L^c \\ N_R \end{bmatrix} + h.c. \tag{2.31}$$

[1] At least two heavy neutral leptons are required to reproduce two mass squared differences.

Considering the limit in which $m_D << M_N$ and by diagonalizing the mass matrix through a unitary transformation, we obtain

$$M = \begin{bmatrix} -m_D^2/M_N & 0 \\ 0 & M_N \end{bmatrix}. \tag{2.32}$$

We see that heavy neutrinos, with mass $\sim M_N$ remains mainly in the sterile neutrino direction, while the light neutrinos are mainly in the active component and they acquire a small mass

$$m_\nu \simeq -m_D \frac{1}{M_N} m_D^T. \tag{2.33}$$

Thus, the smallness of neutrino masses is due to the large hierarchy between m_D and M_N scales. It is useful to consider the number of free parameters. For 3 sterile nuetrinos, a see-saw type I model has 3 heavy masses, 9 real parameters in the Yukawa coupling and 6 phases. Of these only 3 light neutrino masses, 3 mixing angles and 3 phases can be measured at low energy. If the scale is sufficiently low, some additional parameters, e.g. the heavy neutrino masses, might be at reach. A useful parametrization allows to separate the high energy parameters from the low energy observable ones; the so-called Casas-Ibarra parametrization [56], which will be discussed in the next section.

2.4.1 Casas-Ibarra Parametrization

The seesaw can be parametrized in various ways. In the usual "top-down parametrization" of the theory, which applies at energy scales $\Lambda \gtrsim M_i$, and consists in choosing the parameters to be all the high energy ones in Eq. 2.29 and in such a way that they can produce sensible low-energy neutrino mass matrices. To relate various parametrization of the seesaw, it is useful to diagonalize the Yukawa matrix Y by a biunitary transformation: $Y = V_L^\dagger D_Y V_R$. Thus, in the top down approach, the lepton sector can be described by the nine eigenvalues of D_M, D_Y and D_H, and the six phases of V_L and V_R. Another way is to follow a "bottom-up" approach, i.e. we start with the existing experimental information about neutrino masses and then we find out the most general textures for the Yukawa matrix Y_ν and the Majorana mass matrix of the right-handed neutrinos M_M consistent with that experimental data. The Casas-Ibarra parametrization is a bottom-up approach and it is very convenient for calculations [56]. To illustrate this approach we start from Eq. 2.33 and we extract the Higgs VEV $\langle H \rangle = v = 174$ GeV by defining the $\mathcal{K}$ matrix as

$$\mathcal{K} = \frac{m_\nu}{\langle H \rangle^2} = Y^T M_N^{-1} Y. \tag{2.34}$$

Now, following the bottom-up approach we can start with the physical $\mathcal{K}$ matrix al low energy and then we run it up to the "Majorana scale" M, where Eqs. 2.33 and 2.34 are defined. Working in the flavour basis in which the charged-lepton Yukawa matrix and the gauge interactions are flavour-diagonal, the $\mathcal{K}$ matrix is diagonalized by the PMNS matrix U,

$$U^T \mathcal{K} U = \mathrm{diag}(k_1, k_2, k_3) \equiv D_\mathcal{K}, \tag{2.35}$$

where U is a unitary matrix that related flavour to mass eigenstates

$$\begin{bmatrix} \nu_e \\ \nu_\mu \\ \nu_\tau \end{bmatrix} = U \begin{bmatrix} \nu_1 \\ \nu_2 \\ \nu_3 \end{bmatrix}. \tag{2.36}$$

One can always choose to work in a basis of right neutrinos where M_N is diagonal

$$M_N = \mathrm{diag}(M_1, M_2, M_3) \equiv D_M, \tag{2.37}$$

with $M_i \geqslant 0$. Then, from Eqs. 2.34 and 2.35

$$D_{\mathcal{K}} = U^T Y^T D_M^{-1} Y U = U^T Y^T D_{\sqrt{M^{-1}}} D_{\sqrt{M^{-1}}} Y U, \tag{2.38}$$

where $D_{\sqrt{M}} = +\sqrt{D_M}$. Multiplying both members of Eq. 2.38 by $D_{\sqrt{\mathcal{K}^{-1}}}$ from the left and from the right, we get

$$\mathbf{1} = \left[D_{\sqrt{M^{-1}}} Y U D_{\sqrt{\mathcal{K}^{-1}}}\right]^T \left[D_{\sqrt{M^{-1}}} Y U D_{\sqrt{\mathcal{K}^{-1}}}\right], \tag{2.39}$$

whose solution is $D_{\sqrt{M^{-1}}} Y U D_{\sqrt{\mathcal{K}^{-1}}} = R$, with R any orthogonal matrix ($R^T R = 1$). Hence, in order to reproduce the physical, low-energy parameters, i.e. the light neutrino masses (contained in $D_{\mathcal{K}}$ and mixing angles and CP phases (contained in U), the most general Yukawa matrix is given by

$$Y = D_{\sqrt{M}} R D_{\sqrt{\mathcal{K}}} U^\dagger. \tag{2.40}$$

Therefore, beside the physical and measurable low-energy parameters contained in $D_{\mathcal{K}}$ and U, Y depends on the three (unknown) positive mass eigenvalues of the right-handed neutrinos and on the three (unknown) complex parameters defining R. Let us stress that Eq. 2.40 has to be understood at the M scale and in the above-defined bases, i.e. the flavour basis in which the charged-lepton Yukawa matrix, the right-handed Majorana mass matrix and the gauge interactions are flavour diagonal. The R matrix can be written in the following form

$$R = \begin{bmatrix} 1 & 0 & 0 \\ 0 & c_{\omega_1} & s_{\omega_1} \\ 0 & -s_{\omega_1} & c_{\omega_1} \end{bmatrix} \begin{bmatrix} c_{\omega_2} & 0 & s_{\omega_2} \\ 0 & 1 & 0 \\ -s_{\omega_2} & 0 & c_{\omega_2} \end{bmatrix} \begin{bmatrix} c_{\omega_3} & s_{\omega_3} & 0 \\ -s_{\omega_3} & c_{\omega_3} & 0 \\ 0 & 0 & 1 \end{bmatrix}, \tag{2.41}$$

where $c_{\omega_i} \equiv \cos\omega_i$ and $s_{\omega_i} \equiv \sin\omega_i$ with the complex angles given by $\omega_i = x_i + i y_i$ where x_i, y_i are real, free parameters.

Chapter 3

Baryon asymmetry of the universe

In this Chapter we present the problem of the baryon asymmetry of the universe. First, we describe the observations indicating the presence of an asymmetry between matter and antimatter in our universe. Then, we recall the theoretical foundations of baryogenesis: we introduce the Sakharov conditions in Subsec. 3.1.1 which are necessary to generate a baryon asymmetry, and the anomalous $B + L$ violation in the SM, which leads to sphaleron processes in Sec. 3.3.

3.1 Observations

Observations indicate that in the universe the number of baryons is different than the number of antibaryons. This asymmetry is evident if we consider cosmic rays, which provide samples of material from throughout the entire galaxy. In cosmic rays the ratio of antiprotons over protons is of the order of 10^{-4} and the magnitude of the antiproton flux is consistent with the hypothesis that the antiprotons are secondaries produced by cosmic ray collisions with the interstellar medium, and does not seem to indicate the presence of antimatter in the galaxy, even at the 10^{-4} level. Cosmic rays are solid evidence that there is a galactic asymmetry between baryons and antibaryons, and that this asymmetry is maximal [57]. This baryon asymmetry must have been dynamically generated, rather than given as an initial conditions. That's because if we accept inflation as solution of the flatness and horizon problem, and we have good reason to believe that inflation took place based on observed features of the CMB, then any primordial baryon asymmetry would have been exponentially diluted away by the required amount of inflation [20]. Quantitatively, the value of baryon asymmetry of the universe is obtained in two independent ways. The first is by confronting the abundances of the light elements (D, ^{3}He, ^{4}He and ^{7}Li) with the prediction of BBN [58–60]. The crucial time for primordial nucleosynthesis is when the thermal bath temperature becomes smaller than 1 MeV, i.e. when neutrinos decouple from the thermal plasma, weak interactions can no longer keep protons and neutrons in thermal equilibrium. With the assumption of only three light neutrinos, these predictions depend on a single parameter, the *baryon to photon ratio*:

$$\eta \equiv \left. \frac{n_B - n_{\bar{B}}}{n_\gamma} \right|_o , \tag{3.1}$$

where the subscript o means at present time. By using only the abundance of deuterium the baryon to photon ratio is [58]:

$$10^{10}\eta = 5.7 \pm 0.6. \tag{3.2}$$

The second way is from measurements of the CMB anisotropies [61, 62]. The crucial time for CMB is that of recombination, i.e when $T < 1$ eV. CMB observations measure the relative baryon contribution to the energy density of the multiplied by the square of the reduced Hubble constant $h \equiv H_0/(100\text{km sec}^{-1}\,\text{Mpc}^{-1})$

$$\Omega_B h^2 \equiv h^2 \frac{\rho_B}{\rho_{crit}}, \tag{3.3}$$

where $\rho_{crit} = \frac{3H^2}{8\pi G}$ and the density Ω_B is related to η through $10^{10}\eta = 274\Omega_B h^2$. A fit to the most recent observations (WMAP7 data only, assuming ΛCDM model with a scale-free power spectrum for the primordial density fluctuations) gives at 68% [63]:

$$10^2\Omega_B h^2 = 2.258^{+0.057}_{-0.056}. \tag{3.4}$$

There is a third way to express the baryon asymmetry of the Universe, that is, by normalizing the baryon asymmetry to the entropy density $s = g_*(2\pi^2/45)T^3$, where g_* is the number of degrees of freedom in the plasma, and T is the temperature. In this way, we obtain the abundance:

$$Y_{\Delta B} \equiv \left.\frac{n_B - n_{\bar{B}}}{s}\right|_o. \tag{3.5}$$

In terms of $Y_{\Delta B}$ the BBN result (3.2) and the CMB measurements 3.4 read:

$$Y_{\Delta B}^{BBN} = (8.10 \pm 0.85) \times 10^{-11}, \qquad Y_{\Delta B}^{CMB} = (8.79 \pm 0.44) \times 10^{-11}. \tag{3.6}$$

The impressive consistency between the determinations of the baryon density of the Universe from BBN and CMB that, besides being completely independent, also refer to epochs with a six orders of magnitude difference in temperature, provides a striking confirmation of the hot Big Bang cosmology [63].

3.1.1 Sakharov conditions

As we have previously pointed out the baryon asymmetry must have been generated dynamically. The three conditions required for baryogenesis were pointed out by Sakharov [21]:

1. Baryon number violation: This condition is required to evolve from an initial state with $Y_{\Delta B} = 0$ to a state with $Y_{\Delta B} \neq 0$;

2. C and CP violation: If either C or CP were conserved, then the rate $\Gamma(X^c \to Y^c + B^c) = \Gamma(X \to Y + B)$, resulting in an absence of baryon asymmetry. If the universe is initially matter-antimatter symmetric, and without a preferred direction of time, it is represented by a C and CP invariant state $|\phi_0\rangle$, with B = 0. If C and CP were conserved, i.e. $[C, H] = [CP, H] = 0$ (H is the Hamiltonian), then the state of the universe at later time t, $|\phi(t)\rangle = e^{iHt}|\phi_o\rangle$ would be C and CP invariant and, therefore $\Delta B = 0$. The only way to generate a net $\Delta B \neq 0$ is to have C and CP violating interactions.

3. Departure from thermal equilibrium: If all particles in the universe remained in thermal equilibrium, then no direction for time would be defined and CPT invariance would prevent the appearance of any baryon excess, rendering CP violating interactions irrelevant. Furthermore, in chemical equilibrium, there are no asymmetries in quantum numbers that are not conserved, such as B from the first condition.

These ingredients are all present in the Standard Model. However, no SM generating a large enough baryon asymmetry has been found.

1. Baryon number is violated in the Standard Model by the triangle anomaly. At zero temperature B violating processes are too suppressed to have any observable effect, but at high temperatures they occur with unsuppressed rate. So the first condition is quantitatively realized in the early Universe [63].

2. The weak interactions of the SM violate C maximally and violate CP via the Kobayashi-Maskawa mechanism. The CP violation can be parametrized by the Jarlskog invariant which is of order 10^{-20}, so it is impossible to generate $Y_{\Delta B} = 10^{-10}$. This means that there must exist new sources of CP violation, beyond the Kobayashi-Maskawa complex phase of the SM.

3. In the Standard Model, departure from thermal equilibrium occurs at the electroweak phase transition (EWPT). Here, the non-equilibrium condition is provided by the interactions of particles with the bubble wall. However, the experimental lower bound on the Higgs mass implies that this transition is not strongly first order, as required for successful baryogenesis.

This shows that baryogenesis requires new physics that extends the SM in at least two ways: It must introduce new sources of CP violation and it must either provide a departure from thermal equilibrium in addition to the EWPT or modify the EWPT itself. One of the possible new physics mechanism for baryogenesis is given by Leptogenesis, proposed by Fukugita and Yanagida [17]. Its simplest and theoretically best motivated realization is within the seesaw mechanism. To implement the seesaw, new Majorana $SU(2)_L$ singlet neutrinos with a large mass scale M (usually heavier than electroweak breaking scale) are added to the SM particle spectrum. New CP violation sources is provided by the complex Yukawa couplings, departure from thermal equilibrium can occur if their lifetime is not much shorter than the age of the universe when $T \sim M$ and their Majorana masses imply that the lepton number is not conserved. Thus, all three Sakharov conditions are naturally fulfilled in this scenario and leptogenesis is almost unavoidable when one consider seesaw mechanism. So with the introduction of sterile neutrinos lepton asymmetry can be generated dynamically and will be partially converted into a baryon asymmetry by SM sphalerons, that will be discussed in the following sections. A particularly interesting possibility is "thermal leptogenesis" where the heavy Majorana neutrinos are produced by scatterings in the thermal bath starting from a vanishing initial abundance, so that their number density can be calculated solely in terms of the seesaw parameters and of the reheat temperature of the Universe.

3.2 Leptogenesis models

Some possible new mechanism for Leptogenesis are the following:

- **Thermal leptogenesis**. The basic idea of thermal leptogenesis is that a lepton number is created in the Early Universe by the decay of particles with Majorana mass, e.g. heavy sterile neutrinos. In this scenario two different pictures are considered: thermal initial abundance, namely the havey neutrinos are already at thermal equilibrium with the plasma; or vanishing initial abundance, where heavy neutrinos are produced by interactions in the thermal bath. In both cases this is a freeze-out scenario.

- **Resonant leptogenesis**. Resonant leptogenesis is based on the observation that an enhancement of the CP-asymmetry occurs when the mass difference between two heavy Majorana neutrinos is small (quasi-degeneracy). Thanks to this enhancement leptogenesis temperatures of order of TeV are possible.

- **ARS leptogenesis**. This mechanism was first proposed by Akhmedov, Rubakov and Smirnov [27]. In this scenario RHNs are at the electroweak scale (or below), i.e. $M_N \simeq (1-100)$ GeV. Leptogenesis within this mass range is possible via CP-violating oscillations among sterile neutrinos.

In this scenario the neutrino Yukawa couplings are small enough to ensure that some of the sterile states might not reach thermal equilibrium before the electroweak phase transition. Therefore this is a freeze-in scenario.

3.3 Anomalous $B + L$ violation

The baryon number B and the three lepton flavour numbers L_α are conserved in the SM Lagrangian. However, that conservation is spoiled by quantum corrections through the chiral anomaly associated with triangle fermionic loop in external gauge fields. Due to chiral anomaly there are non-perturbative gauge field configurations that can act as source for $B + L_e + L_\mu + L_\tau$. In the early universe, at temperatures above the electroweak phase transition (EWPT), such configurations occur frequently and lead to rapid $B + L$ violation. These configurations are commonly referred to as "sphalerons" [20, 22, 64].

3.3.1 Baryon and Lepton number violations in the Electroweak theory

Baryon and lepton number are symmetries of the classical action, but they are violated by quantum effects. The current conservation is nonzero for the baryon current $J^\mu_B = \sum_q \frac{1}{3}\bar{q}\gamma^\mu q$ and lepton current $J^\mu_L = \sum_l(\bar{l}\gamma^\mu l + \bar{\nu}_l\gamma^\mu\nu_l)$ because of the anomalous triangle diagrams. The calculation gives [64, 65]:

$$\partial_\mu J^\mu_B = \partial_\mu J^\mu_L = N_f\left(\frac{g^2}{32\pi^2}W_{\mu\nu}\tilde{W}^{\mu\nu} - \frac{g'^2}{32\pi^2}Y_{\mu\nu}\tilde{Y}^{\mu\nu}\right) \tag{3.7}$$

where N_f is the number of fermions generations, $W_{\mu\nu}$, $Y_{\mu\nu}$ are the gauge field strength tensors for $SU(2)$ and $U(1)_Y$, respectively, and the tilde means the dual tensor, defined as $\tilde{F}^{\mu\nu} = \frac{1}{2}\epsilon^{\mu\nu\rho\sigma}F_{\rho\sigma}$. From Eq. 3.7 we see that the difference $B - L$ is strictly conserved, and so only the sum $B + L$ is anomalous and can be violated. The product of gauge field strengths on the right hand side of Eq. 3.7 can be written as four-divergences, $W\tilde{W} = \partial_\mu K^\mu_W$, $Y\tilde{Y} = \partial_\mu K^\mu_Y$, where

$$K^\mu_Y = \epsilon^{\mu\nu\alpha\beta}Y_{\nu\alpha}Y_\beta \tag{3.8}$$

$$K^\mu_W = \epsilon^{\mu\nu\alpha\beta}(W^a_{\nu\alpha}W^a_\beta - \frac{g}{3}\epsilon_{abc}W^a_\nu W^b_\alpha W^c_\beta) \tag{3.9}$$

where W_μ, Y_μ are the gauge fields of $SU(2)$ and $U(1)_Y$, respectively. In general total derivatives are unobservable because they can be integrated by parts and drop from the integrals, *i.e.*

$$\int d^4x\partial_\mu J^\mu = \int_{S^3} dA_3 r^3 n_\mu J^\mu \tag{3.10}$$

if $J^\mu \to 0$ at $r \to \infty$ faster than $1/r^3$ the integral vanishes. This holds for the terms in the four-vectors 3.9, 3.8 proportional to the field strengths $W_{\mu\nu}$ and $Y_{\mu\nu}$. Therefore, for the abelian group $U(1)_Y$ the current non conservation induced by quantum effects becomes non observable. However, for gauge fields the integral can be nonzero. Hence, for the non abelian group $SU(2)$ the current non conservation induced by quantum effects becomes observable. Let us define $Q^i(t) = \int d^3x j^i_0$ and $\Delta Q^i = Q^i(+\infty) - Q^i(-\infty)$ and let us suppose that there exist field configurations such that

$$\Delta Q^i = \frac{g^2}{32\pi^2}\int d^4x W^A_{\mu\nu}\tilde{W}^{\mu\nu,A} \tag{3.11}$$

is a non zero integer. This implies that fermions will be created, even though there is no perturbative interaction in the Lagrangian that generates them (see Ref. [20] for details). In the same way we can write $\Delta B = \Delta L = N_f \Delta N_{CS}$, where N_{CS} is the Chern-Simons number characterizing the topology of the gauge field configuration:

$$N_{CS} = \frac{g^2}{32\pi^2} \int d^3x \epsilon^{ijk} \big(W^a_{ij} W^a_k - \frac{g}{3} \epsilon_{abc} W^a_i W^b_j W^c_k \big). \tag{3.12}$$

In fact, since the Baryon number is the charge associated to the current J^μ_B we can write $B = \int d^3x J^0_B$ and

$$N_f \Delta N_{CS} = N_f \int d^4x \partial_\mu K^\mu_W = N_f \int d^4x (\partial_0 K^0_W - \partial_i K^i_W) = N_f \int d^3x K^0_W \Big|^{t_f}_{t_i} = N_f \Delta B \tag{3.13}$$

where in the 3rd expression we dropped the divergence of the spatial current. By Gauss theorem this is equivalent to a surface integral of the flux through it, hence it is possible to choose a gauge in which this vanishes. Now we want to compute ΔB between an initial and a final configuration of gauge fields. We are considering vacuum field strength tensors $W_{\mu\nu}$ which vanish. The corresponding potentials are not necessarily zero but can be represented by purely gauge fields:

$$W_\mu = -\frac{i}{g} U(x) \partial_\mu U^{-1}(x). \tag{3.14}$$

Let's work in temporal gauge which sets $W_0 = 0$. The temporal gauge is a partial gauge fixing condition, as time-independent gauge transformations $U(x)$ leave the gauge fixing condition $W_0 = 0$ fixed: $W_0 \to \frac{i}{g} U(x) \partial_0 U^{-1}(x) = 0$. The vacuum is thus described by the time-independent pure gauge configuration $W(x) = (i/g) U(x) \nabla U^{-1}(x)$. We can make use of the remaining gauge freedom to impose at spatial infinity $|x| \to \infty$ that $W_i = 0$ by choosing $U = 1$. Spatial infinity with infinity identified is equivalent to S^3, indeed the most generic 2×2 unitary matrix with $\det = 1$ may be expressed as $a\mathbb{1} + ib_i\sigma^i$ with $|a|^2 + |b|^2 = 1$, therefore the topology $SU(2) \sim S^3$. Hence, the gauge transformation $U(x)$ becomes a mapping from S^3 to the gauge group $SU(2)$. These mappings fall into homotopy classes categorized by integer winding numbers. Therefore, baryon-number changing processes are closely connected to the topology of the $SU(2)$ gauge plus Higgs fields.

3.3.2 $B + L$ violating rates

In the vacuum the Higgs field can be chosen to be constant and at the minimum of its potential W_μ is a pure gauge. In the $W^a_0 = 0$ gauge, N_{CS} is the gauge field winding number, which is an integer. It is invariant under "small" gauge transformations, *i.e.* gauge transformations continuously connected to the identity, this means that the gauge transformations belong to the same homotopy class. Mappings in different homotopy classes correspond to distinct vacua, which are related by a large gauge transformation. The energy density vanishes in different vacua, but to transition costs a finite energy density. At zero temperature, gauge field configurations that give non-zero $\int d^4x \tilde{W} W$ correspond to tunneling configurations, and are called instantons [20]. They change fermion number by an integer N, so the instanton action is large:

$$\left| \frac{1}{4g^2} \int d^4x W^A_{\mu\nu} W^{\mu\nu A} \right| \geqslant \left| \frac{1}{4g^2} \int d^4x W^A_{\mu\nu} \tilde{W}^{\mu\nu A} \right| \geqslant \frac{64\pi^2 N}{4g^2}. \tag{3.15}$$

The probability of barrier penetration can be calculated using the quasi classical approximation. The euclidean action evaluated at this trajectory gives the probability for barrier penetration as

$$\Gamma \propto e^{-4\pi/\alpha_W} \sim 10^{-162}, \tag{3.16}$$

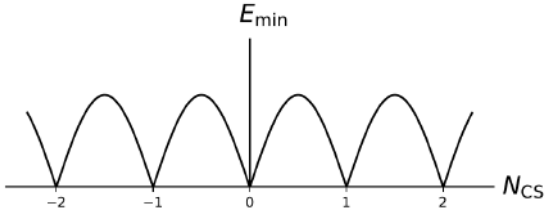

Figure 3.1: Sketch of the minimal field energy for a given value of the Chern-Simons number N_{CS}. Figure taken from Ref. [66].

where the exponent is the instanton action and $\alpha_W = g^2/4\pi$. Therefore, the mediated $B + L$ violation is unobservably small. An instanton acts as a source for three leptons (one from each generation), and nine quarks (all colors and generation), so it induces $\Delta B = \Delta L = 3$ processes. If the ground state of gauge fields is pictured as a periodic potential, with minima labeled by integers, then the instantons correspond to vacuum fluctuations that tunnel between minima. With this analogy, one can imagine that at finite temperature, a thermal fluctuation of the field could climb over the barrier. The sphaleron is such a configuration, in presence of the Higgs vacuum expectation value. Therefore, to change N_{CS} by ± 1, one has to go over an energy barrier. A vacuum-to-vacuum transition along this path would change baryon and lepton number by a multiple of n_f (see Eq. 3.13) [66]. Fig. 3.1 shows the minimal static energy of the gauge-Higgs fields as a function of N_{CS}. The $B + L$ violating rate mediated by sphalerons is Boltzmann suppressed

$$\Gamma_{sph} \propto e^{-E_{sph}/T}, \tag{3.17}$$

where $E_{sph} = 2Bm_W/\alpha_W$ is the height of the barrier at $T = 0$, and $1.5 \lesssim B \lesssim 2.75$ is a parameter that depends on the Higgs mass [22]. For leptogenesis we are interested in the $B + L$ violating rate at temperatures far above the $EWPT$. The large $B + L$ violating gauge field configurations occur frequently at $T \gg m_W$. The rate can be estimated as

$$\Gamma_{\not{B}+\not{L}} \simeq 250\alpha_W^5 T, \tag{3.18}$$

this implies that, for temperatures below $10^{12} GeV$ and above the EWPT, $B + L$ violating rates are in equilibrium. Therefore, leptogenesis is able to provide $B - L \neq 0$, *i.e.* a lepton asymmetry which is not balanced by a baryon asymmetry. As we have already seen, $B - L$ is conserved in the SM, while sphalerons are $B + L$ violating but conserve $B - L$. Since sphalerons are at thermal equilibrium in the temperature range $100 < T < 10^{12}$ GeV, any asymmetry $B + L$ is efficiently washed out. However, the non-zero $B - L$ generated by leptogenesis is partially converted into a baryon asymmetry through these non-perturbative processes. Thus, the final baryon asymmetry of the universe observed today is determined by the lepton asymmetry at the time of sphaleron decoupling, i.e. at the electroweak phase transition. To determine which fraction of $B - L$ asymmetry is converted into B asymmetry we need to consider constraints among various chemical potentials induced by spectator processes.

3.3.3 The relation between Baryon and Lepton asymmetries

Quarks, leptons and Higgs bosons interact via Yukawa and gauge couplings and, also, via the non-perturbative sphaleron processes. In the range $100 < T < 10^{12}$ GeV gauge and sphaleron interactions are in thermal equilibrium, while Yukawa interactions are in equilibrium only in a more restricted temperature range that depends on the strength of the Yukawa couplings. Thus, in different temperature

ranges there are different sets of charges that are conserved, which leads to the "flavor effects" [67]. The corresponding partition function can be written as [66]:

$$Z(\mu, T, V) = \mathrm{Tr} \exp\left[\beta\Big(\sum_i \mu_i Q_i - H\Big)\right], \tag{3.19}$$

where $\beta = 1/T$ and H is the Hamiltionian. For each of the quark, lepton and Higgs fields there is an associated chemical potential μ_i. In the standard model with one Higgs doublet H and N_f families one has $5N_f + 1$ chemical potentials μ_i. p The processes that are at thermal equilibrium, the so-called Spectator processes, yield constraints between the various chemical potentials. The basic way through which they act is that of redistributing the asymmetry generated in the lepton doublets among the other particle species. Their effects can be accounted for by imposing on the thermodynamic system the chemical equilibrium condition appropriate for each specific reaction. The N_{CS}-changing transitions affect only the left-handed fermion fields, so that

$$\sum_i (3\mu_{q_i} + \mu_{l_i}) = 0. \tag{3.20}$$

One also has to take the $SU(3)$ QCD sphaleron processes into account. They change the chiral quark number (the number of right-handed minus number of left-handed quarks) for each quark flavor by the same amount. The corresponding relation between the chemical potentials reads

$$\sum_i (2\mu_{q_i} - \mu_{u_i} - \mu_{d_i}) = 0. \tag{3.21}$$

The Yukawa interactions that are in equilibrium yield relations between the chemical potentials of the left-handed and right-handed fermions and the Higgs:

$$-\mu_{q_i} + \mu_{d_j} = \mu_{q_i} - \mu_{u_j} = -\mu_{l_i} + \mu_{e_i} = \mu_H. \tag{3.22}$$

There is another condition, valid at all temperatures, that arises from the requirement that the total hypercharge of the plasma vanishes. In a weakly coupled plasma, the asymmetry between particle and antiparticle number densities is given by

$$n_i - \bar{n}_i = -\frac{\partial}{\partial \mu_i} \frac{T}{V} \ln Z(\mu, T, V). \tag{3.23}$$

For massless particles one obtains

$$n_i - \bar{n}_i = \frac{g_i T^3}{6} \begin{cases} \beta\mu_i & +O\big((\beta\mu_i)^3\big) \quad \text{(F)} \\ 2\beta\mu_i & +O\big((\beta\mu_i)^3\big) \quad \text{(B)} \end{cases}, \tag{3.24}$$

where g_i denotes the number of internal degrees of freedom. The following analysis is based on these relations for $\beta\mu_i \ll 1$. From this relation and the known hypercharges one obtains

$$\sum_i (\mu_{q_i} + 2\mu_{u_i} - \mu_{d_i} - \mu_{l_i} - \mu_{e_i}) = 2\mu_\phi, \tag{3.25}$$

and using Eq. (3.24), the baryon number density $n_B \equiv gBT^2/6$ and the lepton number densities $n_{L_i} \equiv L_i g T^2/6$ can be expressed in terms of the chemical potentials:

$$B = \sum_i \big(2\mu_{q_i} + \mu_{u_i} + \mu_{d_i}\big), \tag{3.26}$$

$$L_i = 2\mu_{l_i} + \mu_{e_i}, \quad L = \sum_i L_i. \tag{3.27}$$

Consider now the case where all Yukawa interactions are in equilibrium. The asymmetries $L_i - B/N_f$ are then conserved and we have equilibrium between the different generations, $\mu_{l_i} \equiv \mu_l$, $\mu_{q_i} \equiv \mu_q$, etc. Using also the sphaleron relation and the hypercharge constraint, one can express all chemical potentials, and therefore all asymmetries, in terms of a single chemical potential that may be chosen to be μ_l,

$$\begin{aligned} &\mu_e = \frac{2N_f+3}{6N_f+3}\mu_l, \quad \mu_d = \frac{6N_f+1}{6N_f+3}\mu_l \quad \mu_u = \frac{2N_f-1}{6N_f+3}\mu_l \\ &\mu_q = -\frac{1}{3}\mu_l, \quad \mu_H = \frac{4N_f}{6N_f+3}\mu_l. \end{aligned} \tag{3.28}$$

The corresponding baryon and lepton asymmetries are

$$n_B = -\frac{4n_f}{3}\frac{T^2}{6}\mu_l, \quad n_L = \frac{14n_f^2+9n_f}{6n_f+3}\frac{T^2}{6}\mu_l. \tag{3.29}$$

The last equation yields the connection between the B, $B-L$ and L asymmetries:

$$B = c_s(B-L) \quad L = (c_s-1)(B-L), \tag{3.30}$$

where $c_s = (8n_f+4)/(22n_f+13) = 28/79$. The relations 3.30 between B, $B-L$, and L numbers suggest that $B-L$ violation is needed in order to generate a baryon asymmetry at high temperatures where sphaleron processes are in thermal equilibrium. Because the $B-L$ current has no anomaly, the value of $B-L$ at time t_f, where the leptogenesis process is completed, determines the value of the baryon asymmetry today:

$$B(t_0) = c_s(B-L)(t_f). \tag{3.31}$$

Chapter 4

Thermal Leptogenesis

In this Chapter the mechanism of thermal leptogenesis is reviewed. We start by studying the single flavour scenario in Sec. 4.1. In particular, we review the solutions of the Boltzmann Equations in the case with only decays and inverse decays in Sec. 4.2 and we define and compute the contribution to the CP asymmetry factor in Sec. 4.3. Finally, we give a brief description of flavour effects in Sec. 4.4 and resonant leptogenesis in Sec. 4.5.

4.1 Thermal leptogenesis in the single flavour regime

In this section we make the following assumptions [20]:

- The lepton asymmetry is produced in a single flavour α;
- The N-masses are hierarchical: $M_1 \ll M_2, M_3$;
- Thermal production of N_1 and negligible production of N_2, N_3.

The basic idea is the following [20]: Scattering processes produce a population of N_1's at temperatures $T \sim M_1$. When the temperature drops below M_1, the equilibrium number density is exponentially suppressed by a factor $e^{-M_1/T}$, since sterile neutrinos becomes non relativistic. So the N_1 population decays away. If the N_1 interactions are CP violating, asymmetries in all lepton flavours can be produced and if the interactions are out-of-equilibrium the asymmetries may survive. These can the be reprocessed into a baryon asymmetry by SM sphalerons. It is important to notice that in this model the CP asymmetry in the scattering interactions by which the N_1 population is produced is equal in magnitude but opposite in sign to the CP asymmetry in N_1 decays. However a non-zero asymmetry survives because the initial anti-asymmetry made with the N_1 population is depleted by scattering, decays and inverse decays. This depletion is called **washout**. To understand the non-equilibrium processes we need to compare the reaction rates per particle with the Hubble parameter as a function of $z = M/T$. In particular, for $z < 1$ (high temperatures) all processes are out of thermal equilibrium. Around $z \sim 1$, the various processes come into thermal equilibrium. Heavy neutrinos decay and, since their number density slightly exceeds the equilibrium number density, a $B-L$ asymmetry is generated in these decays. As long as washout processes are in equilibrium the asymmetry is partly washed out. At $z > 1$ (low temperatures), N production is kinematically suppressed, while the washout processes eventually get out of equilibrium at some z and the $B - L$ asymmetry is frozen in [66].

4.1.1 Thermal history of Thermal Leptogenesis

The story of leptogenesis begins right after inflation ends, at the reheating temperature T_{reh} which we assume to be larger than the mass of the heavy neutrinos N_j.

At very high temperatures $T \lesssim T_{reh}$ the heavy neutrinos N_j are in thermal equilibrium with the rest of the plasma thanks to their Yukawa interactions: $N_j \leftrightarrow H^0\nu_L$, $N_j \leftrightarrow H^+l$.

As the Universe cools, T becomes smaller than M_j implying the particles in the plasma do not have sufficient energy to produce back right-handed neutrinos, only their decays are allowed: $N_j \to H^0\nu_L$, $N_j \to H^+l$.

Being Majorana neutrinos, N_j can decay both into one channel and its charge conjugate one: $N_j \to H^-l^+$, $N_j \to H^+l^-$.

If the rates of these two processes are different, due to CP violation, then a net charge asymmetry ϵ is generated. This process is not instantaneous and washout effects, due e.g. by inverse decays, will partly erase the asymmetry. The remaining lepton asymmetry can then be converted by sphaleron processes into a baryon asymmetry when $T < M_j$ and $T < 10^{13}$ GeV. As temperature lowers, decays and washout processes freeze out and the sphalerons are fast enough to keep the baryon number at its equilibrium value compared to the lepton number. At the EW scale $T \sim T_{\rm EW} \sim 10^2$GeV we have the EWPT and the sphalerons freeze out due to the Boltzmann suppression factor, and all baryon number violating processes are suppressed from this point. Therefore, the baryon number per comoving volume freezes out to its current value.

4.1.2 Out-of-equilibrium dynamics

Leptogenesis naturally takes place in seesaw models, indeed, besides giving a natural explanation of the light neutrino masses (as we have already seen in Sec. 2.4), the heavy Majorana neutrinos are the source of leptogenesis. From the seesaw Lagrangian in Eq. 2.29 we have that the three Sakharov's conditions are satisfied: lepton number L is violated by the Majorana massive term (see Eq. 2.21), CP is violated by the Yukawa complex couplings $Y_{\alpha j}$ and the departure from thermal equilibrium condition is provided by an additional requirement that N_i decay rate Γ_{N_i} is not very fast compared to the Hubble expansion rate of the Universe $H(T)$ at temperature $T = M_i$. For the initial conditions, we assume that after inflation the Universe reheats to a thermal bath at temperature T_{reheat} which is composed of particles with gauge interactions. The N_1 can be produced by inverse decays $HL_\alpha \to N_1$ and by $2 \to 2$ scatterings involving the top quark or electroweak gauge bosons. N_1 can be produced by s or t channel exchange of a Higgs: $q_L t_R \to H \to L_\alpha N$ or $L_\alpha t_R \to H \to q_L N$. So the production rate can be estimated by a naive dimensional analysis in zero temperature field theory, as

$$\Gamma_{prod} \sim \sum_\alpha \frac{h_t^2 |Y_{\alpha 1}|^2}{4\pi} T, \tag{4.1}$$

where h_t is the Yukawa coupling of the top quark. If $\Gamma_{prod} > H$ then, since $h_t \sim 1$, the N_1 total decay is also in equilibrium:

$$\Gamma_D > H(T = M_1). \tag{4.2}$$

N_i can decay with the following processes:

$$N_i \to Hl, \quad N_i \to H^c l^c. \tag{4.3}$$

Then at tree level we have the diagram in Fig. 4.1 and we can compute the decay rate Γ by considering the N_i particle at rest in the center of mass frame. In this way we have

$$\Gamma = \frac{1}{2M}\int |\mathcal{M}|^2 d\Pi_x, \tag{4.4}$$

where

$$d\Pi_n = d\Pi_l d\Pi_H = \frac{d^3p_l}{(2\pi)^3 2E_l}\frac{d^3p_H}{(2\pi)^3 2E_H}(2\pi)^4\delta^{(4)}(p_N - p_l - p_H). \tag{4.5}$$

When integrating over the phase space we can split the delta and we obtain

$$\int \frac{d^3p_l}{(2\pi)^3 2E_l}\frac{d^3p_H}{(2\pi)^3 2E_H}(2\pi)^4\delta^{(3)}(\vec{p}_N - \vec{p}_l - \vec{p}_H)\delta(E_N - E_H - E_N). \tag{4.6}$$

Now we can integrate over d^3p_H by using the three-dimensional delta, setting $\vec{p}_H = \vec{p}_N - \vec{p}_l$. From momentum conservation we have $\vec{p}_N = \vec{p}_H + \vec{p}_l$ and in the center of mass frame we have $p_N = (M_N, \vec{0})^T$, so we obtain $\vec{p}_H = \vec{p}_l$. Assuming negligible the mass of the scalar and the lepton doublet (respect the mass of the sterile neutrino) we obtain $E_H = E_l$ from mass-shell relation. Going in spherical coordinates we get

$$\int \frac{p_l^2 dp_l d\Omega}{(2\pi)^2 4E_l^2}\delta(M_N - 2E_l) = \int \frac{d\Omega p_l dE_l}{(2\pi)^2 4E_l}\delta(M_N - 2E_l) = \frac{1}{8\pi} \tag{4.7}$$

where in the second passage we used $pdp = EdE$, while in the third we integrated over the solid angle $d\Omega = 4\pi$ and to integrate over dE_l we used the property of the delta $\delta(g(x)) = \frac{\delta(x-x_0)}{|g'(x)|}$. Since the final state in the two different decay channels of N_1 are different, the two amplitudes do not interfere and we can calculate them separately and add only their squares. The amplitude of the diagram in Fig. 4.1 is given by:

$$i\mathcal{M} = \bar{u_l}(p_2)(-iY_{\alpha i})P_R u_N(p_1) \tag{4.8}$$

where $P_R = \frac{1+\gamma_5}{2}$ is the right projector. Now we can take the absolute square and by averaging over the initial spin we find the unpolarized squared amplitude.

$$\begin{aligned}
|\mathcal{M}|^2_{unpol} = \frac{1}{2}\sum_{s_N}\sum_{s_l s_H}\mathcal{M}^*\mathcal{M} =& \frac{1}{2}Y^*_{i\alpha}Y_{\alpha i}Tr[P_L \cancel{p_2} P_R(\cancel{p_1} + M_N)] \\
=& \frac{1}{2}Y^*_{i\alpha}Y_{\alpha i}\frac{1}{2}Tr[\cancel{p_1}\cancel{p_2}] \\
=& Y^*_{i\alpha}Y_{\alpha i}[p_1 \cdot p_2] \\
=& \frac{1}{2}Y^*_{i\alpha}Y_{\alpha i}M^2
\end{aligned} \tag{4.9}$$

where we have used the properties of gamma matrices: $Tr[\gamma^\mu\gamma^\nu] = 4g^{\mu\nu}$ (where $g^{\mu\nu}$ metric tensor), $Tr[\gamma^{\mu_n}] = 0$ if n=odd and using $p_3 = p_1 - p_2$ we find $p_1 \cdot p_2 = M^2/2$ since we have assumed $m_l = m_H = 0$. Considering now the decaying of the right-handed neutrino into an antilepton and a Higgs and following the same steps as before we find that the two amplitudes are equal at tree level. At the end we obtain

$$\Gamma(N_1 \to lH) = \Gamma(N_1 \to \bar{l}H^+) = \frac{1}{32\pi}(Y^+Y)_{11}M_1. \tag{4.10}$$

By summing these two contributions and taking care of a factor of 2 coming from the fact that we are calculating the decay of the right-handed neutrino to any final state, we need to sum over final spin,

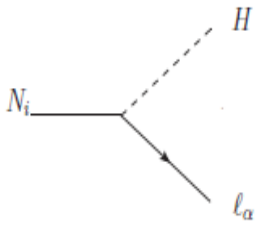

Figure 4.1: tree level Feynman diagram for sterile neutrino decay

flavour and doublet indices[1]. Therefore, we finally obtain

$$\Gamma_D = \sum_\alpha \Gamma_{\alpha\alpha} = \sum_\alpha \Gamma(N_1 \to HL_\alpha, \bar{H}\bar{L}_\alpha) = \frac{1}{8\pi}(Y^+Y)_{11}M_1. \tag{4.11}$$

To study the departure from thermal equilibrium we have to compare this decay rate with the Hubble expansion assuming a universe dominated by radiation (as it was the Early Universe). In this case we have

$$H(T) = \sqrt{\frac{8\pi G\rho_R}{3}} = \frac{2}{3}\sqrt{\frac{\pi^3 g_*}{5}}\frac{T^2}{M_{Pl}}, \tag{4.12}$$

where $M_{\rm Pl} = 1.22 \times 10^{19} GeV$ is the Planck mass and g_* is the total number of relativistic degrees of freedom contributing to the energy density of the Universe. To quantify the departure from thermal equilibrium, it is useful to introduce two dimensional parameters $\tilde{m}$ and m_*, which are of the order of the light neutrino masses, and we can define the decay parameter as

$$K_i \equiv \frac{\Gamma_{N_i}}{H(M_i)} = \frac{\tilde{m_i}}{m_*}, \tag{4.13}$$

where $\tilde{m_i}$ is the *effective neutrino mass* defined as [20]:

$$\tilde{m_i} \equiv \sum_\alpha \tilde{m}_{\alpha\alpha} \equiv \sum_\alpha \frac{Y^\dagger_{\alpha 1} Y_{\alpha 1} v^2}{M_1} = 8\pi \frac{v^2}{M_i}\Gamma_D, \tag{4.14}$$

and

$$m_* \equiv 8\pi \frac{v^2}{M_1^2} H\Big|_{T=M_1} \simeq 1 \times 10^{-3}\text{eV}. \tag{4.15}$$

The decay parameter in Eq. 4.13 controls whether or not N_i decays are in equilibrium and allows to distinguish two regimes:

- **Weak washout regime**. In this scenario $K_i \ll 1$, meaning that the total decay rate $\Gamma(N_i \to L_\alpha H) < H(M_i)$. This implies that the N_i number density does not reach the equilibrium distribution during the evolution of the Universe and any lepton asymmetry created for $z < 1$ will not be erased. In this regime the initial condition on the N_i density is important. If we assume thermal

[1] In fact, if we consider all the lepton and Higgs doublets components we have $\Gamma(N_i \to l_j^- H^+) = \Gamma(N_i \to \nu_{L,j} H^0) = \Gamma(N_i \to l_j^+ H^-) = \Gamma(N_i \to \bar{\nu}_{L,J} H^{0,*}) = 1/(32\pi)|Y_{ij}|^2 M_{N_i}$. To find Γ_D we must sum all these contributions and then sum over the flavors α.

initial abundance of $N_i = N_i^{eq}$, we can ignore the washout when N_i starts decaying at $z \gg 1$. Instead, if we have zero initial N_1 abundance, we have to consider the opposite sign contribution to lepton asymmetry from the inverse decays, namely when N_1 is being populated, and from the period when N_1 starts decaying.

- **Strong washout regime**: In this case $K_i \gg 1$ and any lepton asymmetry generated during the N_1 creation phase is efficiently washed out, resulting in $Y_{\Delta L} \sim 0$. This implies that the solution of Boltzmann equations does not depend on initial conditions. When the temperature drops and the washouts W_{ID} decouples (the inverse decay gets out of equilibrium), the asymmetry created through the decay survives and contributes to $Y_{\Delta L}$

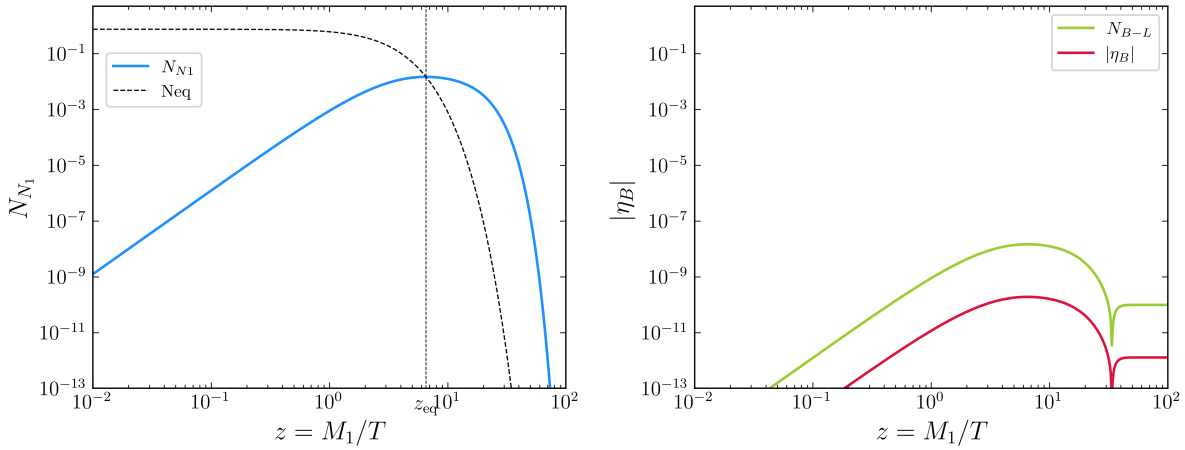

Figure 4.2: Evolution of N_1 number density (on the left) and $B - L$ asymmetry (on the right) in the weak washout case with $K = 10^{-2}$ and vanishing initial abundance. Here, we have $M_1 = 10^{14}$ GeV and $|\epsilon_1| = 10^{-6}$.

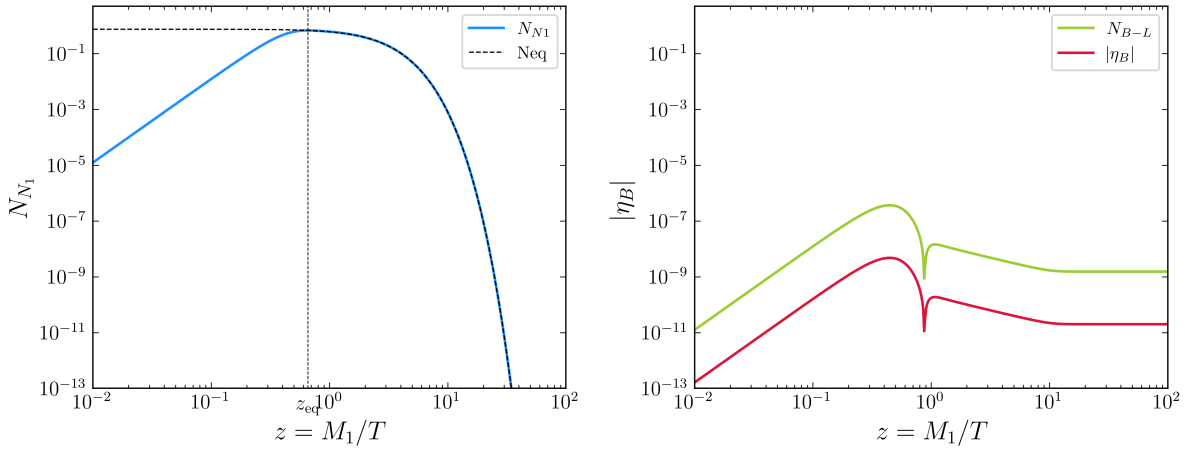

Figure 4.3: Evolution of N_1 number density (on the left) and $B - L$ asymmetry (on the right) in the strong washout case with $K = 100$ and vanishing initial abundance. Here, we have $M_1 = 10^{14}$ GeV and $|\epsilon_1| = 10^{-6}$.

Figs. 4.2 and 4.3 show the N_1 number density and the absolute value of the baryon asymmetry as a

function of $z = M_1/T$ in the case of vanishing initial abundance $N^i_{N_1} = 0$, respectively in the weak and strong washout cases. In the strong washout case we can see that the RHN number density slowly increases with time thanks to its interaction with the SM particles and reaches the equilibrium distribution. In baryon asymmetry plot we can see a dip for $z \simeq 10^0$, this dip represents a change of sign in the baryon asymmetry (as we are considering the absolute value). This happens in the vanishing initial abundance case, since, for $z \ll 1$ we have to consider the opposite sign contribution to lepton asymmetry from the inverse decays, which populate the N_1 sector, resulting in an asymmetry in some direction. In fact, due to CP violation, inverse decay destroy more antileptons than leptons (or viceversa), generating a negative asymmetry. Then, when the RHNs reach the thermal equilibrium distribution, their decay will start dominate the asymmetry production, which will have opposite sign respect to the one created before. The same situation occurs in the weak washout case with vanishing initial abundance, but in this case we see that RHNs number density does not reach the equilibrium distribution and the dip in the absolute BAU is for $z \gg 1$.

4.2 Classical Boltzmann equations

In this section we will write down the classical Boltzmann equations and give a simple analytical estimate of the solution by following Ref. [18]. First we work in the one flavour regime and consider only the decays of the right handed neutrino N_1. If leptogenesis occurs at $T \geqslant 10^{12}$ GeV, then, the charged Yukawa interactions are out of equilibrium, and this defines the one flavor regime. In particular we consider the initial temperature T_i larger than M_1, the mass of N_1. We will also neglect decays of the two heavier neutrinos N_2 and N_3, assuming that a generation of $B - L$ asymmetry from their decays either does not occur at all or that it does not influence the final value of $B - L$, namely this $B - L$ asymmetry will be efficiently washed out by the N_1 interactions. This situation can be realized if for example the reheating temperature after inflation is $T_{RH} \ll M_{2,3}$, such that $N_{2,3}$ are not produced. Further, we restrict ourselves to the non supersymmetric case, and we assume that the lightest heavy neutrino N_1 is the only relevant degree of freedom beyond the standard model particle species. Within this framework the BE reduces to [68]:

$$\frac{dN_{N_1}}{dz} = -(D + S)(N_{N_1} - N^{eq}_{N_1}), \tag{4.16}$$

$$\frac{dN_{B-L}}{dz} = -\epsilon_1 D(N_{N_1} - N^{eq}_{N_1}) - W N_{B-L}. \tag{4.17}$$

where $z = M_1/T$ and, by choosing a comoving volume $a(t_*)^3$ which contains one photon at time t_*, we obtain $N_i(t_*) = n_i a(t_*)^3$ and $N_\gamma(t_*) = 1$ so that $N_{N_1} \equiv n_n/n^{eq}_\gamma$ (n^{eq}_γ is the equilibrium photon density) [69]. ϵ_1 is the CP asymmetry parameter that will be derived in next section. Now we can solve the second Eq. 4.17 and we find:

$$N_{B-L}(z) = N_{B-L}(z_i) e^{-\int_{z_i}^{z} W(z')dz'} - \int_{z_i}^{z} dz' \epsilon_1 D(N_{N_1} - N^{eq}_{N_1}) e^{-\int_{z'}^{z} W(z")dz"}. \tag{4.18}$$

From the other Boltzmann equation 4.16 we can rewrite the result as

$$N_{B-L}(z) = N_{B-L}(z_i) e^{-\int_{z_i}^{z} W(z')dz'} - \int_{z_i}^{z} dz' \epsilon_1 \frac{D}{D+S} \frac{dN_{N_1}}{dz} e^{-\int_{z'}^{z} W(z")dz"}, \tag{4.19}$$

where the last term in the right-hand side is the *efficiency factor* k that measures the amount of asymmetry that has survived the competitive production and wash-out processes. We can define the

efficiency factor as

$$\begin{aligned} k(z) &= \frac{4}{3}\int_{z_i}^{z} dz' \epsilon_1 D(N_{N_1} - N_{N_1}^{eq}) e^{-\int_{z'}^{z} W(z")dz"} = \\ &= -\frac{4}{3}\int_{z_i}^{z} dz' \epsilon_1 \frac{D}{D+S}\frac{dN_{N_1}}{dz} e^{-\int_{z'}^{z} W(z")dz"}, \end{aligned} \tag{4.20}$$

and the Eq. 4.19 becomes

$$N_{B-L}(z) = N_{B-L}(z_i) e^{-\int_{z_i}^{z} W(z')dz'} - \frac{3}{4}\epsilon_1 k(z; \tilde{m}_1, M_1, \bar{m}^2), \tag{4.21}$$

where z_i is some initial temperature when N_1 leptogenesis begin. The efficiency factor $k(z)$ is normalized in such a way that its final value $k_f = k(\infty)$ approaches one in the limit of thermal initial abundance of the heavy neutrinos N_1 and no washout ($W = 0$). In general, for $N_{N_1}^i \leqslant N_{N_1}^{eq} = 3/4$ one has $k_f \leqslant 1$. The first term in Eq. 4.21 accounts for the possible generation of a $B - L$ asymmetry before N_1 decays, *e.g.* from decays of the two heavier neutrinos N_2 and N_3, or from a completely independent mechanism. In the following we shall neglect such an initial asymmetry N_{B-L}^i [18]. As we will see, decays and inverse decays are sufficient to describe qualitatively some properties of the full problem. In the next sections we will find some analytical approximations to study the two regimes of weak and strong washout.

Analytic approximation

Let us first recall some basic definitions and formulae. The decay rate takes the form

$$\Gamma_D(z) = \tilde{\Gamma}_D \left\langle \frac{1}{\gamma} \right\rangle, \tag{4.22}$$

where $\tilde{\Gamma}$ is the decay width

$$\tilde{\Gamma} = \frac{\tilde{m}_1 M_1^2}{8\pi v^2}, \tag{4.23}$$

with the Higgs vacuum expectation value $v = 174GeV$, and $\langle 1/\gamma \rangle$ is the thermally averaged dilation factor. This accounts for the mean time dilation in the decay lifetime of particles, in particular, for particles following a Maxwell-Boltzmann distribution at a temperature $T = m/z$ we get [68]:

$$\left\langle \frac{1}{\gamma} \right\rangle = \left\langle \frac{m}{E} \right\rangle = \frac{\int_z^\infty z\sqrt{x^2 - z^2} e^{-x} dx}{\int_z^\infty x\sqrt{x^2 - z^2} e^{-x} dx} = \frac{\mathcal{K}_1(z)}{\mathcal{K}_2(z)}. \tag{4.24}$$

Where we have integrated the Maxwell-Boltzmann distribution function $f(p) = e^{-E/K_B T}$ in this way

$$n = \int \frac{d^3p}{(2\pi)^3} e^{-E/K_B T} = \frac{1}{2\pi^2}\int \sqrt{E^2 - m^2} E e^{-E/K_B T} dE, \tag{4.25}$$

where we have used $d^3p = p^2 dp d\Omega$ and the fact that if the mass is constant $EdE = pdp$. Then by averaging we get

$$\begin{aligned} \left\langle \frac{m}{E} \right\rangle &= \frac{\frac{1}{2\pi^2}\int \sqrt{E^2 - m^2}\frac{m}{E} E e^{-E/K_B T} dE}{\frac{1}{2\pi^2}\int \sqrt{E^2 - m^2} E e^{-E/K_B T} dE} = \\ &= \frac{\int z\sqrt{x^2 - z^2} z e^{-x} dx}{\int x\sqrt{x^2 - z^2} e^{-x} dx} = \frac{\mathcal{K}_1(z)}{\mathcal{K}_2(z)}, \end{aligned} \tag{4.26}$$

where $\mathcal{K}_1$ and $\mathcal{K}_2$ are the Bessel function. The decay term is written in the form

$$D(z) = Kz\left\langle \frac{1}{\gamma} \right\rangle. \tag{4.27}$$

The inverse decay rate is related to the decay rate by

$$\Gamma_{ID}(z) = \Gamma_D(z)\frac{N_{N_1}^{eq}(z)}{N_l^{eq}}, \tag{4.28}$$

where N_l^{eq} is the equilibrium density of lepton doublets. We can derive the expressions for $N_{N_1}^{eq}(z) = n_{N_1}^{eq}/n_\gamma^{eq}$ and $N_l^{eq}(z) = n_l^{eq}/n_\gamma^{eq}$ from the number density

$$n_{MB}^{eq} = \frac{g}{2\pi}\int_0^\infty \frac{d^3p}{(2\pi)^3}e^{-E/T}, \tag{4.29}$$

with the same passages as in Eq. 4.25 we obtain

$$n_{MB}^{eq} = \frac{gT^3}{2\pi^2}\int_0^\infty x\sqrt{x^2-z^2}e^{-x}dx = \frac{gT^3}{2\pi^2}x^2\mathcal{K}_2(z), \tag{4.30}$$

where g is the number of degrees of freedom for the particle specie. Using Fermi-Dirac or Bose-Einstein statistics $f^{eq}(p) = (e^{E/T} \pm 1)^{-1}$, the number density is given by

$$n_i^{eq} = \frac{g_i T^3}{\pi^2} \times \begin{cases} \zeta(3) & \text{(bosons).} \\ \frac{3}{4}\zeta(3) & \text{(fermions).} \end{cases} \tag{4.31}$$

which are valid in the relativistic limit $m_i << T$. So we can derive

$$N_l^{eq} = \frac{n_l^{eq}}{n_\gamma^{eq}} = \frac{\frac{3}{4}\zeta(3)\frac{2}{\pi^2}T^3}{2\frac{T^3}{\pi^2}\zeta(3)} = \frac{3}{4}, \tag{4.32}$$

where we have used a Fermi-Dirac distribution for the leptons with $g_l = 2$. While, for N_1

$$N_{N_1}^{eq} = \frac{n_{N_1}^{eq}}{n_\gamma^{eq}} = \frac{\frac{3}{4}\zeta(3)\frac{2}{\pi^2}T^3z^2\mathcal{K}_2(z)}{2\frac{T^3}{\pi^2}\zeta(3)} = \frac{3}{8}z^2\mathcal{K}_2(z). \tag{4.33}$$

The contribution of inverse decays to the washout term W is therefore

$$W_{ID}(z) = \frac{1}{2}\frac{\Gamma_{ID}(z)}{H(z)z} = \frac{1}{4}Kz^3\mathcal{K}_1(z), \tag{4.34}$$

which implies

$$W_{ID}(z) = \frac{1}{2}D(z)\frac{N_{N_1}^{eq}(z)}{N_l^{eq}}. \tag{4.35}$$

4.2.1 Decays and inverse decays

Now we consider a simplified picture in which decays and inverse decays are the only processes. Then the kinetic equation 4.16 reduces to (see App. B for a detailed derivation):

$$\frac{dN_{N_1}}{dz} = -D(N_{N_1} - N_{N_1}^{eq}), \tag{4.36}$$

$$\frac{dN_{B-L}}{dz} = -\epsilon_1 D(N_{N_1} - N_{N_1}^{eq}) - W_{ID} N_{B-L}, \tag{4.37}$$

where w_{ID} is the contribution to the washout term due to inverse decays. From Eqs. 4.37 and 4.36 we find that the efficiency factor becomes

$$k(z) = -\frac{4}{3}\int_{z_i}^{z} dz' \frac{dN_{N_1}}{dz'} e^{-\int_{z'}^{z} dz'' W_{ID}(z'')}. \tag{4.38}$$

and by integrating Eq. (4.36) we obtain

$$N_{N_1}(z) = N_{N_1}(z_i) e^{-\int_{z_i}^{z} D(z')dz'} + \int_{z_i}^{z} D(z') N_{N_1}^{eq}(z') e^{-\int_{z'}^{z} D(z'')dz''}. \tag{4.39}$$

4.2.2 Weak washout regime

In the weak washout regime ($K \ll 1$), the initial condition on the N_1 density N_{N_1} is important. Therefore, in this scenario we need to distinguish between two different initial conditions, namely thermal initial abundance and vanishing initial abundance.

Thermal initial abundance

If we assume thermal initial abundance of N_1, i.e. $N_{N_1}(z_i) = N_{N_1}^{eq}(0)$, we can ignore the washout when N_1 starts decaying at $z \gg 1$. In fact, in this case, we can define z_d as the value below which decays are in equilibrium, by $\Gamma_D(z_d)/H(z_d) = z_d D(z_d) = 2$. In the regime far out of equilibrium $K \ll 1$ decays occur at very small temperatures, i.e. $z_d \gg 1$, and the produce $B - L$ asymmetry is not reduced by washout effects (see App. C.1 for further details). Therefore, the integral in Eq. 4.38 for the efficiency factor simply becomes

$$k(z) \simeq -\frac{4}{3}\int_{z_i}^{z} dz' \frac{dN_{N_1}}{dz'} = \frac{4}{3}(N_{N_1}(z_i) - N_{N_1}(z)). \tag{4.40}$$

To find the density of $B-L$ asymmetry today, we integrate between $z_i = 0$ and $z = \infty$ and, by inserting in Eq. 4.21 we finally obtain

$$N_{B-L}(\infty) = \epsilon_1 N_{N_1}^{eq}(0). \tag{4.41}$$

Vanishing initial abundance

On the other hand, if we have zero initial N_1 abundance, i.e. $N_{N_1}(z_i) = 0$, we have to consider the opposite sign contributions to lepton asymmetry from the inverse decays when N_1 is being populated ($N_{N_1} < N_{N_1}^{eq}$) and from the period when N_1 starts decaying ($N_{N_1} > N_{N_1}^{eq}$). Therefore, in this case the efficiency factor in Eq. 4.38 is given by two contributions: k_- and k_+. In order to find these two we define z_{eq} as the time at which $N_{N_1}(z_{eq}) = N_{N_1}^{eq}(z_{eq})$, that corresponds to a maximum for the number density of N_1, see fi. (4.2). The N_{N_1} density at z_{eq} can be computed using some analytical approximations, see App. C.1.2: $N(K) \equiv N_{N_1}(z_{eq}) = (9\pi/16)K$.
For $z < z_{eq}$, we can assume $N_{N_1}^{eq} \gg N_{N_1}$. Then, the asymmetry up to z_{eq} is given by (see Apps. C.1.1 and C.1.2):

$$N_{B-L}(z_{eq}) = \epsilon_1 \int_{z_i}^{z_{eq}} dz' D(z') N_{N_1}^{eq}(z') e^{-\int_{z'}^{z_{eq}} dz'' W_{ID}(z'')} \simeq 2\epsilon_1 (1 - e^{-2/3N(K)}). \tag{4.42}$$

For $z > z_{eq}$, we can write the asymmetry as:

$$N_{B-L}(z) - N_{B-L}(z_{eq}) = -\epsilon_1 \int_{z_{eq}}^{z} dz' D(z')(N_{N_1}(z') - N_{N_1}^{eq}(z'))e^{-\int_{z'}^{z} dz'' W_{ID}(z'')} \tag{4.43}$$

$$= \epsilon_1 \int_{z_{eq}}^{z} dz' \frac{dN_{N_1}}{dz'} e^{-\int_{z'}^{z} dz'' W_{ID}(z'')} \tag{4.44}$$

$$\simeq \epsilon_1 \int_{z_{eq}}^{z} dz' \frac{dN_{N_1}}{dz'} \left(1 - \int_{z'}^{z} dz'' W_{ID}(z'')\right) \tag{4.45}$$

$$\simeq \epsilon_1 (N(K) - N_{N_1}(z)), \tag{4.46}$$

where in the last step we have neglected the negative term. Then the final asymmetry is

$$N_{B-L}(\infty) \simeq \epsilon_1 (N(K) - N_{N_1}(\infty) + 2(1 - e^{-2/3N(K)})) \simeq \epsilon_1 \frac{9\pi^2}{64} K^2 \simeq \epsilon_1 \frac{3\pi^2}{16} N_{N_1}^{eq}(0), \tag{4.47}$$

where we have used approximation in Eq. C.1 in $N_{N_1}^{eq} = 3/8z^2\mathcal{K}_2(z)$ and the fact that $N_l^{eq} = 3/4$. where we have used the fact that $N_{N_1}(\infty) = 0$ and the approximation $N(K) = (9\pi/16)K$.

4.2.3 Strong washout regime

In the strong washout regime ($K \gg 1$) any lepton asymmetry generated during the N_1 creation phase is efficiently washed out. In this regime there exists an interval $z_{in} \leqslant z \leqslant z_{max}$ where inverse decays are in equilibrium. Assuming that the wash-out are effective, any asymmetry generated before z_{in} is fully erased. Therefore, in this case there is no dependence on the initial conditions. An analytical approximation for the asymmetry for $z_{in} \leqslant z \leqslant z_{max}$ can be found by adopting the *Strong washout balance approximation* [70] which states that in the strong washout regime, the lepton asymmetry at each instant takes the value that enforces a balance between the production and the destruction rates of the asymmetry. Therefore, by equating the decay and washout terms in Eq. 4.37 we have

$$N_{B-L}(z) \simeq -\epsilon_1 D(z) \frac{1}{W_{ID}(z)} (N_{N_1} - N_{N_1}^{eq}) \simeq \frac{\epsilon_1}{W_{ID}(z)} \frac{dN_{N_1}^{eq}}{dz} \tag{4.48}$$

$$= \frac{\epsilon_1}{W_{ID}(z)} \frac{d}{dz}\left(\frac{3}{8} z^2 \mathcal{K}_2(z)\right) = \frac{2\epsilon_1}{D(z) N_{N_1}^{eq}} N_l^{eq} \frac{3}{8} z^2 \mathcal{K}_1(z) \tag{4.49}$$

$$= \frac{2\epsilon_1}{Kz} N_l^{eq}. \tag{4.50}$$

where in the second approximation we assume $N_{N_1} = N_{N_1}^{eq}$, then we have used the property of Bessel functions: $d/dz(z^\nu \mathcal{K}_\nu(z)) = -z^\nu \mathcal{K}_{\nu-1}(z)$ and the Eqs. 4.36, 4.33, 4.34, 4.27. After z_{max}, the asymmetry gets frozen so that:

$$N_{B-L}(\infty) \simeq \frac{2\epsilon_1}{K z_{max}} N_l^{eq} = \frac{2\epsilon_1}{K z_{max}} N_{N_1}^{eq}(0), \tag{4.51}$$

where we have used approximation in Eq. C.1 in $N_{N_1}^{eq} = 3/8z^2\mathcal{K}_2(z)$ and the fact that $N_l^{eq} = 3/4$. A more precise analytical approximation is given in Ref. [18] and we give basics of this in App. C.1.3.

4.3 CP asymmetry

To produce a net asymmetry in lepton flavour α, the N_1 must have L_α-violating interactions and different decay rates to final states with particles or anti-particles. The CP asymmetry in lepton flavor

α, produced in the decays of RH neutrinos N_1 is be defined as [63]:

$$\epsilon_{i\alpha} = \frac{\gamma(N_i \to L_\alpha H) - \gamma(N_i \to \bar{L}_\alpha H^*)}{\sum_\alpha \gamma(N_i \to L_\alpha H) + \gamma(N_i \to \bar{L}_\alpha H^*)} \equiv \frac{\Delta\gamma^\alpha_{N_i}}{\gamma_{N_i}}, \tag{4.52}$$

where $\gamma(i \to f)$ is the thermally averaged decay rate defined as

$$\gamma(i \to f) \equiv \int \frac{d^3p_i}{(2\pi)^3 2E_i} \frac{d^3p_f}{(2\pi)^3 2E_f} (2\pi)^4 \delta^{(4)}(p_i - p_f) |\mathcal{M}(i \to f)|^2 e^{-E_i/T}, \tag{4.53}$$

where $\mathcal{M}(i \to f)$ is the decay amplitude and we have assumed Maxwell-Boltzmann distribution for the particle i. $\bar{L}$ denotes the anti-particle of L. N_1 is a Majorana fermion, so $\bar{N}_1 = N_1$. The asymmetry $\epsilon_{\alpha\alpha}$ is normalized of the total decay rate, so that the Boltzmann Equations are linear in flavor space. When we include additional lepton generations, we find that the CP asymmetry is a diagonal element of a matrix, so we give it a double flavor index already. Ignoring all thermal effects the CP asymmetry becomes [20]:

$$\epsilon_{i\alpha} = \frac{\Gamma(N_1 \to L_\alpha H) - \Gamma(N_1 \to \overline{L_\alpha} H^*)}{\Gamma(N_1 \to L_\alpha H) + \Gamma(N_1 \to \overline{L_\alpha} H^*)}. \tag{4.54}$$

The CP asymmetry $\epsilon_{i\alpha}$ arises from the interference of tree-level $\mathcal{M}_0$ and one-loop $\mathcal{M}_1$. In fact, Eq. 4.54 vanishes at tree level but is induced at 1-loop level through this interference. Indeed, if the rates of transitions $i \to f$ are governed by some small parameter λ, so that $|\mathcal{M}(i \to f)|^2 = O(\lambda^k)$, then from Eq. (4.71) we see that any CP-violating difference $|\mathcal{M}(i \to f)|^2 - |\mathcal{M}(f \to i)|^2$ must be at least of order λ^{k+1}. Hence, CP-violating effects must arise from loop corrections to the process $i \to f$ [68].

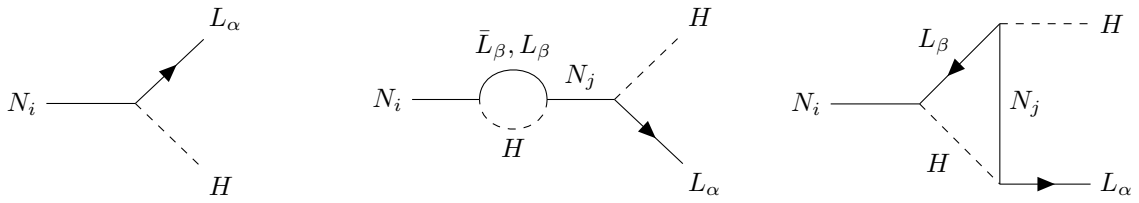

Figure 4.4: Diagrams contributing to the CP asymmetry $\epsilon_{i\alpha}$. The flavor of the internal lepton L_β is summed. The internal L_β and Higgs H are on-shell. The CP asymmetry in type-I seesaw leptogenesis results from the interference between tree and 1-loop wave and vertex diagram.

It is important to consider all the contribution from the 1-loop diagrams, namely both the self-energy, or wave-diagram (in the middle of Fig. 4.4) and the vertex diagram (on the right). The tree and loop matrix elements can each be separated into a coupling constant part c and an amplitude part $\mathcal{A}$ [20]:

$$\mathcal{M} = \mathcal{M}_0 + \mathcal{M}_1 = c_0 \mathcal{A}_0 + c_1 \mathcal{A}_1. \tag{4.55}$$

For instance, in the tree level decay (on the left of Fig. 4.4),

$$c_0 = Y^*_{\alpha 1} \qquad \mathcal{A}_0(N \to H^\dagger \overline{L_\alpha}) = \bar{u}_{L_\alpha} P_R u_N \ . \tag{4.56}$$

The matrix element for the CP conjugate process is

$$\overline{\mathcal{M}} = c_0^* \overline{\mathcal{A}_0} + c_1^* \overline{\mathcal{A}_1}, \tag{4.57}$$

where $|\overline{\mathcal{A}_i}|^2 = |\overline{\mathcal{A}_i}|^2$, since in the CP conjugate amplitude $\overline{\mathcal{A}}$, the u_L spinors are replaced by v_L spinors. However, $\bar{u}_L u_L = \not{p} = \bar{v}_L v_L$, so the squared amplitude is the same. Thus, the CP asymmetry can be written as

$$\epsilon_{i\alpha} = \frac{\int d\Pi_L d\Pi_H \tilde{\delta}|\mathcal{M}|^2 - \int d\Pi_{\bar{L}} d\Pi_{\bar{H}} \tilde{\delta}|\bar{\mathcal{M}}|^2}{\int d\Pi_L d\Pi_H \tilde{\delta}|\mathcal{M}|^2 + \int d\Pi_{\bar{L}} d\Pi_{\bar{H}} \tilde{\delta}|\bar{\mathcal{M}}|^2} \tag{4.58}$$

$$= \frac{\int |c_0\mathcal{A}_0 + c_1\mathcal{A}_1|^2 \tilde{\delta} d\Pi_{H,L} - \int |c_0^*\mathcal{A}_0 + c_1^*\mathcal{A}_1|^2 \tilde{\delta} d\Pi_{\bar{H}\bar{L}}}{2\sum_\alpha \int |c_0\mathcal{A}_0|^2 \tilde{\delta} d\Pi_{H,L}} \tag{4.59}$$

$$= \frac{\mathcal{I}m(c_0 c_1^*)}{\sum_\alpha |c_0|^2} \frac{2\int \mathcal{I}m(\mathcal{A}_0\mathcal{A}_1^*)\tilde{\delta} d\Pi_{H,L}}{\int |\mathcal{A}_0|^2 \tilde{\delta} d\Pi_{L,H}}, \tag{4.60}$$

where

$$d\Pi_l d\Pi_H = \frac{d^3p_l d^3p_H}{2E_l 2E_H} == \frac{d^3p_{\bar{l}} d^3p_{\bar{H}}}{2E_l 2E_H} = d\Pi_{\bar{l}} d\Pi_{\bar{H}}; \tag{4.61}$$

$$\tilde{\delta} = (2\pi)^4 \delta^{(4)}(P_i - P_f), \tag{4.62}$$

and p_i, p_f are, respectively, the incoming four-momentum and the outgoing four-momentum. The loop amplitude has an imaginary part when there are brunch cuts corresponding to intermediate on-shell particle (see Cutkosky Rules [71]), which can arise in the loops in Fig. 4.4 when the H and L_β are on-shell:

$$2\mathcal{I}m(\mathcal{A}_0\mathcal{A}_1^*) = \mathcal{A}_0(N \to HL_\alpha) \sum_\beta \int \mathcal{A}_0^*(N \to \bar{L'}_\beta \bar{H'}) \tilde{\delta'} d\Pi_{L'_\beta H'} \mathcal{A}_0^*(\bar{L}'_\beta \bar{H}' \to HL_\alpha). \tag{4.63}$$

Here, H' and L'_β are the intermediate on-shell particles[2], and $d\Pi_{L'_\beta H'}$ is the integration over their phase space.

4.3.1 Implications of CPT and unitarity for CP violation in decays

We can use S-matrix unitarity and CPT invariance to give some useful constraint on CP violation. Furthermore, we have already seen that the imaginary part of the loop amplitude arises when the intermediate particles are simultaneously on-shell. This contribution can be isolated by the use of the optical theorem. Useful relations, between matrix elements and their CP conjugates can be obtained form the unitarity of the S-matrix, i.e. $SS^+ = S^+S = 1$, where $S = 1 + iT$ we can write

$$1 = SS^+ = (1 + iT)(1 - iT^+) = 1 - iT^+ + iT + TT^+, \tag{4.64}$$

where T is the transition matrix defined as $\langle f|T|i\rangle \equiv (2\pi)^4\delta^4(p_i - p_f)\mathcal{M}(i \to f)$. From Eq. 4.64 we get

$$TT^+ = i(T^+ - T), \tag{4.65}$$

so

$$\langle f|T^+T|i\rangle = \langle f|i(T^+ - T)|i\rangle, \tag{4.66}$$

which becomes

$$[TT^+]_{if} = iT^*_{fi} - iT_{if}, \tag{4.67}$$

[2]Notice that we are considering these particles to be massless, since we are working in the regime where $T > T_{\rm ew}$, where $T_{\rm ew}$ stands for the temperature at electroweak phase transition.

$$i[TT^{+}]_{if} = T_{if} - T^{*}_{fi}, \tag{4.68}$$

where we have used $\langle f|T^{+}|i\rangle = \langle i|T|f\rangle^{*}$. By taking the modulus square of the last equation 4.68 we obtain [68]:

$$\begin{aligned}
|T_{if}|^2 &= |i(TT^{+})_{if} + T^{*}_{fi}|^2 \\
&= |i(\mathcal{R}e(TT^{\dagger})_{if} + i\mathcal{I}m(TT^{\dagger})_{if}) + \mathcal{R}e(T^{*}_{fi}) + i\mathcal{I}m(T_{fi})^{*}|^2 \\
&= |(\mathcal{R}e(T^{*}_{fi}) - \mathcal{I}m(TT^{\dagger}_{if}) + i(\mathcal{R}e(TT^{\dagger})_{if} + \mathcal{I}m(T^{*}_{fi}))|^2 \\
&= (\mathcal{R}e(T^{*}_{fi}) - \mathcal{I}m(TT^{\dagger}_{if})^2 + (\mathcal{R}e(TT^{\dagger})_{if} + \mathcal{I}m(T^{*}_{fi}))^2 \\
&= \mathcal{R}e(T^{*}_{fi})^2 + \mathcal{I}m(TT^{\dagger})^2_{if} - 2\mathcal{R}e(T^{*}_{fi})\mathcal{I}m(TT^{\dagger})_{if} + \\
&\quad + \mathcal{R}e(TT^{\dagger})^2_{if} + \mathcal{I}m(T^{*}_{fi})^2 + 2\mathcal{R}e(TT^{\dagger})_{if}\mathcal{I}m(T^{*}_{fi}).
\end{aligned} \tag{4.69}$$

Now we use the fact that $\mathcal{R}e(T^{*}_{fi}) = \mathcal{R}e(T_{fi})$ and $\mathcal{I}m(T^{*}_{fi}) = -\mathcal{I}m(T_{fi})$, so

$$|T_{if}|^2 = |T_{fi}|^2 + |(TT^{\dagger})_{if}|^2 - 2\mathcal{R}e(T_{fi})\mathcal{I}m(TT^{\dagger})_{if} - 2\mathcal{R}e(TT^{\dagger})_{if}\mathcal{I}m(T_{fi}), \tag{4.70}$$

using the identity $\mathcal{I}m(zy) = \mathcal{R}e(z)\mathcal{I}m(y) + \mathcal{I}m(z)\mathcal{R}e(y)$ (where z and y are complex numbers). In the end, we obtain

$$|T_{if}|^2 - |T_{fi}|^2 = |(TT^{\dagger})_{if}|^2 - 2\mathcal{I}m[(TT^{\dagger})_{if}T_{fi}]. \tag{4.71}$$

This result is related to CP asymmetry and we can see that by considering CPT invariance. Indeed, let $\mathcal{M}(i \to f)$ be the amplitude for a transition from a state i to a state f, and let $\bar{i}$ be the state obtained by applying a CP transformation to i. Then, the CPT theorem implies that [68]:

$$\mathcal{M}(i \to f) = \mathcal{M}(\bar{f} \to \bar{i}). \tag{4.72}$$

In the case of a Majorana initial state $|i\rangle$ becomes

$$\mathcal{M}(i \to f) = \mathcal{M}(\bar{f} \to i). \tag{4.73}$$

Now we have, by using CPT,

$$\begin{aligned}
|T_{if}|^2 &\simeq |\mathcal{M}(i \to f)|^2, \\
|T_{fi}|^2 &\simeq |\mathcal{M}(f \to i)|^2 = |\mathcal{M}(i \to \bar{f})|^2,
\end{aligned} \tag{4.74}$$

inserting this in the CP asymmetry parameter ϵ and using Eq. 4.71 we obtain

$$\epsilon_{i\alpha} = \frac{\int d\Pi_l d\Pi_H (2\pi)^4 \delta^{(4)}(p_N - p_H - p_l)(-2\mathcal{I}m[(TT^{\dagger})_{if}T_{fi}])}{2\sum_{\alpha}\int d\Pi_l d\Pi_H (2\pi)^4 \delta^{(4)}(p_N - p_H - p_l)|\mathcal{M}|^2}. \tag{4.75}$$

This tells us that the CP violation in a N_1 decay can first arise at 1-loop level through the interference between tree and 1-loop diagrams shown in figure 4.4. From these considerations we can proceed to the computation of the CP asymmetry $\epsilon_{i\alpha}$ in Eq. 4.75. First, we focus on the denominator, which is obtained by considering the fact that, as we have already noticed, at tree level $|\bar{\mathcal{M}}|^2 = |\mathcal{M}|^2$. Recalling that the integration over phase space gives a factor of $1/(8\pi)$ (see Eq. 4.7) and the amplitude is given in Eq. 4.9 we obtain that the denominator is

$$Den = \frac{(Y^{\dagger}Y)_{11}M^2_{N_1}}{8\pi}. \tag{4.76}$$

To compute ϵ we need to consider the wave and vertex diagram in figure 4.4 and from Eq. 4.75 we see that we need to compute the following amplitudes [72]:

$$\begin{aligned} &T_{fi} = \langle i|T|f\rangle; \\ &(TT^{+})_{if} = \sum_{k} T_{ik}T^{+}_{kf} = \sum_{k}\langle k|T|i\rangle\langle k|T^{*}|f\rangle; \end{aligned} \tag{4.77}$$

where $|k\rangle$ indicate intermediate states. To compute these amplitudes we follow [37, 71, 72] and we rewrite the Lagrangian in Eq. 2.29 as:

$$\mathcal{L}_{int} = -\sum_{i,\alpha} Y^{*}_{\alpha i}\bar{L}_{\alpha}\tilde{H}P_{R}N_{i} - Y_{\alpha i}\bar{N}_{j}P_{L}H^{\dagger}L_{\alpha} - \sum_{ij}\frac{1}{2}M_{N_{ij}}\bar{N}_{i}N_{j}, \tag{4.78}$$

where $N_i = N_{R_i} + N^{c}_{R_i}$, with $N_{R_i} = P_R N_i$ and $N^{c}_{R_i} = P_L N_i$. At this point we can compute the contribution to the CP asymmetry in the numerator of Eq. 4.75 which is given by the interference between the tree level and the one loop diagrams in Fig. 4.4. The details of the computations are given in App. D. The total contribution is given by:

$$\begin{aligned} \epsilon_{i\alpha} =& \frac{1}{8\pi}\sum_{j\neq i}\frac{\mathcal{I}m((Y^{\dagger}Y)_{ji}Y_{\alpha i}Y^{*}_{\alpha j})}{(Y^{\dagger}Y)_{ii}}\sqrt{x}g \\ &+\frac{1}{8\pi}\sum_{j\neq i}\frac{M_i}{M_i^2 - M_j^2}\frac{\mathcal{I}m((M_i(Y^{\dagger}Y)_{ij} + M_j(Y^{\dagger}Y)_{ji})Y^{*}_{\alpha j}Y_{\alpha i})}{(Y^{\dagger}Y)_{ii}}, \end{aligned} \tag{4.79}$$

where $x = M_j^2/M_i^2$ and $g = 1 - (1+x)\log\left(1 + \frac{1}{x}\right)$. The first term in Eq. 4.79 comes from L-violating wave and vertex diagrams, while the second is from the L-conserving wave diagram. From the $\epsilon_{i\alpha}$ expression we can immediately notice that the terms of the form $(M_i^2 - M_j^2)^{-1}$ are from the wave diagram contributions which can resonantly enhance the CP asymmetry if $M_i \simeq M_j$. We will further explore this case in Sec. 4.5. Let us also note that at least two RHNs are needed, otherwise the CP asymmetry vanishes because the Yukawa couplings combination becomes real. In the one flavor regime, we sum over the flavor index α in Eq. 4.79 and we obtain

$$\epsilon_i \equiv \sum_{\alpha}\epsilon_{i\alpha} = \frac{1}{8\pi}\frac{1}{(Y^{\dagger}Y)_{ii}}\sum_{i\neq j}\mathcal{I}m[(Y^{\dagger}Y)^{2}_{ji}]g\left(\frac{M_j^2}{M_i^2}\right), \tag{4.80}$$

where the second term in Eq. 4.79 vanishes because the combination of the Yukawa couplings is real.

4.3.2 Baryon asymmetry from EW sphaleron

The final lepton asymmetry can be conveniently parametrized as follows[3]

$$Y_{\Delta L}(\infty) = \epsilon_1 k_f Y^{eq}_{N_1}, \tag{4.81}$$

where k_f is the efficiency factor. If leptogenesis ends before EW sphaleron process become active, i.e. for $T \gtrsim 10^{12}$ GeV, the $B-L$ asymmetry $Y_{\Delta B-L}$ is simply given by

$$Y_{\Delta B-L} = -Y_{\Delta L}. \tag{4.82}$$

[3]Here we use the Yields which are obtained by normalizing the particle number density by the entropy density $s = g_*(2\pi^2/45)T^3$, and not by the the comoving volume $a(t_*)^3$ as we did in the previous sections.

At later stage, the $B-L$ asymmetry is partially transferred to a B asymmetry by the EW sphaleron processes trough the relation in Eq. 3.31:

$$Y_{\Delta B}(\infty) = \frac{28}{79} Y_{\Delta B-L}(\infty), \tag{4.83}$$

that holds if the sphalerons decouple before EWPT [73].

4.3.3 Davidson-Ibarra Bound

Assuming a hierarchical spectrum of the RH neutrinos ($M_1 \ll M_2, M_3$) and that the dominant lepton asymmetry is from the N_1 decays, the CP asymmetry can be written from Eq. 4.80 as

$$\epsilon_1 = -\frac{3}{16\pi} \frac{1}{(Y^\dagger Y)_{11}} \sum_{j\neq 1} \mathcal{I}m[(Y^\dagger Y)^2_{j1}] \frac{M_i}{M_j}. \tag{4.84}$$

Assuming three generations of RH neutrinos and using the Casas-Ibarra parametrization (see Sec. 2.4.1), Eq. 4.84 becomes

$$\epsilon_1 = -\frac{3}{16\pi} \frac{M_1}{v^2} \frac{\sum_i m_{\nu_i} \mathcal{I}m(R^2_{1i})}{\sum_i m_{\nu_i} |R_{1i}|^2}. \tag{4.85}$$

Using the orthogonality condition for the matrix R, i.e. $\sum_i R^2_{1i} = 1$, we then obtain the so called Davidson-Ibarra (DI) bound [23]:

$$|\epsilon_1| \leqslant \epsilon_1^{DI} = \frac{3}{16\pi} \frac{M_1}{v^2} (m_{\nu_3} - m_{\nu_1}) = \frac{3}{16\pi} \frac{M_1}{v^2} \frac{\Delta m^2_{atm}}{m_{\nu_1} + m_{\nu_3}}, \tag{4.86}$$

where m_{ν_3} (m_{ν_1}) is the heaviest (lightest) light neutrino mass. Applying the DI bound on Eqs. 4.81-4.83, and requiring that $Y_{\Delta B}(\infty) \geqslant Y_B^{CMB} \simeq 10^{-10}$, we obtain

$$M_1 \left(\frac{0.1 \text{ eV}}{m_{\nu_1} + m_{\nu_3}} \right) k_f^{max}(M_1) \gtrsim 10^9 \text{ GeV}, \tag{4.87}$$

where the $k_f^{max}(M_1)$ is the efficiency factor maximized with respect to K_1 for a particular value of M_1. This allows to find bounds on M_1 and m_{ν_1}. Many numerical studies have been carried out and it was found that succesful leptogenesis with a hierarchical spectrum of the *RH* neutrinos requires $M_1 > 10^9$ GeV and $m_{\nu_1} < 0.1$ eV [63]. This bound implies that the RH neutrinos must be produced at temperatures $T \gtrsim 10^9$ GeV. However, it is important to stress out that the DI bound holds if and only if all the following conditions apply:

- N_1 dominates the contribution to leptogenesis;
- The mass spectrum of RH neutrinos are hierarchical $M_1 \ll M_2, M_3$;
- Leptogenesis occurs in the unflavored regime $T \gtrsim 10^{12}$ GeV.

Therefore, the violation of one of these conditions allows us to lower the scale of leptogenesis.

4.4 Flavour Effects

So far we have discussed leptogenesis in the single lepton flavor regime. This amounts to assuming that the leptons and antileptons which couple to the lightest RH neutrino N_1 maintain their coherence as flavor superpositions throughout the leptogenesis era. This assumption proves to describe the correct final asymmetry only for masses $M_1 \gtrsim 10^{13}$ GeV [74]. In this range of masses the lepton and anti-lepton quantum states produced from the decays of the N_1 can be treated, in flavour space, as pure states between their production at decay and their absorption at a subsequent inverse decay. That is, they can be expressed as a linear combination of flavor eigenstates ($\alpha = e, \mu, \tau$):

$$|l_1\rangle = \sum_\alpha \mathcal{C}_{1\alpha}|l_\alpha\rangle \qquad |\bar{l}_1\rangle = \sum_\alpha \bar{\mathcal{C}}^*_{1\alpha}|\bar{l}_\alpha\rangle, \tag{4.88}$$

with the coefficients $\mathcal{C}_{1\alpha}$ and $\bar{\mathcal{C}}_{1\alpha}$ at tree level given by

$$\mathcal{C}_{1\alpha} = \bar{\mathcal{C}}_{1\alpha} = \frac{Y_{1\alpha}}{\sqrt{(Y^\dagger Y)_{11}}} \tag{4.89}$$

However, since CP is violated by loops, beyond the tree-level approximation the antilepton state $\bar{l}_1$ is not the CP conjugate of the l_1, i.e. $\bar{\mathcal{C}}_{1\alpha} \neq \mathcal{C}_{1\alpha}$. The single flavor regime is realized only at very high temperatures ($T > 10^{12}$ GeV), when both $|l_1\rangle$ and $|\bar{l}_1\rangle$ remain coherent flavor superpositions, and thus are the correct states to describe the dynamics of leptogenesis. This occurs because at high temperatures the lepton-Higgs interactions in the thermal plasma can be neglected. However, at lower temperatures, scatterings induced by the charged lepton Yukawa couplings are sufficiently fast to distinguish the different lepton flavors, $|l_1\rangle$ and $|\bar{l}_1\rangle$ decohere in their flavor components and each flavor state experiences a different time evolution, hence the dynamics of leptogenesis must then be described in terms of the flavor eigenstates l_α [63]. Lepton flavour effects have been studied in [67, 75, 76].
The specific temperature when leptogenesis becomes sensitive to lepton flavor dynamics can be estimated by requiring that the rates of processes Γ_α ($\alpha = e, \mu, \tau$) that are induced by the charged lepton Yukawa couplings h_α become faster than the universe expansion rate $H(T)$. An approximate relation gives [77]:

$$\Gamma_\alpha(T) \simeq 10^{-2} h_\alpha^2 T, \tag{4.90}$$

implying that $\Gamma_\alpha(T) > H(T)$ when $T \lesssim T\alpha$, where $T_e \simeq 4 \times 10^4$ GeV, $T_\mu \simeq 2 \times 10^9$ GeV and $T_\tau \simeq 5 \times 10^{11}$ GeV. From these estimates we see that as the mass scale of Leptogenesis is lowered to $M_1 \sim 10^{12}$ GeV, the single-flavor approximation becomes inaccurate since the SM τ-Yukawa interactions enter in thermal equilibrium. In the same way we can distinguish the two-flavor regime for temperatures 10^9 GeV $\ll T \ll 10^{12}$ GeV, when the τ-Yukawa interactions are in thermal equilibrium while that of muons are not, i.e. $\Gamma_\tau/H \gg 1$ and $\Gamma_\mu/H \ll 1$. Finally, for temperatures $T \ll 10^9$ GeV, also the μ-Yukawa interactions are in thermal equilibrium and all flavors are distinguishable, the coherent superposition in $|l_1\rangle$ and $|\bar{l}_1\rangle$ is destroyed and each flavored asymmetry evolves separately. Therefore, it is necessary to consider also flavor effects if we want to study leptogenesis at scale $T < 10^{12}$ GeV.

4.4.1 The effects on CP asymmetry and washout

The CP violation in N_i decay can manifest itself in two ways:

- The leptons and antileptons are produced at different rates,

$$\gamma_i \neq \bar{\gamma}_i, \tag{4.91}$$

  where $\gamma_i \equiv \gamma(N_i \to l_I H)$ and $\bar{\gamma}_i \equiv \gamma(N_i \to \bar{l}'_i H^*)$.

- The leptons and antileptons produced are not CP conjugate states,

$$\mathrm{CP}(\bar{l}'_i) = l'_i \neq l_i, \tag{4.92}$$

that is, due to loops effects they are slightly misaligned in flavor space.

We can rewrite the CP asymmetry for N_i decays from Eq. 4.52 as follows [63]:

$$\epsilon_{i\alpha} = \frac{P_{i\alpha}\gamma_i - \bar{P}_{i\alpha}\bar{\gamma}_i}{\gamma_i + \bar{\gamma}_i} = \frac{P_{i\alpha} + \bar{P}_{i\alpha}}{2}\epsilon_i + \frac{P_{i\alpha} - \bar{P}_{i\alpha}}{2} \simeq P^0_{i\alpha}\epsilon_i + \frac{\Delta P_{i\alpha}}{2}, \tag{4.93}$$

where terms of order $\mathcal{O}(\epsilon_i \Delta P_{i\alpha})$ and higher have been neglected. $P_{i\alpha}$ is the projector from state L_i into state L_α, and $\Delta P_{i\alpha} = P_{i\alpha} - \bar{P}_{i\alpha}$. At tree level, $P_{i\alpha} = \bar{P}_{i\alpha} \equiv P^0_{i\alpha}$ where the tree level flavor projector is given by

$$P^0_{i\alpha} = \frac{Y_{\alpha i} Y^*_{\alpha i}}{(Y^\dagger Y)_{ii}}. \tag{4.94}$$

From Eq. 4.93 we can see that the first term corresponds to the first type (Eq. 4.91), while the second being of the other type (Eq. 4.92). Since $\sum_\alpha P_{i\alpha} = \sum_\alpha \bar{P}_{i\alpha} = 1$, when summing over flavor indices α, the second term vanishes $\sum_\alpha \Delta P_{i\alpha} = 0$. It is important to notice that, due to flavor misalignment, the CP asymmetry in a particular flavor direction $\epsilon_{i\alpha}$ can be much larger and even of opposite sign from the total CP asymmetry ϵ_i. Actually, the relevance of CP violation of the second type in the flavor regimes is what allows to evade the DI bound. As regard the washout of the lepton asymmetry of flavor α, it is proportional to

$$W_{i\alpha} \propto P_{i\alpha}\gamma_i + \bar{P}_{i\alpha}\bar{\gamma}_i \simeq P^0_{i\alpha} W_i, \tag{4.95}$$

which results in a reduction of washout by a factor of $P^{\leqslant}_{i\alpha} 1$ compared to unflavored case.

4.4.2 Classical flavored Boltzmann Equations

We consider again the case of leptogenesis from the decays and inverse decays of N_1. In this approximation, the BE for the number density of the RHNs is still given by Eq. 4.36, while the BE for $N_{\Delta L_\alpha}$ the lepton asymmetry in the flavor α is given by

$$\frac{dN_{\Delta L_\alpha}}{dz} = \epsilon_{1\alpha} D_1 (N_{N_1} - N^{eq}_{N_1}) - P^0_{1\alpha} W_1 N_{\Delta L_\alpha}. \tag{4.96}$$

Here we are not using a density matrix formalism since we are not interested in the transition between different flavor regimes. As long as L violation from sphalerons is neglected, the BE for $N_{\Delta L_\alpha}$ are independent of each other, and the solutions for the weak and strong washout regimes are given, respectively, by Eqs. 4.47 and 4.51, after replacing $\epsilon_1 \to \epsilon_{1\alpha}$ and $K \to K_{1\alpha} \equiv P^0_{1\alpha} K$.
As an example, we assume leptogenesis at $T \sim 10^{10}$ GeV, that is in the two flavor regime. In this regime, interactions with τ leptons in thermal bath destroy the coherence of the lepton state produced in N_1 decay. Due to fast τ Yukawa interactions l_1 ($\bar{l}_1$) gets projected onto l_τ ($\bar{l}_\tau$) and a coherent mixture of $e + \mu$ eigenstates $l_{e+\mu}$ ($\bar{l}_{e+\mu}$). Hence, one has to consider Boltzmann equations for the components parallel and orthogonal to τ separately [66, 74]. With

$$P_\tau = |\mathcal{C}_{1\tau}|^2, \quad P_{\tau^\perp} = 1 - |\mathcal{C}_{1\tau}|^2 = |\mathcal{C}_{1e}|^2 + |\mathcal{C}_{1\mu}|^2, \quad \langle \tau | \tau^\perp \rangle = 0, \tag{4.97}$$

one obtains

$$\begin{aligned}\frac{dN_N}{dz} &= -D(N_N - N_N^{eq}),\\ \frac{dN_{\tau\tau}}{dz} &= \epsilon_{\tau\tau} D(N_N - N_N^{eq}) - P^0_\tau W N_{\tau\tau},\\ \frac{dN_{\tau^\perp\tau^\perp}}{dz} &= \epsilon_{\tau^\perp\tau^\perp} D(N_N - N_N^{eq}) - P^0_{\tau^\perp} W N_{\tau^\perp\tau^\perp},\end{aligned} \tag{4.98}$$

where $N_{\tau\tau}$ and $N_{\tau^\perp\tau^\perp}$ are respectively the values of the asymmetries in the charges $B/3 - L_\tau$ and $2B/3 - L_{\tau^\perp}$ in a comoving volume. For illustrative purpose, here we consider a scenario in which lepton flavor effects are most prominent. We take both $K_{1\tau}, K_{1e+\mu} \gg 1$, so that both $N_{\tau\tau}$ and $N_{\tau^\perp\tau^\perp}$ are in the strong regime (see Ref. [74] for further details on flavor effects). Then, from Eq. 4.51 we can write down the solution for the produced $B - L$ asymmetry

$$\begin{aligned}N_{B-L}(\infty) &= N_{\tau\tau}(\infty) + N_{\tau^\perp\tau^\perp}(\infty)\\ &= \frac{2}{K_1 z_{max}} N^{eq}_{N_1}(0)\left(\frac{\epsilon_{\tau\tau}}{P^0_{\tau\tau}} + \frac{\epsilon^0_{\tau^\perp\tau^\perp}}{P_{\tau^\perp\tau^\perp}}\right)\\ &\simeq \frac{4\epsilon_1}{K_1 z_{max}} N^{eq}_{N_1}(0) + \frac{1}{K_1 z_{max}} N^{eq}_{N_1}(0)\left(\frac{\Delta P_{1\tau}}{P_{1\tau^0}} + \frac{\Delta P_{1\tau^\perp}}{P^0_{1\tau^\perp}}\right),\end{aligned} \tag{4.99}$$

where in the ast line we have used Eq. 4.93 For temperatures far below T_τ all three lepton flavors have to be taken into account. If $P^0_{1\tau} \simeq P^0_{\tau^\perp}$, then, since $\Delta P_{1\tau} + \Delta P_{1\tau^\perp} = 0$ the second term approximately cancels, and Eq. 4.99 reduces to

$$N_{B-L}(\infty) \simeq \frac{4\epsilon_1}{K_1 z_{max}} N^{eq}_{N_1}(0). \tag{4.100}$$

This approximated expression shows how, compared to the expression obtained in the unflavoured case, large lepton flavour effects can arise only when leptons and anti-leptons have a different flavour composition. If there exists some hierarchy between the flavor projectors, then the second term in Eq. 4.99 plays an important role and can further enhance the asymmetry.

4.5 Resonant Leptogenesis

So far we have considered the case in which we have assumed that $M_{2,3} \gg M_1$. Therefore, we have neglected the effects of $N_{2,3}$ since either $T_{RH} < M_{2,3}$ or N_2, N_3 decouple when N_1 is still in thermal equilibrium. In this section we instead consider the case in which the mass difference between two heavy RHNs species is small, i.e. $M_i \simeq M_j$ (quasi-degeneracy) and is of the order of the decay widths Γ_D. Such a scenario is called "Resonant leptogenesis", see Ref. [25] for a review. This scenario is important since, as we shall see, it leads to a resonant enhancement of the CP asymmetry and, consequently, in this case leptogenesis temperatures of the order of TeV are possible. Also, it is useful to analyze the resonant leptogenesis regime since we will consider small masses for Majorana neutrinos in the ARS scenario in Chapt. 5, which is mainly based on flavor effects and resonant leptogenesis.
The resonant effect is related to the self-energy contribution to the CP asymmetry, i.e. from the wave diagram in Fig. 4.4. In fact, from Eq. 4.79 we see that the self energy contribution is proportional to $M_i/(M_i^2 - M_j^2)$, and, for small mass differences, $|M_i - M_j| \ll \frac{1}{2}(M_i + M_j)$, the CP is dominated by this term. We consider, for simplicity, the case where only N_2 is quasi-degenerate with N_1, i.e. $M_1 \simeq M_2$. Then, a resummation of self-energy effects, namely a resummation of the propagators around their poles, is necessary to solve the singularity arising from the self-energy contribution involving N_2 as an

intermediate state in Eq. 4.79. In resummed perturbation theory one computes the decay rates of heavy neutrinos N_α to leptons l and the Higgs boson: $\Gamma_{\alpha l} \to \Gamma(N_\alpha \to lH)$, $\Gamma^C_{\alpha l} = \Gamma(N_\alpha \to \bar{l}H^*)$, in terms of resummed Yukawa couplings $\bar{h}^\nu_{l\alpha}$ [25]. The CP asymmetries are defined as usual:

$$\epsilon_{\alpha l} \equiv \frac{\Gamma_{\alpha l} - \Gamma^C_{\alpha l}}{\sum_{l=e,\mu,\tau}(\Gamma_{\alpha l} + \Gamma^C_{\alpha l})} = \frac{|\bar{h}^\nu_{\alpha l}|^2 - |\bar{h}^{\nu C}_{l\alpha}|^2}{(\bar{h}^{\nu\dagger}\bar{h}^\nu)_{\alpha\alpha} + (\bar{h}^{\nu C\dagger}\bar{h}^{\nu C})_{\alpha\alpha}}. \tag{4.101}$$

For quasi-degenerate heavy neutrinos the decay rates show the typical resonant enhancement, and for two heavy neutrinos the CP asymmetry parameter ϵ can be expressed as [20, 25, 66]:

$$\epsilon_{\alpha l} \simeq \frac{\mathcal{I}m[(h^{\nu\dagger}_{\alpha l}h^\nu_{l\beta})(h^{\nu\dagger}h^\nu)_{\alpha\beta}]}{(h^{\nu\dagger}h^\nu)_{\alpha\alpha}(h^{\nu\dagger}h^\nu)_{\beta\beta}} \frac{(m^2_{N_\alpha} - m^2_{N_\beta})m_{N_\alpha}\Gamma^{(0)}_{N_\beta}}{(m^2_{N_\alpha} - m^2_{N_\beta})^2 + m^2_{N_\alpha}\Gamma^{(0)2}_{N_\beta}}, \tag{4.102}$$

where $\Gamma^{(0)}_{N_\beta}$ are the tree-level decay widths of the heavy RHN, obtained analogously to Eq. 4.11. In finite-order perturbation theory, the absorptive term $m^2_{N_\alpha}\Gamma^{(0)2}_{N_\beta}$ that occurs in the last denominator on the r.h.s. of Eq. 4.102 is absent, thereby leading to a singular behaviour for $\epsilon_{\alpha l}$ in the mass-degenerate limit $m_{N_\alpha} \to m_{N_\beta}$. However, the appearance of this regulating absorptive term due to the finite width of the heavy Majorana neutrinos should be expected on physical grounds and emerges naturally within the resummation approach [25]. By neglecting flavor effects and considering only N_1 and N_2 we obtain:

$$\epsilon_1 \simeq -\frac{M_1}{M_2}\frac{\Gamma_2}{M_2}\frac{M_2^2\Delta M^2_{21}}{(\Delta M^2_{21})^2 + M_1^2\Gamma_2^2}\frac{\mathcal{I}m[(h^{\nu\dagger}h^\nu)^2_{12}]}{(h^{\nu\dagger}h^\nu)_{11}(h^{\nu\dagger}h^\nu)_{22}}, \tag{4.103}$$

where $\Delta M^2_{21} = M_2^2 - M_1^2$. The resonance condition reads [26]

$$M_2^2 - M_1^2 \simeq M_1\Gamma_2. \tag{4.104}$$

In this case,

$$|\epsilon_1| \simeq \frac{1}{2}\frac{|\mathcal{I}m[(h^{\nu\dagger}h^\nu)^2_{12}]}{(h^{\nu\dagger}h^\nu)_{11}(h^{\nu\dagger}h^\nu)_{22}}. \tag{4.105}$$

The magnitude of the CP asymmetry is governed by the expression

$$\frac{|\mathcal{I}m[(h^{\nu\dagger}h^\nu)^2_{12}]}{|h_{11}|^2|h_{22}|^2} \leqslant 1. \tag{4.106}$$

Thus, in the resonant case, the asymmetry is suppressed by neither the smallness of the light neutrino masses, nor the smallness of their mass splitting, nor small ratios between the singlet neutrino masses. Actually, the CP asymmetry could be of order one, if we consider the maximal case of CP violation in Eq. 4.106 [20]. Therefore, in the framework of resonant leptogenesis, we are able to increase the value of the CP asymmetry by tuning the mass degeneracy between RHNs masses. Therefore, resonant leptogenesis allowas to obtain the observed amount of baryon asymmetry, even by considering small Majorana masses. The price of this mechanism is to require a considerable fine-tuning of the masses.

Chapter 5

ARS Leptogenesis

So far we have considered standard scenarios where leptogenesis takes place during the freeze-out of some heavy states that can decay violating charge-parity CP and lepton number L. This model involves a very high scale of new physics, much higher than the electroweak scale, since it requires RHNs masses M_N to be $M_N \gg v_{\rm ew}$. Akhmedov, Rubakov and Smirnov [27] (ARS) studied the possibility to generate a baryon asymmetry in type I seesaw models at a much lower scale, $M_N \ll v_{\rm ew}$. They suggested that asymmetries in lepton numbers were generated due to oscillations of singlet neutrinos and their interaction with ordinary matter in the early universe. In this scenario, the asymmetry is not produced in the decays of RHNs, but instead while the RHNs are produced and approach equilibrium in the early universe; hence ARS leptogenesis is a freeze-in scenario. In fact, in this low-scale scenario the Yukawa couplings could be small enough to ensure that some of the sterile states might not reach thermal equilibrium before the electroweak phase transition, when sphaleron processes are switched off. The RHNs produced via the SM interactions are generated in their interaction basis, which does not necessarily coincide with their mass basis. Due to this misalignment, the sterile neutrinos oscillate and they generate the asymmetry through these CP violating oscillations. The novel feature of this scenario is that the total lepton number is not violated in these processes, in fact, the important ingredient is separation rather than generation of lepton number, i.e. its redistribution between different species of singlet neutrinos. Lepton-number violating (LNV) processes may be negligible both in the generation of the asymmetries and in the washout as long as Majorana mass of the RHN is small compared to the temperature. Therefore, the initial asymmetries in active leptons are purely flavored and lepton-number conserving (LNC). If this situation survives until the electroweak phase transition, a net baryon asymmetry results, since the eventual equilibration later on can no longer be transmitted to the baryons in absence of effective sphaleron transitions [29, 78, 79]. In the following, we will first describe the ARS mechanism model. Then, we will derive the quantum kinetic equations, first by considering only the LNC processes, valid in the regime $M_N \ll T$, and then we will add the LNV corrections, in order to have the general kinetic equations valid for all regions of the parameter space.

5.1 Model overview

In this section, mainly based on [80], we will provide a detailed description of the ARS leptogenesis model. The model involves the simplest extension of the SM with n_R heavy Majorana singlets

$$\mathcal{L} = \mathcal{L}_{\rm SM} + \bar{N}_{RI} i \not{\partial} N_{RI} - \left(\frac{1}{2} (M_N)_{JI} \bar{N}^c_{RJ} N_{RI} + F_{\alpha k} \bar{L}_\alpha H^c N_{RI} + \text{h.c.} \right), \tag{5.1}$$

where N_{Rk} are the right-handed components of N_k (such that $P_R N_k = N_R$), F is a $3 \times n_R$ Yukawa complex matrix, M_N is a n_R-dimensional complex symmetric matrix, L_α is the SM lepton doublet of flavour α, H the Higgs doublet and $H^c = \epsilon H^*$. When the Higgs doublet develops a VEV, i.e. $\langle H \rangle \neq 0$, these interactions generate a small mass for the active neutrinos through the seesaw mechanism, see Eq. 2.33. Choosing a scalar vev around the electroweak scale $\langle H \rangle \sim 100$ GeV, sterile-neutrino masses around the GeV scale and small Yukawa couplings $F \sim 10^{-7} - 10^{-8}$ we obtain

$$m_\nu \sim 0.1 \text{ eV} \left(\frac{\langle H \rangle}{100 \text{ GeV}} \right)^2 \left(\frac{F}{10^{-7}} \right)^2 \left(\frac{\text{GeV}}{M_N} \right). \tag{5.2}$$

Such small Yukawa couplings between LH leptons and sterile neutrinos, active-sterile neutrino is out of equilibrium in the early universe and does not become rapid until $T \lesssim T_{\text{ew}}$, where $T_{\text{ew}} \sim 140$ GeV is the temperature of sphaleron freeze-out. If there is a negligible concentration of sterile neutrinos immediately following inflation, then the sterile-neutrino abundance remains below its equilibrium value until it re-thermalizes at $T \lesssim T_{\text{ew}}$. As we have already seen, sphaleron processes are active for $T > T_{\text{ew}}$ and violate baryon number B, but preserve $B - L$, processing the primordial lepton asymmetry into a baryon asymmetry.

Sakharov Conditions for ARS Leptogenesis

The Sakharov conditions are satisfied in this model:

- **Violation of the SM lepton number L:** The Yukawa coupling F in Eq. 5.1 preserves a generalized lepton number $L - N$ under which both SM and sterile neutrinos are charged. The $L - N$ symmetry is broken by the sterile neutrino Majorana mass, but rates $(L - N)$-violating processes are suppressed by a factor of M_N^2/T^2 relative to $(L-N)$-preserving rates, and so total lepton number violation is generally ineffective for $T \gtrsim T_{\text{ew}}$. However, scattering processes $L_\alpha \to N_I^\dagger$ through the Yukawa interactions violate SM lepton number, allowing the creation of equal asymmetries in L and N such that $L - N$ is still conserved. Sphalerons then convert the SM L asymmetry into a baryon one.

- **CP violation**: There are three CP phases in the Yukawa couplings $F_{\alpha I}$. These provide a sufficient source for leptogenesis through neutrino oscillations.

- **Departure from thermal equilibrium:** If $M_N \ll T_{\text{ew}}$, sterile neutrino scatterings are out of equilibrium provided there is no abundance of sterile neutrinos in the earliest times following inflation. In this model equilibration occurs only after the sphalerons freeze-out at T_{ew}.

Since the three Sakharov conditions are satisfied we can proceed to examine which are the physical processes responsible for leptogenesis. Immediately following inflation there is no sterile neutrinos abundance and the sterile sector starts being populated by out-of-equilibrium scatterings mediated by the Yukawa couplings F, as shown on the left side of Fig. 5.1. The production mechanism of singlet neutrinos conserves CP, i.e. for each type equal numbers of particles and antiparticles (particles of opposite helicities, since we are in the Majorana case) are produced [27]. Sterile neutrinos are produced in flavor combinations that get modified in propagation, because they are a superposition of the mass eigenstates. Moreover, the sterile neutrinos remain coherent as long as the active-sterile Yukawa coupling remains out of equilibrium, since in this minimal model there are no other interactions involving the sterile neutrinos. Note that none of these processes violates the total lepton number $L_{tot} = \sum_i L_i$, where i denotes the types of Majorana neutrinos $i = 1, 2, 3$. However, CP is not conserved due to mixing in the singlet neutrino sector. Therefore the initially created state with individual lepton numbers

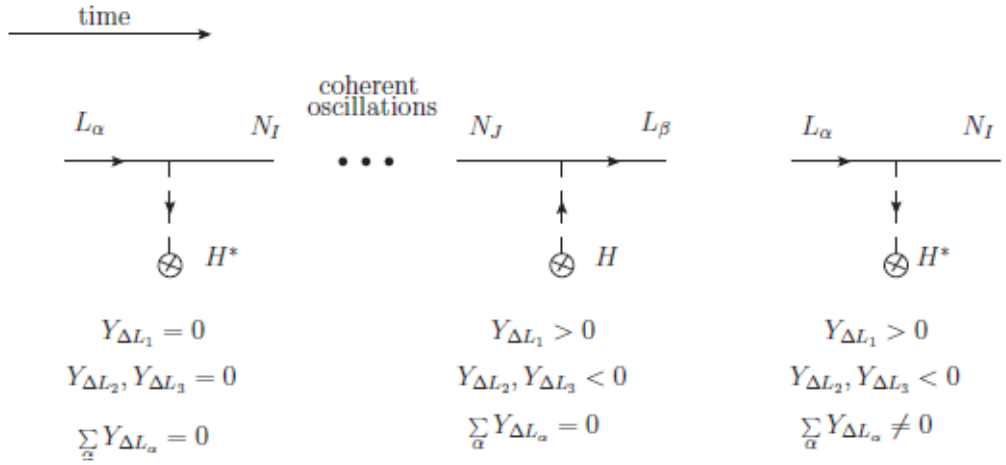

Figure 5.1: The basic stages leading to the generation of a total lepton asymmetry from left to right: Out of equilibrium scattering of LH leptons begin to populate the sterile neutrino abundance at order $\mathcal{O}(|F|^2)$; after some time of coherent oscillations, a small fraction of the sterile neutrinos scatter back into LH leptons and create an asymmetry in individual lepton flavours at order $\mathcal{O}(|F|^4)$. Finally, at order $\mathcal{O}(|F|^6)$, a total lepton asymmetry is generated due to a difference in scattering rate into sterile neutrinos among the different active flavours. Figure taken from Ref. [80].

$L_1 = L_2 = L_3 = 0$ evolves through the oscillations into a state in which $L_1 \neq 0$, $L_2 \neq 0$, $L_3 \neq 0$, but still $L_{tot} = 0$. Therefore, the total lepton number gets unevenly distributed between different species of sterile neutrinos. Some time later, sterile neutrinos communicate their lepton asymmetry to ordinary neutrinos and charged leptons through their Yukawa couplings. In fact, a subset of sterile neutrinos scatter back into LH leptons, mediating $L_\alpha \to L_\beta$ transitions, as shown in the center of Fig. 5.1. Since the sterile neutrinos remain in a coherent superposition in the intermediate time between scatterings, the transition rate $L_\alpha \to L_\beta$ includes an interference between propagation mediated by the different sterile neutrino mass eigenstates. The different mass eigenstates have different phases resulting from time evolution; for sterile neutrinos N_I and N_J, the relative phase accumulated during a small time dt is $e^{-i(\omega_I - \omega_J)dt}$, where (see Subsec. 2.2.1):

$$\omega_I - \omega_J \sim \frac{(M_N)_I^2 - (M_N)_J^2}{2T} \equiv \frac{(M_N)_{IJ}^2}{2T}. \tag{5.3}$$

In the interaction basis, this CP-even phase results from an oscillation between different sterile neutrino flavours. When combined with the CP-odd phases from the Yukawa matrix $F_{\alpha I}$, neutrino oscillations lead to a difference between the $L_\alpha \to L_\beta$ rate and its complex conjugate [80]:

$$\Gamma(L_\alpha \to L_\beta) - \Gamma(L_\alpha^\dagger \to L_\beta^\dagger) \propto \sum_{I \neq J} \mathrm{Im}\left[\exp\left(-i \int_0^t \frac{M_{IJ}^2}{2T(t')} dt' \right) \right] \times \mathrm{Im}(F_{\alpha I} F_{\beta I}^* F_{\alpha J}^* F_{\beta J}). \tag{5.4}$$

In absence of efficient washout interactions, which is ensured by the out-of-equilibrium condition, this difference in rates creates asymmetries in the individual LH lepton flavours L_α. Denoting the individual LH flavour abundances by $Y_{L_\alpha} \equiv n_{L_\alpha}/s$, where s is the entropy density, and the asymmetries by $Y_{\Delta L_\alpha} \equiv Y_{L_\alpha} - Y_{L_\alpha^\dagger}$, we note that the processes of order $\mathcal{O}(|F|^4)$ only convert L_α into L_β, conserving

the overall SM lepton number, i.e.

$$Y_{\Delta L_{tot}} = \sum_{\alpha} Y_{\Delta L_\alpha} = 0 \qquad \text{at } \mathcal{O}(|F|^4). \tag{5.5}$$

Therefore, at this level no net baryon asymmetry is generated $Y_{\Delta B_{tot}} = 0$, since sphalerons couple to the total SM lepton number. However, the total lepton asymmetry is generated at order $\mathcal{O}(|F|)^6$: the excess in each individual LH lepton flavour due to the asymmetry from Eq. 5.4 leads to a slight increase of the rate of $L_\alpha \to N^\dagger$ vs. $L_\alpha^\dagger \to N$. The result is that active-sterile lepton scatterings can convert individual lepton flavour asymmetries into asymmetries in the sterile neutrinos. But, since the rates of conversion, $\Gamma(L_\alpha \to N^\dagger)$, are generically different for each lepton flavour α, this leads to a depletion of some of the individual lepton asymmetries at a faster rate than others, leading to an overall SM lepton asymmetry and an overall neutrino asymmetry. Because $L_{tot} - N$ is conserved for $T \gg m_N$, this gives

$$\frac{dY_{\Delta N_{tot}}}{dt} = \frac{dY_{\Delta L_{tot}}}{dt} = \sum_{\alpha, I} Y_{\Delta L_\alpha} \Gamma(L_\alpha \to N_I^\dagger). \tag{5.6}$$

Therefore, while the sum of the LH lepton flavour asymmetries vanishes at $\mathcal{O}(|F|^4)$ as in Eq. 5.5, the fact that the LH leptons scatter at different rates into the sterile sector results in a non-vanishing total lepton asymmetry at $\mathcal{O}(|F|^6)$. Two scales are therefore relevant in the generation of the asymmetry: the time when the oscillation rate is similar to the Hubble expansion (oscillation time), and the equilibration time when the scattering rate is of the order of the Hubble expansion. First, we consider the oscillation time. In absence of a sterile-neutrino mass splitting, the sterile-neutrino masses and couplings can be simultaneously diagonalized, and there is no coherent oscillation. The size of the mass splitting dictates the time scale at which the phases of the coherently evolving sterile neutrino eigenstates become substantially different. From Eq. 5.4 and the Hubble parameter in a radiation-dominated universe:

$$H = \frac{1.66\sqrt{g_*}T^2}{M_{\rm Pl}}, \tag{5.7}$$

we have an $\mathcal{O}(1)$ phase from oscillation at

$$t_{\rm osc} \propto (\Delta M_{N_{IJ}}^2 M_0)^{-1/3}, \tag{5.8}$$

where $M_0 \equiv M_{\rm Pl}/1.66\sqrt{g_*}$. From the probability of oscillation in Eq. 2.12 we see that the frequency of oscillation is $\propto 1/L_{\rm osc} = \Delta m_{ij}^2/2E$ (where we have used natural units). By comparing the oscillation frequency with the Hubble parameter and by requiring $\Gamma_{\rm osc} \simeq H$ we obtain Eq. 5.8. From Eq. 5.8 we see that the oscillation time is later for smaller mass splittings. At later times, the rates of scattering between active-sterile neutrinos is larger relative to the Hubble scale, and the asymmetry is consequently larger. Therefore, small but non-zero sterile neutrino mass splittings enhance the size of the baryon asymmetry, as long as active-sterile neutrino scatterings is not so rapid as to decohere the sterile neutrinos prior to coherent oscillations. At early times, $t \ll t_{\rm osc}$ the oscillation phase is small and the rate of asymmetry is slow. At later times, $t \gg t_{\rm osc}$, the oscillation rate is rapid compared to the Hubble scale, and sterile neutrinos produced at different times have different phases. Consequently, averaging over the entire ensemble results in a cancellation of the asymmetry production from each sterile neutrino. Therefore, the lepton flavour asymmetries are dominated by production at $t \sim t_{\rm osc}$. The equilibration time is obtained by requiring that the scattering rate is of the order of the Hubble expansion

$$t_{\rm eq}(\alpha) \propto (F^2 M_0)^{-1} \sim \left(\frac{m_\nu m_N M_0}{v^2}\right)^{-1}. \tag{5.9}$$

Therefore the magnitude of the Yukawa couplings is an important element for generating a non-zero baryon asymmetry, since it determines the rates of processes generating the lepton asymmetry. As we have already seen, the rate of production of individual lepton flavour asymmetries is $\mathcal{O}(|F|^4)$. This implies that increasing the magnitude of Yukawa couplings both enhances the individual flavour asymmetries and gives a more rapid transfer rate from the individual lepton flavour asymmetries into a total lepton asymmetry at order $\mathcal{O}(|F|^6)$. However, increase in the Yukawas also enhances the washout processes. The characteristic time scale associated with the washout of lepton flavour α is

$$t_{\alpha\,\text{washout}} \sim \frac{1}{\Gamma(L_\alpha \to N^\dagger)} \sim \frac{1}{(FF^\dagger)_{\alpha\alpha}T}. \tag{5.10}$$

If the Yukawa couplings is too large, then washout occurs before the electroweak phase transition, and all lepton flavour asymmetries are erased in the equilibrium limit. Unless the mass eigenestates are extremely degenerate, there is a hierarchy of scales:

$$t_{\text{osc}} \ll t_{\text{eq}} \sim t_{\text{EW}}. \tag{5.11}$$

From these considerations we see that the generation of the asymmetry in the different flavors is effective at $t \sim t_{\text{osc}}$, so it takes place at temperatures much higher than the electroweak phase transition. At later times, when oscillations are very fast, quantum effects are no longer possible and the lepton asymmetries no longer grow, but the total lepton asymmetry keeps evolving because the equilibration rate of different flavors is different. The presence of lepton flavour dependence in scattering rates is crucial to generate a lepton asymmetry. In fact, in the absence of lepton flavour dependence effects, the individual scattering rates are all equal, i.e. $\Gamma(L_e \rightharpoonup N^\dagger) = \Gamma(L_\mu \rightharpoonup N^\dagger) = \Gamma(L_\tau \rightharpoonup N^\dagger)$, and the total lepton asymmetry remains zero[1]. After all the states reach the equilibration time $t > t_{\text{eq}}$, the asymmetry drops exponentially. If the electroweak phase transition happens before that, the subsequent evolution of the lepton asymmetries no longer affects the baryons and therefore whatever baryon asymmetry survives until t_{ew} remains.

5.1.1 Derivation of quantum kinetic equations

The described mechanism can be realized by a simple framework called as the neutrino MSM (νMSM), in which three right-handed neutrinos are introduced with Majorana masses below the electroweak scale. The lightest sterile neutrino N_1 with mass $\sim$ 10 keV can be a candidate of dark matter, while the other two N_2 and N_3 with masses $\sim$ 1 GeV can generate the BAU through ARS leptogenesis. In order to describe a series of processes generating asymmetries, we have to deal with the coherent evolution of sterile neutrinos with the flavour oscillations, and also the incoherent scattering processes with surrounding medium for the destruction and production of sterile neutrinos. We then use the Raffelt-Sigl formalism [81], i.e. the formulation with the matrix of densities. As we have already seen in previous chapters, we describe the early universe as a thermodynamical ensemble, which can be described by a density matrix ρ and the expectation value of any operator is given by the average, see Eq. E.40. To characterize ρ are necessary all matrix elements of ρ, or, equivalently, all n-point correlation functions for all quantum fields [2]. The leptonic charges can be expressed in terms of field

[1] There is already evidence for lepton flavour dependence in the interactions with neutrinos. First, the structure of the LH neutrino masses and mixing angles tells us that their Yukawa couplings are non-universal, and proportional to the mxing angles θ_{ij}. Second, the CP phases appear in very particular terms in the interaction: for instance, the Dirac phase δ appears only in terms proportional to $\sin\theta_{13}$. Changing the phase can lead to constructive or destructive interference of rates involving a specific lepton flavour [80].

[2] Notice that, since the ensemble can be in infinitely many states, infinitely many numbers are necessary to exactly characterize ρ. Therefore, any practically computable description requires truncation

bilinears, thus it is sufficient to concentrate on the two-point functions. We will consider bilinears in the ladder operators a_I, $a_I^\dagger$ for sterile, and a_α, $a_\alpha^\dagger$ for active neutrinos. The starting point of this formalism is to consider the time evolution of number density matrices represented by the expectation values of the number density operators for the particle states (right or positive helicity states) and antiparticles (left or negative helicity states):

$$\begin{aligned}\langle a_j^\dagger(\mathbf{k})a_i(\mathbf{k'})\rangle_T &\equiv (2\pi)^3\delta^3(\mathbf{k}-\mathbf{k'})(\rho(k))_{ij},\\ \langle b_i^\dagger(\mathbf{k})b_j(\mathbf{k'})\rangle_T &\equiv (2\pi)^3\delta^3(\mathbf{k}-\mathbf{k'})(\bar{\rho}(k))_{ij},\end{aligned} \tag{5.12}$$

The matrix of interest here is one in the flavor space consisting of sterile neutrinos N_2 and N_3 with positive helicities, $\bar{N}_2$ and $\bar{N}_3$ with negative helicities, active leptons $L_\alpha,\ \alpha = e,\mu,\tau$ and their antiparticles $\bar{L}_\alpha,\ \alpha = e,\mu,\tau$, which leads to a 10×10 matrix. The diagonal elements of this matrix will be the usual occupation numbers, and the off-diagonal elements contain correlation of the flavour mixing.

$$\rho = \begin{bmatrix} \rho_{LL} & \rho_{L\bar{L}} & \rho_{LN} & \rho_{L\bar{N}} \\ \rho_{\bar{L}L} & \rho_{\bar{L}\bar{L}} & \rho_{\bar{L}N} & \rho_{\bar{L}\bar{N}} \\ \rho_{NL} & \rho_{N\bar{L}} & \rho_{NN} & \rho_{N\bar{N}} \\ \rho_{\bar{N}L} & \rho_{\bar{N}\bar{L}} & \rho_{\bar{N}N} & \rho_{\bar{N}\bar{N}} \end{bmatrix} \tag{5.13}$$

where different entries ρ are matrices describing the neutrino states in different sectors. Notice that we have only considered terms that contain exactly one creation and one annihilation operator. In fact, terms contatining two creation or two annihilation operators, such as $\langle a_I a_J\rangle$, or $\langle a_\alpha^\dagger \alpha_\beta^\dagger\rangle$, can be related to processes that violate lepton number and are suppressed at $T > M$. For $T \lesssim M$ they could in principle contribute, but we neglect them for the moment since the leading order contribution in the Yukawa coupling F to the corresponding rate $\frac{d}{dt}\langle a_I a_J\rangle$ etc. oscillate fast. We will go back to these fast modes in the next sections, but for the moment we will focus only on the lepton number conserving processes. It is important to notice that in absence of lepton number violating (LNV) processes, the total asymmetry summed over both the active and singlet sector must vanish. Hence, the asymmetries produced in the active and singlet sector are of equal value, but have opposite sign. However, sphaleron processes act only on the asymmetry in the SM sector, partially converting it into the observed baryon asymmetry. In this way, leptogenesis occurs even if the total generalised lepton number is conserved (approximately). In the situation under consideration, the density matrix can be simplified. First, active leptons possess gauge interactions and Yukawa interactions with right-handed charge leptons in addition to neutrino Yukawa interactions, which induce large energy gaps between active and sterile states through the thermal effect. Then, the transitions between active and sterile leptons are highly suppressed, and the elements corresponding to the mixing between L_α and N_I (and also $\bar{L}_\alpha$ and $\bar{N}_I$) are neglected. At this stage, the matrix of densities in the system is decomposed into two 2×2 matrices ρ_N for $N_{2,3}$ and $\bar{\rho}_N$ for $\bar{N}_{2,3}$, and two 3×3 matrices ρ_L and $\rho_{\bar{L}}$[3] for active leptons L_α and $\bar{L}_\alpha$, with $\alpha = e,\mu,\tau$. Secondly, the off-diagonal elements of ρ_L and $\rho_{\bar{L}}$ can be neglected for the temperatures of interest. This is because the flavour transitions among active leptons are also suppressed due to the medium effects induced by the Yukawa interactions of charged leptons with hierarchical coupling constants. Therefore, the system can be described in the density matrix formalism by two differential matrix equations, one for the single neutrino N (anti-neutrino $\bar{N}$) and one for the active leptons L (anti-leptons $\bar{L}$). First, we consider the kinetic equation for the sterile neutrinos, which can be written in the form [81]:

$$\frac{d\rho}{dt} = -i[H,\rho] - \frac{1}{2}\{\Gamma^a,\rho\} + \frac{1}{2}\{\Gamma^p, 1-\rho\}, \tag{5.14}$$

[3] ρ_L is considered to be the sum of two contributions of lepton doublets, i.e. $\rho_L = \rho_\nu + \rho_e = N_D\rho_\nu$.

$$\frac{d\rho_L}{dt} = -i[H_L, \rho_L] - \frac{1}{2}\{\Gamma^a_L, \rho_L\} + \frac{1}{2}\{\Gamma^p_L, 1-\rho_L\}, \tag{5.15}$$

where $H = H^0 + V_N$ is the Hermitian effective Hamiltonian incorporating the medium effects on neutrino propagation in the thermal plasma and can be written as (see Ref. [56] for details on the computation):

$$H \equiv \frac{M_N^2}{2k_0} + \frac{T^2}{8k_0}F^\dagger F, \tag{5.16}$$

where we have excluded those effects that are flavor blind, i.e. proportional to the identity in flavor which drop from the commutator [29]. The first term of Eq. 5.14 describes the coherent evolution of ρ_N and the oscillation of sterile neutrinos occurs due to the off-diagonal elements of the effective potential V_N , which is found from the self energy for sterile neutrinos at finite temperatures (see Ref. [82] for details). These equations can be simplified by taking the active species to be in thermal equilibrium with a chemical potential μ_α, $\rho_L(k_L, T, \mu_\alpha) = N_D\rho_F(k_L/T, \mu_\alpha)I$, with $\rho_F(k_L/T, \mu_\alpha) = (\exp(k_L/T - \mu_\alpha))^{-1}$, denoting the Fermi-Dirac distribution with momentum k_L and chemical potential normalized by the temperature $\mu_\alpha = \mu_\alpha/T$. We can further notice that the chemical potentials μ_α are small parameter, since they are directly related to the generated baryon asymmetry. Therefore, they may be used for a perturbative analysis. Γ^p_N and Γ^a_N are the production and annihilation rates, respectively. For a process $a(E_1) + b(E_2) \to c(E_3) + N(p_N)$

$$\Gamma^p_N = \frac{1}{2k_N}F^\dagger\bigg(\int\prod_{f=1}^{3}\frac{d^3p_f}{(2\pi)^3}(2\pi)^4\delta^{(4)}(p_1+p_2-p_3-p_N)|\mathcal{M}|^2\rho_a(E_1)\rho_b(E_2)(1\pm\rho_c(E_3)\bigg)F, \tag{5.17}$$

$$\Gamma^a_N = \frac{1}{2k_N}F^\dagger\bigg(\int\prod_{f=1}^{3}\frac{d^3p_f}{(2\pi)^3}(2\pi)^4\delta^{(4)}(p_1+p_2-p_3-p_N)|\mathcal{M}|^2(1\pm\rho_a(E_1))(1\pm\rho_b(E_2))\rho_c(E_3)\bigg)F, \tag{5.18}$$

where ρ_i are the distribution functions. Eqs. 5.18 can be re-written as

$$\Gamma^p_{N_{ij}} = F^\dagger_{i\alpha}\rho_F\bigg(\frac{k_0}{T} - \mu_\alpha\bigg)\gamma_N(k, \mu_\alpha)F_{\alpha j}, \tag{5.19}$$

$$\Gamma^a_{N_{ij}} = F^\dagger_{\alpha i}\bigg(1 - \rho_F\bigg(\frac{k_0}{T} - \mu_\alpha\bigg)\bigg)\gamma_N(k, \mu_\alpha)F_{\alpha j}, \tag{5.20}$$

where γ_N contains the contribution from all $2 \to 2$ processes that produce an N:

$$\bar{Q}t \to \bar{l}N;\ tl \to QN;\ Wl \to \bar{H}N;\ lH \to WN;\ WH \to \bar{l}N, \tag{5.21}$$

and $1 \leftrightarrow 2$ processes: $H \to \bar{l}N$ including resummed soft-gauge interactions (see Refs. [28, 29, 78, 82]). These contributions have been computed, including also the effected of a lepton chemical potential to linear order, in Ref. [78]. Expanding in μ_α

$$\gamma_N(k, \mu_\alpha) \simeq \gamma^{(0)}_N(k) + \gamma^{(2)}_N(k)\mu_\alpha, \tag{5.22}$$

and defining

$$\gamma^{(1)}_N(k) \equiv \gamma^{(2)}_N(k) - \frac{\rho'_F(k)}{\rho_F(k)}\gamma^{(0)}_N(k), \tag{5.23}$$

with $\rho'_F \equiv \frac{d\rho_F(y)}{dy}$, the functions $\gamma^{(i)}_N$ get contributions from quark (Q), gauge scattering (V) and the $1 \to 2$ resummed processes (LPM):

$$\gamma^{(i)}_N = \gamma^{(i)}_{LPM} + y_t^2\gamma^{(i)}_Q + (3g^2 + g'^2)\bigg(\gamma^{(i)}_V + \gamma^{(i)}_{IR}\log\bigg(\frac{1}{3g^2+g'^2}\bigg)\bigg). \tag{5.24}$$

The functions $\gamma^{(i)}_{Q,V}$ depend only on the ratio k_0/T, while $\gamma^{(i)}_{LPM}$ has non-trivial temperature dependence due to the runnings of the coupling constants; for details see [83, 84]. Inserting Eqs. 5.22-5.23) in the kinetic equations 5.14 we get

$$\begin{aligned}
\frac{d\rho}{dt} &= -i[H,\rho] - \frac{1}{2}\{\Gamma^a,\rho\} + \frac{1}{2}\{\Gamma^p, 1-\rho\} \\
&= -i[H,\rho] - \frac{1}{2}\left\{F^\dagger(1-\rho_F(k,\mu))\gamma_N F,\rho_N\right\} + \frac{1}{2}\left\{F^\dagger\rho_F(k,\mu)\gamma_N F, 1-\rho_N\right\} \\
&= -i[H,\rho] - \frac{1}{2}\left\{F^\dagger\gamma_N F,\rho_N\right\} + \frac{1}{2}\left\{F^\dagger\rho_F(k,\mu)\gamma_N F,\rho_N\right\} + \frac{1}{2}\left\{F^\dagger\rho_F(k,\mu)\gamma_n F, 1\right\} \\
&\quad - \frac{1}{2}\left\{F^\dagger\rho_F(k,\mu)\gamma_N F,\rho_N\right\} \\
&= -i[H,\rho] - \frac{1}{2}\left\{F^\dagger(\gamma^{(0)}_N + \gamma^{(2)}_N\mu_\alpha)F,\rho_N\right\} + \frac{1}{2}\left\{F^\dagger\rho_F(k,\mu)(\gamma^{(0)}_N + \gamma^{(2)}_N\mu_\alpha)F, 1\right\} \\
&= -i[H,\rho] - \frac{1}{2}\left\{F^\dagger\gamma^{(0)}_N F,\rho_N\right\} - \frac{1}{2}\left\{F^\dagger\gamma^{(2)}_N\mu_\alpha F,\rho_N\right\} + F^\dagger\rho_F(k,\mu)\gamma^{(0)}_N F \\
&\quad + F^\dagger\rho_F(k,\mu)\gamma^{(2)}_N\mu F.
\end{aligned} \tag{5.25}$$

At this point we can expand at first order in the chemical potential $\rho_F(k_0/T-\mu_\alpha) \simeq \rho_F(k_0/T) - \rho'_F(k_0/T)\mu_\alpha$ and we obtain

$$\begin{aligned}
\frac{d\rho_N}{dt} &= -i[H,\rho] - \frac{1}{2}\left\{F^\dagger\gamma^{(0)}_N F,\rho_N\right\} - \frac{1}{2}\left\{F^\dagger\gamma^{(2)}_N\mu_\alpha F,\rho_N\right\} + F^\dagger\rho_F(k,\mu)\gamma^{(0)}_N F \\
&\quad + F^\dagger(\rho_F(k) - \mu\rho'_F(k))\gamma^{(2)}_N(k)\mu F \\
&= -i[H,\rho] - \frac{1}{2}\left\{F^\dagger\gamma^{(0)}_N F,\rho_N\right\} - \frac{1}{2}\left\{F^\dagger\gamma^{(2)}_N\mu_\alpha F,\rho_N\right\} + F^\dagger(\rho_F(k) - \mu\rho'_F(k))\gamma^{(0)}_N F \\
&\quad + F^\dagger\rho_F(k)\gamma^{(1)}_N(k)\mu F + F^\dagger\rho'_F(k)\gamma^{(0)}_N\mu F - F^\dagger\mu^2\rho'_F(k)\gamma^{(2)}_N F \\
&= -i[H,\rho_N] - \frac{1}{2}\left\{F^\dagger\gamma^{(0)}_N F,\rho_N - \rho_F\right\} - \frac{1}{2}\left\{F^\dagger\gamma^{(2)}_N\mu F,\rho_N\right\} + F^\dagger\rho_F\gamma^{(1)}_N\mu F + \mathcal{O}(\mu^2),
\end{aligned} \tag{5.26}$$

where $\mu \equiv \mathrm{diag}(\mu_\alpha)$. The equation for $\bar{N}$ are given by CP conjugation, i.e. by taking $\rho_N \to \bar{\rho}_N$ and $\mu \to -\mu$, $F \to F^*$. In this way we immediately obtain

$$\frac{d\bar{\rho}_N}{dt} = -i[H^*,\bar{\rho}_N] - \frac{1}{2}\left\{F^T\gamma^{(0)}_N F^*,\bar{\rho}_N - \rho_F\right\} + \frac{1}{2}\left\{F^T\gamma^{(2)}_N\mu_\alpha F^*,\bar{\rho}_N\right\} - F^T\rho_F\gamma^{(1)}_N\mu F^*. \tag{5.27}$$

Finally, we need the equations describing the lepton asymmetry $\rho_L - \rho_{\bar{L}}$. To derive these equations we start by considering the evolution of active species L (see Eq. 5.15) and we can find the evolution of $\rho_{\bar{L}}$ by taking $L \to \bar{L}$, $\mu_L \to -\mu_L$. The corresponding decay and production rates of the active species, which describes the exact same processes from the point of view of these particles, can be related to Eqs. 5.26-5.27. In fact, from the processes in Eq. 5.21 we see that the production of leptons l corresponds to the destruction of the RHNs, therefore, we can substitute

$$\begin{aligned}
\{\Gamma^p_L, 1-\rho_L\} &\to \{\Gamma^a_N,\rho_N\}, \\
\{\Gamma^a_L,\rho_L\} &\to \{\Gamma^p_N.1-\rho_N\},
\end{aligned} \tag{5.28}$$

and for the lepton asymmetry we need to consider $\rho_L - \rho_{\bar{L}}$ (see Ref. [82] for a detailed estimate of the rates). From these considerations we can deduce that the kinetic equation for the asymmetry can be

derived by taking $\frac{d}{dt}(\rho_N - \rho_{\bar{N}})$. We can also notice that the lepton asymmetry can be related to the chemical potential, since

$$\int \frac{d^3k_L}{(2\pi)^3}[\rho_F(k_L/T,\mu_L) - \rho_F(k_L/T,-\mu_L)] \sim -2\mu_L \int \frac{d^3k_L}{(2\pi)^3}\rho'_F(k_L/T) = \frac{T^3}{6}\mu_L, \tag{5.29}$$

where we have used the fact that $\frac{d}{dy}(e^y+1)^{-1} = -e^y/(1+e^y)^2$ and we obtain:

$$\frac{1}{e^{k/T-\mu_L}+1} - \frac{1}{e^{k/T+\mu_L}+1} = \frac{e^{k/T}(e^{\mu_L}-e^{-\mu_L})}{(e^{k/T}+1)^2} \simeq -2\mu_L\rho'_F. \tag{5.30}$$

Hence, the chemical potentials can be written as (see Ref. [85] for details):

$$\mu_\alpha = \frac{6}{T^3 N_D}\int \frac{d^3k_L}{(2\pi)^3}(\rho_L - \rho_{\bar{L}})_{\alpha\alpha}, \tag{5.31}$$

and we can obtain the kinetic equations for the chemical potentials from the equations for $\rho_L - \rho_{\bar{L}}$, i.e. from $\rho_N - \rho_{\bar{N}}$. Note that the off-diagonal elements of ρ_L and $\rho_{\bar{L}}$ do not enter in Eq. 5.26, and hence it is sufficient to solve the kinetic equation for diagonal components only, implying that the commutator in Eq. 5.15 can be dropped. Actually, the above approach is incorrect, as it neglects the effects of interactions between SM fields, which are rapid compared to the active-sterile neutrino scatterings. Because of these scatterings, the asymmetries in individual lepton flavours created by sterile neutrino oscillations are rapidly distributed among all SM fields. Since the asymmetries are destroyed only through interactions of the LH leptons with sterile neutrinos, this modifies the relative rates of asymmetry creation and destruction. Therefore, we must take into account the so-called spectator processes. In fact, as we have already pointed out in Sec. 3.3.3, these processes distribute the asymmetry among various species of the thermal bath, conserving $B-L$, but violating $B+L$. Hence, to incorporate these processes, we include in our density matrices only quantities that are preserved by the equilibrium SM interactions, justifying the absence of such rapid interactions in the evolution equations. For this reason we consider the evolution of the asymmetries $B/3 - L_\alpha$, which are non anomalous and exactly conserved in the SM [80]. The relation between the leptonic chemical potentials and the approximately conserved charges, $B/3 - L_\alpha$, is given by [85]:

$$\mu_\alpha = 2\sum_\beta C_{\alpha\beta}\mu_{B/3-L_\alpha}, \qquad C_{\alpha\beta} = -\frac{1}{711}\begin{bmatrix} 257 & 20 & 20 \\ 20 & 257 & 20 \\ 20 & 20 & 257 \end{bmatrix}. \tag{5.32}$$

From the considerations above we can now finally find the kinetic equation for the conserved charges $B/3 - L_\alpha$ as

$$\begin{aligned}\frac{dn_{B/3-L_\alpha}}{dt} = -2\int_k \Bigg\{ &\frac{\gamma_N^{(0)}}{2}(F\rho_N F^\dagger - F^*\rho_{\bar{N}}F^T)_{\alpha\alpha} \\ &+ \mu_\alpha\left(\frac{\gamma_N^{(2)}}{2}(F\rho_N F^\dagger + F^*\rho_{\bar{N}}F^T)_{\alpha\alpha} - \gamma_N^{(1)}\mathrm{Tr}[FF^\dagger P_\alpha]\rho_F\right)\Bigg\},\end{aligned} \tag{5.33}$$

where P_α is the projector on flavor α. It is important to notice that the evolution equations satisfy the relation $\mathrm{Tr}(\rho_{\mathrm{N}-\bar{\mathrm{N}}} - \rho_{\mathrm{L}-\bar{\mathrm{L}}}) \simeq 0$ which reflects the conservation of the global $L-N$ charge. Indeed, as we have already pointed out, if we neglect the LNV processes the total asymmetry summed over both the active and singlet sector must vanish. Thus, if the system starts with the lepton symmetric

universe, the asymmetry of sterile neutrinos is always opposite to that of active leptons. Namely, the kinetic equations we have derived here do not describe the generation of the lepton asymmetry, but the separation into sterile and active sectors [82].
Introducing finally the expansion of the Universe and changing variables to the scale factor $x = a = T^{-1}$ and $y = ka$, the time derivative of the distribution functions changes to:

$$\frac{d\rho_N(T,k)}{dt} \to xH(x)\frac{\partial\rho_N(x,y)}{\partial x}\bigg|_{y\text{ fixed}}, \qquad \frac{dn_{B/3-L_\alpha}}{dt} \to -2xH(x)\frac{d\mu_{B/3-L_\alpha}}{dx}\int_k \rho'_F, \tag{5.34}$$

where $H(x) = T^2/M_0$, with $M_0 = M_{\rm Pl}/(1.66 g_{*,s})$, is the Hubble parameter in a radiation dominated universe. In this case we have a constant number of relativistic degrees of freedom $g_*(T_0) \simeq 106.75$ for $T_0 \geqslant T_{\rm ew}$, then $xT =$ const. that we can fix to one. Solving the kinetic equations 5.26 and 5.27 is challenging since they are integro-differential equations as ρ_N and $\bar\rho_N$ depend upon momenta and the collision terms are integrals of the density matrices themselves. Therefore, to simplify the numerical solution of these equations, it is common to assume that the heavy neutrinos fulfill the weaker condition of kinetic equilibrium, $\rho_N(k_N,T)_{IJ} = R_N(T)_{IJ}\rho_F(k_N/T, \mu = 0)$. In this way we approximate the neutrino and anti-neutrino density matrices as a Fermi-Dirac distribution with vanishing chemical potential and with a temperature T, multiplied by time-dependent matrices R_N and $R_{\bar N}$ which encode the neutrino asymmetries as well as flavour correlations. With this we can factor out the momentum-independent variable $R_N(T)$ in the integrals above, and replace the integrated rates with thermally averaged destruction and production rates:

$$\langle\gamma(T)\rangle = \frac{\int d^3p\gamma(p,T)\rho_F(p/T)}{\int d^3p\rho_F(p/T)}. \tag{5.35}$$

By changing variables as in Eq. 5.34 we finally find the kinetic equations:

$$xH\frac{dR_N}{dx} = -i[\langle H\rangle, R_N] - \frac{\langle\gamma_N^{(0)}\rangle}{2}\{F^\dagger F.R_N - 1\} + \langle\gamma_N^{(1)}\rangle F^\dagger\mu F - \frac{\langle\gamma^{(2)}\rangle}{2}\{F^\dagger\mu F, R_N\} \tag{5.36}$$

$$xH\frac{dR_{\bar N}}{dx} = -i[\langle H^*\rangle, R_{\bar N}] - \frac{\langle\gamma_N^{(0)}\rangle}{2}\{F^T F^*, R_{\bar N} - 1\} - \langle\gamma_N^{(1)}\rangle F^T\mu F^* + \frac{\langle\gamma_N^{(2)}\rangle}{2}\{F^T\mu F^*, R_{\bar N}\} \tag{5.37}$$

$$xH\frac{d\mu_{B/3-L_\alpha}}{dx} = \frac{\int_k \rho_F}{\int_k \rho'_F}\bigg\{\frac{\langle\gamma^{(0)}\rangle}{2}(FR_NF^\dagger - F^*R_{\bar N}F^T)_{\alpha\alpha} + \mu_\alpha\bigg(\frac{\langle\gamma_N^{(2)}\rangle}{2}(FR_NF^\dagger - F^*R_{\bar N}F^T)_{\alpha\alpha} \tag{5.38}$$

$$- \langle\gamma_N^{(1)}\rangle{\rm Tr}[F^\dagger F P_\alpha]\bigg)\bigg\}. \tag{5.39}$$

So far we have neglected lepton number violating (LNV) processes because the Majorana mass of the RHNs is small compared to the temperature. In this situation the initial asymmetries in active leptons are purely flavored and lepton-number conserving (LNC) and we have seen that total asymmetries in the active sector arise and are approximately counterbalanced by those in the sterile sector, i.e. ${\rm Tr}(\rho_{L-\bar L} - \rho_{N-\bar N}) \simeq 0$. But in other regions of the parameter space LNV contributions may be relevant and then must be accounted for, namely when M/T corrections to the rates cannot be neglected. In fact, since the sterile neutrinos are massive, they carry both helicities. The two helicities states experience different interactions: one state interacts with Standard Model leptons and the other with antileptons. Therefore, both helicities play a role and in presence of a lepton asymmetry they are produced and equilibrate at a different rate. It turns out that at a good approximation the two helicity states have no direct overlap with each other and we can describe the neutrino ensemble with the two distinguished

matrices ρ_N and $\rho_{\bar{N}}$. This approximation is valid in the limit $M_N \ll T$ (or if all Majorana masses are set to zero), the theory has an additional conserved charged, called "fermion number". In this limit the Majorana spinor can be replaced by a chiral Dirac spinor and the conserved charge then counts the total asymmetry in right-handed and left-handed leptons. Keeping instead the Majorana character intact, the fermion number is defined as the sum of the helicity asymmetry of the sterile neutrinos and the lepton asymmetry of the Standard Model sector. Therefore, we need to take into account the helicity-conserving (fermion number violating) terms in the quantum kinetic Eqs. 5.37-5.39, by adding the LNV corrections to the rates that have been computed in Ref. [84]. By following Ref. [79] we neglect the hypercharge chemical potential[4], which is a small effect, and we write the LNV contributions analogously to the LNC rates in Eqs. 5.22-5.23, but with the following substitutions:

$$\gamma_N^{(0)} \to S_N^{(0)}, \qquad \gamma_N^{(1),(2)} \to -S_N^{(1),(2)}, \qquad F_{\alpha i} \to F_{\alpha i}^* \frac{M_N}{T}. \tag{5.40}$$

As we have already pointed out, one helicity state couples to leptons, while the other to antileptons. Since here we are considering helicity conserving terms, we must have both helicities and, therefore, the term proportional to the chemical potential μ have a different sign, since they couple to antileptons (leptons). For this reason we change the sign in the middle of Eq. 5.40. In the last substitution of Eq. 5.40, we have inserted the term M_N/T since we are considering LNV terms, while the Yukawa coupling becomes its complex conjugate since it enters in the quantum kinetic equations with opposite helicity. With these substitutions we finally obtain

$$\begin{aligned}
xH\frac{dR_N}{dx} &= -i[\langle H\rangle, R_N] - \frac{\langle\gamma_N^{(0)}\rangle}{2}\{F^\dagger F, R_N - 1\} - x^2\frac{\langle S_N^{(0)}\rangle}{2}\{MF^T F^* M, R_N - 1\} \\
&\quad + \langle\gamma_N^{(1)}\rangle F^\dagger \mu F - x^2\langle S_N^{(1)}\rangle MF^T\mu F^* M - \frac{\langle\gamma^{(2)}\rangle}{2}\{F^\dagger\mu F, R_N\} \\
&\quad + x^2\frac{\langle S_N^{(2)}\rangle}{2}\{MF^T\mu F^* M, R_N\}, \\
xH\frac{dR_{\bar{N}}}{dx} &= -i[\langle H^*\rangle, R_{\bar{N}}] - \frac{\langle\gamma_N^{(0)}\rangle}{2}\{F^T F^*, R_{\bar{N}} - 1\} - x^2\frac{\langle S_N^{(0)}\rangle}{2}\{MF^\dagger FM, R_{\bar{N}} - 1\} \\
&\quad - \langle\gamma_N^{(1)}\rangle F^T\mu F^* + x^2\langle S_N^{(1)}\rangle MF^\dagger\mu FM + \frac{\langle\gamma_N^{(2)}\rangle}{2}\{F^T\mu F^*, R_{\bar{N}}\} \\
&\quad - x^2\frac{\langle S_N^{(2)}\rangle}{2}\{MF^\dagger\mu FM, R_{\bar{N}}\}, \\
xH\frac{d\mu_{B/3-L_\alpha}}{dx} &= \frac{\int_k \rho_F}{\int_k \rho_F'}\left\{\frac{\langle\gamma^{(0)}\rangle}{2}(FR_N F^\dagger - F^* R_{\bar{N}} F^T) - x^2\frac{\langle S_N^{(0)}\rangle}{2}(F^* MR_N MF^T - FMR_{\bar{N}} MF^\dagger)\right. \\
&\quad - \mu_\alpha\big(\langle\gamma_N^{(1)}\rangle FF^\dagger + x^2\langle S_N^{(1)}\rangle FM^2F^\dagger\big) + \frac{\langle\gamma_N^{(2)}\rangle}{2}\mu_\alpha\big(FR_N F^\dagger + F^* R_{\bar{N}} F^T\big) \\
&\quad \left. + x^2\frac{\langle S_N^{(2)}\rangle}{2}\mu_\alpha\big(FMR_{\bar{N}} MF^\dagger + F^* MR_N MF^T\big)\right\}_{\alpha\alpha}.
\end{aligned}$$

[4]Within perturbation theory, the presence of $\mu_{L_\alpha}, \mu_B \neq 0$ implies that the temporal component of the hypercharge gauge potential develops an expectation value (μ_Y), guaranteeing the neutrality of the plasma.

5.2 ARS Leptogenesis with additional singlet scalar

In this section we are going to study how the ARS Leptogenesis mechanism is modified when we add an additional scalar particle to the νMSM scenario. In particular, we are going to add a complex scalar particle Φ and a global $U(1)_{B-L}$ symmetry. Therefore, the symmetry group of the theory is:

$$\big(SU(3)_c \times SU(2)_l \times U(1)_Y\big) \times U(1)_{(B-L)_{global}}. \tag{5.41}$$

The additional scalar is a singlet under the SM gauge group and has a $B-L=+2$ charge. The Lagrangian of this theory will be made by $\mathcal{L}=\mathcal{L}_{\rm SM}+\mathcal{L}_{kin(N_R,\Phi)}+\mathcal{L}_{int}-V(H,\Phi)$. To write it we need to consider all the possible terms respecting the symmetry group. In this way, we can construct the gauge invariant interacting Lagrangian as:

$$\mathcal{L}_{int}=-F_{\alpha i}\bar{L}_\alpha \epsilon H^* N_I-\frac{Y_{IJ}}{2}\Phi\bar{N}_I^c N_J+\text{h.c.}\,, \tag{5.42}$$

and the high-energy potential invariant under the symmetry group is given by

$$V(H,\Phi)=\mu_H^2 H^\dagger H+\lambda_H(H^\dagger H)^2+\mu_\phi^2\Phi^\dagger\Phi+\lambda_\phi(\Phi^\dagger\Phi)^2+\lambda_{H\phi}H^\dagger H\Phi^\dagger\Phi, \tag{5.43}$$

with $\lambda_H>0$ to have a potential limited from below. We can verify that this Lagrangian is invariant under the $U(1)_{B-L}$ global symmetry, indeed, if we transform the scalar as $\Phi\to e^{i\alpha}\Phi$ the Lagrangian does not change. This is not true for the vacuum of the system, which is not trivial when $\mu_\phi^2<0$ and leads to Spontaneous Symmetry Breaking (SSB). To find the ground state of the system we compute the minimum of the potential, first by assuming that $\mu_\phi^2,\mu_H^2,\lambda_H,\lambda_\phi,\lambda_{\phi H}>0$

$$\begin{aligned}\frac{\partial V}{\partial|\Phi|}=&2\mu_|\phi|^2\Phi+4\lambda_\phi|\Phi|^3+2\lambda_{\lambda H}|H|^2\Phi=0,\\ \frac{\partial V}{\partial|H|}=&2\mu_H^2|H|+4\lambda_H|H|^3+2\lambda_{H\phi}H|\Phi|^2=0.\end{aligned} \tag{5.44}$$

These conditions are satisfied for

$$|H|=0, \qquad |H|^2=-\frac{\mu_H^2+\lambda_{H\phi}|\Phi|^2}{2\lambda_H}, \tag{5.45}$$

$$|\Phi|=0, \qquad |\Phi|^2=-\frac{\mu_\phi^2+\lambda_{H\phi}|H|^2}{2\lambda_\phi}. \tag{5.46}$$

Since we are assuming $\mu_\phi^2,\mu_H^2>0$ we must choose the solutions $|\Phi|=0$ and $|H|=0$ and by computing the second derivative we find the Hessian matrix:

$$\begin{aligned}\frac{\partial^2 V}{\partial|\Phi|^2}=&2\mu_\phi^2+12\lambda_\phi|\Phi|^2+\lambda_{\lambda H}|H|^2\Big|_{\Phi=0,H=0},\\ \frac{\partial^2 V}{\partial|H|^2}=&2\mu_H|H|^2+12\lambda_H H^2+2\lambda_{H\phi}|\Phi|^2\Big|_{\phi=0,H=0},\\ \frac{\partial^2 V}{\partial\Phi\partial H}=&4\lambda_{H\phi}|H||\Phi|\Big|_{\Phi=0,H=0},\end{aligned} \tag{5.47}$$

$$H=\begin{bmatrix}2\mu_\phi^2 & 0\\ 0 & 2\mu_H^2\end{bmatrix}. \tag{5.48}$$

Therefore, we see that if $\mu_\phi^2 > 0$ and $\mu_H^2 > 0$ the Hessian matrix is positive definite and we have a trivial minimum in the point $\{\Phi = 0, H = 0\}$. But we immediately notice that if instead $\mu_\phi^2 < 0$ we are in a saddle point. Indeed, by taking $\mu_\phi^2 \to -\mu_\phi^2$ we see that we have another possible minimum configuration given by[5]:

$$\begin{aligned} |\Phi|^2 =& \frac{\mu_\phi^2 - \lambda_{H\phi}|H|^2}{2\lambda_{H\phi}}, \\ |H| =& 0. \end{aligned} \tag{5.49}$$

By substituting these conditions in Eq. 5.47 and by taking $\mu_\phi^2 \to -\mu_\phi^2$ we obtain a positive definite Hessian matrix:

$$H = \begin{bmatrix} 4\mu_\phi^2 & 0 \\ 0 & 2\mu_H^2 + \frac{\lambda_H \mu_\phi^2}{\lambda_\phi} \end{bmatrix}, \tag{5.50}$$

so we have a minimum. Recalling that we can rewrite a complex scalar field as the linear combination of two real fields $\Phi = \frac{\phi + i\theta}{\sqrt{2}}$, so $\Phi^\dagger\Phi = \frac{1}{2}(\phi^2 + \theta^2)$. We see that the first equation in Eq. 5.49 represents a circle in the complex plane, which is invariant under the global $U(1)_{B-L}$ symmetry. Every point on this circle defines a minimum of energy and, consequently, we have a set of infinite degenerate vacua. However, once we choose a particular point on the minima configuration, the global invariance would be broken. By combining the two solutions in Eq. 5.49 we have

$$\Phi^\dagger\Phi = \frac{\mu_\phi^2}{2\lambda_\phi} \equiv \frac{v_\phi^2}{2}, \tag{5.51}$$

where $v_\phi^2 = \mu_\phi^2/\lambda_\phi$ is the Vacuum Expectation Value. Therefore, we have spontaneous breaking of a continuous symmetry and, from the Goldstone Theorem we know that when this happens, massless particles, i.e. Goldstone Bosons, must arise. The Goldstone theorem also states that the number of Goldstone bosons produced is equal to the difference between the dimension of the broken symmetry group and the dimension of the subgroup, which leaves the symmetry unbroken. In our case, the group $U(1)_{B-L}$ is completely broken, and, since it has only one generator, we expect one goldstone boson to emerge. For simplicity, we can choose the ground state of our theory such as

$$\langle \phi_0 \rangle = v_\phi, \quad \langle \theta_0 \rangle = 0, \tag{5.52}$$

where we have used the parametrization

$$\Phi = \frac{1}{\sqrt{2}}(\phi + i\theta). \tag{5.53}$$

This choice would imply that the θ would corresponds to the Goldstone boson. In order to see that we explore the spectrum we shift the field in order to rewrite the Lagrangian in terms of displacement from the physical vacuum.

$$\phi(x) = \langle \phi_0 \rangle + \hat{\phi} = v_\phi + \hat{\phi}, \qquad \theta(x) = \langle \theta_0 \rangle + \tilde{\theta}(x) = \tilde{\theta}(x). \tag{5.54}$$

So we expect the field θ to be massless, while ϕ will be massive. To verify that we insert the parametrization in Eq. 5.53 in the Lagrangian in Eq. 5.42 and then we shift the fields as in Eq. 5.54, which corresponds to take

$$\Phi = \frac{v_\phi + \hat{\phi} + i\hat{\theta}}{\sqrt{2}}. \tag{5.55}$$

[5]We still have $H = 0$ since we are assuming $U(1)_{B-L}$ symmetry breaks before the EWSB. In fact, we want to dynamically generate the masses of the RHNs before EWPT, in order to have sterile neutrino oscillations and, consequently, the generation of the lepton asymmetry.

First we focus on the potential part[6] and we find

$$\begin{aligned} V(H,\Phi) &= -\frac{\mu_\phi^2}{2}(\theta^2+\phi^2) + \frac{\lambda_\phi}{4}(\phi^2+\theta^2)^2 + \mu_H^2 H^\dagger H + \lambda_H (H^\dagger H)^2 + \frac{\lambda_{H\phi}}{2} H^\dagger H(\phi^2+\theta^2) \\ &= -\frac{\mu_\phi^2}{2}v_\phi^2 - \frac{\mu_\phi^2}{2}\hat{\phi}^2 - \mu_\phi^2 v_\phi \hat{\phi} - \frac{\mu_\phi^2}{2}\hat{\theta}^2 + \frac{\lambda_\phi}{4}(v_\phi+\hat{\phi})^4 + \frac{\lambda_\phi}{4}\hat{\theta}^4 + \frac{\lambda_\phi}{2}\hat{\phi}^2\hat{\theta}^2 + \frac{\lambda_\phi}{2}v_\phi^2\hat{\theta}^2 + \frac{\lambda_\phi}{2}2v_\phi\hat{\phi}\hat{\theta} \\ &+ \frac{\lambda_{H\phi}}{2}H^\dagger H\hat{\phi}^2 + \frac{\lambda_{H\phi}}{2}H^\dagger H v_\phi^2 + \lambda_{H\phi}H^\dagger H v\hat{\phi} + \frac{\lambda_{H\phi}}{2}H^\dagger H\hat{\theta}^2 + \mu_H^2 H^\dagger H + \lambda_H (H^\dagger H)^2. \end{aligned} \tag{5.56}$$

By considering the quadratic terms and recalling that $v_\phi^2 = \mu_\phi^2/\lambda_\phi$ we find

$$V_{quad}(\phi,\theta) = -\frac{\mu_\phi^2}{2}\hat{\phi}^2 + \frac{3}{2}\lambda_\phi v_\phi^2\hat{\phi}^2 - \frac{\mu_\phi^2}{2}\hat{\theta}^2 + \frac{\lambda_\phi}{2}v_\phi^2\hat{\theta}^2 = \mu_\phi^2\hat{\phi}^2. \tag{5.57}$$

As expected, we see that there is no massive term for the field θ and we can conclude that it is the Goldstone boson, which in the case of $U(1)_{B-L}$ SSB is called the Majoron. Instead, for the particle ϕ we have a massive term and we can conclude that at tree level and at zero temperature, the scalar mass is $M_\phi^0 = \sqrt{\lambda_\phi}v_\phi$. Now we insert the parametrization in Eq. 5.55 in the kinetic terms in the scalar sector of the Lagrangian and we have

$$\partial_\mu\Phi^\dagger\partial^\mu\Phi \rightarrow \partial_\mu\left(\frac{v_\phi+\hat{\phi}+i\hat{\theta}}{\sqrt{2}}\right)\partial^\mu\left(\frac{v_\phi+\hat{\phi}+i\hat{\theta}}{\sqrt{2}}\right) = \frac{1}{2}\partial_\mu\hat{\phi}\partial^\mu\hat{\phi} + \frac{1}{2}\partial_\mu\hat{\theta}\partial^\mu\hat{\theta}. \tag{5.58}$$

So we see that the Goldstone bosons θ enter in $\mathcal{L}$ is via derivatives. Lastly, we consider the RHNs sector of our Lagrangian, by substituting Eq. 5.55 in the interacting Lagrangian in Eq. 5.42 we obtain

$$\mathcal{L}_{int} = -\sum_{I,J}\frac{Y_{IJ}}{2}\bar{N}_I^c N_J\left(\frac{\hat{\phi}+v_\phi+i\hat{\theta}}{\sqrt{2}}\right) = \frac{Y_{IJ}}{2\sqrt{2}}\bar{N}^c N\hat{\phi} + \frac{Y_{IJ}}{2\sqrt{2}}v_\phi\bar{N}^c N + i\frac{Y_{IJ}}{2\sqrt{2}}\bar{N}^c N\hat{\theta}, \tag{5.59}$$

where we take the couplings Y_{IJ} to be real and flavour universal i.e. $Y_{IJ} = y_N\delta_{IJ}$. From this Lagrangian we see that after the SSB of the $U(1)_{B-L}$ symmetry a massive term for the RHNs arise and $m_N = v_\phi y_N$. With the addition of the singlet scalar Φ we have that in the early universe RHNs can be produced in four possible ways: in SM Higgs boson decays and $2 \leftrightarrow 2$ scattering via the coupling $F_{\alpha I}$ as in standard ARS model, in ϕ and θ decays and annihilations through the coupling Y_{IJ}.

5.2.1 New interactions

As we have seen in the previous section, the additional scalar modifies the Lagrangian with the introduction of a new interaction that can populate the RHNs, with some consequences on the asymmetry produced. In particular, we expect that if the RHNs are brought in thermal equilibrium at a temperature such that $z_{eq} \ll z_{osc}$, namely before the time it takes for the RHN state to oscillate once, the asymmetry gets cut off. In the following we will estimate how the new interaction modify the abundance of RHNs. Furthermore, we will focus in the temperature range $T > 100$ GeV, i.e. before the EW sphaleron freeze-out, since we know that in the ARS mechanism the lepton asymmetry is produced before the electroweak phase transition.
We assume that the scalar Φ is at thermal equilibrium with the plasma after reheating, and after the

[6] Here we are taking $\mu_\phi^2 \rightarrow -\mu_\phi^2$ since we are in the configuration which breaks the symmetry.

SSB of the $U(1)_{B-L}$ symmetry we have two possible interactions: $\phi \leftrightarrow NN$ and $\phi\phi \leftrightarrow NN$. We can argue that the decay of the scalar particle is kinematically forbidden for $M_\phi < 2m_N$ i.e. for $\sqrt{\lambda_\phi} < y_N$ and so in this case the $2 \leftrightarrow 2$ would dominate, but we must take into account the fact that we are assuming that the scalar singlet is at thermal equilibrium with the thermal plasma, therefore it will receive some thermal correction to the mass[7]. In fact, from the effective potential at one-loop (see App. E) we find that the scalar mass is proportional to the temperature (see App. E.3 for details in the computation) and we obtain:

$$M_\Phi(T)^2 = M_\Phi(0)^2 + c_\phi T^2, \tag{5.60}$$

where

$$c_\phi = \frac{1}{12}(2\lambda_{H\phi} + 4\lambda_\phi). \tag{5.61}$$

At this point we can compute the interaction rate for the scalar decay and the $2 \to 2$ process to determine the time of equilibration of the RHNs, defined as the time at which the total RHN production rate is equal to the Hubble expansion rate.
First we focus on the scalar decay:

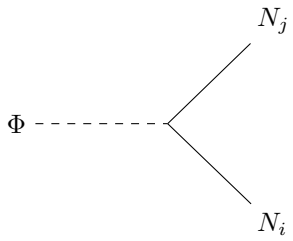

By computing the decay rate in the center of mass frame we find (see App. F.1):

$$\Gamma = \frac{1}{2M_\phi^2} y_N^2 (M_\phi^2 - 4m_N^2) \frac{1}{8\pi} \sqrt{1 - \frac{4m_N^2}{M_\phi^2}} = \frac{y_N^2}{16\pi} M_\phi \left(1 - \frac{4m_N^2}{M_\phi^2}\right)^{3/2}. \tag{5.62}$$

Now, to compute the thermal averaged decay rate, defined as

$$\langle \Gamma_{i \to jk} \rangle = \frac{\int \frac{d^3\vec{p}_i}{(2\pi^3)} f_i^{\text{eq}} \Gamma}{\int \frac{d^3\vec{p}_i}{(2\pi)^3} f_i^{\text{eq}}}, \tag{5.63}$$

we assume that the scalar ϕ follows a Maxwell-Boltzmann equilibrium distribution and we find (see App. F.1 for details in the computation):

$$\langle \Gamma_{\phi \to NN} \rangle = M_\phi(T) \left(1 - \frac{4m_N^2}{M_\phi(T)^2}\right)^{3/2} \frac{\mathcal{K}_1(M_\phi(T)/T)}{\mathcal{K}_2(M_\phi(T)/T)}. \tag{5.64}$$

To determine whether this process bring the RNOs at thermal equilibrium or not, we need to compare the averaged rate with the Hubble parameter $H = T^2/M_0$, with $M_0 = 7.1 \times 10^{17}$ GeV, in a radiation dominated universe. In order to do that we need to fix the zero temperature scalar mass $M_\Phi(0) = \sqrt{\lambda_\phi} v_\phi$, i.e. the vev v_ϕ and the coupling λ_ϕ, and the RHNs mass $m_N = y_N v_\phi$. We also need to fix the coupling $\lambda_{H\phi}$, since this coupling enters into thermal scalar mass, see Eq. 5.61.

[7] It is worth noting that the RHNs do not develop a thermal mass since they are produced out of equilibrium, i.e. they do not interact with the thermal plasma.

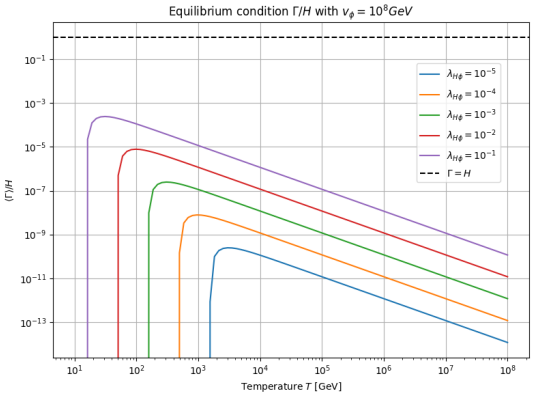

(a) $v_\phi = 10^8$ GeV, $y_N = 10^{-8}$, $\lambda_\phi = 10^{-18}$.

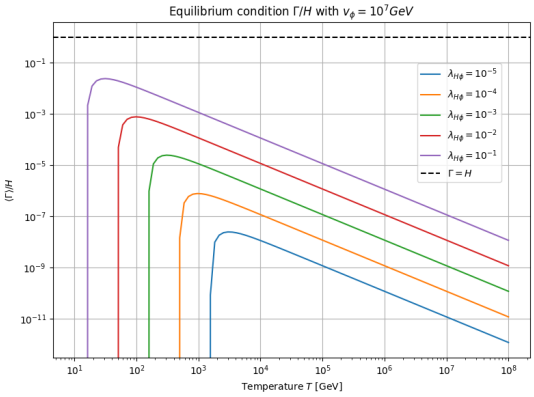

(b) $v_\phi = 10^7$ GeV, $y_N = 10^{-7}$, $\lambda_\phi = 10^{-14}$

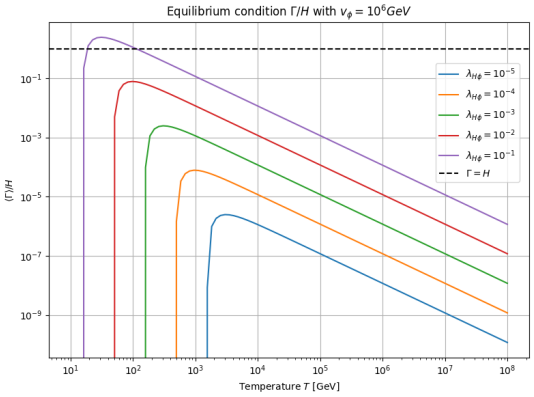

(c) $v_\phi = 10^6$ GeV, $y_N = 10^{-6}$, $\lambda_\phi = 10^{-14}$

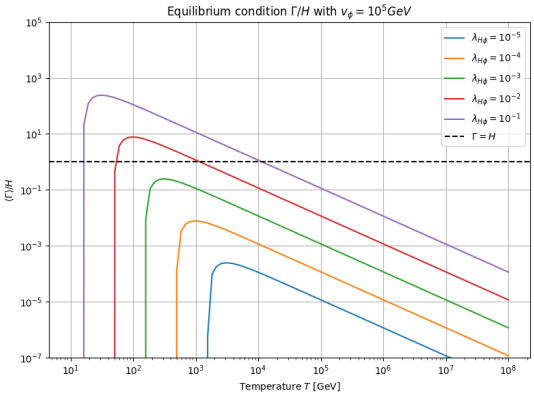

(d) $v_\phi = 10^5$ GeV, $y_N = 10^{-5}$, $\lambda_\phi = 10^{-10}$

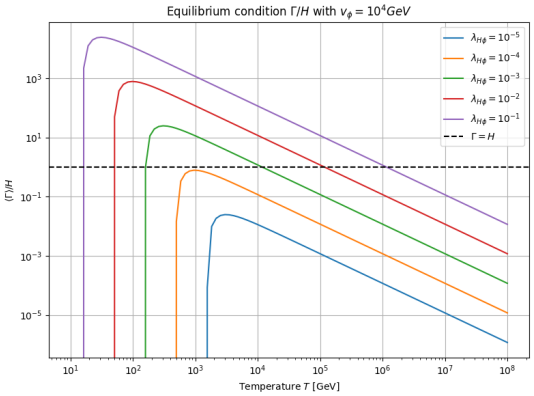

(e) $v_\phi = 10^4$ GeV, $y_N = 10^{-4}$, $\lambda_\phi = 10^{-10}$.

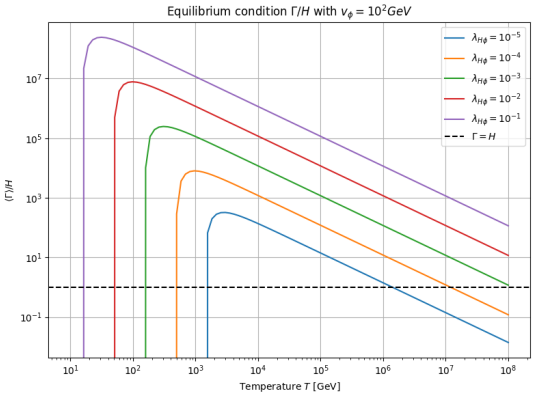

(f) $v_\phi = 10^2$ GeV, $y_N = 10^{-2}$, $\lambda_\phi = 10^{-6}$

Figure 5.2: $\langle \Gamma_{\phi \to NN} \rangle / H$ ratio as a function of the temperature T with fixed M_ϕ^0 and m_N.

As a benchmark point, we first consider the scalar mass $M_\phi^0 = 0.1$ GeV and the RHNs mass

$m_N = 1$ GeV[8]. With this choice we can then vary the scalar vev and the couplings y_N and λ_ϕ to find the equilibrium temperature. In the plots listed in Fig. 5.2 we show the ratio $\langle\Gamma_{\phi\to NN}\rangle/H$ for different values of the $\lambda_{H\phi}$ coupling. When this fraction is higher than 1, the process is in thermal equilibrium with the plasma. From these plots we see that for VEV v_ϕ up to $(10^6 - 10^7)$ GeV the scalar decay brings the RHNs in thermal equilibrium before the electroweak phase transition. Therefore, we expect that when the symmetry spontaneously breaks at $T \lesssim 10^6$ GeV, then the scalar decay brings the RHNs in thermal equilibrium before EWPT. This situation holds for this particular choice of m_N and $M_\phi(0)$; i.e. the equilibrium temperature depends on four free parameters: y_N, v_ϕ, λ_ϕ and $\lambda_{H\phi}$. In the following sections, we will explore the phenomenology for other parameter choices.
For the process $\phi\phi \to NN$ we have the diagrams in Fig. 5.3.

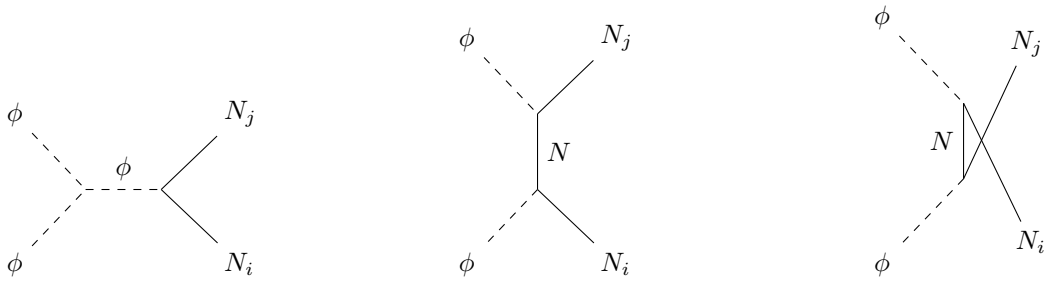

Figure 5.3: Feynman diagrams contributing to the $\phi\phi \to NN$ interaction.

As in the previous case, we determine the interaction rate $\Gamma_{\phi\phi\to NN} = n_\phi^{eq}\langle\sigma v_{12}\rangle$ and we compare it with the Hubble parameter in order to see whether this process brings the RHNs in thermal equilibrium or not. The computation is shown in App. F.2 and the results are showed in Fig. 5.4. From these results we see that the $2 \to 2$ process does not bring the RHNs in thermal equilibrium for VEV up to $v_\phi \simeq 10^2$ GeV. We can notice that if the symmetry is not broken up until $T \simeq 10^2$ GeV, then the RHNs are not massive and they cannot oscillate. Therefore, for this VEV the lepton asymmetry will not be generated before sphaleron freeze-out. Thus, we can conclude that the scalar decay is the dominant process, thus we do not include further the $2 \to 2$ processes in out analysis.

From these considerations we expect that the interactions with the new scalar singlet will bring the RHNs in thermal equilibrum before t_{osc}, consequently the asymmetry will be erased. Before computing the dominant contribution coming from the scalar ϕ decay, we must consider also the interaction with the Majoron. In fact, from the Lagrangian in Eq. 5.59 we see that we have also an interaction term between the Majoron θ and the RHNs. In particular we have that the Majoron will be at thermal equilibrium with the plasma, so it may decay in two RHNs as ϕ. However, thanks to the Goldstone theorem, the Majoron has a vanishing mass at tree level. Therefore the Majoron decay is kinematically forbidden. We can argue that the Majoron may have some thermal correction to the mass, but to compute the corrections to the ϕ masses we have chosen a vacuum such that the Majoron has no thermal correction (see App. E.3). Actually, there may also be another process contributing to the population of the RHNs sector, i.e. the t and u channels of the process $\theta\theta \to NN$, see Fig. 5.5.

[8]We choose these masses for the scalar and the RHNs because in ARS leptogenesis RHNs masses are in the range $m_N \in [0.1, 100]$ GeV and if $M_\phi(0) > 2m_N$ the scalar decay would be the dominant process. Therefore, we focus in the case with $M_\phi(0) < m_N$ to see if the scalar decay remains the leading contribution.

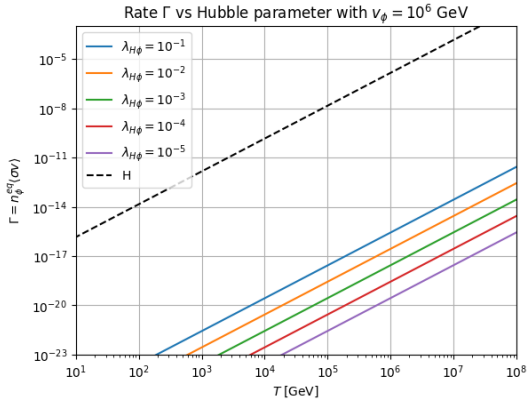

(a) $v_\phi = 10^6$ GeV, $y_N = 10^{-6}$, $\lambda_\phi = 10^{-14}$

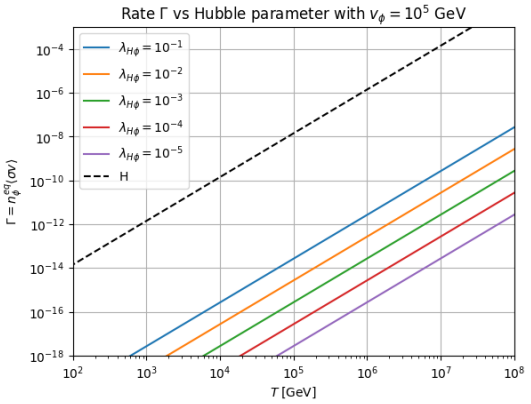

(b) $v_\phi = 10^5$ GeV, $y_N = 10^{-5}$, $\lambda_\phi = 10^{-10}$

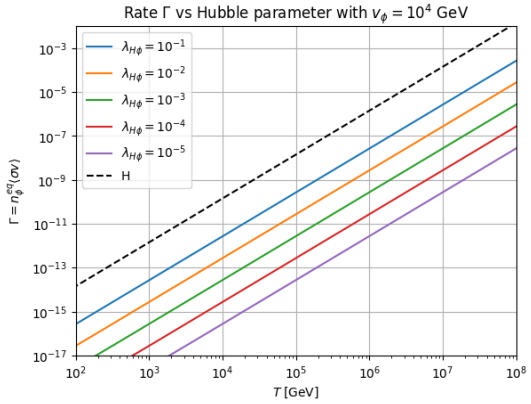

(c) $v_\phi = 10^4$ GeV, $y_N = 10^{-4}$, $\lambda_\phi = 10^{-10}$

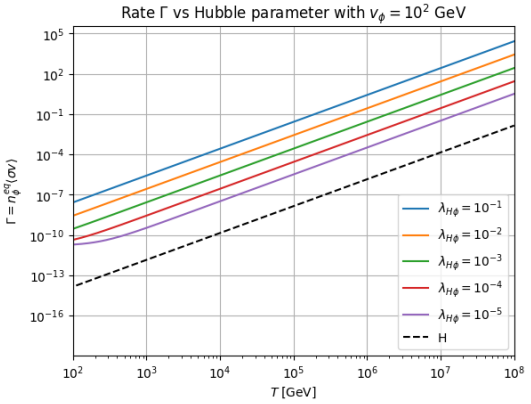

(d) $v_\phi = 10^2$ GeV, $y_N = 10^{-2}$, $\lambda_\phi = 10^{-6}$

Figure 5.4: $\langle\Gamma_{\phi\phi\to NN}\rangle/H$ ratio as a function of the temperature T with fixed M_ϕ^0 and m_N.

We expect that these processes will bring the RHNs at thermal equilibirum. Indeed, we start with vanishing abundance of RHNs and they will be populated by the process $\theta\theta \to NN$. This process is kinematically allowed since the majorons θ are at thermal equilibrium with the plasma and, from the equipartition theorem, we know that for a relativistic gas of bosons $\langle E_\theta\rangle \approx 3T$, hence $E_{\rm cm} \simeq 2\langle E_\theta\rangle \approx 6T \gg 2m_N$ if $T \gtrsim 100$GeV, therefore, the condition $E_{cm} > 2m_N$ is satisfied[9] since in the c.o.m. frame $\vec{p}_1 + \vec{p}_2 = \vec{p}_3 + \vec{p}_4 = \vec{0}$, so $E_{cm} = E_1 + E_2$. As the RHN sector is being populated, the inverse process $NN \to \theta\theta$ will also contribute and RHNs will reach thermal equilibrium. Consequently, if we consider also these processes the asymmetry will be further reduced. Therefore, in our model we will consider only the decay of the ϕ scalar, which is the dominant process and it is enough to see the erasing of the asymmetry. Before discussing this process, we can argue that the interaction $NN \to \theta\theta$ could bring the RHNs out of thermal equilibrium with some consequences for the lepton asymmetry. But this would happen only when the condition $E_{cm} > 2m_N$ does not hold anymore, i.e. when $T \lesssim m_N$ (far below the EWSB), so this would not affect the erasure of the lepton asymmetry, which takes place via ϕ decays at much higher scales.

[9]Recall that we are in the regime $T > 100$ GeV and RHN are relativistic.

Figure 5.5: Feynman diagrams for the process $NN \to \theta\theta$

5.2.2 Boltzmann Equation with scalar decay

As we have seen in the previous section, the scalar has an effective mass that is proportional to the temperature. Therefore, the condition $M(T) \geqslant 2m_N$ is satisfied and the scalar ϕ can decay in two sterile neutrinos. This additional interaction will modify the Boltzmann Equation for the R_N matrix which becomes:

$$\frac{dR_N}{dt} = ARS + \langle \mathcal{I}_{NN\leftrightarrow\phi} \rangle, \tag{5.65}$$

where the collisional term resulting from the process $N(E_1) + N(E_2) \leftrightarrow \phi(E_3)$ can be written as [86]:

$$\begin{aligned} \mathcal{I} = \frac{1}{2E_1} \int \frac{d^3\vec{p}_2}{(2\pi)^3 2E_2} \frac{d^3\vec{p}_3}{(2\pi)^3 2E_3} (2\pi)^4 \delta^4(p_1 + p_2 - p_3) \times |\mathcal{M}|^2 \\ \times \frac{1}{2}\big(f_\phi\{1-\rho_1, 1-\rho_2\} - (1+f_\phi)\{\rho_1, \rho_2\}\big), \end{aligned} \tag{5.66}$$

where f_i are the distribution functions. To simplify the computations we neglect quantum statistic and we assume flavour universality of the coupling y_N. In this way $(1 + f_i) \simeq 1$ and the collisional term becomes

$$\mathcal{I} = \frac{1}{2E_1} \int \frac{d^3\vec{p}_2}{(2\pi)^3 2E_2} \frac{d^3\vec{p}_3}{(2\pi)^3 2E_3} (2\pi)^4 \delta^4(p_1 + p_2 - p_3) \times |\mathcal{M}|^2 \times \frac{1}{2}\big(2f_\phi - \{\rho_1, \rho_2\}\big). \tag{5.67}$$

The momentum averaged collisional term reads:

$$\begin{aligned} \langle \mathcal{I} \rangle = \frac{1}{\int \frac{d^3\vec{p}_1}{(2\pi)^3} f_1^{eq}} \int \frac{d^3\vec{p}_1}{(2\pi)^3 2E_1} \frac{d^3\vec{p}_2}{(2\pi)^3 2E_2} \frac{d^3\vec{p}_3}{(2\pi)^3 2E_3} (2\pi)^4 \delta^4(p_1 + p_2 - p_3) \times |\mathcal{M}|^2 \\ \times \frac{1}{2}\big(2f_\phi - 2f_1^{eq} f_2^{eq} R_N^2\big), \end{aligned} \tag{5.68}$$

where we have used the ansatz $\rho(x, y) = f_{FD}(y) R_N(x)$. Now, from Eq. 5.63 we can notice that for the direct and inverse decay respectively we have

$$\langle \Gamma_{\phi\to NN} \rangle = \frac{\sum_{spins} \int d\Pi_1 d\Pi_2 d\Pi_3 |\mathcal{M}_{1\to 23}|^2 (2\pi)^4 \delta^{(4)}(p_{fin} - p_{in}) f_\phi^{eq}}{n_\phi^{eq}}, \tag{5.69}$$

$$\langle \Gamma_{NN\to\phi} \rangle = \frac{\sum_{spins} \int d\Pi_1 d\Pi_2 d\Pi_3 |\mathcal{M}_{23\to 1}|^2 (2\pi)^4 \delta^{(4)}(p_{fin} - p_{in}) f_N^{eq} f_N^{eq}}{n_N^{eq} n_N^{eq}}, \tag{5.70}$$

where $n_i = \int \frac{d^3\vec{p}_i}{(2\pi)^3} f_i^{eq}$. From the principle of detailed balance we have that

$$f_1^{eq} = f_2^{eq} f_3^{eq}, \tag{5.71}$$

and unitarity yields the equation [87]:

$$\sum_{spins} \int d\Pi_1 d\Pi_2 d\Pi_3 |\mathcal{M}_{1\to 23}|^2 (2\pi)^4 \delta^{(4)}(p_{fin} - p_{in}) = \sum_{spins} \int d\Pi_1 d\Pi_2 d\Pi_3 |\mathcal{M}_{23\to 1}|^2 (2\pi)^4 \delta^{(4)}(p_{fin} - p_{in}), \tag{5.72}$$

hence we obtain

$$\langle \Gamma_{\phi\to NN} \rangle n_\phi^{eq} = \langle \Gamma_{NN\to\phi} \rangle n_N^{eq} n_N^{eq}. \tag{5.73}$$

Now we employ the principle of detailed balance in the collisional integral by inserting Eq. 5.71 in Eq. 5.68 and we obtain

$$\begin{aligned} \langle \mathcal{I} \rangle = & \frac{1}{\int \frac{d^3\vec{p}_1}{(2\pi)^3} f_1^{eq}} \int \frac{d^3\vec{p}_1}{(2\pi)^3 2E_1} \frac{d^3\vec{p}_2}{(2\pi)^3 2E_2} \frac{d^3\vec{p}_3}{(2\pi)^3 2E_3} (2\pi)^4 \delta^4(p_1 + p_2 - p_3) \times |\mathcal{M}|^2 \\ & \times \frac{1}{2}\big(2f_\phi - 2f_\phi^{eq} R_N^2\big) \\ & \frac{1}{\int \frac{d^3\vec{p}_1}{(2\pi)^3} f_1^{eq}} \int \frac{d^3\vec{p}_1}{(2\pi)^3 2E_1} \frac{d^3\vec{p}_2}{(2\pi)^3 2E_2} \frac{d^3\vec{p}_3}{(2\pi)^3 2E_3} (2\pi)^4 \delta^4(p_1 + p_2 - p_3) \times |\mathcal{M}|^2 \\ & \times \frac{1}{2}\big(2f_\phi^{eq} - 2f_\phi^{eq} R_N^2\big), \end{aligned} \tag{5.74}$$

where in the last line we have used the fact that the distribution function for the scalar is $f_\phi = e^{-(E_\phi - \mu_\phi)/T}$, so we can write $f_\phi = f_\phi^{eq} e^{-\mu_\phi/T}$ and by assuming that $\mu_\phi = 0$ we get $f_\phi^{eq} = e^{-E_\phi/T}$.[10] Finally by inserting Eq. F.11 and using Eq. 5.73 in Eq. 5.74 we get

$$\frac{dR_N}{dt} = ARS + \frac{n_\phi^{eq}}{n_N^{eq}} \langle \Gamma_{\phi\to NN} \rangle (1 - R_N^2). \tag{5.75}$$

By inserting Eq. 5.62 in Eq. 5.75, and recalling that for n_ϕ^{eq} we use $f_\phi^{eq} = e^{-E_\phi/T}$ (see Eq. F.25 in App. F.1), we obtain the new Boltzmann Equation for ARS Leptogenesis with the additional scalar

$$\frac{dR_N}{dt} = \langle ARS \rangle + \frac{1}{n_N^{eq}} \frac{y_N^2}{32\pi^3} T M_\phi^3 \left(1 - \frac{4m_N^2}{M_\phi^2}\right)^{3/2} \mathcal{K}_1\left(\frac{M_\phi}{T}\right)(1 - R_N^2), \tag{5.76}$$

where for n_N^{eq} the expression

$$n_N^{eq} = \int \frac{d^3\vec{p}}{(2\pi)^3} f_{FD}^{eq} = g \frac{3}{4} \frac{T^3}{\pi^2} \zeta(3), \tag{5.77}$$

where $g = 2$ for a Majorana particle.

5.3 Numerical Analysis

Having derived the new BE including the additional interaction from the scalar decay $\phi \to NN$, we now aim to solve these equations to compare what is different in the evolution of the N_1 number density

[10] we assume vanishing chemical potential since we are assuming no asymmetry between ϕ and ϕ^*.

and, consequently of the BAU, in the standard ARS scenario with that in the case where the N_1 mass is dynamically generated. We consider the scenario where ϕ is at thermal equilibrium with the thermal plasma. From the scalar potential (see Eq. 5.43) we see that the interaction of Φ with the Higgs doublet H could bring Φ at thermal equilibrium, and, by a naive dimensional analysis we find that the coupling $\lambda_{H\phi}$ must be $\lambda_{H\phi} > 10^{-4}$ to have Φ at thermal equilibrium at temperatures higher than T_{ew}[11], i.e. before sphaleron freeze-out. From these considerations we fix $\lambda_{H\phi} = 10^{-2}$, since with this choice we have that Φ is at thermal equilibrium for $T < 10^9$ GeV. At temperatures T_ϕ the scalar Φ develops its vev v_ϕ and, for simplicity, we assume $T_\phi = v_\phi$ with $T_\phi > T_{ew}$, since we require that the RHNs acquire a mass before EWPT.
To solve the new Boltzmann Equations 5.76 we make use of the latest version of the ULYSSES Python package [88, 89], which has been modified to account for the contributions to the RHN number density due to the scalar decay.

5.3.1 Model parametrization

First we consider the standard ARS model with the Lagrangian given in Eq. 5.1. At low temperatures, $T \ll M_N$, the SM neutrinos acquire a mass in the effective theory, see Eq. 2.33. In Sec. 2.4 we have already noticed that at least two Heavy Neutral Leptons are necessary to explain the two observed mass splittings in the active neutrino sector, therefore we focus on the minimal scenario with two heavy neutrinos. We choose the mass of the RHN N_1 to be $M_1 \simeq 0$ while the masses of the other two RHNs are $M_2 \simeq M_3$. Hence, we are in the case of two right-handed neutrinos with quasi-degenerate masses. The masses of the light neutrinos m_ν are constrained by the neutrino oscillation experiments (neutrino mass squared splittings are taken from the central values of NuFIT 5.1 global fit data [90]). Out of the 9 parameters in the light neutrino mass matrix, 5 are already measured, namely the two mass differencies and three mixing angles. The remaining unknown parameters are the mass of the lightest neutrino $m_{1/3}$, two Majorana phases and the Dirac phase δ. The measured low-energy parameters imply that the choice of heavy neutrino masses M_N and Yukawa couplings F is not completely free. Also, the magnitudes of the Yukawa couplings $F_{\alpha 2}$, $F_{\alpha 3}$ are crucial for successful leptogenesis. To better understand the connection between the Yukawa couplings and physical parameters, we work in Casas-Ibarra parametrization (see Subsec. 2.4.1) for the type I seesaw [32].

$$F = \frac{i}{v_{ew}} U_{\rm PMNS} \sqrt{\hat{m}_\nu} R \sqrt{\hat{M}_N}, \tag{5.78}$$

where $\hat{m}_\nu$ is the diagonal neutrino mass matrix, $\hat{M}_N$ is the diagonal mass matrix for RHNs and U is the PMNS matrix, see Eq. 2.4. Therefore, what we need to specify, besides the PMNS matrix parameters and the lightest neutrino mass $m_{1/3}$, are the six degrees of freedom of the orthogonal matrix R defined in Eq. 2.41 and the RHNs masses. To choose the real parameters x_i and y_i we have considered the mixing between active and sterile neutrinos. In fact, the important parameters for phenomenology of sterile neutrinos N_2 and N_3 are their masses $M_{2,3}$ and the mixing matrix Θ. The latter is crucial to specify the strength of interactions with other SM particles. In the case of two heavy neutrinos there is only one relevant Majorana phase in the PMNS matrix in Eq. 2.4. We parametrize it as $\eta = \frac{1}{2}(\alpha_{21} - \alpha_{31})$ for normal, and $\eta = \frac{1}{2}\alpha_{21}$ for inverted neutrino mass hierarchy with $\eta \in [0, 2\pi]$. The light neutrino mass matrix $\sqrt{\hat{m}_\nu} = \text{diag}(m_1, m_2, m_3)$ with $m_1 = 0$ for NO, and $m_2 = 0$ for IO. In the model with two

[11] To find this parameter we have considered a $2 \leftrightarrow 2$ process involving 2 Higgs doublets and 2 scalars, and by requiring $\Gamma \gtrsim H$ we find the condition $T^3 \lambda_{H\phi}/T^2 \gtrsim T^2/M_0$.

right-handed neutrinos the matrix R (see Eq. 2.41) depend on the neutrino mass hierarchy and we have

$$R^{\rm NO} = \begin{bmatrix} 0 & 0 \\ \cos\omega & \sin\omega \\ -\xi\sin\omega & \xi\cos\omega \end{bmatrix} \qquad R^{\rm IO} = \begin{bmatrix} \cos\omega & \sin\omega \\ -\xi\sin\omega & \xi\cos\omega \\ 0 & 0 \end{bmatrix}. \tag{5.79}$$

with a complex angle $\omega = x_1 + iy_1$ and the discrete parameter $\xi = \pm\xi$. The complex angle ω parametrizes the misalignment between sterile neutrino mass and interaction eigenstates. Notice that when $\omega = 0$, the Yukawa interactions can be diagonalized in the sterile neutrino mass basis, and the interference necessary for leptogenesis is absent. The change of the sign of ξ can be compensated by $\omega \to -\omega$ along with $N_3 \to -N_3$, so we fix $\xi = +1$ [32].
As a consequence of the seesaw mechanism, the heavy neutrino mass eigenstates are mixed with the doublet neutrinos, and can interact with the rest of the standard model, the interaction states $\nu_{L\alpha}$ are superpositions of the mass eigenstates ν_i and N_I:

$$\nu_{L\alpha} = [U_\nu]_{\alpha i}\nu_i + \Theta_{\alpha i}N_I^c. \tag{5.80}$$

The mixing angle between a heavy neutrino N_I and the active neutrinos $\nu_{L\alpha}$ is expected to be small, and is approximately given by

$$\Theta_{\alpha i} \simeq \frac{vF_{\alpha i}}{M_I}. \tag{5.81}$$

The mixing angle appears in amplitudes for heavy neutrino production, which means that the heavy neutrino production is suppressed by

$$U^2_{\alpha i} \equiv |\Theta_{\alpha i}|^2. \tag{5.82}$$

The overall mixing between the heavy and light neutrinos can be quantified by introducing the parameter

$$U^2 \equiv \sum_{\alpha i} U^2_{\alpha i}. \tag{5.83}$$

The total mixing angle, defined in Eq. 5.83 can be written as

$$U^2 = \frac{\sum_i m_i}{M}\cosh\left(2\mathcal{I}m\omega\right). \tag{5.84}$$

CP violation

CP violation is an effect related to the presence of physical complex couplings that generically involve many flavor parameters. Within the considered Casas-Ibarra parametrization, the CP-violating matrices can be either $U_{\rm PMNS}$, R or both. In particular, there are three source of CP violation: the Majorana phase η, the Dirac phase δ and the complex sterile neutrino mixing angle ω. According to Sakharov conditions, a source of CP violation is required to generate a baryon asymmetry. Except where δ, η and $\mathcal{I}m(\omega)$ all vanish, there is generically an $\mathcal{O}(1)$ phase contributing to baryogenesis coming from a combination of these individual phases [80].
All the CP-violating observables should be flavor basis invariant and be sensitive to the physical phases, the so-called CP-violating invariants. A well-known example is that of the Jarlskog invariant, defined in Eq. 2.6, which determines the magnitude of CP-violation in $\nu_\alpha \to \nu_\beta$ and $\bar\nu_\alpha \to \bar\nu_\beta$ oscillations ($\alpha \neq \beta$). Several CP-invariants can be derived in the type-I seesaw extension of the SM starting from the flavor parameters in the model, i.e. the physical parameters in the matrices F and M_N. The CP invariants relevant for leptogenesis can be constructed out of two building blocks [79]: $J^{LNC}_\alpha = \Im[F^*_{\alpha 1}F_{\alpha 2}(F^\dagger F)_{21}]$ and $J^{LNV}_\alpha = \Im[F^*_{\alpha 1}F_{\alpha 2}(F^\dagger F)_{12}]$ (see also Refs. [91–93]).

In the following, we focus in the case of low-energy CP violation [89], i.e. CP violation solely from the Dirac phase. Therefore, in this case the only CP-violating matrix is $U_{\rm PMNS}$, with R matrix being CP-conserving. This situation can be achieved by taking $x_1 = k\pi$ and $y_1 \neq 0$[12]. The phases in the PMNS matrix should be CP-violating, i.e. $\delta \neq 0, \pi$ and/or $\alpha_{21} \neq k_{21}\pi$ and/or $\alpha_{31} \neq k_{31}\pi$, with $k_{21} = 0, 1, 2, ...,$, $k_{31} = 0, 1, 2, ...$

Parameter scan standard ARS leptogenesis

First, we will reproduce the parameter space in the classical ARS model, namely without the additional scalar. In order to calculate the baryon asymmetry yield in this scenario we solve the ARS BE (see Eq. 5.14) and use the ULYSSES Python package. Once we have reproduced the parameter space, we choose sets of parameters such that the corresponding mixing U^2 is in the region of viable leptogenesis. In this work we have focused on the minimal scenario with two heavy neutrinos: N_2 and N_3, with $M_3 > M_2 \sim (0.1 - 100)$ GeV and a mass splitting $\Delta M \equiv M_3 - M_2 \ll M_3$ in the range $\Delta M/M_2 \sim (10^{-10} - 10^{-8})$.

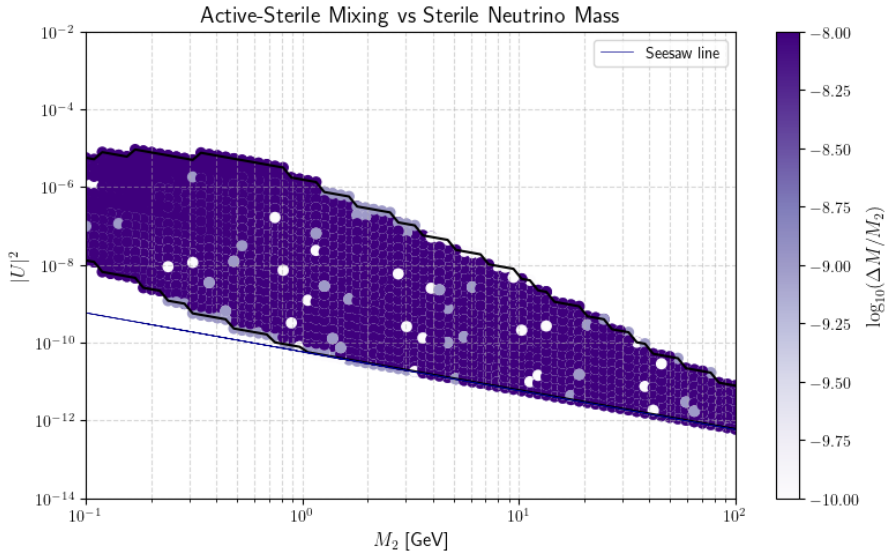

Figure 5.6: The range of the total mixing angle U^2 consistent with both the seesaw mechanism and leptogenesis as a function of RHNs' mass M. Here we considered the NO case, with $x_1 = 0$, $\delta = 270$, $\alpha_{21} = \pi$, $\alpha_{31} = 0$.

The parameter space of leptogenesis is quite large, in total we have six unknown parameters: the average mass M, defined as $(M_2 + M_3)/2$, the mass splitting ΔM, one Dirac and one Majorana phases of the PMNS matrix; the real and imaginary parts of the angle $\omega = x_1 + iy_1$. Instead of directly constraining these parameters, we see how they are related to the experimentally observable quantities. Among these the most relevant are the masses of the heavy neutrinos and their mixing angles. These are particularly important for direct searches as the size of the mixing angle determines the number of heavy neutrinos that can be produced [32]. Also, the condition of reproducing both the baryon

[12] We focus on this scenario since it is associated with relative large values of the mixing U^2 and we are interested in connecting with experimental searches of heavy Majorana neutrinos, but there are also other possible settings leading to low-energy CP-violation, see Refs. [89, 94].

asymmetry of the universe and the light neutrino masses imposes constraints on the allowed mixing angles of the heavy neutrinos. To perform the study of the parameter space we follow Ref. [89] and we set the phases $\delta = 3\pi/2$, $\alpha_{21} = \pi$, $\alpha_{31} = 0$ and $\mathcal{R}e(\omega) = x_1$. Once these are fixed, we scan over the remaining parameters. We focus exclusively on the normal hierarchy as a benchmark, since our results also qualitatively hold in the inverted hierarchy and easily generalize to that scenario. We limit the RHNs masses to the range $(0.1 - 100)$ GeV with splitting $\Delta M/M_2$ in the range $(10^{-10} - 10^{-8})$ and we vary y_1 to the range $(-10, 10)$ rad. The results are showed in Fig. 5.6. The upper (lower) solid black line is the curve of maximal (minimal) mixing $|U|^2$ compatible with viable leptogenesis. The area between the two black lines correspond to successful Leptogenesis for certain values of $\Delta M/M_2$. The region under the blue line (seesaw line) is forbidden in the type-I seesaw mechanism of light neutrino mass generation. In fact, by re-expressing the seesaw relation $m_\nu = -m_D M_M^{-1} m_D^T$ (see Eq. 2.33) with Eq. 5.81 as $m_\nu = -\Theta M_M \Theta^T$ it is obvious that m_ν in the seesaw relation vanishes identically if all $\Theta_{\alpha i}$ are zero. Therefore, the requirement to explain the neutrino masses $m_{\nu,i}$ must impose a lower bound on the mixing $|U|^2$ [95]. This line can be obtained by taking a vanishing imaginary part $\mathcal{I}m\omega = y_1$ in Eq. 5.84.

At this point we can perform a numerical analysis to see how the scenario changes with the introduction of the scalar singlet. In order to do that, we first fix the parameters such that the corresponding mixing is in the region of viable leptogenesis. Therefore, we fix θ_{ij} according to experimental data (see Sec. 2.2.1) and we set the Dirac and Majorana phases as we already did to produce the parameter scan. Then, we need to fix the parameters x_1 and y_1 to find the corresponding mixing $|U|^2$. In the ARS with the additional singlet scenario, we also need to fix other parameters, namely the couplings y_N, $\lambda_{H\phi}$, λ_ϕ and the scalar vev v_ϕ. Fixing these parameters corresponds to choose the RHNs masses and the scalar mass.

In the following, we first focus on some scenarios by fixing the RHNs masses and the scalar mass (at zero temperature). Then, we will conclude our analysis by performing a parameter scan to find the parameter space of viable leptogenesis with an additional scalar.

Table 5.1: Input parameter values.

Parameter	**Unit**	**Code input**	**Value**
δ	[°]	delta	270
α_{21}	[°]	a21	180
α_{31}	[°]	a31	0.0
θ_{23}	[°]	t23	48.59
θ_{12}	[°]	t12	33.84
θ_{13}	[°]	t13	8.66
x_1	[°]	x1	0.00
y_1	[°]	y1	40.107
x_2	[°]	x2	0.00
y_2	[°]	y2	0.00
x_3	[°]	x3	0.00
y_3	[°]	y3	0.00
$\log_{10}(m_{1/3})$	[eV]	m	-100
$\log_{10}(M_1)$	[GeV]	M1	-100
$\log_{10}(M_2)$	[GeV]	M2	0.0
$\log_{10}(M_3)$	[GeV]	M3	$4.343 \cdot 10^{-9}$

5.3.2 The case with $M_2 \simeq M_3 \simeq 1$ GeV

We start by considering the case with $M_2 \simeq M_3 \simeq 1$ GeV and $M_\phi = 10$ GeV. First, we assume Normal Hierarchy (NO), i.e. $m_1 < m_2 < m_3$. We choose the following set of parameters listed in Tab. 5.1. For these parameters we have mixing $|U|^2 = 1.26395 \cdot 10^{-10}$ and the baryon-to-photon ratio for standard ARS is $\eta_B = 8.13 \cdot 10^{-10}$. The ULYSSES code solves the BEs in terms of number densities of particles

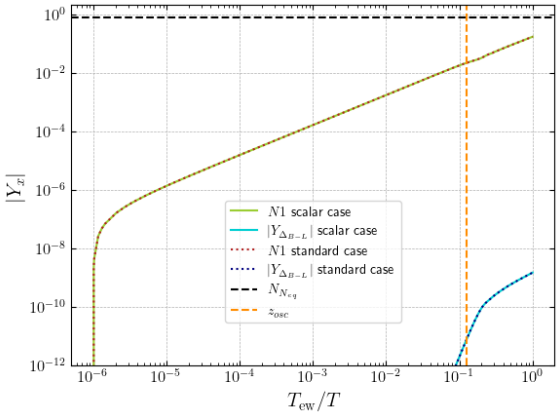

(a) $v_\phi = 10^8$ GeV, $y_N = 10^{-8}$, $\lambda_\phi = 10^{-14}$

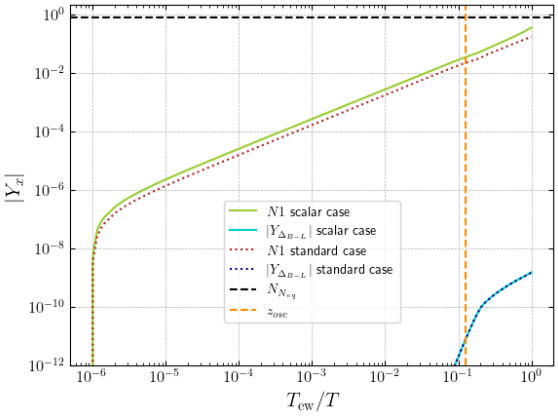

(b) $v_\phi = 10^6$ GeV, $y_N = 10^{-6}$, $\lambda_\phi = 10^{-10}$

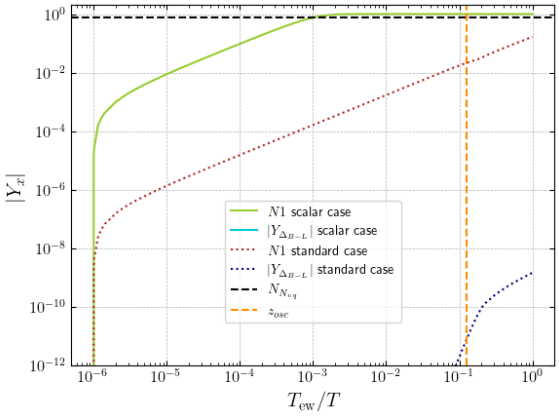

(c) $v_\phi = 10^4$ GeV, $y_N = 10^{-4}$, $\lambda_\phi = 10^{-6}$

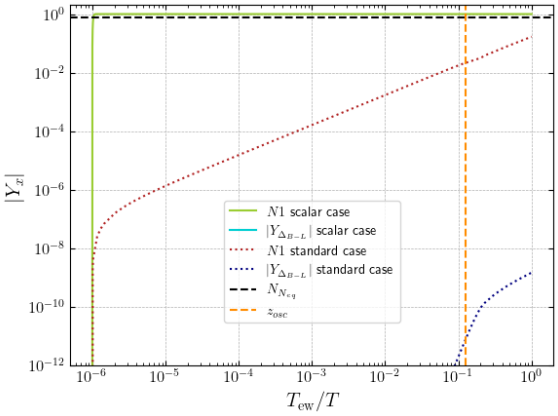

(d) $v_\phi = 10^2$ GeV, $\lambda_\phi = 10^{-2}$, $y_N = 10^{-2}$

Figure 5.7: Evolution of N_1 and B-L asymmetry Yields in NO case with parameters listed in Tab. 5.1. We have fixed $m_N = 1$ GeV and the zero temperature scalar mass $M_\phi(0) = 0.1$ GeV. The coupling $\lambda_{H\phi} = 10^{-2}$ for all four plots.

and particle asymmetries, normalized to a comoving volume containing one photon. Therefore, the normalized equilibrium abundance of the right-handed neutrino is the same as in Eq. 4.33. In our case we have $z \ll 1$, therefore we can use the approximation in Eq. C.1 and $N_N^{eq} = 3/4$, corresponding to the dashed black line in the plots. The results are plotted in Fig. 5.7. In the case $v_\phi > 10^6$ GeV we see that the Yukawa couplings are so small that the RHNs do not enter in thermal equilibrium, and therefore the asymmetry with the additional interaction is essentially the same as in the case without the scalar. In the range $v_\phi > 10^4$ GeV and $v_\phi < 10^6$ GeV we notice that the Yukawa couplings are big enough to bring the right handed neutrinos at thermal equilibrium, therefore the asymmetry gets washed-out.

In particular, we focus on the case with $v_\phi = 10^5$ GeV in Fig. 5.8: In this case, we observe that the

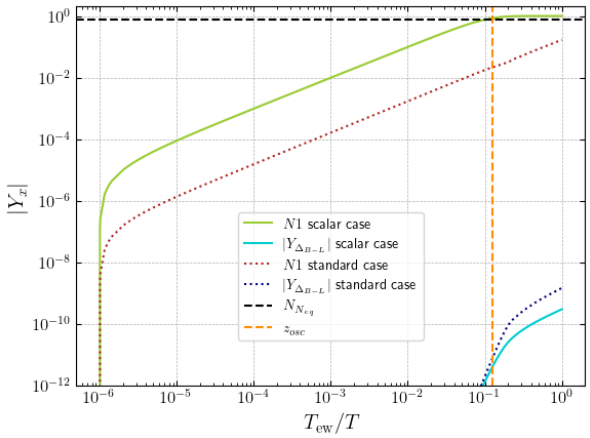

Figure 5.8: Evolution of N_1 and B-L asymmetry Yields in NO case with parameters listed in Tab. 5.1. In this case we have chosen: $v_\phi = 10^5$ GeV, $\lambda_\phi = 10^{-8}$, $M_\phi = 10$ GeV, $y_N = 10^{-5}$.

asymmetry in the scalar case start to decrease due to the fact that RHNs go in thermal equilibrium, but it is not completely washed out. This is due to the fact that RHNs go in thermal equilibrium at $z_{eq} \simeq z_{osc}$, implying that some RHNs could still oscillate and produce a lepton asymmetry.
For what concerns the range $v_\phi < 10^4$ GeV, the RHNs enter in thermal equilibrium at much higher temperatures, as plotted in Fig. 5.7c. In this case the asymmetry production is inhibited as the third Sakharov condition (departure from thermal equilibrium) is no longer satisfied. It is important to notice the case when $v_\phi \sim 10^2$ GeV, in Fig. 5.7d, the scalar obtains a mass near the EWPT, i.e. at $T_{ew}/T = 10^0$. In this way the RHNs are not massive until the EWPT but this would imply that they do not oscillate. So in this situation we have that the asymmetry is not generated since the first Sakharov condition (lepton number violation) is not satisfied. In fact if RHNs have no mass this would imply that we do not have a Majorana massive term in the Lagrangian, therefore no Lepton number violation. This situation is very interesting, since it would imply that in this case the Baryon asymmetry could be generated by another mechanism, but it would not be washed out by this process. Also, we can conclude that if the scalar singlet takes a vev after EWPT, it would generate a lepton asymmetry, but since sphalerons are already freezed-out, the lepton asymmetry is not converted into a baryonic one, hence, there is no visible effect today.
From these considerations we see that, as expected, the lepton asymmetry gets erased when the RHNs go in thermal equilibrium before the time z_{osc}, i.e. the dimensionless time corresponding to approximately one oscillation among the RHN mass eigenstates. This time, in the ULYSSES package is given by

$$z_{osc} \equiv \left(\frac{12 T_{ew}^3}{\Delta M_{32}^2 M_0} \right)^{1/3} . \tag{5.85}$$

Viceversa, if the RHNs equilibration time z_{eq}, i.e. the dimensionless time such that $\Gamma_N(z_{eq})/H(z_{eq}) \equiv 1$, is $z_{eq} > z_{osc}$[13] the asymmetry generation is not inhibited by the new RHN interaction and we obtain the same result as in the ARS standard case.
These graphs were obtained for a fixed value of $\lambda_{H\phi}$, but from the thermal mass of the scalar singlet in Eqs. 5.60 and 5.61 we see that the mass depends both on $\lambda_{H\phi}$ and λ_ϕ. Therefore, by varying these

[13] since $z_{osc} = T_{ew}/T_{osc}$ and $z_{eq} = T_{ew}/T_{eq}$ and in the early universe $T \propto t^{-1}$.

parameters we have that the RHNs enter in thermal equilibrium at different temperatures, modifying the picture that we have considered so far. In fact, fixing the zero temperature mass of the scalar equal to $M_\phi = 0.1$ GeV will imply that the λ_ϕ coupling will be small, since we are considering a vev v_ϕ in the range $T \in [10^8 \text{ GeV}; 10^2 \text{ GeV}]$. Therefore, from Eq. 5.61 we conclude that in this temperature range the term proportional to $\lambda_{H\phi}$ will dominate. For this reason, we fix the vev v_ϕ, the masses $M_\phi(0)$, m_N and the couplings y_N, λ_ϕ and by varying the coupling $\lambda_{H\phi}$ we find an interesting result, see Figs. 5.9.

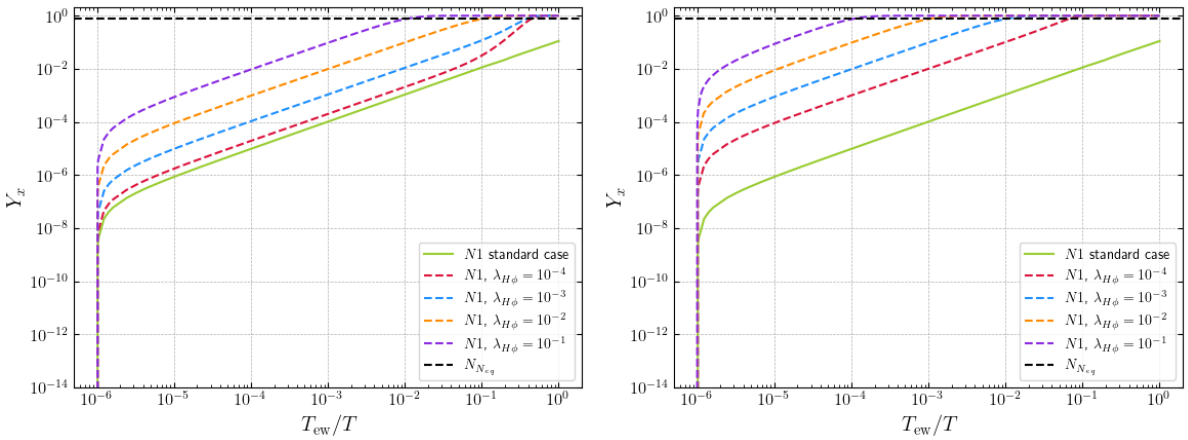

Figure 5.9: Dependence of the N_1 yield on the coupling $\lambda_{H\phi}$. On the left the other parameters were fixed as: $v_\phi = 10^5$ GeV, $\lambda_\phi = 10^{-8}$, $M_\phi = 10$ GeV, $y_N = 10^{-5}$. On the right the other parameters are: $v_\phi = 10^4$ GeV, $\lambda_\phi = 10^{-6}$, $M_\phi = 10$ GeV, $y_N = 10^{-4}$. The parameters used for the Casas-Ibarra parametrization are the ones listed in Tab. (5.1), and we have considered the NO case.

The plots in Fig. 5.9 show that RHNs enter thermal equilibrium at higher temperatures as $\lambda_{H\phi}$ increases.

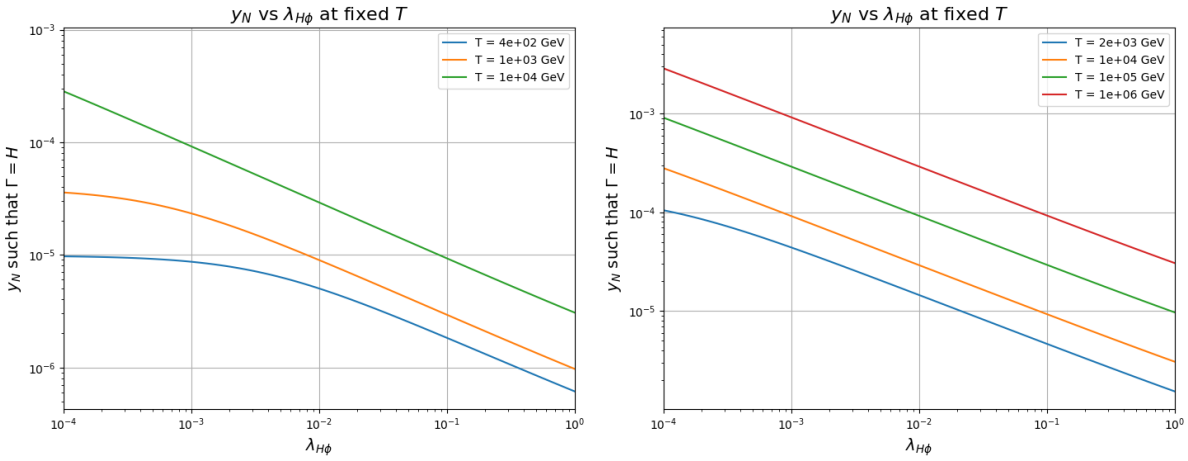

Figure 5.10: Dependence of the Yukawa couplings on the coupling $\lambda_{H\phi}$, for fixed $m_N = 1$ GeV and λ_ϕ. On the left we have fixed $v_\phi = 10^5$ GeV and $\lambda_\phi = 10^{-8}$. On the right we have the case for $v_\phi = 10^4$ GeV and $\lambda_\phi = 10^{-6}$.

This effect is important to highlight, since a naive dimensional analysis would suggest that RHNs

enter in thermal equilibrium at temperatures much higher than those actually observed. In fact, one could naively estimate that the condition $\Gamma \gtrsim H$ for the scalar decay is given by $y_N^2 T \gtrsim T^2/M_0$, where $M_0 \equiv M_{\rm Pl}/(1.66\sqrt{g_{*,s}}) = 7.1 \cdot 10^{17}$. But from this estimate we would find a much higher equilibrium temperature, e.g. choosing $y_N = 10^{-4}$ gives $T_{eq} \simeq 10^9$ GeV, i.e. $z = T_{ew}/T \simeq 10^{-7}$, which is significantly different from the result showed in Fig. 5.9, left panel. This discrepacy arises from the fact that the scalar mass $M_\phi(T)$ depends on $\lambda_{H\phi}$. This behavior may be verified by imposing the condition Γ/H in order to find a relation between y_N and $\lambda_{H\phi}$ for fixed λ_ϕ and T. Therefore, we consider the decay rate in Eq. F.26 and we compare it with the Hubble parameter. Then, we consider the temperatures in Fig. 5.9 such that the RHNs enter at thermal equilibrium and we find the expected behavior, as plotted in Fig. 5.10.
From the plots in Fig. 5.10 we see that for the selected temperatures T we obtain the expected Yukawa coupling corresponding to the $\lambda_{H\phi}$ value in the plots in Fig. 5.9. Notice that in the left panel we have selected three temperatures since in the case with $v_\phi = 10^5$ GeV RHNs go in thermal equilibrium at the same temperature for the choices $\lambda_{H\phi} = 10^{-4}$ and $\lambda_{H\phi} = 10^{-3}$ (see left panel Fig. 5.9).

At this point we want to see if our considerations are valid also for different zero temperature masses for the scalar ϕ. Since the mixing between active and sterile neutrino does not depend only on the Yukawa matrix Y, the Higgs vev and the RHNs masses, we take the same parameters listed in Tab. 5.1 and we change the scalar mass $M_\phi(0) = \sqrt{\lambda_\phi} v_\phi$.
From the plots in Fig. 5.11 we see that the situation is very similar to the previous with $M_\phi = 0.1$ GeV, (see Figs. 5.7, 5.8). In fact, the RHN reach thermal equilibrium for temperatures of the same order as

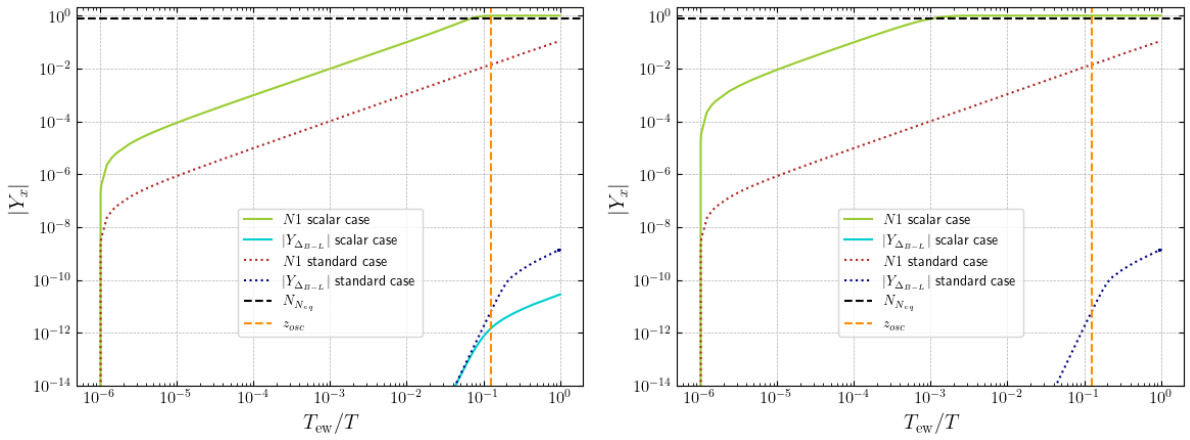

Figure 5.11: Evolution of N_1 and $B-L$ asymmetry Yields with a scalar mass (at zero temperature) $M_\phi(0) = 100$ GeV. Here we have the case of NO with parameters listed in Tab. 5.1. On the left we have chosen: $v_\phi = 10^5$ GeV, $\lambda_\phi = 10^{-6}$, $M_\phi = 100$ GeV, $y_N = 10^{-5}$. On the right: $v_\phi = 10^4$ GeV, $\lambda_\phi = 10^{-4}$, $y_N = 10^{-4}$. In both cases we have fixed $\lambda_{H\phi} = 10^{-2}$.

previous case. This is due to the fact that the chosen zero temperature mass $M_\phi(0)$ still is too small to have a visible effect, i.e. the dominant term still is $\lambda_{H\phi}$.

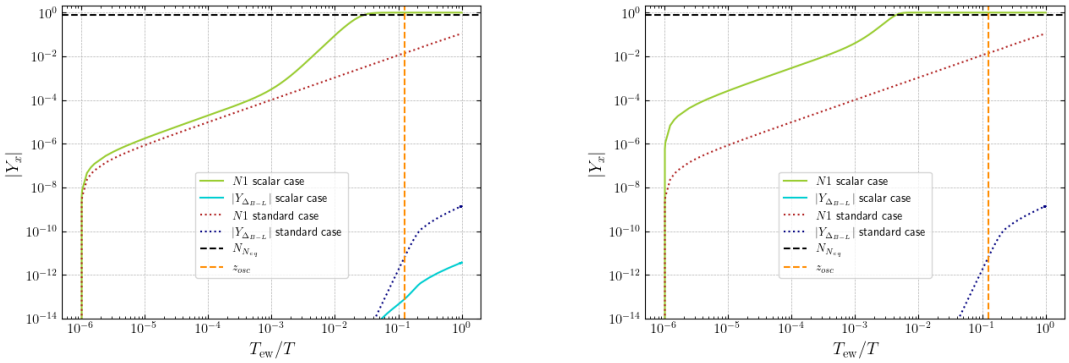

Figure 5.12: Evolution of N_1 and $B-L$ asymmetry Yields with a scalar mass $M_\phi(0) = 10^4$ GeV. Here we have the case of NO with parameters listed in Tab. 5.1. On the left we have chosen: $v_\phi = 10^6$ GeV, $\lambda_\phi = 10^{-4}$, $y_N = 10^{-6}$. On the right: $v_\phi = 10^5$ GeV, $\lambda_\phi = 10^{-2}$, $y_N = 10^{-5}$. In both cases we have fixed $\lambda_{H\phi} = 10^{-2}$.

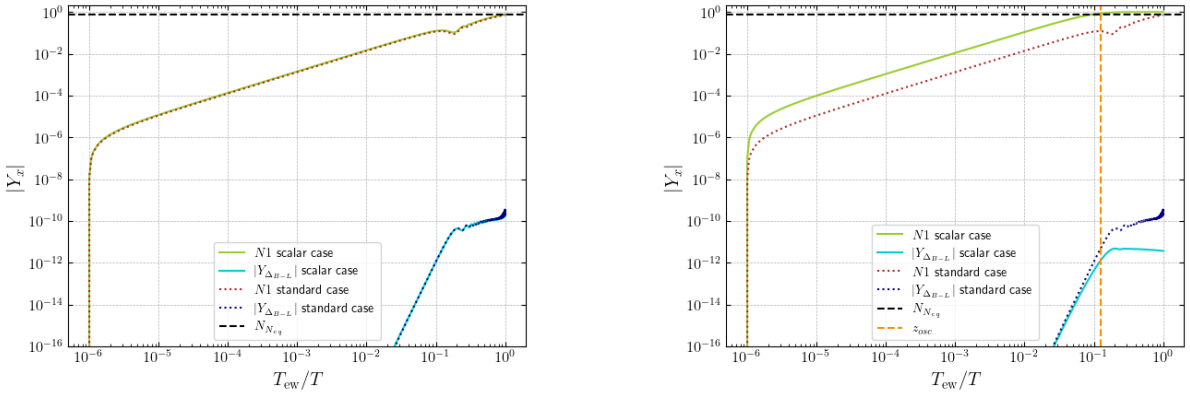

(a) $v_\phi = 10^6$ GeV, $y_N = 10^{-6}$, $\lambda_\phi = 10^{-10}$

(b) $v_\phi = 10^5$ GeV, $y_N = 10^{-5}$, $\lambda_\phi = 10^{-8}$

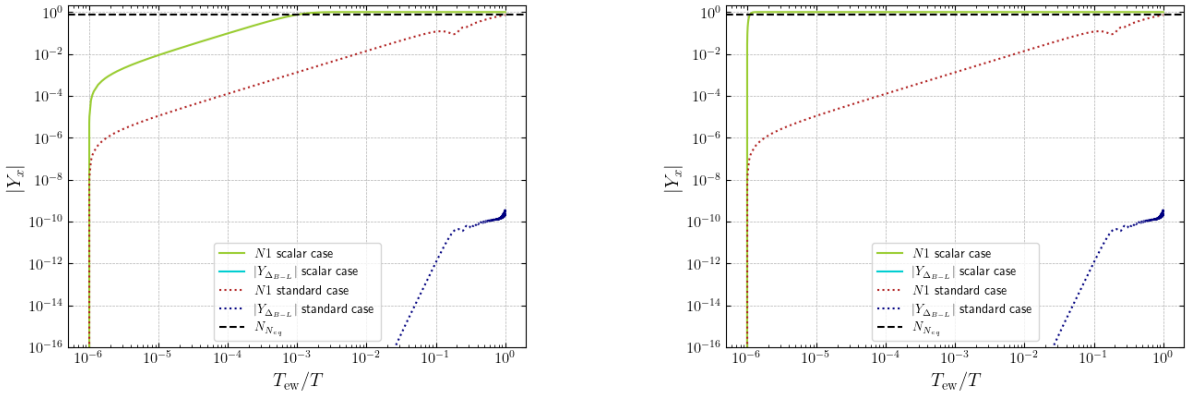

(c) $v_\phi = 10^4$ GeV, $y_N = 10^{-4}$, $\lambda_\phi = 10^{-6}$

(d) $v_\phi = 10^2$ GeV, $\lambda_\phi = 10^{-2}$, $y_N = 10^{-2}$

Figure 5.13: Evolution of N_1 and B-L asymmetry Yields in IO case with parameters listed in Tab. 5.1, with the substitution $y_1 = 120.00$. We have fixed $m_N = 1$ GeV and the zero temperature scalar mass $M_\phi(0) = 10$ GeV. The coupling $\lambda_{H\phi} = 10^{-2}$ for all four plots.

Therefore, to neglect the dependence on the parameter $\lambda_{H\phi}$ we need a bigger mass, in order to have $\lambda_\phi >> \lambda_{H\phi}$. For this reason we now fix $M_\phi(0) = 10^4$ GeV and we keep $\lambda_{H\phi} = 10^{-2}$. With this choice we obtain the plots in Fig. 5.12. From these results we see that for a heavier scalar the RHNs enter in thermal equilibrium at higher temperatures. Indeed, from the plot on the left of Fig. 5.12, where we have chosen a vev $v_\phi = 10^6$ GeV, we see that the RHNs enter in thermal equilibrium for $z_{eq} \simeq z_{osc}$ and the asymmetry is not completely erased. While, for $v_\phi = 10^5$ GeV we have that the RHNs enter in thermal equilibrium at higher temperatures and the asymmetry is completely washed-out. Therefore, we can conclude that the behaviour of the lepton asymmetry is governed by the vev v_ϕ and by the couplings y_N, λ_ϕ and $\lambda_{H\phi}$.

Now we consider the case of inverted hierarchy (IO) and we choose the same parameters listed in Tab. 5.1, but now we consider $y_1 = 120.00$. This choice leads to a mixing $|U|^2 = 3.27192 \cdot 10^{-9}$ and a baryon-to-photon ratio for standard ARS case is $|\eta_B| = 6.254 \cdot 10^{-10}$.
As we can see from the Fig. 5.13 the situation is very similar to the case with NO. In fact, the RHNs go in thermal equilibrium when the scalar vev is $v_\phi \simeq 10^5$ GeV, but only when $v_\phi \simeq 10^4$ GeV the lepton asymmetry is completely erased as we have already noticed in the previous case. Therefore, in the following, we will focus only on the NO case, since our results hold qualitatively also in the IO scenario.

5.3.3 The case with $M_2 \simeq M_3 \simeq 500$ MeV

At this point we can modify the RHNs masses to see if the situation changes. We start by considering NO and we take the RHNs masses to be $M_2 \simeq M_3 \simeq 500$ MeV, while the zero temperature scalar mass is fixed at $M_\phi = 10$ GeV. The first set of parameters, for which we have a mixing $|U^2| = 4.09358 \cdot 10^{-10}$ and the baryon-to-photon ratio for the standard ARS case is $\eta_B = 6.127 \cdot 10^{-10}$, is given in Tab. 5.2.

Table 5.2: Set of parameters in NO with RHNs masses $M_2 \simeq M_3 \simeq 500$ MeV.

Parameter	**Unit**	**Code input**	**Value**
δ	[°]	delta	270
α_{21}	[°]	a21	180
α_{31}	[°]	a31	0.0
θ_{23}	[°]	t23	48.59
θ_{12}	[°]	t12	33.84
θ_{13}	[°]	t13	8.66
x_1	[°]	x1	0.00
y_1	[°]	y1	55.00
x_2	[°]	x2	0.00
y_2	[°]	y2	0.00
x_3	[°]	x3	0.00
y_3	[°]	y3	0.00
$\log_{10}(m_{1/3})$	[eV]	m	-100
$\log_{10}(M_1)$	[GeV]	M1	0.00
$\log_{10}(M_2)$	[GeV]	M2	-0.301000005
$\log_{10}(M_3)$	[GeV]	M3	-0.3010

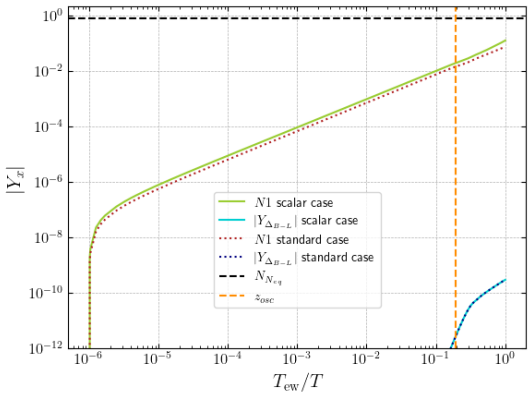

(a) Case with $v_\phi = 10^6$ GeV, $y_N = 5{\cdot}10^{-7}$, $\lambda_\phi = 10^{-10}$

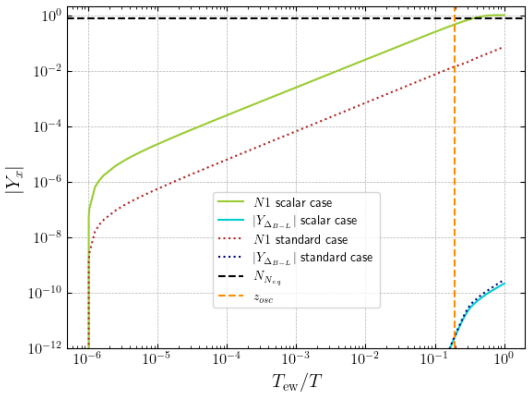

(b) Case with $v_\phi = 10^5$ GeV, $y_N = 5\cdot10^{-6}$, $\lambda_\phi = 10^{-8}$

Figure 5.14: Evolution of N_1 and $B-L$ asymmetry Yields with fixed $m_N = 500$ MeV, $M_\phi(0) = 0.1$ GeV and $\lambda_{H\phi} = 10^{-6}$

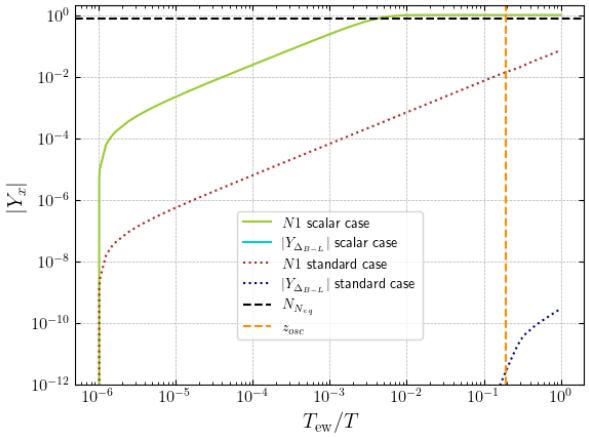

Figure 5.15: Evolution of N_1 and $B-L$ asymmetry Yields with fixed $m_N = 500$ MeV, $M_\phi(0) = 0.1$ GeV and $\lambda_{H\phi} = 10^{-6}$. Here, we present the case with $v_\phi = 10^4$ GeV, $y_N = 5\cdot10^{-5}$, $\lambda_\phi = 10^{-10}$

From Figs. 5.14 and 5.15 we notice that in the case with smaller masses the asymmetry is completely erased when the Yukawa coupling is $y_N \gtrsim 10^{-5}$. In this case the situation is similar to the previous one, i.e. the asymmetry production is inhibited for $v_\phi < 10^4$ GeV. It is interesting to notice that in the case $v_\phi = 10^5$ GeV (see right panel of Fig. 5.14), the RHNs enter in thermal equilibrium after z_{osc}, consequently the asymmetry is not washed out.

5.3.4 The case with $M_2 \simeq M_3 \simeq 10$ GeV

In the next set of parameters we explore the phenomenology for heavier sterile neutrinos by fixing $M_2 \simeq M_3 \simeq 10$ GeV, while the zero temperature scalar mass is fixed at $M_\phi = 10$ GeV. The chosen set of parameters, for which we have a mixing $|U^2| = 2.42214 \cdot 10^{-11}$ and the baryon-to-photon ratio for the standard ARS case is $\eta_B = 1.6930 \cdot 10^{-8}$, is given in Tab. 5.2.

Table 5.3: Set of parameters in NO with RHNs masses $M_2 \simeq M_3 \simeq 10$ GeV.

Parameter	**Unit**	**Code input**	**Value**
δ	[°]	delta	270
α_{21}	[°]	a21	180
α_{31}	[°]	a31	0.0
θ_{23}	[°]	t23	48.59
θ_{12}	[°]	t12	33.84
θ_{13}	[°]	t13	8.66
x_1	[°]	x1	0.00
y_1	[°]	y1	60.00
x_2	[°]	x2	0.00
y_2	[°]	y2	0.00
x_3	[°]	x3	0.00
y_3	[°]	y3	0.00
$\log_{10}(m_{1/3})$	[eV]	m	-100
$\log_{10}(M_1)$	[GeV]	M1	0.00
$\log_{10}(M_2)$	[GeV]	M2	1.00
$\log_{10}(M_3)$	[GeV]	M3	1.00000005

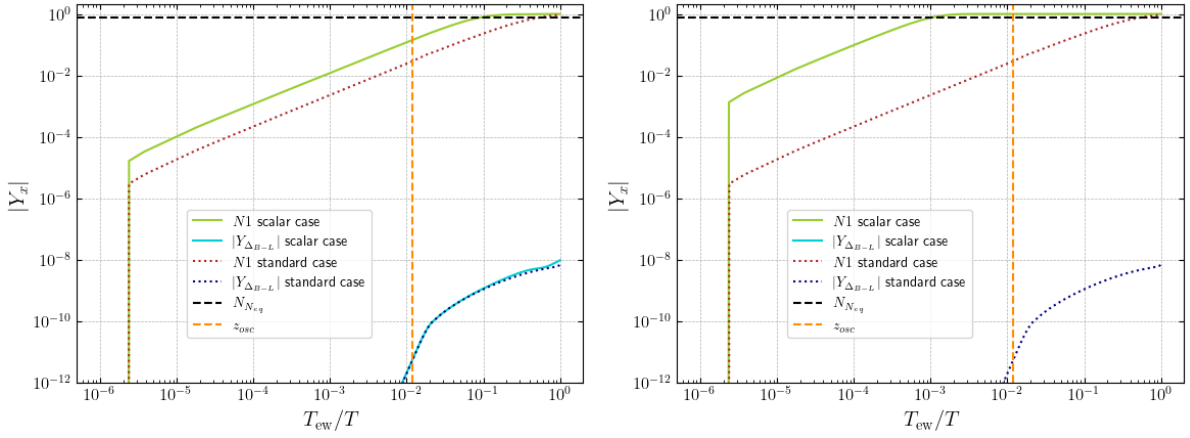

Figure 5.16: Evolution of N_1 and $B-L$ asymmetry Yields with fixed $m_N = 10$ GeV, $M_\phi(0) = 10$ GeV and $\lambda_{H\phi} = 10^{-2}$. On the left we have the case with $v_\phi = 10^6$ GeV, $y_N = 10^{-5}$, $\lambda_\phi = 10^{-10}$. On the right $v_\phi = 10^5$ GeV, $y_N = 10^{-4}$, $\lambda_\phi = 10^{-8}$.

From Figs. 5.16 we notice that in the case with heavier RHNs the asymmetry is completely erased when $v_\phi = 10^5$ GeV. Indeed, in this case the RHNs enter in thermal equilibrium before z_{osc}. It is worth noting that in this case $z_{osc} = 0.0119$, i.e. it is smaller than 0.1. This implies that oscillations starts earlier and we cannot solve the full set of quantum kinetic equations including all oscillations. Therefore, we truncate the generation of the flavour asymmetries at a dimensionless time $z_{cut} = 10 \cdot z_{osc}$.
It is particularly interesting the case with $v_\phi = 10^6$ GeV, shown on the left of Fig. 5.16. In this scenario, the RHNs enter in thermal equilibrium for $z_{eq} > z_{osc}$ and we expect to obtain an asymmetry comparable to the standard case. However, the resulting asymmetry is slightly larger than in the standard ARS scenario. This can be understood by noting that, at $z = z_{osc}$, the RHNs number density in the presence

of the additional scalar is higher than in the standard case. Therefore, a large population of RHNs oscillates leading to an enhancement of asymmetry. This feature does not appear in the case with $m_N \simeq 500$ GeV (see Fig. 5.14), where the RHNs enter thermal equilibrium immediately after z_{osc}, leaving no time for additional asymmetry to be generated.

5.3.5 Non vanishing initial asymmetry

In this section, we are going to analyze the case with non-vanishing initial lepton asymmetry. We focus on the NO case and we choose the parameters listed in Tab. 5.1. We fix the RHNs masses equal to 1 GeV and the zero temperature scalar mass $M_\phi(0) = 10$ GeV; in this way we are in the same situation described in Sec. 5.3.2. The results are plotted in Fig. 5.17.

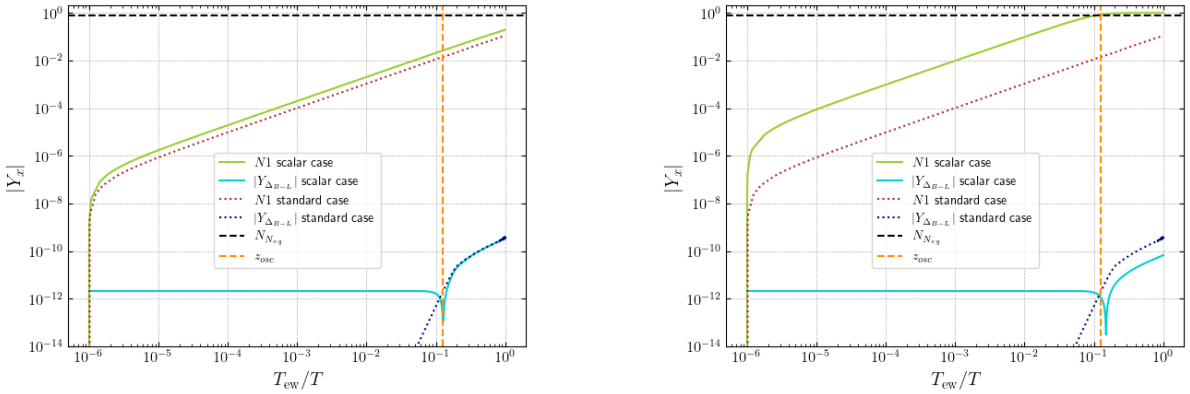

(a) Case with $v_\phi = 10^6$ GeV, $y_N = 10^{-6}$, $\lambda_\phi = 10^{-10}$.

(b) Case with $v_\phi = 10^5$ GeV, $y_N = 10^{-5}$, $\lambda_\phi = 10^{-8}$.

Figure 5.17: Evolution of N_1 and $B - L$ asymmetry Yields with fixed $m_N = 1$ GeV, $M_\phi(0) = 10$ GeV and $\lambda_{H\phi} = 10^{-2}$.

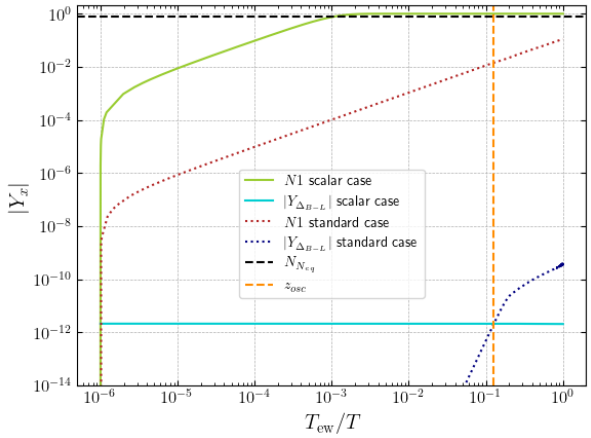

Figure 5.18: Evolution of N_1 and $B - L$ asymmetry Yields with fixed $m_N = 1$ GeV, $M_\phi(0) = 10$ GeV and $\lambda_{H\phi} = 10^{-2}$. Here, we present the case with $v_\phi = 10^4$ GeV, $y_N = 10^{-4}$, $\lambda_\phi = 10^{-6}$.

In the case plotted in Fig. 5.17a the scalar gets a vev at $T \simeq 10^6$ GeV and, as in the case with vanishing initial asymmetry, the RHNs do not enter in thermal equilibrium. Therefore, the obtained asymmetry is the same as in the standard ARS case. In this case the plot shows a dip for $z \simeq z_{osc}$, which is due to the standard ARS washout processes. In fact, we have already seen that for $v_\phi \gtrsim 10^6$ GeV the scalar decay does not modify the standard picture.
For smaller values of the scalar vev the situation is different. First, we focus on the plot in Fig. 5.17b. In this case $v_\phi = 10^5$ GeV and the RHNs enter in thermal equilibrium, due to the scalar decay, at $z_{eq} \simeq z_{osc}$. Therefore, some RHNs can still oscillate to produce a lepton asymmetry and for this reason we still see a dip for $z \simeq z_{osc}$. It is important to notice that also in this case the washout processes are those of standard ARS leptogenesis. As expected, the asymmetry produced is smaller than the one produced without the additional scalar singlet, since in this case some RHNs are already at thermal equilibrium.
In the last plot (Fig. 5.18) the scalar acquires a vev equal to 10^4 GeV. In this case the scalar decay brings the RHNs in thermal equilibrium for higher temperatures, namely $z_{eq} \ll z_{osc}$, and the RHNs cannot oscillate to produce the lepton asymmetry. Also, in this case the standard washouts are not present since the RHNs are already at thermal equilibrium. It is worth noting that the scalar decay is a LNC process and, for this reason, the thermal initial asymmetry is not washed out, even if the RHNs enter in thermal equilibrium. Therefore, for smaller vevs the lepton asymmetry production via oscillation is inhibited, but an initial lepton asymmetry abundance will not be erased.

5.3.6 Parameter scan

In the previous sections, we have shown that the evolution of the lepton asymmetry is influenced by the behaviour of the RHNs number density. In fact, if the RHNs go in thermal equilibrium before the oscillation time z_{osc}, the asymmetry is washed out. To have an overall picture of this mechanism we perform a numerical scan of the parameter space of viable leptogenesis. In particular, we want to see how the parameter space changes with the introduction of the new interaction with the scalar. We have already seen that, for certain values of the scalar vev, the asymmetry is washed out. Therefore, we expect that the region of viable leptogenesis in Fig. 5.6 will be reduced. To perform the numerical scan we fix the parameters as described in Sec. 5.3.1 and we fix the mass splitting of RHNs equal to 10^{-8}. Then, we vary the scalar vev in the range $(10^3 - 10^6)$ GeV, since for these values we have observed that the lepton asymmetry is washed out. We also fix the coupling $\lambda_{H\phi} = 10^{-2}$ and we select three benchmark points, according to the value of the scalar mass at zero temperature $M_\phi(0) = [10,\ 10^2,\ 10^3]$ GeV.

M_N	U^2_{ARS}	$\lvert\eta_B\rvert_{ARS}$
1 GeV	$1.26395 \cdot 10^{-10}$	$8.13 \cdot 10^{-10}$
0.5 GeV	$4.09358 \cdot 10^{-10}$	$6.127 \cdot 10^{-10}$
10 GeV	$2.42214 \cdot 10^{-11}$	$1.6930 \cdot 10^{-10}$

Table 5.4: Summary of the considered benchmark points for the numerical analysis. The parameters are the RHNs mass, with splitting fixed equal to 10^{-8}. Given are the mixing angle and the produced BAU (in terms of the Baryon to photon ratio) in the standard ARS case.

We start by considering the case where the zero-temperature scalar mass is equal to 10 GeV. In Fig. 5.19 we show the range of the total mixing angle U^2 consistent with both the seesaw mechanism and leptogenesis as a function of RHN masses. The upper (lower) dashed black line in the plots corresponds to the curve of maximal (minimal) mixing compatible with viable leptogenesis in the standard ARS case, with mass splitting fixed at $\Delta M/M = 10^{-8}$, see Fig. 5.6. The shaded points correspond to successful

leptogenesis for certain choices of the scalar vev v_ϕ. In Fig. 5.19 the red stars represent the points that we have analyzed in previous section, which are summarized in Tab. 5.4.
From the plot in the left panel we observe that, as expected, the parameter space is not significantly different from that of the standard ARS case, since we have considered vev values as high as 10^6 GeV. From our numerical analysis in Sec. 5.3, we have already shown that for $v_\phi = 10^6$ GeV the RHNs do not enter in thermal equilibrium before z_{osc}. Consequently, we obtain the same result as in standard ARS case. In the right panel we show the case with $v_\phi \in [10^3, 10^5]$ GeV. As expected, the points represented by the red stars do not correspond to successful leptogenesis, since for these vevs the asymmetry production is washed out and/or inhibited. In this case we observe that the parameter space of viable leptogenesis is slightly reduced.

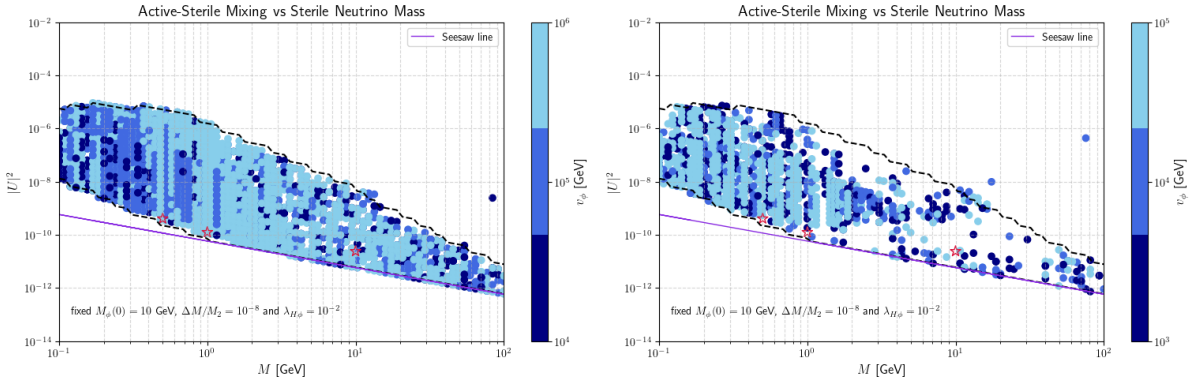

Figure 5.19: The parameter space of viable leptogenesis with the additional scalar singlet. Here we considered the case with $M_\phi = 10$ GeV. On the left panel we show the case with scalar vev varying in the range $[10^4, 10^6]$ GeV, whereas on the right panel we focused on the case with $v_\phi \in [10^3, 10^5]$ GeV.

Now we focus on the case with $M_\phi = 100$ GeV, shown in Fig. 5.20. Similarly to the case with $M_\phi(0) = 10$ GeV, we notice that the parameter space is reduced when the scalar vev varies in the range $[10^3, 10^5]$. This implies that when the scalar acquires a vev at these temperatures[14], the RHNs equilibrate before their oscillations could start resulting in the erasure of the lepton asymmetry. This effect is shown in the right panel of Fig. 5.20. From this plot we can also notice that larger values of the mixing angle U^2 are not allowed when the scalar vev satisfies $v_\phi < 10^5$ GeV. This indicates that the RHNs enter in thermal equilibrium before their oscillation temperature, resulting in an erasing of the asymmetry. This behaviour was not present in the case with a smaller scalar mass $M_\phi(0) = 10$ GeV, where the parameter space for $m_N \leqslant 1$ GeV nearly coincides with that of the standard ARS case and larger mixing are allowed. In the left panel of Fig. 5.20 the case with $v_\phi \in [10^4, 10^6]$ GeV is shown. As expected, the parameter space is more similar to that of the standard ARS case. By comparing this plot with the one in the left panel of Fig. 5.19, we notice that for the same range of vevs the parameter space is more reduced when considering larger zero-temperature scalar masses. This situation becomes even more evident for higher scalar masses, as shown in the left panel of Fig. 5.21. Therefore, we can conclude that increasing the zero-temperature scalar mass further reduces the parameter space of viable leptogenesis. This behaviour is more noticeable in the right panel of Fig. 5.21, where we observe that the asymmetry is almost completely washed out for $m_N \leqslant 1$ GeV, whereas some scattered points remain for larger values of the neutrino masses.
It is interesting to notice that in all the three cases the darker points, which correspond to lower values of the scalar vev, do not follow a clear pattern but are instead scattered across the entire RHN mass

[14] Recall that we are assuming that the scalar vev corresponds to the temperature of $U(1)_{B-L}$ SSB.

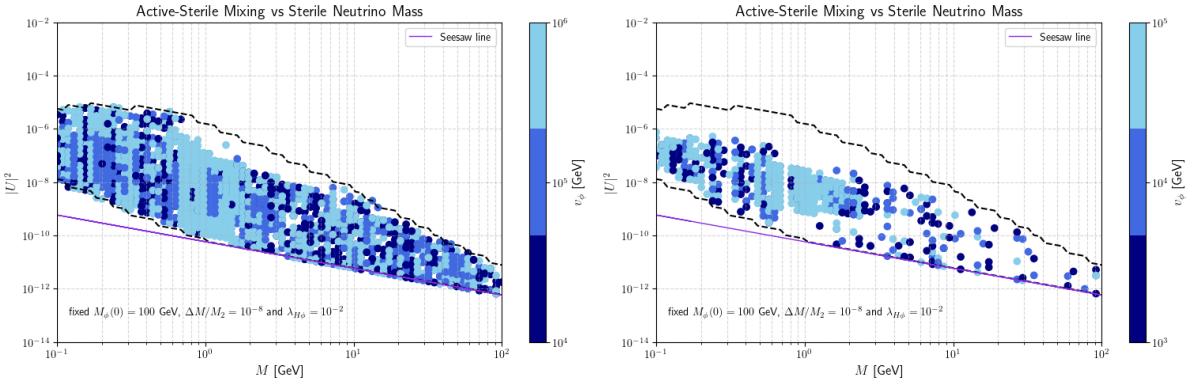

Figure 5.20: The parameter space of viable leptogenesis with the additional scalar singlet. Here we considered the case with $M_\phi = 100$ GeV. On the left panel we show the case with scalar vev varying in the range $[10^4, 10^6]$ GeV, whereas on the right panel we focused on the case with $v_\phi \in [10^3, 10^5]$ GeV.

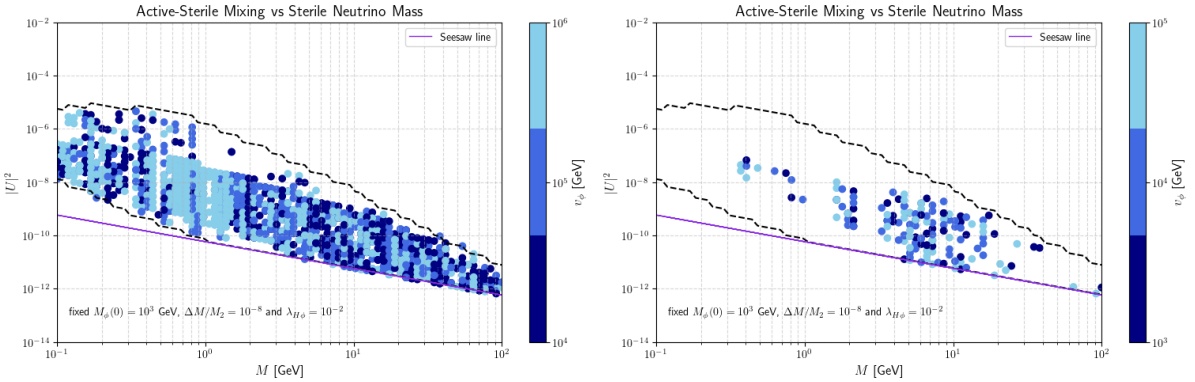

Figure 5.21: The parameter space of viable leptogenesis with the additional scalar singlet. Here we considered the case with $M_\phi = 10^3$ GeV. On the left panel we show the case with scalar vev varying in the range $[10^4, 10^6]$ GeV, whereas on the right panel we focused on the case with $v_\phi \in [10^3, 10^5]$ GeV.

range. One would expect that, for smaller values of the scalar vev, the lighter RHNs would not reach thermal equilibrium due to the smallness of their Yukawa coupling. Despite that, we observe points with $v_\phi \simeq 10^3,\ 10^4$ GeV that yield successful leptogenesis even for larger RHNs masses. This is likely because these points correspond to Casas-Ibarra configurations in which the RHNs remain out of equilibrium, preventing the washout of the asymmetry. This consideration may be verified in further analysis.

From these parameter scans we can conclude that introducing a scalar singlet to the SM particle content and a $U(1)_{B-L}$ global symmetry to the SM symmetry group modifies the parameter space of viable leptogenesis when the SSB occurs at $T \leqslant 10^6$ GeV. In particular, in the range $v_\phi \in [10^2, 10^6]$ the thermalised scalar leads to an enhancement in the RHNs production at early times. As a consequence, the RHNs enter in thermal equilibrium for $z_{eq} < z_{osc}$, leading to a reduction of the predicted BAU compared to the standard ARS picture. Therefore, we found that, in our model, the BAU of the standard ARS scenario is reproduced when the scalar vev is at least as large as $\mathcal{O}(10^7)$ GeV and/or the Yukawa coupling is $y_N \leqslant 10^{-5}$. Actually, this is a conservative bound since when the zero-temperature scalar masses are at most as large as $\mathcal{O}(10)$ GeV, the standard ARS scenario can be reproduced for $v_\phi \leqslant 10^6$ GeV, as shown in Fig. 5.19. Hence, the parameter space of viable leptogenesis also depends on the choice of the scalar self-coupling λ_ϕ. These considerations lead us to conclude that the standard ARS scenario is reproduced when $v_\phi \geqslant 10^7$ GeV and/or $y_N \leqslant 10^{-5}$. This bound can be lowered to $v_\phi \geqslant 10^6$ GeV when $\lambda_\phi \leqslant 10^{-10}$. To further improve our results, one could find a relation between the Yukawa coupling y_N and the self-scalar coupling λ_ϕ mass for a fixed value of v_ϕ, in order to define the minimum scalar mass corresponding to each sterile neutrino mass for which leptogenesis is successful. It is also worth noting that all these considerations hold for a fixed value of the coupling $\lambda_{H\phi} = 10^{-2}$. As already shown in Fig. 5.9, RHNs enter in thermal equilibrium at lower temperatures as $\lambda_{H\phi}$ decreases. Therefore, we expect that for smaller $\lambda_{H\phi}$ the parameter space will be reduced for smaller values of the scalar vev. We leave these analysis for future works.

Chapter 6

Conclusions

In this thesis we have investigated how the baryon asymmetry of the universe could be affected by the introduction of a complex scalar singlet, Φ, and a global symmetry $U(1)_{B-L}$ in a seesaw tipe I extension of the SM with two quasi-degenerate right handed neutrinos.

In Chapters 3 we reviewed the problem of the baryon asymmetry of the universe and discussed one of the most extensively studied proposed solutions, i.e. baryogenesis via leptogenesis. We then provided an overview of the current leptogenesis scenarios, focusing on thermal leptogenesis in Chapt. 4. Subsequently, we explored low scale leptogenesis models, such as resonant leptogenesis in Sec. 4.5 and leptognesis via oscillations (ARS leptogenesis). Our study focused particularly on ARS leptogenesis, an appealing scenario in which the RHNs have masses at the GeV scale, making it potentially testable in upcoming experiments.
In Chapter 5 we presented our original proposal. We first provided an overview of the ARS mechanism and we have derived the quantum kinetic equations. Then, we go beyond this model to explore how the masses of the RHNs could be dynamically generated through the spontaneous breaking of a new symmetry. Therefore, we introduced a new scalar degree of freedom, Φ, and a global symmetry $U(1)_{B-L}$ under which the scalar carries charge $+2$ and the RHNs -1. This construction introduces additional terms in the scalar potential, namely the self interacting terms of Φ and a scalar portal given by the interaction of Φ with the Higgs boson through the coupling $\lambda_{H\phi}$. The new scalar also couples with the RHNs and the breaking of the $U(1)_{B-L}$ will generate a Majorana mass for the sterile neutrinos. It is important to note that, in order to generate a lepton asymmetry, the RHNs must acquire a mass before the electroweak phase transition, otherwise sterile oscillations would not occur. For this reason we focused on the scenario in which the scalar Φ acquires a vev at temperature above 10^2 GeV.
Once the $U(1)_{B-L}$ is spontaneously broken, two real scalar degrees of freedom emerge, ϕ and θ, where ϕ corresponds to the massive radial mode and θ is the massless Goldstone bosons, commonly reffered to as the Majoron. This results in new interactions between these scalars and the RHNs, with some consequences on the leptogenesis process. These effects have been studied by looking at the quantum kinetic equations. In order to do that, we first identified the dominant contributions in Sec. 5.2.1. In particular, we assumed that the scalar Φ is in thermal equilibrium thanks to its interaction with the Higgs boson. As a consequence, the scalar singlet acquires a thermal mass, computed in App. E.3, whereas the RHNs do not have a thermal mass since they do not interact with the thermal plasma, as we are considering a freeze-in mechanism. It is worth noting that the thermal mass was computed by choosing a vacuum configuration such that the Majoron remain massless; hence, the thermal correction affects only the scalar ϕ.

The presence of the thermal mass allows ϕ to decay in two RHNs even if its zero temperature mass satisfies $M_\phi(0) < M_N$. Therefore the dominant process is the scalar decay. We have also considered the $2 \to 2$ interactions between ϕ and RHNs and we have found them to be subdominant; for this reason, we have not considered them in our framework.

Once the scalar decay was identified as the dominant process, we derived the corresponding collisional term in the quantum kinetic equations and performed a numerical study to investigate how this process modifies the ARS leptogenesis picture. First, we considered three benchmark points by fixing the zero temperature scalar mass and varying the RHNs masses. The results are presented in Sec. 5.3. Interestingly, we observed that the timing of the scalar acquiring a vev significantly affects the leptogenesis dynamics. We have found that in our model the baryon asymmetry of the standard ARS model is reproduced when the scalar vev, which we have assumed to be equal to the SSB temperature, is at least as large as $\mathcal{O}(10^7)$ GeV. For smaller values of the vev the scalar decay leads to an enhancement of sterile neutrino production. Particularly, if scalar decay brings the RHNs in thermal equilibrium for temperatures such that $T_{eq} > T_{osc}$, i.e. the RHNs enter in thermal equilibrium before the time it takes for the RHNs to oscillate once, the lepton asymmetry is washed out. In particular, we have to distinguish two cases:

- For $T_{eq} \gg T_{osc}$ the asymmetry generation is inhibited because the third Sakharov condition (departure from thermal equilibrium) is not satisfied.
- For $T_{eq} \simeq T_{osc}$, the asymmetry is partially erased thanks to the washout processes associated with the interaction $\phi \leftrightarrow NN$.

This behaviour has been verified in Subec. 5.3.5, where we considered the scenario with non-vanishing initial asymmetry. When $T_{eq} \simeq T_{osc}$, the asymmetry is reduced, but not completely erased; whereas for $T_{eq} \gg T_{osc}$ we do not observe any washout in the asymmetry, neither from the scalar interactions nor from the standard ARS picture. This situation occurs because, if the RHNs enter in thermal equilibrium too early, the asymmetry is not produced at all, as the third Sakharov condition is not satisfied for long enough to allow the asymmetry generation.
Another interesting scenario arises when the SSB occurs at $T \simeq T_{ew}$, i.e. $v_\phi = 10^2$ GeV. In this case, the asymmetry is not generated because the RHNs acquire a mass only at the time of sphaleron freeze-out, preventing oscillations before the EWPT, resulting in the absence of the CP violation necessary to generate the letpon asymmetry. From these results, we conclude that to reproduce the same asymmetry as the one produced in the standard ARS picture, the SSB should occur at sufficiently high temperatures such that the RHNs do not reach thermal equilibrium before their oscillation temperature.

Having studied these benchmark points for a fixed value of the zero temperature scalar mass, we then performed a parameter scan to investigate how varying the scalar mass affects this picture. In order to do that we have fixed $M_\phi(0) = 10, 10^2, 10^3$ GeV and we varied the scalar vev in the range $[10^3, 10^6]$ GeV. The results of these scans of the parameters are shown in Sec. 5.3.6. From them, we can conclude that the parameter space of viable leptogenesis is significantly reduced when the scalar particle acquires a vev at temperature $T \leqslant 10^5$ GeV. This occurs for all three choices of the scalar mass. The parameter space is slightly reduced for $v_\phi \leqslant 10^6$ GeV when the scalar mass is $M_\phi(0) > 10$ GeV, whereas for $M_\phi(0) \leqslant 10$ GeV the parameter space of standard ARS leptogenesis is reproduced when $v_\phi \geqslant 10^6$ GeV. From these considerations, we can conclude that in general the standard ARS scenario can be reproduced when the spontaneous breaking of the $U(1)_{B-L}$ symmetry occurs at $T \geqslant 10^7$ GeV, and that this temperature bound can be lowered if the scalar mass is smaller, i.e. $M_\phi(0) \leqslant 10$ GeV.

Our analysis can be improved in different ways. As already mentioned in Sec. 5.3.6, a possible improvement could be to investigate how the parameter space of viable leptogenesis changes by varying

the coupling $\lambda_{H\phi}$ and it could be also interesting to find a minimum scalar mass corresponding to each sterile neutrino mass for which leptogenesis is successful.

Another possible development is to include in the quantum kinetic equations the contribution involving the Majoron. The decay of this particle is forbidden since it is a massless particle, but the $2 \to 2$ process could be present and contribute to bring the RHNs in thermal equilibrium, resulting in a further erasement of the BAU. In particular, we expect that the introduction of the $\theta\theta \leftrightarrow NN$ process in the collisional term of the Quantum Kinetic Equations could bring the RHNs in thermal equilibrium at higher temperatures, since, in this process the interaction rate will depend only on the Yukawa coupling y_N and the scalar vev v_ϕ. Indeed, we need to consider only the u and t-channels, as shown in Fig. 5.5, and the rate of this process will not depend on the scalar mass $M_\phi(T)$, but only on the coupling y_N and the mass of the RHNs.

Finally, it could be also interesting to investigate the scenario with a gauge $U(1)_{B-L}$ symmetry. This results in the introduction of a massive gauge boson which can interact with the RHNs. Also in this case one could verify whether the interaction with the gauge boson can bring the RHNs in thermal equilibrium before t_{osc} and how this additional particle modifies the leptogenesis picture. We leave these further developments for future works.

In summary, we found that including a physical explanation of the RHNs masses by the spontaneous breaking of a $U(1)_{B-L}$ global symmetry can significantly affect leptogenesis. Only for very large values of the scalar vev, so that the Yukawa couplings are sufficiently small, the RHNs do not enter in thermal equilibrium and leptogenesis can proceed as in the standard ARS case. Our results may be useful once sterile neutrinos and scalar particles are discovered in the laboratory, with their masses and Yukawa couplings determined. In that case, one could assess whether the ARS mechanism can account for the baryon asymmetry of the Universe, or whether an alternative explanation must be considered.

Acknowledgements

I would like to sincerely thank my supervisor, Prof. Silvia Pascoli for proposing me this thesis project. I am deeply grateful for her continuous guidance, support and insightful discussion throughout the development of this work, as well as for her valuable advice to help me prepare for the PhD interviews. I am also sincerely thankful to Dr. Alessandro Granelli for his constant guidance, encouragement and availability. His expertise and support have been fundamental throughout every stage of this research. Finally, I am grateful for the stimulating environment provided by the theoretical physics group at the University of Bologna, and I would like to thank my colleagues for their support and for sharing this journey with me during my Master's degree.

Appendix A

Charge conjugation

In this appendix we will give a brief review of charge conjugation in the SM. Following Ref. [44], we define the charge conjugate of a fermion field as

$$(\psi)^c(x) \equiv \xi_c C\bar{\psi}^T(x), \tag{A.1}$$

where ξ_c is the charge parity of the field. C is the charge conjugation matrix which satisfies the following properties

$$C\gamma_\mu^T C^{-1} = -\gamma_\mu, \tag{A.2}$$

$$C^\dagger = C^{-1}, \tag{A.3}$$

$$C^T = -C. \tag{A.4}$$

In the Dirac representation of the γ_μ matrices, one has $C = i\gamma^2\gamma^0$. Since two charge conjugation transformations must bring back the field to its initial value

$$\psi \xrightarrow{c} \xi_c C\bar{\psi}^T \xrightarrow{c} |\xi_c|^2\psi, \tag{A.5}$$

we find $|\xi_c|^2 = 1$. The parameter ξ_c is a phase which represents the intrinsic charge parity of the field. From here onward we take $\xi_c = 1$ for left-handed neutrinos, since weak interactions violate the charge conjugation symmetry, the charge parity of neutrinos is arbitrary. Under a charge conjugation transformation, we have $\mathcal{U}_c\psi(x)\mathcal{U}_c^\dagger = \psi^c(x)$. We must notice an important property, that is, the charge conjugate of a left-handed field is right-handed and viceversa. In fact, using the left-handed projector P_L, one can show

$$P_L C\bar{\psi_L}^T = C(\bar{\psi_L}P_L)^T = C\Big((P_R\psi_L)^\dagger\gamma^0\Big)^T = 0. \tag{A.6}$$

Under a charge conjugation transformation, we find that $\mathcal{U}_c\psi_L\mathcal{U}_c^\dagger = (\psi_R(x))^c$. Therefore, a Lagrangian which contains only left-handed fields, such as the charge and neutral current terms in the Standard Model one, cannot preserve charge conjugation as a symmetry.

A.1 Majorana fields

A Majorana field is defined as

$$\psi = \psi^c. \tag{A.7}$$

This condition means that particle and antiparticle are indistinguishable and therefore can only apply to neutral fields. Majorana fields have several specific properties:

- Majorana fields satisfy the Dirac equation for particles and antiparticles

$$(i\gamma^\mu \partial_\mu - m)\psi = 0. \tag{A.8}$$

- In terms of its chiral components the Majorana condition implies that the field can be written as

$$\psi = \psi_L + \psi_L^c, \tag{A.9}$$

  where we have used the fact that $(\psi_L)^c = (\psi^c)_R$.

- Majorana fields have only 2 degrees of freedom, differently from Dirac ones which have 4
- Majorana fields are quantized in terms of only one type of creation operator.
- Their electromagnetic current $j^\mu = q\bar{\psi}\gamma^\mu\psi$ vanishes exactly.

In the SM only neutrinos are neutral fermions and can be Majorana particles. As they cannot carry any charge, since the associated current vanishes, this implies that lepton number is not a conserved symmetry if neutrinos are Majorana type. This is evident form the fact that the Majorana condition is not invariant under a $U(1)_L$ transformation.

Appendix B

Derivation of Boltzmann equations

In this appendix we review the derivation of the Boltzmann Equations for thermal leptogenesis that we have used in Chapt. 4.
We work in the one flavour regime and consider only the decays of the right handed neutrino N_1. In particular we consider the initial temperature T_i larger than M_1, the mass of N_1. We will also neglect decays of the two heavier neutrinos N_2 and N_3, assuming that a generation of $B-L$ asymmetry from their decays either does not occur at all or that it does not influence the final value of $B-L$, namely this $B-L$ asymmetry will be efficiently washed out by the N_1 interactions. Therefore we will drop the subscript "1", and refer to the lightest right-handed neutrino simply as N in the following. Further, we assume that the lightest heavy neutrino N_1 is the only relevant degree of freedom beyond the standard model particle species. The Boltzmann equation for a right-handed neutrino in a FLRW framework can be written as [96]

$$\frac{\partial f_N}{\partial t} - |\mathbf{p}_N| H \frac{\partial f_N}{\partial |\mathbf{p}_N|} = C_D[f_N] + C_S[f_N], \tag{B.1}$$

where f_N is the phase space distribution of the RHN, $\mathbf{p}_N$ the RHN momentum. On the right-hand side, the collision integral $C_D[f_N]$ and $C_S[f_N]$ encode, respectively, the interactions of the RHN due to decays into lepton and Higgs (D) and scattering processes via Yukawa interactions with the top quark (S). Similarly, the Boltzmann equation for leptons and anti-leptons is

$$\frac{\partial f_{l-\bar{l}}}{\partial t} - |\mathbf{p}_l| H \frac{\partial f_{l-\bar{l}}}{\partial |\mathbf{p}_l|} = C_D[f_{l-\bar{l}}] + C_S[f_{l-\bar{l}}], \tag{B.2}$$

where we have defined

$$f_{l-\bar{l}} \equiv f_l - f_{\bar{l}}. \tag{B.3}$$

Integrating $f_{l-\bar{l}}$ over the lepton phase space

$$n_{l-\bar{l}} \equiv \frac{g_l}{(2\pi)^3} \int d^3 p_l f_{l-\bar{l}}, \tag{B.4}$$

with $g_l = 2$, we obtain the lepton asymmetry per co-moving photon,

$$N_{l-\bar{l}} \equiv \frac{n_{l-\bar{l}}}{n_\gamma^{eq}}, \tag{B.5}$$

where $n_\gamma^{eq} = (\zeta(3)/\pi^2) g_\gamma T^3$ with $g_\gamma = 2$ is the equilibrium photon density. The two Boltzmann equations can be simplified by transforming to dimensionless coordinates $z = M/T$ and $y_i = |\mathbf{P}_i|/T$ where M is the

mass of the sterile neutrino. Using the relation $dT/dt = -HT$, the differential operator $\partial_t - |\mathbf{p}_i|H\partial_{|\mathbf{p}_i|}$ becomes $zH\partial_z$, and consequently BE becomes:

$$\frac{\partial f_N(z,y)}{\partial z} = \frac{z}{H(M)}(C_D[f_N(z,y)] + C_S[f_N(z,y)]), \tag{B.6}$$

and

$$\frac{\partial f_{l-\bar{l}}(z,y)}{\partial z} = \frac{z}{H(M)}(C_D[f_{l-\bar{l}}(z,y)] + C_S[f_{l-\bar{l}}(z,y)]), \tag{B.7}$$

where $H(M) = H(T)z^2$. The Boltzmann Equations B.7-B.6 encode how a lepton asymmetry is generated and washed out in an expanding universe given some specific particle interaction.

B.1 Decay and inverse decay

First we consider a simplified picture in which decays and inverse decays of N_1 are the only process, i.e. we impose $C_S[f_N]$ in Eqs. B.7 and B.6. The collision integral for the RHN has the following form:

$$\begin{aligned} C_D[f_N] = \frac{1}{2E_N}\int \frac{d^3p_l}{2E_l(2\pi)^3}\frac{d^3p_\Phi}{2E_\Phi(2\pi)^3}(2\pi)^4\delta^4(p_N - p_l - p_\Phi) \\ \times [f_\Phi f_l(1-f_N)(|\mathcal{M}_{\Phi l\to N}|^2 + |\mathcal{M}_{\Phi\bar{l}\to N}|^2) - \\ f_N(1-f_l)(1+f_\Phi)(|\mathcal{M}_{N\to\Phi l}|^2 + |\mathcal{M}_{N\to\Phi\bar{l}}|^2)]. \end{aligned} \tag{B.8}$$

where E_i and p_i are, respectively, the energy and 4-momenta of the particle species i and $\mathcal{M}_A$ denotes the matrix element for the process A. At tree level, the squared matrix element is the one we have derived in Eq. 4.9, which we rewrite as [96]

$$|\mathcal{M}_{N\to\Phi l}|^2 = \frac{(m_D^+ m_D)_{11}}{v^2} p_l p_N, \tag{B.9}$$

where we have inserted the expression of the Dirac masses $m_D = yv/\sqrt{2}$ and $v = 174GeV$ is the VEV of the Higgs particle. The integral in Eq. B.8 can be reduced to a one dimensional form

$$C_D[f_N] = \frac{M\tilde{\Gamma}}{E_N p_N}\int_{(E_N-p_N)/2}^{(E_N+p_N)/2} dp_\Phi [f_\Phi f_l(1-f_N) - f_N(1-f_l)(1+f_\Phi)]. \tag{B.10}$$

For leptons participating in the same decay and inverse decay processes the collisional term is given by

$$\begin{aligned} C_D[f_l] = \frac{1}{2E_l}\int \frac{d^3p_N}{2E_l(2\pi)^3}\frac{d^3p_\Phi}{2E_\Phi(2\pi)^3}(2\pi)^4\delta^4(p_N - p_l - p_\Phi) \\ \times [f_N(1-f_l)(1+f_\Phi)(|\mathcal{M}_{N\to\Phi l}|^2 - f_\Phi f_l(1-f_N)(|\mathcal{M}_{\Phi l\to N}|^2]. \end{aligned} \tag{B.11}$$

From CPT invariance the decay neutrino amplitude can be written as

$$\begin{aligned} |\mathcal{M}_{N\to\Phi l}|^2 = |\mathcal{M}_{\Phi\bar{l}}|^2 = |\mathcal{M}_0|^2(1+\epsilon), \\ |\mathcal{M}_{N\to\Phi\bar{l}}|^2 = |\mathcal{M}_{\Phi l\to N}|^2 = |\mathcal{M}_0|^2(1-\epsilon), \end{aligned} \tag{B.12}$$

where $|\mathcal{M}_0|^2$ is the tree level amplitude given in Eq. B.9.

Integrated Boltzmann equations

To integrate the Boltzmann equations we make some assumptions. First, we neglect quantum effects such as the Pauli exclusion principle and we assume $1 \pm f_i \sim 1$. Secondly, all standard model particles are taken to be in thermal equilibrium due to their gauge interactions and their distribution functions approximated by a Maxwell-Boltzmann distribution $f_i^{eq} = e^{-E_i/T}$. With these assumptions and using energy conservation we find

$$f_\Phi f_l = e^{-(E_\Phi + E_l)/T} = e^{-E_N/T} = f_N^{eq}, \tag{B.13}$$

so the collision integral in Eq. B.8 becomes

$$C_D[f_N] = \frac{M\Gamma}{E_N p_N} \int_{(E_N - p_N)/2}^{(E_N + p_N)/2} dp_\Phi [f_N^{eq} - f_N] \tag{B.14}$$

Integrating over p_Φ and inserting into Eq. B.6 the Boltzmann Equation becomes

$$\frac{\partial f_N}{\partial z} = \frac{z\Gamma M}{H(M) E_N} (f_N^{eq} - f_N). \tag{B.15}$$

Assuming kinetic equilibrium for right-handed neutrinos we have $f_N/f_N^{eq} \sim n_N/n_N^{eq}$, where n_N is the number density. By integrating we find

$$\frac{\partial n_N}{\partial z} = zK \left\langle \frac{M}{E_N} \right\rangle (n_N^{eq} - n_N). \tag{B.16}$$

where $K \equiv \tilde{\Gamma}/H(M)$. Dividing by the equilibrium photon density n_γ we obtain the Boltzmann Equation 4.36.

For what concerns the evolution of lepton asymmetry ($\Delta L = L - \bar{L}$), besides the RHN decays and inverse decays we have to consider also the $\Delta L = 2$ scattering terms, in order to obtain the out-of equilibrium condition, i.e. that no lepton asymmetry is generated in thermal equilibrium [97]. Without the subtraction of the scattering term, decays and inverse decays lead to the generation of a lepton asymmetry in thermal equilibrium, in contradiction with general theorems [18]. It is important to notice that in the $2 \to 2$ scattering, the contribution from on-shell s-channel N_1-exchange is already accounted for by the decays and inverse decays. Indeed, the amplitude for $2 \to 2$ due to s-channel exchange of a single X contains two terms: a part corresponding to the propagation of an on-shell intermediate X and a part accounting for off-shell X exchange [68]. The physical intermediate states, which are called *Real Intermediate States* (RIS) are already included in the Boltzmann equation as successive lower order ($2 \to 1$ and $1 \to 2$ processes), so it is necessary to remove this contribution to avoid double counting and we do that by considering a subtracted amplitude. Instead, for what concerns the t- and u-channel N_1 exchange no RIS can appear, hence there are no on-shell contributions to be subtracted. To derive the Boltzmann equation for the density of lepton doublets we follow Ref. [18]. Asssuming kinetic equilibrium and rewriting the Liouville operator in terms of number densities the Boltzmann equation for the density of lepton doublets becomes

$$\begin{aligned} \frac{n_l}{dt} + 3Hn_l =& \frac{n_{N_1}}{n_{N_1}^{eq}} \gamma^{eq}(N_1 \to lH) - \frac{n_l}{n_l^{eq}} \gamma^{eq}(lH \to N_1) \\ &+ \frac{n_{\bar{l}}}{n_l^{eq}} \gamma_{sub}^{eq}(\bar{l}\bar{H} \to lH) - \frac{n_l}{n_l^{eq}} \gamma_{sub}^{eq}(lH \to \bar{l}\bar{H}) \\ &+ \gamma^{eq}(\bar{H}\bar{H} \to ll) - \left(\frac{n_l}{n_l^{eq}}\right)^2 \gamma^{eq}(l\bar{l} \to \bar{H}\bar{H}). \end{aligned} \tag{B.17}$$

where γ^{eq} are the reaction densities in thermal equilibrium

$$\gamma(i \to f) \equiv \int \frac{d^3p_i}{(2\pi)^3 2E_i} \frac{d^3p_f}{(2\pi)^3 2E_f} (2\pi)^4 \delta^4(p_i - p_f) |\mathcal{M}(i \to f)|^2 e^{-E_i/T}, \tag{B.18}$$

and we assumed the Higgs doublets H are in thermal equilibrium. The CP asymmetry is defined in such a way that

$$\gamma^{eq}(N_1 \to lH) = \gamma^{eq}(\bar{l}\bar{H} \to N_1) = \frac{1+\epsilon_1}{2}\gamma_{N_1}, \tag{B.19}$$

$$\gamma^{eq}(N_1 \to \bar{l}\bar{H}) = \gamma^{eq}(lH \to N_1) = \frac{1-\epsilon_1}{2}\gamma_{N_1}. \tag{B.20}$$

Where ϵ_1 is the CP violation parameter defined in Eq. 4.54 and $\gamma_{N_1} = \gamma^{eq}(N_1 \to H + l) + \gamma^{eq}(N_1 \to H + \bar{l}) = \tilde{\Gamma}_D n^{eq}_{N_1} \frac{\mathcal{K}_1}{\mathcal{K}_2}$. For the $2 \to 2$ processes we have

$$\gamma^{eq}_{sub}(\bar{l}\bar{\phi} \to l\phi) = \gamma^{eq}(\Delta L = 2, +) - \frac{1}{2}\epsilon_1 \gamma_{N_1}, \tag{B.21}$$

$$\gamma^{eq}_{sub}(l\phi \to \bar{l}\bar{\phi}) = \gamma^{eq}(\Delta L = 2, +) + \frac{1}{2}\epsilon_1 \gamma_{N_1}, \tag{B.22}$$

$$\gamma^{eq}(\bar{\phi}\bar{\phi} \to ll) = \gamma^{eq}(\overline{ll} \to \phi\phi) = \gamma^{eq}_{\Delta L=2,t}. \tag{B.23}$$

Where $\gamma^{eq}_{\Delta L=2,+}$ is the unsubtracted reaction density. Introducing a lepton, or $B-L$ asymmetry,

$$n_l = n^{eq}_l - \frac{1}{2}n_{B-L}, \qquad n_{\bar{l}} = n^{eq}_l + \frac{1}{2}n_{B-L}, \tag{B.24}$$

assuming $n_{B-L} = n_{\bar{l}} - n_l = O(\epsilon_1)$ and keeping only terms $O(\epsilon_1)$ the kinetic equation for the $B-L$ asymmetry reads

$$\frac{dn_{B-L}}{dt} + 3Hn_{B-L} = -\epsilon_1 \left(\frac{n_{N_1}}{n^{eq}_{N_1}} - 1\right)\gamma_{N_1} - \frac{n_{B-L}}{n^{eq}_l}\left(\frac{1}{2}\gamma_{N_1} + \gamma_{\Delta L=2}\right), \tag{B.25}$$

where

$$\gamma_{\Delta L=2} = 2\gamma^{eq}_{\Delta=2,+} + 2\gamma_{\Delta L=2}. \tag{B.26}$$

The CP violating part of γ^{eq}_{sub} yields the term $+\epsilon_1\gamma_{N_1}$ which guarantees that for $n_{N_1} = n^{eq}_{N_1}$ no asymmetry is generated. Neglecting the off-shell contribution $\gamma_{\Delta L=2}$, using the relation

$$\gamma_{N_1} = n^{eq}_{N_1} zHD = 2n^{eq}_l zHW_{ID}, \tag{B.27}$$

and changing variables from t to $z = M_1/T$ and from number densities to particle numbers in a comoving volume ($n_j = N_j/a(t_*)^3$) we find that the right-hand side of Eq. B.25 becomes

$$\frac{zH}{a(t_*)^3}(-\epsilon_1(N_{N_1} - N^{eq}_{N_1})D - N_{B-L}W_{ID}), \tag{B.28}$$

while for the left-hand side we can use the fact that $T \propto a(t)^{-1}$ and notice that

$$\frac{1}{a(t_*)^3}\frac{dN_{B-L}}{dt} = \frac{dn_{B-L}}{dt} + 3Hn_{B-L}, \tag{B.29}$$

$$\frac{dN_{B-L}}{dt} = \frac{dN_{B-L}}{dz}\frac{dz}{dT}\frac{dT}{dt} = zH\frac{dN_{B-L}}{dz}. \tag{B.30}$$

Finally, by combining Eqs. B.30 and B.29 we obtain the Boltzmann Equation 4.17.

Appendix C

Analytical approximation for the Solutions of BE

In this appendix we will give further details on the analytical approximations for the solutions of the Boltzmann Equations that we have already seen in Chapt. 4.2.1. In order to do that we will mainly follow Ref. [18]. First, we consider the quantities in Sec. 4.2, which are given in terms of the Bessel functions $\mathcal{K}_1$ and $\mathcal{K}_2$, whose asymptotic limit at high temperature $z << 1$ is

$$\mathcal{K}_2(z) \simeq \frac{2}{z}\mathcal{K}_1(z) \simeq \frac{2}{z^2}, \tag{C.1}$$

whereas at low temperatures $z >> 1$

$$\mathcal{K}_2(z) \simeq \frac{1}{z}\left(\frac{15}{8}+z\right)\mathcal{K}_1(z) \simeq \frac{1}{z^2}\left(\frac{15}{8}+z\right)\sqrt{\frac{\pi}{2}}ze^{-z}. \tag{C.2}$$

Interpolating functions for $\mathcal{K}_1(z)$ and $\mathcal{K}_2(z)$ for all values of z are

$$\mathcal{K}_2(z) \simeq \frac{1}{z}\left(\frac{15}{8}+z\right)\mathcal{K}_1(z) \simeq \frac{1}{z^2}\left(\frac{15}{8}+z\right)\sqrt{1+\frac{\pi}{2}}ze^{-z}. \tag{C.3}$$

In the approximation in Eq. C.3 we get

$$\left\langle\frac{1}{\gamma}\right\rangle(z) \simeq \frac{z}{\frac{15}{8}+z}, \tag{C.4}$$

$$D(z) \simeq K\frac{z^2}{\frac{15}{8}+z} \tag{C.5}$$

$$W_{ID}(z) \simeq \frac{1}{4}Kz^2\sqrt{1+\frac{\pi}{2}}ze^{-z}. \tag{C.6}$$

It is useful to define a value z_d corresponding to a decay temperature T_d below which decays are in equilibrium

$$\frac{\Gamma_D(z_d)}{H(z_d)} = z_d D(z_d) = 2. \tag{C.7}$$

The value of z_d is determined by K and in the approximation in Eq. C.5 we obtain

$$z_d^3 - \frac{2}{K}\left(z_d + \frac{15}{8}\right) \simeq 0. \tag{C.8}$$

For $K << 1$ this yields $z_d \simeq \sqrt{2/K}$, whereas $z_d \simeq (15/4K)^{1/3}$ for $K >> 1$. Inverse decays are in equilibrium if $W_{ID}(z) \geqslant 1$. From Eq. C.6 one can find that W_{ID} reaches its maximal value $W_{ID}(z_{max}) \simeq 0.3K$ at $z_{max} \simeq 2.4$. Hence, for $K > 3$ there exists an interval $z_{in} \leqslant z_{max} \leqslant z_{out}$, where inverse decays are in equilibrium. For $K < 3$ no such interval exists and inverse decays are always out of equilibrium. Thanks to these analytical approximations we can see from Eq. 4.37 that the final amount of baryon asymmetry depend by just two parameters: ϵ, indicating the amount of CP-violation, and K, the washout parameter (which indicate the strength of decay compared to the mass of heavy neutrinos).

C.1 Out-of-equilibrium decays

In the regime far out of equilibrium $K \ll 1$, decays occur at very small temperatures $z_d \gg 1$. At these temperatures the washout effects become less significant and we can ignore it ($W = 0$). So the produced $B - L$ asymmetry is not reduced by washout effects. In this case the integral for the efficiency factor becomes

$$k(z) \simeq -\frac{4}{3}\int_{z_i}^{z} dz' \frac{dN_{N_1}}{dz'} \simeq \frac{4}{3}(N_{N_1}^i - N_{N_1}(z)), \tag{C.9}$$

where we have neglected the washout factor W_{ID}. For $z < z_d$ no asymmetry is generated because the heavy neutrinos do not decay. They also cannot be produced since inverse decays are switched off. Hence, in this regime the dynamics is completely frozen. For $z > z_d$ the equilibrium abundance is negligible, due to the exponential suppression in the approximation in Eq. C.3 for the Bessel function, and from Eq. 4.36 we find

$$\begin{aligned} N_{N_1}(z) &\simeq N_{N_1}^i e^{-\int_{z_i}^{z} dz' D(z')} \\ &\simeq N_{N_1}^i e^{-K\left(\frac{z^2}{2} - \frac{15z}{8} + \left(\frac{15}{8}\right)^2 \ln\left(1 + \frac{8}{15}z\right)\right)}. \end{aligned} \tag{C.10}$$

The final value of the efficiency factor $k_f = k(\infty)$ is proportional to the initial N_1^i abundance. In particular, if the initial abundance is zero, then $k_f = 0$ as well. Therefore in this region one has to invoke some external mechanism to produce the initial abundance of neutrinos. Thus in the regime $K \ll 1$ the results strongly depend on the initial conditions and the picture is not self-contained.

C.1.1 Dynamical initial abundance

In order to obtain the efficiency factor in the case of vanishing initial N_1-abundance, $N_{N_1}(z_i) \equiv N_{N_1}^i \simeq 0$, one has to calculate how heavy neutrinos are dynamically produced by inverse decays. This requires solving Eq. 4.36 with the initial condition $N_{N_1}^i = 0$. First, we define a value z_{eq} such that

$$N_{N_1}(z_{eq}) = N_{N_1}^{eq}(z_{eq}), \tag{C.11}$$

so if $z = z_{eq}$ we obtain, from Eq. 4.36, that the number density N_{N_1} reaches its maximum, since $dN_{N_1}/dz = 0$ and $d^2N_{N_1}/dz^2 = DdN_{N_1}^{eq}/dz < 0$. An approximate solution can be found by noting that for $z < z_{eq}$ inverse decays dominate and thus

$$\frac{dN_{N_1}}{dz} \simeq DN_{N_1}^{eq} > 0. \tag{C.12}$$

By inserting Eqs. 4.27, 4.24, 4.33 and integrating we find for $z < z_{eq}$

$$\begin{aligned} N_{N_1}(z) &\simeq \frac{3}{8} K \int_{z_i}^{z} dz' z'^3 \mathcal{K}_1(z') \\ &\simeq \frac{3}{2} \int_{z_i}^{z} dz' W_{ID}(z'). \end{aligned} \tag{C.13}$$

In the case $z_i \ll z < 1$ we can use approximation in Eq. C.1 and we find

$$N_{N_1}(z) \simeq \frac{K}{8} z^3. \tag{C.14}$$

Now we can calculate the corresponding approximate solution for the efficiency factor $k(z)$. For $z < z_{eq}$ the efficiency factor $k \equiv k^-$ is negative since $N_{N_1} < N_{N_1}^{eq}$ (since we are considering the inverse decays when N_1 is being populated). From Eqs. 4.38 and C.12 we get

$$\begin{aligned} k^-(z) &\simeq -\frac{4}{3} \int_{z_i}^{z} dz' D(z') N_{N_1}^{eq}(z') e^{-\int_{z'}^{z} dz" W_{ID}(z")} \\ &= -2 \int_{z_i}^{z} dz' W_{ID}(z') e^{-\int_{z'}^{z} dz" W_{ID}(z")} \\ &= -2\big(\big(1 - e^{\int_{z_i}^{z} dz' W_{ID}(z')}\big) \\ &\simeq -2\big(1 - e^{-\frac{2}{3} N_{N_1}}\big), \end{aligned} \tag{C.15}$$

where we have used Eq. 4.34 and in the third passage we have used the fact that

$$\frac{d}{dz'}\left(e^{-\int_{z'}^{z} dz" W_{ID}(z")}\right) = W_{ID}(z') e^{-\int_{z'}^{z} dz" W_{ID}(z")}. \tag{C.16}$$

For $N_{N_1} \ll 1$ the efficiency factor is proportional to N_{N_1}, up to corrections which correspond to washout effects. For $z > z_{eq}$ k^- is reduced by washout effects. For $z \geqslant z_{eq}$, there is an additional positive contribution to the efficiency factor, corresponding to the period in which N_{N_1} starts decaying.

$$k^+(z) \simeq \frac{4}{3} \int_{z_{eq}}^{z} dz' D(z') (N_{N_1}(z') - N_{N_1}^{eq}(z')) e^{-\int_{z'}^{z} dz" W_{ID}(z")}. \tag{C.17}$$

Then, the total efficiency factor is the sum of both contributions,

$$k_f(z) = k^+(z) + k^-(z). \tag{C.18}$$

For $z \gtrsim z_{eq}$ we now have to distinguish two different situations, the weak and strong washout regimes.

C.1.2 Weak washout regime

In the case of weak washout[1] $K \ll 1$ we have $z_{eq} \gg 1$ since

$$K = \frac{\tilde{m_1}}{m_1^*} = \frac{(Y^+Y)_{11} v^2}{M_1} \frac{3\sqrt{5} M_{Pl}}{16 \pi^{5/2} v^2 \sqrt{g_*}} \ll 1 \tag{C.19}$$

[1] We are here focusing in the case of weak washout with vanishing initial abundance

implies

$$M_1 \gg (Y^+Y)_{11}\frac{3\sqrt{5}}{16\pi^{5/2}\sqrt{g_*}}M_{Pl}, \tag{C.20}$$

so N_1 decays when they are not relativistic and at very small temperatures. For $z < z_{eq}$ inverse decays dominate and we can employ the following analytical approximation:

$$N_{N_1}(z_{eq}) \simeq \frac{9\pi}{16}K \equiv N(K). \tag{C.21}$$

For $z > z_{eq} \gg 1$ decays dominate over inverse decays such that

$$\frac{dN_{N_1}}{dz} = -DN_{N_1} < 0. \tag{C.22}$$

By integrating we obtain

$$N_{N_1}(z) = N^{eq}_{N_1}(z_{eq})e^{-\int_{z_{eq}}^{z} dz' D(z')}. \tag{C.23}$$

For $z > z_{eq}$, $W_{ID}(z)$ is exponentially suppressed and washout effects can be neglected in first approximation. For the negative part of the efficiency factor $k^-(z)$ we obtain from Eq. C.15:

$$k^- = -2\big(1 - e^{-\frac{2}{3}N(K)}\big). \tag{C.24}$$

While, for the positive part, we obtain from Eq. (C.17)

$$k^+(z) = \frac{4}{3}(N(K) - N_{N_1}(z)). \tag{C.25}$$

Then the efficiency factor $k(z)$ is given by

$$k_f(K) \simeq \frac{4}{3}N(K) - 2\big(1 - e^{-\frac{2}{3}N(K)}\big). \tag{C.26}$$

To first order in $N(K) \propto K$ the final efficiency factor vanishes. This corresponds to the approximation where washout effects are completely neglected. To obtain a non-zero asymmetry the washout in the period $z < z_{eq}$ is crucial. It reduces the absolute value of the negative contribution $k^-(z)$, yielding a positive efficiency factor of order $\mathcal{O}(K^2)$

$$k_f(K) \simeq \left[\frac{2}{3}N(K)\right]^2 \simeq \frac{9\pi^2}{64}K^2 \tag{C.27}$$

This equation does not hold for $K > 1$, since in this case z_{eq} becomes small and washout effects for $z \geqslant z_{eq}$ are also important.

C.1.3 Strong washout regime

As we have already seen for $K \gg 1$ there exists an interval $z_{in} \leqslant z \leqslant z_{max}$ where inverse decays are in equilibrium. Assuming that the wash-out are effective, any asymmetry generated before z_{in} is fully erased. Therefore, in this case there is no dependence on the initial conditions. As K increases, z_{eq} decreases and at $K \simeq 3$ the maximal number density $N(K)$ reaches the equilibrium density N_{eq} at $z_{eq} \simeq 1$. For $K \gg 1$, one obtains from Eq. C.14:

$$N_{N_1}(z_{eq}) = \simeq \frac{K}{8}z_{eq}^3 \Rightarrow z_{eq} \simeq \left(\frac{3}{4}\frac{8}{K}\right)^{1/3} \simeq \left(\frac{6}{K}\right)^{1/3} \simeq z_d \ll 1, \tag{C.28}$$

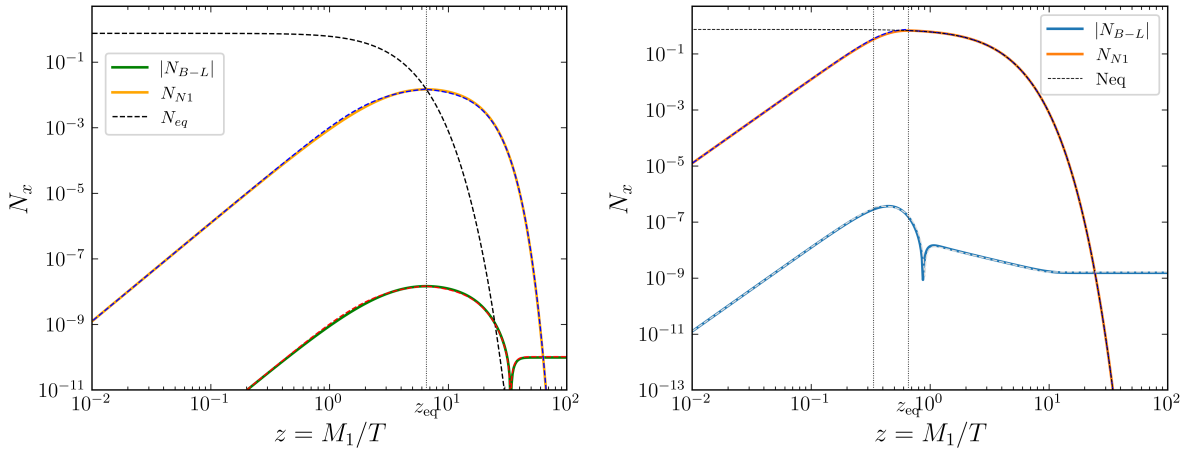

Figure C.1: Comparison analytical (dashed lines) and numerical results for heavy neutrino production and B-L asymmetry in the case of zero initial abundance for weak washout with $K = 10^{-2}$ and $|\epsilon_1| = 10^{-6}$ (left) and strong washout with $K = 100$ and $|\epsilon| = 10^{-6}$ (right).

where we have used $N_{N_1}(z_{eq}) = N^{eq}_{N_1}(z_{eq}) = 3/4$. Since $z_{eq} \ll 1$, we can use $N^{eq}_{N_1} \simeq 3/4$ in Eq. 4.36 and, by integrating we find

$$N_{N_1}(z) = \frac{3}{4}\left(1 - e^{-\frac{1}{6}Kz^3}\right). \tag{C.29}$$

In this case we can neglect the k^- contribution to the efficiency factor since assuming that the asymmetry generated at high temperatures is efficiently washed out is equivalent to assume thermal initial abundance. For $K \gtrsim 3$, inverse decays are in equilibrium in the range $z_{in} < z < z_{out}$, with $z_{in} \simeq 2/\sqrt{K}$, and any asymmetry generated before z_{in} is efficiently washed-out. For $z \lesssim z_d \simeq [15/(4K)]^{1/3}$ decays are not effective in tracking the equilibrium distribution, since in this case $T_D < T$ (T_D is the decay temperature, below which decays are in equilibrium). The departure from equilibrium Δ, defined by the difference

$$\Delta = N_{N_1}(z) - N^{eq}_{N_1}(z), \tag{C.30}$$

with $N_{N_1}(0) = N^{eq}_{N_1}(0) = 3/4 \equiv N_{eq}$, drives the production of $B - L$ asymmetry. In the case $z \lesssim z_d$ one has

$$\Delta(z) \simeq N^i_{N_1} - N^{eq}_{N_1}(z) \simeq \frac{3}{16}z^2. \tag{C.31}$$

The corresponding efficiency factor is given by (cfr. Eq. 4.38)

$$k(z) \simeq \frac{4}{3}\int_{z_i}^{z} dz' D(z')\Delta(z') \simeq \frac{2K}{75}z^5. \tag{C.32}$$

In the case $z > z_d$ the neutrino abundance tracks closely the equilibrium behavior. Since $D \propto K$, we can solve the Boltzmann equation in power of 1/K

$$\Delta(z) = -\frac{1}{D}\frac{dN^{eq}_{N_1}}{dz} + O(\frac{1}{K^2}). \tag{C.33}$$

substituting the expression in Eq. 4.33 and using the property of the Bessel functions:

$$\frac{d}{dx}[x^\nu \mathcal{K}_\nu(x)] = -x^\nu \mathcal{K}_{\nu-1}(x), \tag{C.34}$$

we find

$$\frac{dN_{N_1}^{eq}}{dz} = -\frac{3}{8}z^2\mathcal{K}_1(z) = -\frac{3}{2Kz}W_{ID}(z). \tag{C.35}$$

Now we can compute the efficiency factor:

$$\begin{aligned} k(z) &= -\frac{4}{3}\int_{z_i}^{z} dz' \frac{dN_{N_1}}{dz'} e^{-\int_{z'}^{z} dz'' W_{ID}(z'')} = -\frac{4}{3}\int_{z_i}^{z} dz' \left(-\frac{3}{2Kz}W_{ID}(z)\right) e^{-\int_{z'}^{z} dz'' W_{ID}(z'')} \\ &= \frac{2}{K}\int_{z_i}^{z} dz' \frac{W_{ID}(z')}{z'} e^{-\int_{z'}^{z} dz'' W_{ID}(z'')} \equiv \int_{z_i}^{z} dz' e^{-\psi(z',z)}. \end{aligned} \tag{C.36}$$

This integral is dominated by the contribution from a region around the value $\bar{z}$ where $\psi(z', z)$ has a minimum. The integral can be solved by replacing in the exponent of the integrand $W_{ID}(z)$ by

$$\bar{W}_{ID}(z) = \frac{\bar{z}}{z}W_{ID}(z) = -\frac{K\bar{z}}{4}\frac{d}{dz}(z^2\mathcal{K}_2(z)). \tag{C.37}$$

Then the efficiency factor becomes

$$\frac{2}{K\bar{z}}\int_{z_i}^{z} dz' \bar{W}_{ID}(z') e^{-\int_{z'}^{z} dz'' \bar{W}_{ID}(z'')} = \frac{2}{K\bar{z}}(1 - e^{-\int_{z_i}^{z} dz' \bar{W}_{ID}(z')}). \tag{C.38}$$

So for $z_d \lesssim z < z_B$, $k \propto 1/z$, while for $z \geqslant z_B$ the efficiency factor gets frozen at a final value $k_f \simeq 2/(Kz_B)$. Finally, we can find global solutions for all values of z by interpolating the asymptotic solution for $z < z_d$ and $z > z_d$ respectively. From Eqs. C.33 and C.31 one obtains

$$\Delta(z) \simeq \left(1 + \frac{Kz^3}{\frac{15}{4} + 2z}\right)^{-1} \frac{3}{16}z^3\mathcal{K}_1(z). \tag{C.39}$$

Similarly we can interpolate the results for the efficiency factor and we obtain

$$k(z) \simeq \left(1 + \frac{K^2\bar{z}z^5}{75}\right)^{-1} \frac{2K}{75}z^5. \tag{C.40}$$

Appendix D

CP asymmetry computation

D.1 Wave diagrams contribution

First we consider the following wave diagram:

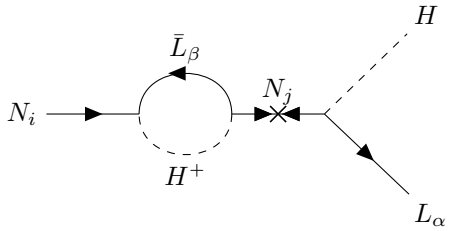

In this diagram (and also in the following ones) we have a line direction which is the "left-handedness" and the X represents a Majorana mass insertion. We start by considering the amplitude

$$\langle i|T|f\rangle = \langle N_i|T(-i\int d^4x Y_{\alpha i}\bar{N}_j P_L H^+ L)|L_\alpha H\rangle = -iY_{\alpha i}\bar{u}_i P_L u_\alpha, \tag{D.1}$$

where T is the time ordering operator. This amplitude corresponds to the following diagram

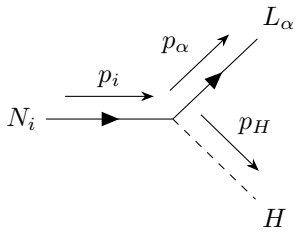

We can study the kinematics of this diagram in the center of mass frame. In this case N_i is at rest so the four-momentum is

$$p_i = \begin{bmatrix} M_i \\ \vec{0} \end{bmatrix}, \tag{D.2}$$

from momentum conservation we have $\vec{p_i} = \vec{p}_\alpha + \vec{p}_H$, so $\vec{p}_\alpha = -\vec{p}_H$. Now we can compute

$$p_i \cdot p_\alpha = \begin{pmatrix} M_i \\ \vec{0} \end{pmatrix} \cdot \begin{pmatrix} E_\alpha \\ \vec{p}_\alpha \end{pmatrix} = M_i \cdot E_\alpha. \tag{D.3}$$

From this we find

$$E_\alpha = \frac{p_i \cdot p_\alpha}{M_i} = \frac{(p_\alpha + p_H) \cdot p_\alpha}{M_i} = \frac{M_i}{2}, \tag{D.4}$$

where, in the last passage we have used the fact that $p_i = p_\alpha + p_H$, so $p_i^2 = p_\alpha^2 + p_H^2 + 2p_\alpha \cdot p_H$ and we have assumed $p_\alpha^2 = m_\alpha^2 = 0$, $p_H^2 = m_H^2 = 0$, since the scale of the heavy neutrinos is so much larger than the electroweak scale, it is reasonable to work directly in the symmetric phase where all particles except the heavy Majorana neutrinos are massless, and all components of the neutral and charged complex Higgs fields are physical [19]. Thus we can conclude that

$$p_\alpha = \begin{pmatrix} \frac{M_i}{2} \\ \vec{p}_\alpha \end{pmatrix}, \qquad p_H = \begin{pmatrix} \frac{M_i}{2} \\ -\vec{p}_\alpha \end{pmatrix}. \tag{D.5}$$

Secondly we consider the amplitude

$$\begin{aligned} \langle k|T|i\rangle &= \langle \bar{L}_\beta H|T\big(-i\int d^4x Y_{\beta i}\bar{N}_i P_L H^+ L_\beta\big)|N_i\rangle = \\ &= -iY_{\beta i}\langle \bar{L}_\beta|\bar{N}_i P_L L_\beta|N_i\rangle = \\ &= iY_{\beta i}\langle \bar{L}_\beta|L_\beta^+ P_L^T C^{-1} N_i|N_i\rangle = \\ &= iY_{\beta i}(v_\beta^T P_L^T C^{-1} u_i) = \\ &= iY_{\beta i}(\bar{u}_\beta C^T P_L^T C^{-1} u_i) = \\ &= -iY_{\beta i}(\bar{u}_\beta P_L u_i). \end{aligned} \tag{D.6}$$

where, in the second line we have neglected the contraction of the scalar since it gives just a phase and in the third line, we have used the fact that $\bar{N}_i P_L L_\beta = (\bar{N}_i P_L L_\beta)^T$ since it is a fermionic bilinear. In fact, recalling that for Grassman variables $(AB)^T = -B^T A^T$ we get

$$(\bar{N}_i P_L L_\beta)^T = -L_\beta^T P_L^T \bar{N}_i^T, \tag{D.7}$$

and

$$\begin{aligned} &\bar{N}_i P_L L_\beta = \bar{N}_i (P_L)_{i\beta} L_\beta = \bar{N}_i L_\beta (P_L)_{i\beta} = -L_\beta \bar{N}_i (P_L)_{i\beta} = \\ &= -L_i \bar{N}_\beta (P_L)_{\beta i} = -L_i (P_L)_{i\beta}^T \bar{N}_\beta = -L_i^T (P_L)_{i\beta}^T \bar{N}_\beta^T = -L_\beta^T P_L^T \bar{N}_i^T. \end{aligned} \tag{D.8}$$

We have also used the fact that for Majorana neutrinos $\bar{N}_j^T = C^{-1} N_j$ and in the last line we have used the identities: $u = C\bar{v}^T$ and $v = C\bar{u}^T$. This amplitude corresponds to the following diagram:

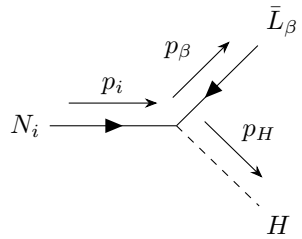

For this diagram the kinematics is analogous to the previous one so we can immediately conclude that

$$p_\beta = \begin{pmatrix} \frac{M_i}{2} \\ \vec{p}_\beta \end{pmatrix}, \qquad p_H = \begin{pmatrix} \frac{M_i}{2} \\ -\vec{p}_\beta \end{pmatrix}. \tag{D.9}$$

Finally we need to compute

$$\langle k|T|f\rangle^* = \langle \bar{L}_\beta H|T|L_\alpha H\rangle^*, \tag{D.10}$$

this expression comes from $\langle\Omega|TH\bar{L}_\beta L_\alpha H|\Omega\rangle = \frac{\langle 0|TH\bar{L}_\beta L_\alpha H \exp(i\int d^4x\mathcal{L}_{int})|0\rangle}{\langle 0|\exp(i\int d^4x\mathcal{L}_{int})|0\rangle}$. Taylor expanding the numerator we get that the leading contribution comes from the second order term, since the first order contains an odd number of fields and vanishes because of Wick's theorem. So we consider

$$\langle \bar{L}_\beta H|T\big(-i\int d^4x Y_{\alpha i}\bar{N}_j P_L H^+ L_\alpha\big)\big(-i\int d^4y Y_{\beta i}\bar{N}_j P_L H^+ L_\beta\big)|L_\alpha H\rangle^*, \tag{D.11}$$

now we take the transpose of the term $(...)_x$ in order to have the contraction $N_i\bar{N}_i$ which gives the fermion propagator $\langle\Omega|T\psi(x)\bar{\psi}(y)|\Omega\rangle = i\frac{\not{p}+m}{p^2-m^2+i\epsilon}$ [37]. So we find[1]

$$\begin{aligned}
&\langle \bar{L}_\beta|T\big(-i\int d^4x Y_{\alpha i}(\bar{N}_j P_L L_\alpha)^T\big)\big(-i\int d^4y Y_{\beta i}\bar{N}_j P_L L_\beta\big)|L_\alpha\rangle^* \\
&= -Y^*_{\alpha j}Y^*_{\beta j}(-v_\beta^T P_L^T C^{-1}\left(\frac{i(\not{p}_j + M_j)}{p^2 - M_j^2}\right)P_L u_\alpha)^* \\
&= \frac{-iY^*_{\alpha j}Y^*_{\beta j}}{p^2-M^2}(v_\beta^T P_L^T C^{-1}(\not{p}_j + M_j)P_L u_\alpha)^* \\
&= \frac{-iY^*_{\alpha j}Y^*_{\beta j}}{p^2-M^2}(\bar{u}_\beta C^T P_L^T C^{-1}(\not{p}_j + M_j)P_L u_\alpha)^* \\
&= \frac{iY^*_{\alpha j}Y^*_{\beta j}}{p^2-M^2}(\bar{u}_\beta P_L(\not{p}_j + M_j)P_L u_\alpha)^* \\
&= \frac{iY^*_{\alpha j}Y^*_{\beta j}}{p^2-M^2}(\bar{u}_\beta P_L M_j u_\alpha)^+ \\
&= \frac{iY^*_{\alpha j}Y^*_{\beta j}}{p^2-M^2}\bar{u}_\alpha M_j P_R u_\beta.
\end{aligned} \tag{D.12}$$

where we have used the properties of the charge conjugation matrix: $C^T = C^{-1} = -C$ and $C\gamma^5 C^{-1} = (\gamma^5)^T$, and of the projectors: $P_L^2 = P_L$ and $P_L P_R = 0$. This amplitude corresponds to the diagram:

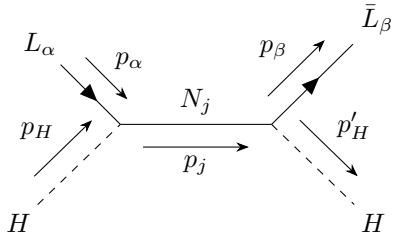

[1] As in the previous case we neglect the contribution of the Higgs since its contractions gives just a 1 factor

This is an s-channel and in the center of mass frame we have $E_{CM} = \sqrt{s} = p_\alpha + p_H = p_\beta + p_{H'}$ and

$$p_j = \begin{pmatrix} E_{CM} \\ \vec{0} \end{pmatrix} = \begin{pmatrix} M_i \\ \vec{0} \end{pmatrix}. \tag{D.13}$$

Now we sum the three contribution over polarizations:

$$\begin{aligned}
\mathcal{M}_{unpol} &= \frac{1}{2}\sum_{pol}(-iY_{\alpha i}\bar{u}_i P_L u_\alpha)\left(\frac{iY^*_{\alpha j}Y^*_{\beta j}}{p_j^2 - M^2}\bar{u}_\alpha M_j P_R u_\beta\right)(-iY_{\beta i}\bar{u}_\beta P_L u_i) \\
&= \frac{1}{2}\sum_{pol}(-i)\frac{Y_{\alpha i}Y^*_{\alpha j}Y^*_{\beta j}Y_{\beta i}}{p_j^2 - M^2}M_j(\bar{u}_i P_L u_\alpha \bar{u}_\alpha P_R u_\beta \bar{u}_\beta P_L u_i) \\
&= \frac{1}{2}(-i)\frac{Y_{\alpha i}Y^*_{\alpha j}Y^*_{\beta j}Y_{\beta i}}{p_j^2 - M^2}M_j tr(\bar{u}_i P_L \not{p}_\alpha P_R \not{p}_\beta P_L u_i) \\
&= \frac{1}{2}(-i)\frac{Y_{\alpha i}Y^*_{\alpha j}Y^*_{\beta j}Y_{\beta i}}{p_j^2 - M^2}M_j tr(\bar{u}_i P_L \not{p}_\alpha \not{p}_\beta u_i) \\
&= \frac{1}{2}(-i)\frac{Y_{\alpha i}Y^*_{\alpha j}Y^*_{\beta j}Y_{\beta i}}{p_j^2 - M^2}M_j \frac{1}{2}tr[(1-\gamma^5)\not{p}_\alpha \not{p}_\beta(\not{p}_i + M_i)] \\
&= \frac{-i}{4}\frac{Y_{\alpha i}Y^*_{\alpha j}Y^*_{\beta j}Y_{\beta i}}{p_j^2 - M^2}M_j tr(\not{p}_\alpha \not{p}_\beta M_i) \\
&= (-i)\frac{Y_{\alpha i}Y^*_{\alpha j}Y^*_{\beta j}Y_{\beta i}}{p_j^2 - M^2}M_j M_i p_\alpha p^\alpha.
\end{aligned} \tag{D.14}$$

Where we have used: $\sum_s u_s(p)_\alpha \bar{u}_s(p)_\beta = (\not{p} + m)_{\alpha\beta}$ and the properties of gamma matrices trace $tr(\gamma^{\mu_1}...\gamma^{\mu_N}) = 0$, $tr(\gamma^5\gamma^{\mu_1}...\gamma^{\mu_N}) = 0$ if N =odd, $tr(\gamma^5\gamma^\mu\gamma^\nu) = 0$ and $tr(\gamma^\alpha\gamma^\beta) = 4\eta^{\alpha\beta}$. Now we can use Eq. D.13 in the denominator and Eq. D.21 to compute the product $p_\alpha p^{\alpha\,2}$ and Eq.(D.14) becomes

$$\begin{aligned}
&= \frac{-iY_{\alpha i}Y^*_{\alpha j}Y^*_{\beta j}Y_{\beta i}}{M_i^2 - M_j^2}M_j M_i\left(\frac{M_i^2}{4} - \frac{M_i^2}{4}\cos\theta_{\alpha\beta}\right) \\
&= \frac{-iY_{\alpha i}Y^*_{\alpha j}Y^*_{\beta j}Y_{\beta i}}{M_i^2 - M_j^2}\frac{M_j M_i^3}{4}\left(1 - \cos\theta_{\alpha\beta}\right).
\end{aligned} \tag{D.15}$$

[2] we are using the Minkowski metric $\eta_{\alpha\beta} = diag(+,-,-,-)$

Since we are using the optical theorem we need to integrate over the on-shell cut momenta and we obtain:

$$\begin{aligned}
&\int d\Pi_{L_\beta} d\Pi_{H'} (2\pi)^4 \delta^{(4)}(p_N - p_{L_\beta} - p_{H'})(-i)\frac{Y_{\alpha i}Y^*_{\alpha j}Y^*_{\beta j}Y_{\beta i}}{M_i^2 - M_j^2}\frac{M_j M_i^3}{4}(1-\cos\theta_{\alpha\beta}) \\
&= \frac{-iY_{\alpha i}Y^*_{\alpha j}Y^*_{\beta j}Y_{\beta i}}{M_i^2 - M_j^2}\frac{M_j M_i^3}{4}\int \frac{d^3p_\beta}{(2\pi)^3 2E_\beta}\frac{d^3p_{H'}}{(2\pi)^3 2E_{H'}}(2\pi)^4\delta(E_N - E_\beta - E_{H'})\times \\
&\quad \delta^{(3)}(\vec{p_N} - \vec{p_{L_\beta}} - \vec{p_{H'}})(1-\cos\theta_{\alpha\beta}) \\
&= \frac{-iY_{\alpha i}Y^*_{\alpha j}Y^*_{\beta j}Y_{\beta i}}{M_i^2 - M_j^2}\frac{M_j M_i^3}{4}\int \frac{d^3p_\beta}{(2\pi)^2 2E_\beta 2E_{H'}}\delta(E_N - E_\beta - E_{H'})(1-\cos\theta_{\alpha\beta})\big|_{\vec{p}_\beta = -\vec{p}_{H'}} \\
&= \frac{-iY_{\alpha i}Y^*_{\alpha j}Y^*_{\beta j}Y_{\beta i}}{M_i^2 - M_j^2}\frac{M_j M_i^3}{4}\int \frac{d^3p_\beta}{(2\pi)^2 4E_\beta^2}\delta(E_N - 2E_\beta)(1-\cos\theta_\beta) \\
&= \frac{-iY_{\alpha i}Y^*_{\alpha j}Y^*_{\beta j}Y_{\beta i}}{M_i^2 - M_j^2}\frac{M_j M_i^3}{4(2\pi)}\int \frac{p_\beta^2 dp_\beta d\cos\theta_\beta}{4E_\beta^2}\delta(E_N - 2E_\beta)(1-\cos\theta_\beta) \\
&= \frac{-iY_{\alpha i}Y^*_{\alpha j}Y^*_{\beta j}Y_{\beta i}}{M_i^2 - M_j^2}\frac{M_i^3 M_j}{32\pi}.
\end{aligned} \tag{D.16}$$

Where in the third line we have integrated over the three dimensional delta. We have also used mass-shell relation $E_j = \sqrt{|\vec{p}_j|^2 + m_j^2},\ for\ j = \alpha, \beta, H, H'$, where $m_j^2 = 0$ and in the fifth line we passed to spherical coordinates. Also, in order to have an integral containing variables related to L_β only, we changed $\cos\theta_{\alpha\beta}$ to $\cos\theta_\beta$ since we can perform a rotation to have one of the reference frames axis aligned with the emission direction of L_α. Finally, we use this result in Eq. 4.75. First, we consider the numerator and we integrate over the phase space

$$\begin{aligned}
&\int d\Pi_l d\Pi_H (2\pi)^4 \delta^{(4)}(p_N - p_H - p_{L_\alpha})(-2\mathcal{I}m[(TT^\dagger)_{if}T_{fi}]) \\
=&\frac{\mathcal{I}m(Y_{\alpha i}Y^*_{\alpha j}Y^*_{\beta j}Y_{\beta i})}{M_i^2 - M_j^2}\frac{M_i^3 M_j}{16\pi}\int \frac{d^3p_\alpha}{(2\pi)^3 2E_\alpha}\frac{d^3p_H}{(2\pi)^3 2E_H}(2\pi)^4\delta(E_N - E_\alpha - E_{H'}) \\
&\quad \times \delta^{(3)}(\vec{p_N} - \vec{p_{L_\alpha}} - \vec{p_H}) \\
=&\frac{1}{8\pi}\frac{\mathcal{I}m(Y_{\alpha i}Y^*_{\alpha j}Y^*_{\beta j}Y_{\beta i})}{M_i^2 - M_j^2}\frac{M_i^3 M_j}{16\pi}.
\end{aligned} \tag{D.17}$$

Now we divide this result by the denominator previously obtained (cf. Eq. 4.76) and we obtain

$$\frac{1}{16\pi}\frac{\mathcal{I}m(Y_{\alpha i}Y^*_{\alpha j}Y^*_{\beta j}Y_{\beta i})}{\sum_\alpha |Y_{\alpha i}|^2}\frac{M_i M_j}{M_i^2 - M_j^2}, \tag{D.18}$$

by introducing $x = M_j^2/M_i^2$ we can rewrite this result in the following form

$$\frac{1}{16\pi}\frac{\mathcal{I}m(Y_{\alpha i}Y^*_{\alpha j}Y^*_{\beta j}Y_{\beta i})}{\sum_\alpha |Y_{\alpha i}|^2}\frac{\sqrt{x}}{1-x}. \tag{D.19}$$

The second wave diagram contribution is given by the following diagram:

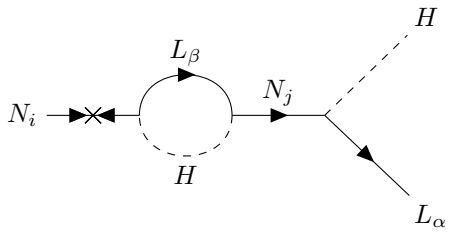

The amplitude $\langle i|T|f\rangle$ has already been computed in the previous diagram, see Eq. D.1. Therefore, we proceed by computing the next amplitude:

$$\langle k|T|i\rangle = \langle L_\beta H|T\left(i\int d^4x(-Y^*_{\beta i}\bar{L}_\beta\tilde{H}P_R N_i)\right)|N_i\rangle = -iY^*_{\beta i}\bar{u}_\beta P_R u_i, \tag{D.20}$$

which corresponds to the following diagram

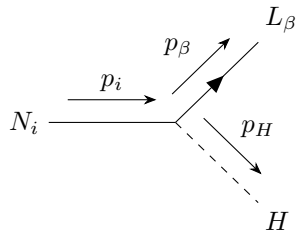

As in previous case we study the kinematics of this diagram in the center of mass frame and we obtain:

$$p_\beta = \begin{pmatrix}\frac{M_i}{2}\\ \vec{p}_\beta\end{pmatrix}, \qquad p_H = \begin{pmatrix}\frac{M_i}{2}\\ -\vec{p}_\beta\end{pmatrix}, \tag{D.21}$$

where we have used the fact that N_i is at rest in the CM frame, namely $P_i = (M_i, \vec{0})$, and from momentum conservation we have $\vec{p}_\beta = -\vec{p}_H$. The last amplitude we need to compute is

$$\begin{aligned}
\langle k|T|f\rangle^* =& \langle L_\beta H|T\left(i\int d^4x(-Y^*_{\beta j}\bar{L}_\beta\tilde{H}P_R N_j)\right)\left(-i\int d^4y(Y_{\alpha j}\bar{N}_j P_L H^\dagger L_\alpha)\right)|L_\alpha H\rangle^*\\
=& -Y_{\beta j}Y^*_{\alpha i}(\bar{u}_\beta P_R i\left(\frac{\not{p}_j + M_j}{p_j^2 - M_j^2}\right)P_L u_\alpha)^*\\
=& \frac{iY_{\beta j}Y^*_{\alpha j}}{p_j^2 - M_j^2}(\bar{u}_\beta P_R \not{p}_j u_\alpha)^*\\
=& \frac{iY_{\beta j}Y^*_{\alpha j}}{p_j^2 - M_j^2}(\bar{u}_\beta P_R \not{p}_j u_\alpha)^\dagger\\
=& \frac{iY_{\beta j}Y^*_{\alpha j}}{p_j^2 - M_j^2}\bar{u}_\alpha \not{p}_j P_L u_\beta
\end{aligned} \tag{D.22}$$

This amplitude corresponds to the diagram:

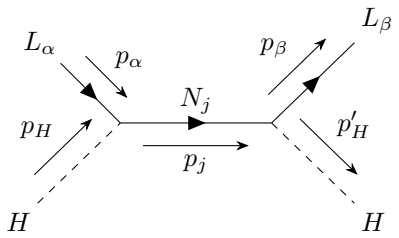

This is an s-channel and in the center of mass frame we have $E_{CM} = \sqrt{s} = P_\alpha + P_H = P_\beta + P_{H'}$ and $P_j = (E_{CM}, \vec{0}) = (M_i, \vec{0})$. Now we can proceed to sum the three contributions over polarizations:

$$\begin{aligned}
\mathcal{M}_{unpol} =& \frac{1}{2}\sum_s (-iY_{\alpha i}\bar{u}_i P_L u_\alpha)\left(\frac{iY_{\beta j}Y^*_{\alpha j}}{p_j^2 - M_j^2}\bar{u}_\alpha \not{p}_j P_L u_\beta\right)(-iY^*_{\beta i}\bar{u}_\beta P_R u_i) \\
=& \frac{1}{2}\sum_s \left(\frac{-iY_{\alpha i}Y_{\beta j}Y^*_{\alpha j}Y^*_{\beta i}}{P_j^2 - M_j^2}\right)(\bar{u}_i P_L u_\alpha \bar{u}_\alpha \not{p}_j P_L u_\beta \bar{u}_\beta P_R u_i) \\
=& \frac{1}{2}\left(\frac{-iY_{\alpha i}Y_{\beta j}Y^*_{\alpha j}Y^*_{\beta i}}{P_j^2 - M_j^2}\right) Tr[P_L \not{p}_\alpha \not{p}_j P_L \not{p}_\beta P_R(\not{p}_i + M_i)] \\
=& \frac{1}{4}\left(\frac{-iY_{\alpha i}Y_{\beta j}Y^*_{\alpha j}Y^*_{\beta i}}{P_j^2 - M_j^2}\right) Tr[(1-\gamma_5)\not{p}_\alpha \not{p}_j \not{p}_\beta(\not{p}_i + M_i)] \\
=& \frac{1}{4}\left(\frac{-iY_{\alpha i}Y_{\beta j}Y^*_{\alpha j}Y^*_{\beta i}}{P_j^2 - M_j^2}\right)[4(p_\alpha p^j_\mu p_\beta p^i_\nu)(\eta^{\alpha\mu}\eta^{\beta\nu} - \eta^{\alpha\beta}\eta^{\mu\nu} + \eta^{\alpha\nu}\eta^{\mu\beta}) + 4ip_\alpha p^j_\mu p_\beta p^i_\nu \epsilon^{\alpha\mu\beta\nu}] \\
=& \frac{1}{4}\left(\frac{-iY_{\alpha i}Y_{\beta j}Y^*_{\alpha j}Y^*_{\beta i}}{P_j^2 - M_j^2}\right)(p_\alpha \cdot p_j p_{\beta\cdot i} - p_\alpha \cdot p_\beta p_j \cdot p_i + p_\alpha \cdot p_j p_\beta \cdot p_i)
\end{aligned} \tag{D.23}$$

where in the last step we have used the fact that $\epsilon^{\alpha\mu\beta\nu}$ is antisymmetric while the product $p_\alpha p^j_\mu p_\beta p^i_\nu$ is symmetric, so their contraction is equal to zero. Now we consider the kinematics of the process and we have that the scalar product becomes

$$\begin{aligned}
p_\alpha \cdot p_j p_\beta \cdot p_i =& p_\alpha \cdot p_j p_\beta \cdot p_i = \frac{M_i^4}{4} \\
p_\alpha \cdot p_\beta p_j \cdot p_i =& \left(\frac{M_i^4}{4} - \vec{p}_\alpha \vec{p}_\beta \cos\theta_{\alpha\beta}\right) M_i^2 = \frac{M_i^4}{4}(1 - \cos\theta_{\alpha\beta}).
\end{aligned} \tag{D.24}$$

Thus, the Eq. D.23 becomes

$$\begin{aligned}
&\left(\frac{-iY_{\alpha i}Y_{\beta j}Y^*_{\alpha j}Y^*_{\beta i}}{M_j^2 - M_j^2}\right)\left[\frac{M_i^4}{4} - \frac{M_i^4}{4}(1 - \cos\theta_{\alpha\beta} + \frac{M_i^4}{4}\right] \\
=& \frac{-i}{4}\left(\frac{Y_{\alpha i}Y_{\beta j}Y^*_{\alpha j}Y^*_{\beta i}}{M_j^2 - M_j^2}\right) M_i^4(1 + \cos\theta_{\alpha\beta}).
\end{aligned} \tag{D.25}$$

Now we can integrate over phase space of on-shell cuts

$$\begin{aligned}
&\int d\Pi_{L_\beta} d\Pi_H (2\pi)^4 \delta^{(4)}(p_N - p_{L_\beta} - p_H)(-i)\frac{Y_{\alpha i}Y_{\beta j}Y^*_{\alpha j}Y^*_{\beta i}}{M_i^2 - M_j^2}\frac{M_i^4}{4}(1+\cos\theta_{\alpha\beta}) \\
&= \frac{-iY_{\alpha i}Y_{\beta j}Y^*_{\alpha j}Y^*_{\beta i}}{M_i^2 - M_j^2}\frac{M_i^4}{4}\int \frac{d^3p_\beta}{(2\pi)^3 2E_\beta}\frac{d^3p_H}{(2\pi)^3 2E_H}(2\pi)^4\delta(E_N - E_\beta - E_H)\times \\
&\quad \delta^{(3)}(\vec{p_N} - \vec{p_{L_\beta}} - \vec{p_H})(1+\cos\theta_{\alpha\beta}) \\
&= \frac{-iY_{\alpha i}Y_{\beta j}Y^*_{\alpha j}Y^*_{\beta i}}{M_i^2 - M_j^2}\frac{M_i^4}{4}\int \frac{d^3p_\beta}{(2\pi)^2 2E_\beta 2E_H}\delta(E_N - E_\beta - E_H)(1+\cos\theta_{\alpha\beta})\big|_{\vec{p}_\beta = -\vec{p}_H} \\
&= \frac{-iY_{\alpha i}Y_{\beta j}Y^*_{\alpha j}Y^*_{\beta i}}{M_i^2 - M_j^2}\frac{M_i^4}{4}\int \frac{d^3p_\beta}{(2\pi)^2 4E_\beta^2}\delta(E_N - 2E_\beta)(1+\cos\theta_\beta) \\
&= \frac{-i}{4(2\pi)^2}\frac{Y_{\alpha i}Y_{\beta j}Y^*_{\alpha j}Y^*_{\beta i}}{M_i^2 - M_j^2}\frac{M_i^4}{4}\int \frac{p_\beta^2 dp_\beta d\cos\theta_\beta}{4E_\beta^2}\delta(E_N - 2E_\beta)(1-\cos\theta_\beta) \\
&= \frac{-i}{32\pi}\frac{Y_{\alpha i}Y_{\beta j}Y^*_{\alpha j}Y^*_{\beta i}}{M_i^2 - M_j^2}M_i^4.
\end{aligned} \tag{D.26}$$

As in the previous case, in order to have an integral containing variables related to L_β only, we changed $cos\theta_{\alpha\beta}$ to $cos\theta_\beta$ by performing a rotation to align the emission direction of L_β with one of the reference frame axes. In the end, we can use this result in Eq. 4.75. By considering the numerator we integrate over the phase space

$$\begin{aligned}
&\int d\Pi_l d\Pi_H (2\pi)^4 \delta^{(4)}(p_N - p_H - p_{L_\alpha})(-2\mathcal{I}m[(TT^\dagger)_{if}T_{fi}]) \\
&= -2\int \frac{d^3p_\alpha}{(2\pi)^3 2E_\alpha}\frac{d^3p_H}{(2\pi)^3 2E_H}(2\pi)^4\delta^{(4)}(P_{N_i} - P_\alpha - P_H)\left[\frac{-\mathcal{I}m(Y_{\alpha i}Y_{\beta j}Y^*_{\alpha j}Y^*_{\beta i})}{32\pi(M_i^2 - M_j^2)}M_i^4\right] \\
&= \frac{1}{16\pi}\frac{\mathcal{I}m(Y_{\alpha i}Y_{\beta j}Y^*_{\alpha j}Y^*_{\beta i})}{M_i^2 - M_j^2}\frac{M_i^4}{(2\pi)^2}\int \frac{d^3p_\alpha}{4E_\alpha^2}\delta(E_{N_i} - 2E_\alpha)\big|_{\vec{p}_\alpha = -\vec{p}_H} \\
&= \frac{1}{8\pi}\frac{\mathcal{I}m(Y_{\alpha i}Y_{\beta j}Y^*_{\alpha j}Y^*_{\beta i})}{M_i^2 - M_j^2}\frac{M_i^4}{16\pi}.
\end{aligned} \tag{D.27}$$

Now we can divide by the denominator in Eq. (4.76) and we obtain:

$$\frac{1}{16\pi}\frac{\mathcal{I}m(Y_{\alpha i}Y_{\beta j}Y^*_{\alpha j}Y^*_{\beta i})}{\sum_\alpha |Y_{\alpha i}|^2}\frac{M_i^2}{M_i^2 - M_j^2} = \frac{1}{16\pi}\frac{\mathcal{I}m(Y_{\alpha i}Y_{\beta j}Y^*_{\alpha j}Y^*_{\beta i})}{\sum_\alpha |Y_{\alpha i}|^2}\frac{1}{1-x}, \tag{D.28}$$

where $x = M_j^2/M_i^2$.

D.2 Vertex diagram contribution

The last diagram we need to compute is the following

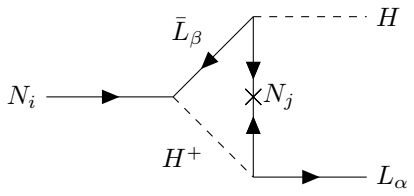

As in the previous case, the amplitude $\langle i|T|f\rangle$ has already been computed in Eq. D.1. To study the kinematics of this process we can proceed in the same way as in Eq. D.1 and we obtain the same result as in Eq. D.21. Now by assuming that the particle L_α is emitted in the xy plane, we can explicit the angle dependence and we have

$$p_\beta = \begin{pmatrix} \frac{M_i}{2} \\ |\vec{p}_\alpha| \cos\theta_\alpha \\ |\vec{p}_\alpha| \sin\theta_\alpha \\ 0 \end{pmatrix}, \qquad p_H = \begin{pmatrix} \frac{M_i}{2} \\ -|\vec{p}_\alpha| \cos\theta_\alpha \\ -|\vec{p}_\alpha| \cos\theta_\alpha \\ 0 \end{pmatrix}, \tag{D.29}$$

where θ_α is the scattering angle.
The second diagram we need to consider is

$$\begin{aligned} \langle k|T|i\rangle =& \langle \bar{L}_\beta H' | T\left(-i \int d^4x Y_{\beta i} \bar{N}_i P_L H^\dagger L_\beta\right) |N_i\rangle \\ =& -iY_{\beta i}(\bar{u}_\beta P_L u_i), \end{aligned} \tag{D.30}$$

where we have performed the same computations as for the first wave diagram, see Eq. D.6. This amplitude corresponds to the diagram

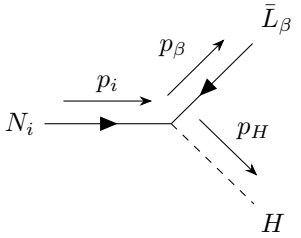

In the center of mass frame the kinematics is analogous as in the previous cases and we can conclude that

$$p_\beta = \begin{pmatrix} \frac{M_i}{2} \\ \vec{p}_\beta \end{pmatrix}, \qquad p_H = \begin{pmatrix} \frac{M_i}{2} \\ -\vec{p}_\beta \end{pmatrix}. \tag{D.31}$$

Now by assuming that the particle $\bar{L}_\beta$ is emitted in the xy plane, we can explicit the angle dependence and we have

$$p_\beta = \begin{pmatrix} \frac{M_i}{2} \\ |\vec{p}_\beta| \cos\theta_\beta \\ |\vec{p}_\beta| \sin\theta_\beta \\ 0 \end{pmatrix}, \qquad p_H = \begin{pmatrix} \frac{M_i}{2} \\ -|\vec{p}_\beta| \cos\theta_\beta \\ -|\vec{p}_\beta| \cos\theta_\beta \\ 0 \end{pmatrix}, \tag{D.32}$$

where θ_β is the scattering angle. The last diagram we need to compute is

$$\begin{aligned}
\langle \bar{L}_\beta H|T|L_\alpha H\rangle^* =& \langle \bar{L}_\beta H|T\big(-i\int d^4x Y_{\alpha i}\bar{N}_j P_L H^\dagger L_\alpha\big)\big(-i\int d^4y Y_{\beta i}\bar{N}_j P_L H^\dagger L_\beta\big)|L_\alpha H\rangle^* \\
=& \frac{-iY^*_{\alpha j}Y^*_{\beta j}}{p^2-M^2}(v_\beta^T P_L^T C^{-1}(\not{p}_j + M_j)P_L u_\alpha)^* \\
=& \frac{-iY^*_{\alpha j}Y^*_{\beta j}}{p^2-M^2}(\bar{u}_\beta C^T P_L^T C^{-1}(\not{p}_j + M_j)P_L u_\alpha)^* \\
=& \frac{iY^*_{\alpha j}Y^*_{\beta j}}{p^2-M^2}(\bar{u}_\beta P_L(\not{p}_j + M_j)P_L u_\alpha)^* \\
=& \frac{iY^*_{\alpha j}Y^*_{\beta j}}{p^2-M^2}(\bar{u}_\beta P_L M_j u_\alpha)^\dagger \\
=& \frac{iY^*_{\alpha j}Y^*_{\beta j}}{p^2-M^2}\bar{u}_\alpha M_j P_R u_\beta,
\end{aligned} \tag{D.33}$$

where we have performed the same computation as in Eq. D.12. Now in this case this amplitude corresponds to the diagram

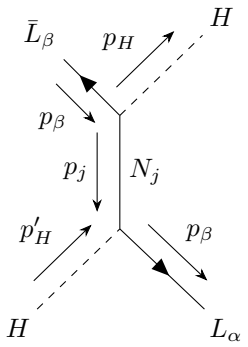

This diagram corresponds to a t-channel and in the center of mass frame we have $t = (p_\beta - p_H)^2 = (p_\alpha - p_{H'})^2$. From momentum conservation we see that $t^2 = p_j^2$ and we have massless L_α and H, since we are working before EW symmetry breaking. Therefore

$$t = p_\alpha^2 + p_{H'}^2 - 2p_\alpha \cdot p_{H'} = -2\left(\frac{M_i^2}{4} - \frac{M_i^2}{4}(-\cos\theta_\beta)\right) = -\frac{M_i^2}{2}(1+\cos\theta_\beta). \tag{D.34}$$

At this point we can sum the three amplitude contributions over polarizations

$$\begin{aligned}
\mathcal{M}_{unpol} =& (-iY_{\alpha i}\bar{u}_i P_L u_\alpha)\left(\frac{iY^*_{\alpha j}Y^*_{\beta j}}{P_j^2 - M_j^2}\bar{u}_\alpha M_j P_R u_\beta\right)(-iY_{\beta i}\bar{u}_\beta P_L u_i) \\
=& \frac{-iY_{\alpha i}Y^*_{\alpha j}Y^*_{\beta j}Y_{\beta i}}{P_j^2 - M_j^2} M_j M_i p_\alpha \cdot p_\beta \\
=& -iY_{\alpha i}Y^*_{\alpha j}Y^*_{\beta j}Y_{\beta i}M_j M_i \frac{\frac{M_i^4}{4}(1-\cos\theta_\beta)}{-\frac{M_i^2}{2}(1+\cos\theta_\beta) - M_j^2} \\
=& \frac{i}{2}Y_{\alpha i}Y^*_{\alpha j}Y^*_{\beta j}Y_{\beta i}M_j M_i \frac{1-\cos\beta}{1+\cos\theta_\beta + 2\frac{M_j^2}{M_i^2}}.
\end{aligned} \tag{D.35}$$

Now we integrate over the on-shell cuts

$$\begin{aligned}
&\int d\Pi_{L_\beta} d\Pi_{H'} (2\pi)^4 \delta^{(4)}(p_N - p_{L_\beta} - p_{H'})(-i)\frac{i}{2} Y_{\alpha i} Y^*_{\alpha j} Y^*_{\beta j} Y_{\beta i} M_j M_i \frac{1-\cos\beta}{1+\cos\theta_\beta + 2\frac{M_j^2}{M_i^2}} \\
=&\frac{i}{2} Y_{\alpha i} Y^*_{\alpha j} Y^*_{\beta j} Y_{\beta i} M_j M_i \int \frac{d^3 p_\beta}{(2\pi)^3 2E_\beta} \frac{d^3 p_{H'}}{(2\pi)^3 2E_{H'}} (2\pi)^4 \delta(E_N - E_\beta - E_{H'}) \times \\
&\qquad \delta^{(3)}(\vec{p_N} - \vec{p_{L_\beta}} - \vec{p_{H'}}) \frac{1-\cos\beta}{1+\cos\theta_\beta + 2\frac{M_j^2}{M_i^2}} \\
=&\frac{i}{2} Y_{\alpha i} Y^*_{\alpha j} Y^*_{\beta j} Y_{\beta i} M_j M_i \int \frac{d^3 p_\beta}{(2\pi)^3 2E_\beta 2E_{H'}} \delta(E_N - E_\beta - E_{H'}) \frac{1-\cos\beta}{1+\cos\theta_\beta + 2\frac{M_j^2}{M_i^2}} \Big|_{\vec{p}_\beta = -\vec{p}_{H'}} \\
=&\frac{i}{2} Y_{\alpha i} Y^*_{\alpha j} Y^*_{\beta j} Y_{\beta i} M_j M_i \int \frac{d^3 p_\beta}{(2\pi)^3 4E_\beta^2} \delta(E_N - 2E_\beta) \frac{1-\cos\beta}{1+\cos\theta_\beta + 2\frac{M_j^2}{M_i^2}} \Big|_{\vec{p}_\beta = -\vec{p}_{H'}} \\
=&\frac{i}{8\pi^2} Y_{\alpha i} Y^*_{\alpha j} Y^*_{\beta j} Y_{\beta i} M_j M_i (2\pi) \int \frac{p_\beta^2 dp_\beta}{4E_\beta^2} \delta(E_N - 2E_\beta) \int_{-1}^{+1} d\cos\theta_\beta \frac{1-\cos\theta_\beta}{1+\cos\theta_\beta + 2\frac{M_j^2}{M_i^2}} \\
=&\frac{-i}{16\pi} Y_{\alpha i} Y^*_{\alpha j} Y^*_{\beta j} Y_{\beta i} M_j M_i \left(1 - (1+x)\log\left(1+\frac{1}{x}\right)\right),
\end{aligned} \tag{D.36}$$

where, ad before, we have defined $x = M_j^2/M_i^2$. Finally, we use this result in Eq. 4.75. First, we consider the numerator and we integrate:

$$\begin{aligned}
&\int d\Pi_l d\Pi_H (2\pi)^4 \delta^{(4)}(p_N - p_H - p_{L_\alpha})(-2\mathcal{I}m[(TT^\dagger)_{if} T_{fi}]) \\
=&\frac{1}{8\pi} \mathcal{I}m(Y_{\alpha i} Y^*_{\alpha j} Y^*_{\beta j} Y_{\beta i}) M_j M_i \left(1 - (1+x)\log\left(1+\frac{1}{x}\right)\right) \int d\Pi_l d\Pi_H (2\pi)^4 \delta^{(4)}(p_N - p_H - p_{L_\alpha}) \\
=&\frac{1}{16\pi} \mathcal{I}m(Y_{\alpha i} Y^*_{\alpha j} Y^*_{\beta j} Y_{\beta i}) M_j M_i \left(1 - (1+x)\log\left(1+\frac{1}{x}\right)\right),
\end{aligned} \tag{D.37}$$

Now, we divide by the denominator and we obtain

$$\frac{1}{8\pi} \frac{\mathcal{I}m(Y_{\alpha i} Y^*_{\alpha j} Y^*_{\beta j} Y_{\beta i})}{\sum_\alpha |Y_{\alpha i}|^2} \sqrt{x} \left(1 - (1+x)\log\left(1+\frac{1}{x}\right)\right). \tag{D.38}$$

Now we can add all the three contributions and we get

$$\epsilon_{i\alpha} = \frac{1}{8\pi} \frac{\mathcal{I}m(Y_{\alpha i} Y^*_{\alpha j} Y^*_{\beta j} Y_{\beta i})}{\sum_\alpha |Y_{\alpha i}|^2} \sqrt{x} g + \frac{1}{16\pi} \frac{\mathcal{I}m(Y_{\alpha i} Y_{\beta j} Y^*_{\alpha j} Y^*_{\beta i})}{\sum_\alpha |Y_{\alpha i}|^2} \frac{1}{1-x} + \frac{1}{16\pi} \frac{\mathcal{I}m(Y_{\alpha i} Y^*_{\alpha j} Y^*_{\beta j} Y_{\beta i})}{\sum_\alpha |Y_{\alpha i}|^2} \frac{\sqrt{x}}{1-x}, \tag{D.39}$$

where $g = 1 - (1+x)\log\left(1+\frac{1}{x}\right)$. Now we sum over the internal d.o.f, that is, over β and j and multiply by 2 the contributions coming from the wave diagram, since in these diagrams both the neutral and charged components of the lepton doublet run in the loop. Also, we do not include in the sum over the flavour of the intermediate neutrinos in the case $j = i$, since in general states degenerate with the initial one do not contribute to the CP violating asymmetry and, in the vertex contribution, if we consider the contribution from $j = i$ we will get a term proportional to $\mathcal{I}m(Y^\dagger Y)^2_{ii} = 0$ [19]. Putting all these results together we obtain the expression for the ϵ parameter given in Eq. 4.79.

Appendix E

The effective potential

In Sec. 1.2 we have seen that the classical potential of a quantum field theory plays a crucial role in studying the question of symmetry breaking. However, sometimes radiative corrections in a quantum theory may change the behaviour of the classical potential. The minimum of the classical potential may be unstable under radiative corrections and a symmetry that is spontaneously broken at classical level may be restored or an unbroken symmetry at classical level may be spontaneously broken because of quantum effects. For this reason the important quantity to consider is the effective potential which takes into account the quantum corrections in a theory. In our discussion we will restrict to the effective potential taking into account only the one loop corrections, since we are interested in using it to find the thermal masses of a scalar singlet.

E.1 The effective potential at zero temperature

First, we consider the case at zero temperature and we will follow the review [64].

Generating functionals

Let us consider a theory described by a scalar field ϕ with an action

$$S[\phi] = \int d^4x \mathcal{L}(\phi(x)). \tag{E.1}$$

The generating functional is given by the path integral representation

$$Z[j] = \int d\phi \exp\left(iS[\phi] + i\int d^4x \phi(x) j(x)\right). \tag{E.2}$$

From this definition we can obtain the connected generating functional $W[j]$

$$Z[j] \equiv \exp(iW[j]), \tag{E.3}$$

and the effective action $\Gamma[\bar{\phi}$ as the Legendre transform of Eq. E.3

$$\Gamma[\bar{\phi}] = W[j] - \int d^4x \frac{\delta W[j]}{\delta j(x)} j(x), \tag{E.4}$$

where

$$\bar{\phi}(x) = \frac{\delta W[j]}{\delta j(x)}. \tag{E.5}$$

The field $\bar{\phi}$ is also called the mean field and it represents the connected 1-point function with the source $j(x)$ kept alive. From this definition we can see that if we set the source $j(x) = 0$, we get

$$\bar{\phi}(x)|_{j=0} = \langle\bar{\phi}\rangle_c \equiv \phi_c, \tag{E.6}$$

i.e. the mean field $\bar{\phi}$, which represents the vacuum expectation value of the field ϕ, would be a constant independent of space-time when the source is turned off because of the Lorentz invariance of the vacuum. From these definitions we can find the vacuum of the theory in absence of external sources as

$$\left.\frac{\delta\Gamma[\bar{\phi}]}{\partial\bar{\phi}}\right|_{j=0} = 0. \tag{E.7}$$

We can now expand the generating functional in a power series of j, to obtain its representation in terms of Green functions $G_{(n)}$ as

$$Z[j] = \sum_{n=0}^{\infty} \frac{i^n}{n!} \int d^4x_1...d^4x_n j(x_1)...j(x_n) G_{(n)}(x_1, ..., x_n), \tag{E.8}$$

and

$$iW[j] = \sum_{n=0}^{\infty} \frac{i^n}{n!} \int d^4x_1...d^4x_n j(x_1)...j(x_n) G^c_{(n)}(x_1, ..., x_n), \tag{E.9}$$

where we have used

$$\begin{aligned} G_{(n)}(x_1, ..., x_n) =& \langle\phi^1...\phi^n\rangle = \frac{1}{i^n}\frac{\delta^n Z[j]}{\delta j_1...\delta j_n}\bigg|_{j=0}, \\ G^c_{(n)}(x_1, ..., x_n) =& \langle\phi^1...\phi^n\rangle_c = \frac{1}{i^n}\frac{\delta^n iW[j]}{\delta j_1...\delta j_n}\bigg|_{j=0}. \end{aligned} \tag{E.10}$$

Similarly, the effective action can be expanded in powers of $\bar{\phi}$ as

$$\Gamma[\bar{\phi}] = \sum_{n=0}^{\infty} \frac{1}{n!} \int d^4x_1...d^4x_n \bar{\phi}(x_1)...\bar{\phi}(x_n) \Gamma^{(n)}(x_1, ..., x_n), \tag{E.11}$$

where $\Gamma^{(n)}$ are the $1PI$ Green functions:

$$\langle\phi_1, ..., \phi_n\rangle_{1PI} = \Gamma^{(n)}(x_1, ..., x_n) = \frac{\delta^n i\Gamma[\bar{\phi}]}{\delta\bar{\phi}^1...\delta\bar{\phi}^n}\bigg|_{\bar{\phi}=0}. \tag{E.12}$$

Now we can Fourier transform $\Gamma[\bar{\phi}]$ and $\bar{\phi}$ as

$$\Gamma^{(n)}(x) = \int \prod_{i=1}^{n} \left[\frac{d^4p_i}{(2\pi)^4} \exp(ip_i x_i)\right] (2\pi)^4 \delta^{(4)}(p_1 + ... + p_n) \Gamma^{(n)}(p) \tag{E.13}$$

$$\tilde{\phi}(p) = \int d^4x e^{-ipx} \bar{\phi}(x) \tag{E.14}$$

and we obtain the effective action in Eq. E.4 as

$$\Gamma[\bar{\phi}] = \sum_{n=0}^{\infty} \int \prod_{i=1}^{n} \left[\frac{d^4 p_i}{(2\pi)^4} \tilde{\phi}(-p_i) \right] (2\pi)^4 \delta^{(4)}(p_1 + ... + p_n) \Gamma^{(n)}(p_1, ..., p_n). \tag{E.15}$$

Recaling Eq. E.6 and by removing an overall factor of space-time volume, we define the effective potential $V_{eff}(\phi_c)$ as

$$\Gamma[\phi_c] = -\int d^4 x V_{eff}(\phi_c). \tag{E.16}$$

Since Γ represents an effective action, it contains both the classical and quantum parts of the action. Therefore, V_{eff} contains quantum corrections of all orders to the original classical potential. However, it does not have a closed form and for this reason its structure has to be studied order by order in perturbation theory. A perturbative expansion is in terms of the number of loops of a Feynman diagram which also coincides with an expansion in powers of $\hbar$. In particular, the zero-loop contribution is simply the classical (tree-level) potential. The one-loop contribution can be written in closed form for any field theory containing spinless particles, spin 1/2 fermions and gauge bosons, but we will focus on scalar fields.

E.2 One-loop potential

The perturbative expansion of the potential at one-loop order can be written as

$$V_{eff} = V_0 + \hbar V_1 + O(\hbar^2). \tag{E.17}$$

We will follow Ref. [98] and we will calculate the one loop corrections to the effective potential in a way that generalizes to the case of finite temperature. We consider the simplest model of a real scalar field ϕ and let us assume that ϕ_0 represents a solution of the tree level Euler-Lagrange equation[1]

$$\left. \frac{\delta S^J(\phi)}{\delta \phi(x)} \right|_{\phi=\phi_0} = 0, \tag{E.18}$$

which implies

$$\frac{\delta S}{\delta \phi(x)} = -J(x). \tag{E.19}$$

Therefore, we can expand the field variables around this classical solution as

$$\phi(x) = \phi_0(x) + \sqrt{\hbar}\chi(x), \tag{E.20}$$

correspondingly, the classical action would have the expansion around $\phi = \phi_0$

$$S^J(\phi) = S^J(\phi_0 + \sqrt{\hbar}\chi) = S^J(\phi_0) - \frac{\hbar}{2} \int d^4x d^4y \chi(x) G^{-1}(x,y) \chi(y) + ... \tag{E.21}$$

where the linear term in χ vanishes since we have used Eq. E.18 and since the source terms in S^J are linear in the field variables, they do not contribute to the second derivative terms and we have defined

$$G^{-1}(x,y) = -\left. \frac{\delta^2 S^J}{\delta\phi(x)\delta\phi(y)} \right|_{\phi_0} = -\left. \frac{\delta^2 S}{\delta\phi(x)\delta\phi(y)} \right|_{\phi_0}, \tag{E.22}$$

[1] We call $S^J = S[\phi] + \int d^4x \phi(x) j(x)$

which is the inverse of a propagator in the presence of a background field and would correspond to a propagator with an effective mass. Substituting the expansion in the expression for the generating functional and we integrate over the quantum part χ by keeping the background field ϕ_0 fixed, we get

$$\begin{aligned} Z[j] =& \int D\chi e^{i/\hbar S^J(\phi_0+\sqrt{\hbar}\chi)} \\ =& e^{\frac{i}{\hbar}S^J(\phi_0)} \int D\chi e^{-\frac{i}{2}\int d^4x d^4y \chi(x) G^{-1}(x,y)\chi(y)} \\ =& e^{\frac{i}{\hbar}S^J(\phi_0)} [\det(G^{-1})]^{-1/2} \end{aligned} \tag{E.23}$$

Therefore we also have

$$W[j] = S^J(\phi_0) + \frac{\hbar}{i}\ln\left[\det G^{-1}\right]^{-1/2} = S^J(\phi_0) + \frac{i\hbar}{2} Tr \ln G^{-1} \tag{E.24}$$

Considering now the effective action, we note that the mean field ϕ_c can also be expanded in powers of $\hbar$. But, since it satisfies the classical equation in the limit $\hbar \to 0$[2], we can write its expansion as

$$\phi_c(x) = \phi_0(x) + \phi_1(x) + ... \tag{E.25}$$

With this we note that

$$\begin{aligned} S(\phi_c) \sim& S(\phi_0 + \phi_1) \\ =& S(\phi_0) + \int d^4x \phi_1 \frac{\delta S}{\delta\phi(x)}\bigg|_{\phi_0} + O(\hbar^2) \\ =& S(\phi_0) - \int d^4x J(x)\phi_1(x) \end{aligned} \tag{E.26}$$

where we have used Eq. E.19 and have neglected higher order terms. It follows that the effective action at one-loop order has the form

$$\begin{aligned} \Gamma[\phi_c] =& W[j] - \int d^4x \phi_c(x) j(x) \\ =& S^J(\phi_0) + \frac{i\hbar}{2} Tr\ln G^{-1} - \int d^4x(\phi_0+\phi_1)j \\ =& S(\phi_0) + \int d^4x \phi_o j + \frac{i\hbar}{2} Tr\ln G^{-1} - \int d^4x(\phi_o+\phi_1)j \\ =& S(\phi_c) + \frac{i\hbar}{2} Tr\ln G^{-1}. \end{aligned} \tag{E.27}$$

For constant field configurations from Eq. E.16 we write the effective action as

$$\Gamma(\phi_c) = -\Omega V(\phi_c) = -\Omega V^0(\phi_c) + \frac{i\hbar}{2} Tr\ln G^{-1}, \tag{E.28}$$

where we have called $\Omega = \int d^4x$, and we obtain

$$V(\phi_c) = V^0(\phi_c) - \frac{i\hbar}{2}\Omega^{-1} Tr\ln G^{-1} \tag{E.29}$$

[2]Since all connected diagrams can either be computed with $W[j]$ using $S[\phi]$ to all orders in $\hbar$, or they can be computed with the equivalent of $W[j]$ constructed using $\Gamma[\phi]$ instead of $S[\phi]$ in the $\hbar \to 0$ limit [37]

Therefore the one loop contribution to the effective potential is given by

$$V^1(\phi_c) = -\frac{i\hbar}{2}\Omega^{-1} Tr \ln G^{-1}. \tag{E.30}$$

Now, as we have seen in Eq. E.22 G behaves as a propagator with an effective mass. In fact, if we consider as an example an action given by $S = \int d^4x(1/2\partial_\mu\phi\partial^\mu\phi - m^2\phi^2/2 - \lambda\phi^4/4!)$ and we compute the inverse propagator by taking the second derivative of the action we find $G^{-1}(x,y) = (\Box + m^2 + \lambda/2\phi_c^2)\delta^4(x-y)$ and we can define the effective mass $m_{eff}^2 = m^2 + \lambda/2\phi_c^2$. Therefore, in general we obtain

$$G^{-1}(x,y) = (\Box + m_{eff}^2)\delta^4(x-y). \tag{E.31}$$

Going in momentum space we find

$$G^{-1}(k,k') = (-k^2 + m_{eff}^2)\delta^4(k-k'). \tag{E.32}$$

We can now obtain

$$\begin{aligned} Tr \ln G^{-1} &= \int d^4x \langle x| \ln G^{-1} |x\rangle \\ &= \int d^4x d^4k d^4k' \langle x|k\rangle\langle k| \ln G^{-1} |k'\rangle\langle k'|x\rangle \\ &= \int d^4x d^4k d^4k' \frac{e^{-i(k-k')\cdot x}}{(2\pi)^4} \ln(-k^2 + m_{eff}^2)\delta^4(k-k') \\ &= \Omega \int \frac{d^4k}{(2\pi)^4} \ln(-k^2 + m_{eff}^2). \end{aligned} \tag{E.33}$$

Therefore, we can identify

$$V^1(\phi_c) - \frac{i\hbar}{2}\int \frac{d^4k}{(2\pi)^4} \ln(-k^2 + m_{eff}^2). \tag{E.34}$$

Now that we have found an expression for the effective potential at one-loop order, we will illustrate a method to calculate it, by following Ref. [64]. This method consists in computing the derivative of the effective potential in the shifted theory and then integrating. Given a scalar theory with a Lagrangian $\mathcal{L}$, we define another Lagrangian $\hat{\mathcal{L}}$ in this way:

$$\int d^4x \hat{\mathcal{L}}(\phi_c;\phi(x)) \equiv S[\phi_c + \phi] - S[\phi_c] - \phi\frac{\delta S[\phi_c]}{\delta\phi_c}. \tag{E.35}$$

The second term makes the vacuum energy equal to zero and the third term is there to cancel the tadpole part of the shifted action. Now we denote

$$i\mathcal{D}^{-1}(\phi_c, x-y) = \left.\frac{\delta^2 S[\phi]}{\delta\phi(x)\delta\phi(y)}\right|_{\phi=\phi_c} \tag{E.36}$$

and by $i\mathcal{D}^{-1}(\phi_c,p)$ its Fourier transform, the effective potential is found to be given by

$$V_{eff}(\phi_c) = V^0(\phi_c) - \frac{i}{2}\int \frac{d^4p}{(2\pi)^4} \ln(\det i\mathcal{D}^{-1}(\phi_c,p)) + i\Big\langle \exp\left[i\int d^4x \hat{\mathcal{L}}_I(\phi_c,\phi(x))\right]\Big\rangle. \tag{E.37}$$

The first term is the classical tree-level potential, the second term is the one-loop potential, where the determinant operates on any possible internal indices defining the propagator, and the last term denotes

higher order loops. As an example we can consider again the Lagrangian $\mathcal{L} = 1/2\partial_\mu\phi\partial^\mu\phi - m^2\phi^2/2 - \lambda\phi^4/4!$ and by applying the definition in Eq. E.35 we find $\hat{V} = 1/2m^2(\phi_c)\phi^2 + \lambda/3!\phi_c\phi^3 + \lambda/4\phi^4$ where the shifted mass $m^2(\phi_c)$ coincides with the effective mass $m^2_{eff} = m^2 + \lambda/2\phi_c^2$. Therefore the shifted propagator will coincide with the one in Eq. E.31 and we obtain the same result as in Eq. E.34 for the one-loop effective potential. To conclude, we can notice that the "field-shifting" method is identical to the background field method, where we write the classical action S as a function of the field ϕ plus an arbitrary background ϕ_c field. With this shifting we find a new generating functional Z_B and, consequently, the effective action Γ_B. By employing the definiton $\phi = \phi_c + \phi$ ad by shifting the variable of integration in Z_B and Γ_B as $\phi \to \phi - \phi_c$ (see Ref. [99] for details) we find that $\Gamma_B[\phi;\phi_c] = \Gamma[\phi + \phi_c]$ and, by taking $\phi = 0$ we find $\Gamma_[\phi_c] = \Gamma_B[0;\phi_c]$. Therefore, we find that the background effective action is just a conventional effective action computed in the presence of a background field. Now, $\Gamma_B[0;\phi_c]$ has no dependence on the field ϕ so it generates no graphs with external lines. The background field method allows to calculate the effective action by summing only vacuum graphs. Therefore, from the Eq. E.16 we see that we can compute the effective potential by computing the sum sum of $1PI$ diagrams in the presence of the background field.

One-loop effective potential at finite temperature

At this point we can construct the one-loop effective potential at finite temperature and we will do that by using imaginary time formalism. We need to consider quantum field theory at finite temperature as in the early stages of the universe, at high temperatures, the environment had a non-negligible matter and radiation density. Therefore, we need to consider the background state as a thermal bath. In order to do that we first recall some concepts from statistical mechanics. The statistical behaviour of a quantum mechanical system, in thermal equilibrium, is studied thorugh an appropriate ensemble, where an ensemble is a collection of an infinitely large number of identical and independent systems. In general, a density matrix for the ensemble is defined as

$$\rho(\beta) = \frac{e^{-\beta\mathcal{H}}}{Z(\beta)}, \tag{E.38}$$

where β represents the inverse of the equilibrium temperature $\beta = T^{-1}$ and$H$is an appropriate Hamiltonian for the particular ensemble. $Z(\beta)$ is a normalization factor and is known as the partition function of the ensemble. In the most general case we have

$$\mathcal{H} = H - \mu N - \sum_i \mu_{Q_i} Q_i, \tag{E.39}$$

where H denotes the conventional dynamical Hamiltonian, N represent the number operator, μ corresponds to the chemical potential and μ_{Q_i} represent the totality of all characteristics of equilibrium besides the temperature T, i.e. they are the equilibrium state properties. From Eq. E.38 we can define the ensemble average of any observable $\mathcal{O}$ as

$$\langle\mathcal{O}\rangle \equiv Tr(\mathcal{O}\rho), \tag{E.40}$$

which satisfies the property $\langle 1\rangle = 1$. Similarly, the thermal average of the correlation function of any two operators A and B, with different coordinates can similarly be written as

$$\langle AB\rangle = Tr(\rho(\beta)AB) = Z^{-1}(\beta)Tr(e^{-\beta\mathcal{H}}AB) \tag{E.41}$$

E.2.1 Generating functionals

As in reference [64] we consider the case of a real scalar field $\phi(x)$, carrying no charges, with vanishing chemical potential and with Hamiltonian H *i.e.*

$$\phi(x) = e^{itH}\phi(0,\vec{x})e^{-itH}, \tag{E.42}$$

where the time $x^0 = t$ is analitically continued to the complex plane. We define the thermal Green function as the average of the ordered product of the n field operators

$$G^{(c)}(x_1,...,x_n) \equiv \langle T_C\phi(x_1),...,\phi(x_n)\rangle, \tag{E.43}$$

where the T_C ordering means that fields should be ordered along the path C in the complex t-plane, *i.e.*

$$T_c\phi(x)\phi(y) = \theta_C(x^0-y^0)\phi(x)\phi(y) + \theta_C(y^0-x^0)\phi(y)\phi(x) \tag{E.44}$$

if we parametrize C as $t = x(\tau)$, where $\tau \in \Re$, T_C ordering means standard ordering along τ. Therefore the step delta functions can be given as $\theta_C(t) = \theta(\tau)$, $\delta_C(t) = (\partial z/\partial\tau)^{-1}\delta(\tau)$. The rules of the functional formalism can be applied as usual, with the prescription $\delta j(y)/\delta j(x) = \delta_C(x^0-y^0)\delta^{(3)}(\vec{x}-\vec{y})$, and the generating functional becomes

$$Z^\beta[j] = \sum_{n=0}^{\infty}\frac{i^n}{n!}\int_C d^4x_1,...,d^4x_n j(x_1)...j(x_n)G^{(C)}(x_1,...,x_n) \equiv \exp\left(iW^\beta[j]\right), \tag{E.45}$$

which is normalized to $Z^\beta[0] = \langle 1\rangle = 1$ and where the integral along t is supposed to follow the path C in the complex plane. Similarly, the generating functional fot the $1PI$ Green functions $\Gamma^\beta[\bar{\phi}]$ is defined by the Legendre transformation

$$\Gamma^\beta[\bar{\phi}] = W^\beta[j] - \int_C d^4x\frac{\delta W^\beta[j]}{\delta j(x)}j(x), \tag{E.46}$$

where the classical field $\bar{\phi}(x) = \delta W^\beta[j]/\delta j(x)$. It follows that $\delta\Gamma^\beta[\bar{\phi}]/\delta\bar{\phi}(x) = -j(x)$ and $\bar{\phi}(x) = \langle\phi(x)\rangle$ is the average of the field. As in the previous section, we have that when $j = 0$, $\bar{\phi} = \phi_c$, where ϕ_c is a constant. In this case, by removing the overall factor of space-time volume arising in each term of $\Gamma^\beta[\phi_c]$, we can define the effective potential at finite temperature as

$$\Gamma^\beta[\phi_c] = -\int d^4x V^\beta_{eff}(\phi_c) \tag{E.47}$$

and symmetry breaking occurs whenn

$$\frac{\partial V^\beta_{eff}(\phi_c)}{\partial\phi_c} = 0 \tag{E.48}$$

for $\phi_c \neq 0$.

Green functions

From Eqs. E.44 and E.43 we can write the two-point Green function as

$$G^{(C)}(x-y) = \theta_C(x^0-y^0)G_+(x-y) + \theta_C(y^0-x^0)G_-(x-y) \tag{E.49}$$

where

$$G_+(x-y) = \langle\phi(x)\phi(y)\rangle, \qquad G_-(x-y) = G_+(y-x). \tag{E.50}$$

Not all contours are allowed if we require Green functions to be analytic with respect to t. In order to find a condition on t, we take the complete set of states $|n\rangle$ with eigenvalues E_n; $H|n\rangle = E_n|n\rangle$ and we can compute $G_+(x-y)$ at the point $\vec{x} = \vec{y} = 0$ as

$$\begin{aligned} G_+(x^0 - y^0) &= Tr[Z^{-1}(\beta)e^{-\beta H}\phi(0)\phi(0)] \\ &= Z^{-1}(\beta)\sum_m \langle m|e^{-\beta H}\phi(0)e^{\beta H}e^{-\beta H}\phi(0)|m\rangle \\ &= Z^{-1}(\beta)\sum_{n,m} \langle m|e^{-\beta H}e^{itH}\phi(0)e^{-itH}e^{\beta H}|n\rangle\langle n|e^{-\beta H}\phi(0)|m\rangle \\ &= Z^{-1}(\beta)\sum_{n,m} e^{iE_m(t+i\beta)}\langle m|\phi(0)|n\rangle e^{-iE_n(t+i\beta)}e^{-E_n\beta}\langle n|\phi(0)|m\rangle \\ &= Z^{-1}(\beta)\sum_{n,m} \langle n|\phi(0)|m\rangle^*\langle n|\phi(0)|m\rangle e^{-iE_nt}e^{iE_m(t+i\beta)} \\ &= Z^{-1}(\beta)\sum_{m,n} |\langle m|\phi(0)|n\rangle|^2 e^{-iE_n(x^0-y^0)}e^{iE_m(x^0-y^0+i\beta)} \end{aligned} \tag{E.51}$$

where we have used Eqs. E.41, E.42 and the completeness relation $\sum_n |n\rangle\langle n| = 1$. The convergence of the sum implies that $-\beta \leqslant \mathcal{I}m(x^0 - y^0) \leqslant 0$, which requires $\theta_C(x^0 - y^0) = 0$ for $\mathcal{I}m(x^0 - y^0) > 0$. Similarly, from the condition in Eq. E.50 we find that for the convergence of $G_-(x^0 - y^0)$ the condition $0 \leqslant \mathcal{I}m(x^0 - y^0) \leqslant \beta$ must be satisfied. This requires that $\theta_C(x^0 - y^0) = 0$ for $\mathcal{I}m(x^0 - y^0) < 0$, and the final condition for the convergence of the complete Green function is

$$-\beta \leqslant \mathcal{I}m(x^0 - y^0) \leqslant \beta \tag{E.52}$$

and we define $\theta_C(t)$ such that $\theta_C(t) = 0$ for $\mathcal{I}m > 0$, which implies that C must be such that a point moving along it has a monotically decreasing or constant imaginary part. From the definitions in Eq. E.50 we can deduce (by using Eqs. E.41, E.42) and the cyclic permutation property of the trace) the so called **Kubo-Martin-Schwinger** (KMS) relation:

$$G_+(t - i\beta, \vec{x}) = G_-(t, \vec{x}). \tag{E.53}$$

This relation leads to periodicity and anti-periodicity properties in bosonic and fermionic two point Green's functions at finite temperature.

Imaginary time formalism

The computation of the propagators depends on the chosen path C going from an initial arbitrary time t to $t - i\beta$, provided by the periodicity properties of Green functions. The simplest path is to take a straight line along the imaginary axis $t = -i\tau$. Therefore we can perform a Wick rotation, *i.e.* send $t \to i\tau$ (Euclidean time) and we see that the condition in Eq. E.52 becomes $-\beta \leqslant (\tau - \tau') \leqslant \beta$. Since the Green functions are defined within a finite time interval and are periodic for bosons (anti-periodic for fermions) thanks to the KMS relation, they can be written as a Fourier series involving only discrete frequencies:

$$G_\beta(\tau) = \frac{1}{\beta}\sum_n e^{i\omega_n\tau}G_\beta(\omega_n). \tag{E.54}$$

For periodic boundary conditions (for bosons), the Green function has to satisfy (see Eq. E.53)

$$G_\beta(0) = G_\beta(\beta) \tag{E.55}$$

or,

$$\frac{1}{\beta}\sum_n G_\beta(\omega_n) = \frac{1}{\beta}\sum_n e^{i\omega_n\beta}G_\beta(\omega_n), \tag{E.56}$$

which determines

$$\omega_n = \frac{2n\pi}{\beta}, \quad n = 0, \pm1, \pm2, ... \tag{E.57}$$

These frequencies are called the *Matsubara frequencies*. The inverse transform of Eq. E.54 can be obtained

$$G_\beta(\omega_n) = \int_{-\beta}^{\beta} d\tau e^{-i\omega_n\tau}G_\beta(\tau). \tag{E.58}$$

In contrast to the imaginary time variable τ at finite temperature taking values in a finite interval in the Green function $G_\beta(\tau)$, the spatial coordinates have an infinite range. Therefore, putting in all the coordinates, we can write

$$G_\beta(\tau, \vec{x}) = \frac{1}{\beta}\sum_n \int \frac{d^3\vec{k}}{(2\pi)^3} e^{i(\omega_n\tau + \vec{k}\cdot\vec{x})}G_\beta(\omega_n, \vec{k}); \tag{E.59}$$

$$G_\beta(\omega_n, \vec{k}) = \int_{-\beta}^{\beta} d\tau \int d^3x e^{-i(\omega_n\tau + \vec{k}\cdot\vec{x})}G_\beta(\tau, \vec{x}). \tag{E.60}$$

Therefore, for taking the Fourier transformation of the propagator in going from Minkowski space to finite temperature Euclidean space we need to substitute:

$$\begin{aligned} \int_{-\infty}^{\infty}\frac{dk^0}{2\pi} &\to \frac{1}{\beta}\sum_{n=-\infty}^{\infty}, \\ \int_{-\infty}^{\infty}\frac{d^3k}{(2\pi)^3} &\to \int_{-\infty}^{\infty}\frac{d^3k}{(2\pi)^3}. \end{aligned} \tag{E.61}$$

Therefore we can derive the form of the propagator for a bosonic theory at finite temperature[3]. For example, we consider the free Klein-Gordon theory of a massive real scalar field ϕ and the Green function satisfies

$$(\partial_t^2 - \nabla^2 + m^2)G(x) = -\delta^4(x). \tag{E.62}$$

The momentum space Green function, in this case, has the form

$$G(k_0, \vec{k}) = \frac{1}{k_0^2 - \vec{k}^2 - m^2}. \tag{E.63}$$

Going in imaginary time, *i.e.* by rotating $x^0 = t \to -i\tau$, $k^0 = k_0 \to ik_4 = i\omega_n$ and $G \to -G_\beta$ we obtain

$$\left(\frac{\partial^2}{\partial\tau^2} + \nabla^2 - m^2\right)G_\beta(\tau, \vec{x}) = -\delta(\tau)\delta^3(x), \tag{E.64}$$

and, from Eq. E.63

$$G(k_0, \vec{k}) = \frac{1}{k_0^2 - \vec{k}^2 - m^2} \to \frac{1}{-\omega_n^2 + \vec{k}^2 - m^2} = -G_\beta(\omega_n, \vec{k}). \tag{E.65}$$

[3]The same considerations are valid also for fermionic theory, but here we focus on a scalar theory since we are interested only in computing the effective potential.

Now that we have find the expression for the propagator and by using the rules in Eq. E.61 we can derive an expression for the one-loop effective potential at finite temperatures. Indeed, by going in imaginary time and recalling Eqs. E.33 and E.65 we find

$$V^1(\phi_c) = \frac{1}{2\beta} \sum_{n=-\infty}^{\infty} \int \frac{d^3k}{(2\pi)^3} \ln(\omega_n^2 + \omega^2), \tag{E.66}$$

where ω_n are the Matsubara frequencies and

$$\omega^2 = \vec{k}^2 + m_{eff}^2(\phi_c). \tag{E.67}$$

The sum over n diverges, but the infinite part does not depend pm ϕ_c. The finite part can be computed by the following method [64]. Define

$$v(\omega) = \sum_{n=-\infty}^{\infty} \ln(\omega_n^2 + \omega^2), \tag{E.68}$$

then

$$\frac{\partial v}{\partial \omega} = \sum_{n=-\infty}^{\infty} \frac{2\omega}{\omega_n^2 + \omega^2}. \tag{E.69}$$

Using the identity

$$f(y) = \sum_{n=1}^{\infty} \frac{y}{y^2 + n^2} = -\frac{1}{2y} + \frac{\pi}{2} \coth(\pi y) = -\frac{1}{2y} + \frac{\pi}{2} + \pi \frac{e^{-2\pi y}}{1 - e^{-2\pi y}}, \tag{E.70}$$

with $y = \beta\omega/2\pi$ we obtain

$$\frac{\partial v}{\partial \omega} = 2\beta \left[\frac{1}{2} + \frac{e^{-\beta\omega}}{1 - e^{-\beta\omega}} \right] \tag{E.71}$$

and

$$v(\omega) = 2\beta \left[\frac{\omega}{2} + \frac{1}{\beta} \ln(1 - e^{-\beta\omega}) \right] + \omega - ind.terms. \tag{E.72}$$

Substituting this result in Eq. E.66 we finally obtain

$$V_1^{\beta}(\phi_c) = \int \frac{d^3k}{(2\pi)^3} \left[\frac{\omega}{2} + \frac{1}{\beta} \ln(1 - e^{-\beta\omega}) \right]. \tag{E.73}$$

One can prove that the first integral is the one-loop effective potential at zero temperature (see Ref. [64] for details). Therefore we focus on the temperature dependent part that can be written as

$$\frac{1}{\beta} \int \frac{d^3k}{(2\pi)^3} \ln(1 - e^{-\beta\omega}) = \frac{1}{2\pi^2\beta^4} J_B[m^2(\phi_c)\beta^2], \tag{E.74}$$

where the thermal bosonic function J_B is defined as

$$J_B[m^2\beta^2] = \int_0^{\infty} dx x^2 \ln\left[1 - e^{-\sqrt{x^2 + \beta^2 m^2}}\right] \tag{E.75}$$

E.2.2 Symmetry restoration

As we have seen in the previous sections when the mass term has a negative sign a non trivial vacuum exists leading to a spontaneous breaking of the symmetry. On the other hand, we expect that if a particle moves in a hot medium, it must pick up a temperature dependent effective mass, and this temperature corrections come with a positive sign. Therefore, we expect that above a certain temperature, this temperature correction will take over the tree level negative mass squared term and symmetry will be restored. The main point is that at finite temperature, the equilibrium value of the scalar field ϕ, $\langle\phi(T)\rangle$, does not correspond to the minimum of the effective potential $V_{\mathbf{eff}}^{T=0}(\phi)$ at zero temperature, but to the minimum of the finite temperature effective potential $V_{\mathbf{eff}}^{\beta}(\phi)$. Thus, even if the minimum of the $V_{\mathbf{eff}}^{T=0}(\phi)$ occurs ar $\langle\phi\rangle = v \neq 0$, for sufficiently large temperatures, the minimum of $V_{\mathbf{eff}}^{\beta}(\phi)$ occurs at $\langle\phi(T)\rangle = 0$. This phenomenon is known as symmetry restoration at high temperature and gives rise to the phase transition from $\phi(T) = 0$ to $\phi = v$. The cosmological scenario can be drawn as follows: In the theory of the Hot Big Bang, the universe is initially at very high temperature and it can be in the symmetric phase $\langle\phi(T)\rangle = 0$, *i.e.* $\phi = 0$ can be the stable absolute minimum. At some critical temperature T_c the minimum $\phi = 0$ becomes metastable and the phase transition may proceed.

E.3 Derivation of thermal mass of the scalar singlet

As we have seen in Sec. E.2 we expect that if a particle moves in a hot medium, it must pick up a temperature dependent effective mass. Therefore, to compute the one-loop correction to the mass of the scalar singlet Φ we can first compute the one-loop effective potential and then by taking its second derivative we will find the effective mass. First we parametrize the Higgs doublet and the scalar singlet in terms of real scalar fields

$$H = \frac{1}{\sqrt{2}}\begin{bmatrix}\chi_1 + i\chi_2 \\ h + i\chi_3\end{bmatrix} \tag{E.76}$$

$$\Phi = \frac{1}{\sqrt{2}}(\phi + i\theta). \tag{E.77}$$

With these parametrizations, the potential in Eq. (5.43) becomes

$$\begin{aligned} V^0 = &-\frac{\mu_\phi^2}{2}(\phi^2+\theta^2) + \frac{\lambda_\phi}{4}(\phi^2+\theta^2)^2 - \frac{\mu_H^2}{2}(\chi_1^2+\chi_2^2+\chi_3^2+h^2) \\ &+ \frac{\lambda_H}{4}(\chi_1^2+\chi_2^2+\chi_3^2+h^2)^2 + \frac{\lambda_H\phi}{4}(\phi^2+\theta^2)(\chi_1^2+\chi_2^2+\chi_3^2+h^2) \end{aligned} \tag{E.78}$$

To compute the effective potential we use Eq. E.35 and we shift the scalar fields as

$$\begin{aligned} h &\to h_c + h \\ \phi &\to \phi_c + \phi \\ \theta &\to \theta \\ \chi_i &\to \chi_i \quad i = 1,2,3 \end{aligned} \tag{E.79}$$

where h_c and ϕ_c are constant backgrounds. We have chosen this shift since we know that after SSB the field θ will be the Goldstone boson and after EWSB we have 3 Goldstone bosons χ_i $i = 1,2,3$. With

this shifting, the quadratic part of the $\hat{\mathcal{V}}$ (see Eq. E.35) will become[4]

$$\begin{aligned} V_{quad} = &- \frac{\mu_\phi^2}{2}(\phi^2+\theta^2) + \frac{3}{2}\lambda_\phi \phi_c^2 \phi^2 + \frac{\lambda_\phi}{2}\phi_c^2\theta^2 - \frac{\mu_\phi^2}{2}(\chi_1^2+\chi_2^2+\chi_3^2+h^2) \\ &+ \frac{3}{2}\lambda_H h_c^2 h^2 + \frac{\lambda_H}{2}h_c^2(\chi_1^2+\chi_2^2+\chi_3^2) + \frac{\lambda_{H\phi}}{4}\phi_c^2(\chi_1^2+\chi_2^2+\chi_3^2) \\ &+ \frac{\lambda_{H\phi}}{4}\phi_c^2 h^2 + \frac{\lambda_{H\phi}}{4}h_c^2\phi^2 + \frac{\lambda_{H\phi}}{4}h_c^2\theta^2. \end{aligned} \tag{E.80}$$

We can rewrite this potential as

$$V_{quad} = \frac{1}{2}M_\phi^2\phi^2 + + \frac{1}{2}M_\theta^2\theta^2 + \frac{1}{2}M_{\chi_1}^2\chi_1^2 + \frac{1}{2}M_{\chi_2}^2\chi_2^2 + \frac{1}{2}M_{\chi_3}^2\chi_3^2 + \frac{1}{2}M_h^2 h^2 \tag{E.81}$$

where

$$\begin{aligned} M_\phi^2 &= -\mu_\phi^2 + 3\lambda_\phi\phi_c^2 + \frac{\lambda_{H\phi}}{2}h_c^2 \\ M_\theta^2 &= -\mu_\phi^2 + \lambda_\phi\phi_c^2 + \frac{\lambda_{H\phi}}{2}h_c^2 \\ M_{\chi_1}^2 &= -\mu_h^2 + \lambda_h h_c^2 + \frac{\lambda_{H\phi}}{2}\phi_c^2 \\ M_{\chi_2}^2 &= -\mu_h^2 + \lambda_h h_c^2 + \frac{\lambda_{H\phi}}{2}\phi_c^2 \\ M_{\chi_3}^2 &= -\mu_h^2 + \lambda_h h_c^2 + \frac{\lambda_{H\phi}}{2}\phi_c^2 \\ M_h^2 &= -\mu_h^2 + 3\lambda_H h_c^2 + \frac{\lambda_{H\phi}}{2}\phi_c^2 \end{aligned} \tag{E.82}$$

and we see that these masses correspond to the effective (or shifted) masses. At this point the effective potential at one loop can be written as (see Eq. E.34)

$$V^1(\phi_c, h_c) = -\frac{i}{2}\int \frac{d^4k}{(2\pi)^4}\Big[\ln(-k^2+M_\phi^2) + \ln(-k^2+M_{\chi_i}^2) + \ln(-k^2+M_\theta^2) + \ln(-k^2+M_h^2)\Big]. \tag{E.83}$$

To find the one-loop potential at finite temperature T we need to go in imaginary time, and, in order to do that we have to rotate to Euclidean space with the energies taking discrete values (Matsubara frequencies) and the integration over energy will be replaced by a sum. Thus the effective potential becomes

$$V^1(\phi_c, h_c) = \frac{1}{2\beta}\sum_n \int \frac{d^3k}{(2\pi)^3}\Big[\ln(\omega_n^2+\omega_\phi^2) + \ln(\omega_n^2+\omega_\theta^2) + \ln(\omega_n^2+\omega_{\chi_i}^2) + \ln(\omega_n^2+\omega_h^2)\Big], \tag{E.84}$$

where with ω_n we indicate the Matsubara frequencies, which, in the case of bosons are $\omega_n = 2n\pi/\beta$; and with $\omega_i = \vec{k}^2 + M_i^2$, with $i = \phi, \theta, h, \chi_1, \chi_2, \chi_3$. In order to find an expression for the effective potential, we evaluate a generic expression of the form [98]:

$$\begin{aligned} I(M) =& \frac{1}{2\beta}\sum_n \int \frac{d^3k}{(2\pi)^3}\ln\left(\left(\frac{2n\pi}{\beta}\right)^2 + \vec{k}^2 + M^2\right) \\ =& \int \frac{d^3k}{(2\pi)^3}\tilde{I}(\omega) \end{aligned} \tag{E.85}$$

[4]We consider only the quadratic part since we are interested in computing the thermal masses only.

where $\omega^2 = \vec{k}^2 + M^2$. Taking the derivative of $\tilde{I}(\omega)$ with respect to ω, we obtain

$$\frac{\partial \tilde{I}(\omega)}{\partial \omega} = \frac{1}{\beta} \sum_n \frac{\omega}{\omega^2 + (2n\pi/\beta)^2} \tag{E.86}$$

This sum can be evaluated by using the identities:

$$\sum_{n=-\infty}^{\infty} \frac{1}{n^2 + y^2} = \frac{\pi}{y} \coth(\pi y) \tag{E.87}$$

$$\coth(\beta x) = 1 + 2n_B(2x) \tag{E.88}$$

where n_b is the Bose-Einstein distribution function $n_B = \frac{1}{e^{\beta x} - 1}$. Therefore we obtain

$$\frac{\partial \tilde{I}(\omega)}{\partial \omega} = \frac{1}{2} + \frac{1}{e^{\beta\omega} - 1} \tag{E.89}$$

Finally, by integrating we obtain

$$\int d\omega \frac{\partial \tilde{I}(\omega)}{\partial \omega} \to \tilde{I}(\omega) = \frac{\omega}{2} + \frac{1}{\beta} \ln(1 - e^{-\beta\omega}) \tag{E.90}$$

Therefore we can write

$$I(M) = \int \frac{d^3k}{(2\pi)^3} \left(\frac{\omega}{2} + \frac{1}{\beta} \ln(1 - e^{\beta\omega}) \right) \tag{E.91}$$

From this expression we can notice that for vanishing temperatures, i.e. $\beta \to \infty$, only the first term contributes and it corresponds to the one-loop effective potential at zero temperature. Instead, the second term (which will be indicated as $I^\beta(M)$ in the integrand represents the true temperature corrections. This term cannot, in general, be evaluated in closed form. However, the first few dominant term can be calculated and is enough to give an approximate critical temperature for symmetry restoration. In fact, we can notice that

$$I^\beta(M)\Big|_{M^2=0} = \frac{1}{2\pi^2\beta^4} \int_0^\infty dx x^2 \ln(1 - e^{-x}) = -\frac{\pi^2}{90\beta^4} \tag{E.92}$$

$$\frac{\partial I^\beta(M)}{\partial M^2}\Big|_{M^2=0} = \frac{1}{4\pi^2\beta^2} \int_0^\infty dx \frac{x}{e^x - 1} = \frac{1}{24\beta^2} \tag{E.93}$$

Therefore we can write

$$I^\beta(M) = -\frac{\pi^2}{90\beta^4} + \frac{M^2}{24\beta^2} + ... \tag{E.94}$$

At this point we can put everything in in Eq. E.84 to compute the integral, and we can write

$$\begin{aligned} V(\phi_c, h_c) =& V^{(0)}(\phi_c, h_c) + V^{(1)}(\phi_c, h_c) \\ =& V^{(0)}(\phi_c, h_c) - \frac{6\pi^2}{90\beta^4} + \frac{M_\phi^2 + M_\theta^2 + M_{\chi_i}^2 + M_h^2}{24\beta^2} \end{aligned} \tag{E.95}$$

The second derivative of the zero temperature effective potential $V^{(0)}$ would give the renormalized mass of the theory, while the thermal masses will be obtained by computing the second derivative of the

one-loop potential in the minimum of the theory. Notice that at high temperature we have a symmetry restoration (see Subsec. E.2.2), therefore the minimum will be given by $\phi_c = 0$ and $h_c = 0$.

$$\left.\frac{\partial^2 V^{(1)}(\phi_c, h_c)}{\partial \phi_c^2}\right|_{\phi_c=0, h_c=0} = \frac{1}{24\beta^2}(8\lambda_\phi + 4\lambda_{H\phi}) \tag{E.96}$$

$$\left.\frac{\partial^2 V^{(1)}(\phi_c, h_c)}{\partial h_c^2}\right|_{\phi_c=0, h_c=0} = \frac{1}{24\beta^2}(\lambda_{H\phi} + 6\lambda_H) \tag{E.97}$$

Therefore we can write the thermal mass of the scalar Φ as

$$M_\phi^2(T) = -M^2(0) + \frac{T^2}{12}(4\lambda_\phi + 2\lambda_{H\phi}) \tag{E.98}$$

where $M^2(0)$ is the renormalized tree level mass. Notice that from this derivation we can also find the thermal corrections to the mass of the Higgs scalar. It is important to notice that, since we have shifted the scalars as in Eq. E.79, the Majoron with this choice does not get a thermal mass.

Appendix F

New interactions computation

In this appendix we present the computations that led to the thermal averaged rates presented in the main text in Sec. 5.2.1.

F.1 Scalar decay

First, we consider the scalar decay $\phi \to NN$

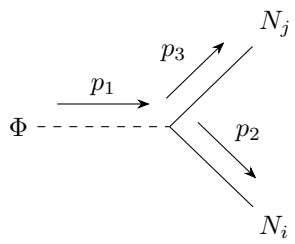

First, we compute the square amplitude of this process

$$\begin{aligned}
&\langle N_i N_j | T\left(-\frac{-i}{2\sqrt{2}}\int d^4x \phi \bar{N}^c N\right)|\phi\rangle \\
=&\langle N_i N_j | T\left(\frac{-i}{2\sqrt{2}}\int d^4x \phi \bar{N}^c C \bar{N}^T\right)|\phi\rangle \\
=&-\frac{i}{2\sqrt{2}} y_N \bar{u}_j C \bar{u}_i^T \times 2 \\
=&\frac{-i}{2\sqrt{2}} y_N \bar{u}_j v_i,
\end{aligned} \tag{F.1}$$

where in the first line we have used $N^c = N$ and $N^c = C\bar{N}^T$, while in the last step we multiplied by 2 since we can exchange $i \leftrightarrow j$ in the RHNs in the final state and we have used the relation $v_i = C\bar{u}_i^T$.

$$\begin{aligned}|\mathcal{M}(\phi \to N_i N_j)|^2_{unpol} &= \sum_s \frac{1}{2} y_N^2 (\bar{v}_i u_j \bar{u}_j v_i) = \frac{1}{2} y_N^2 Tr(\bar{v}_i u_j \bar{u}_j v_i) \\ &= \frac{1}{2} y_N^2 Tr\big((\not{p}_j + m_N)(\not{p}_i - m_N)\big) = \frac{y_N^2}{2} Tr\big(\not{p}_3 \not{p}_2 - m_N^2\big) \\ &= 2y_N^2 (p_3 \cdot p_2 - m_N^2).\end{aligned} \tag{F.2}$$

In the center of mass frame we have that the decaying particle is still, thus we have that the four-momentum is

$$P_\phi = \begin{bmatrix} M_\phi \\ 0 \end{bmatrix}, \tag{F.3}$$

and from momentum conservation we have $P_\phi = P_2 + P_3$, so $M_\phi = P_2 + P_3$. From this relation, we can derive an expression for the scalar product $p_2 \cdot p_3 = \frac{M_\phi^2 - 2m_N^2}{2}$. Finally, the square amplitude is

$$|\mathcal{M}(\phi \to N_i N_j)|^2_{unpol} = y_N^2 \big(M_\phi^2 - 4m_N^2\big). \tag{F.4}$$

At this point, we can compute the decay rate width:

$$d\Gamma = \frac{1}{2M} |\mathcal{M}|^2_{unpol} d\Pi_2, \tag{F.5}$$

where M is the energy in the center of mass frame, which corresponds to the mass of the decaying particle, and $d\Pi_2$ is the two-dimensional phase space element in the center of mass frame

$$\int d\Pi_2 = \int d\Omega \frac{1}{16\pi^2} \frac{|\vec{p}|_f}{E_{cm}} = \int d\Omega \frac{1}{16\pi^2} \frac{|\vec{p}|_f}{M_\phi}. \tag{F.6}$$

We can find the expression for $|\vec{p}_f|$ by considering the four-momenta: $P = (M_\phi,\ \vec{0})^T$ and $p_2 = (E_2,\ \vec{p}_2)^T$.So, we obtain

$$P \cdot p_2 = M_\phi \cdot E_2 \to E_2 = \frac{(p_2 + p_3) \cdot p_2}{M_\phi} = \frac{m_N^2 + \frac{M_\phi^2 - 2m_N^2}{2}}{M_\phi} = \frac{M_\phi}{2}, \tag{F.7}$$

and, from the mass-shell relation $|\vec{p}_f| = \sqrt{E_2^2 - m_N^2}$ we finally obtain

$$|\vec{p}_f| = \sqrt{\frac{M_\phi^2}{4} - m_N^2} = \frac{M_\phi}{2} \sqrt{1 - \frac{4m_N^2}{M_\phi^2}}. \tag{F.8}$$

Therefore, the integrated 2-phase space element becomes

$$\int d\Pi_2 = \int d\Omega \frac{1}{16\pi^2} \frac{M_\phi}{2} \sqrt{1 - \frac{4m_N^2}{M_\phi^2}} \frac{1}{M_\phi} = \frac{1}{8\pi} \sqrt{1 - \frac{m_N^2}{M_\phi^2}}. \tag{F.9}$$

Finally the decay rate width is

$$\Gamma = \frac{1}{2M_\phi^2} y_N^2 (M_\phi^2 - 4m_N^2) \frac{1}{8\pi} \sqrt{1 - \frac{4m_N^2}{M_\phi^2}} = \frac{y_N^2}{16\pi} M_\phi \left(1 - \frac{4m_N^2}{M_\phi^2}\right)^{3/2}. \tag{F.10}$$

At this point we consider the thermal averaged decay rate:

$$\langle \Gamma_{\phi\to NN}\rangle = \frac{\sum_{spins}\int d\Pi_1 d\Pi_2 d\Pi_3 |\mathcal{M}_{1\to 23}|^2 (2\pi)^4\delta^{(4)}(p_{fin}-p_{in}) f_\phi^{eq}}{n_\phi^{eq}}. \tag{F.11}$$

First, we focus on the numerator and, from Eq. F.11 and by taking $f_\phi^{\rm eq} = e^{-E_\phi/T}$ we can compute

$$\begin{aligned}\text{Num} &= \int \frac{d^3\vec{p}_1}{(2\pi)^3 2E_1}\frac{d^3\vec{p}_2}{(2\pi)^3 2E_2}\frac{d^3\vec{p}_3}{(2\pi)^3 2E_3} y_N^2 M_\phi^2\left(1-\frac{4m_N^2}{M_\phi^2}\right)(2\pi)^4\delta^{(4)}(p_1-p_2-p_3)e^{-E_1/T}\\ &= \int \frac{d^3\vec{p}_1}{(2\pi)^3 2E_1}\frac{d^3\vec{p}_2}{(2\pi)^3 2E_2}\frac{d^3\vec{p}_3}{(2\pi)^3 2E_3} y_N^2 M_\phi^2\left(1-\frac{4m_N^2}{M_\phi^2}\right)(2\pi)^4\delta^{(0)}(E_1-E_2-E_3)\\ &\quad \delta^{(3)}(\vec{p}_1-\vec{p}_2-\vec{p}_3)e^{-E_1/T},\end{aligned} \tag{F.12}$$

now we integrate over the 3-delta using the fact that in the center of mass frame $p_\phi = (M_\phi,\, \vec{0})$

$$= \int \frac{d^3\vec{p}_1}{(2\pi)^3 2E_1}\frac{d^3\vec{p}_2}{(2\pi)^3 2E_2 2E_3} y_N^2 M_\phi^2\left(1-\frac{4m_N^2}{M_\phi^2}\right)(2\pi)^4\delta^{(0)}(E_1-E_2-E_3)e^{-E_1/T}|_{\vec{p}_2=-\vec{p}_3}, \tag{F.13}$$

now we go in polar coordinates $d^3\vec{p}_2 = |\vec{p}|^2 dp\sin\theta d\theta d\phi$ and, from the condition $|\vec{p}_2| = |\vec{p}_3| = \vec{p}$ and the fact that $m_2 = m_3 = m_N$ we have $E_2 = E_3 = E_N$

$$= \int \frac{d^3\vec{p}_1}{(2\pi)^3 2E_1}\frac{|\vec{p}|^2 dp}{4\pi E_N^2} y_N^2 M_\phi^2\left(1-\frac{4m_N^2}{M_\phi^2}\right)\delta^{(0)}(E_1-2E_N)e^{-E_1/T}, \tag{F.14}$$

to integrate over the delta we use the property

$$\delta(g(x)) = \sum_k \frac{\delta(x-x_k)}{|g'(x)|}, \tag{F.15}$$

and we obtain

$$\int \frac{p^2 dp}{E_N^2}\frac{\delta\left(p-\frac{E_\phi}{2}\sqrt{1-\frac{4m_N^2}{M_\phi^2}}\right)}{\frac{pE_\phi}{E_N^2}} = \frac{1}{2}\sqrt{1-\frac{4m_N^2}{M_\phi^2}}, \tag{F.16}$$

by inserting in Eq. F.14

$$\begin{aligned}&= \int \frac{d^3\vec{p}_1}{(2\pi)^3 2E_1}\frac{1}{4\pi} y_N^2 M_\phi^2\left(1-\frac{4m_N^2}{M_\phi^2}\right)\frac{1}{2}\sqrt{1-\frac{4m_N^2}{M_\phi^2}}e^{-E_1/T}\\ &= \int \frac{p_1^2 dp_1}{(2\pi)^3 2E_1}\frac{y_N^2 M_\phi^2}{2}\left(1-\frac{4m_N^2}{M_\phi^2}\right)^{3/2}e^{-E_1/T}\\ &= \int \frac{E_1 p_1 dE_1}{(2\pi)^3 2E_1}\frac{y_N^2 M_\phi^2}{2}\left(1-\frac{4m_N^2}{M_\phi^2}\right)^{3/2}e^{-E_1/T}\\ &= \int \frac{\sqrt{E_1^2-M_\phi^2}dE_1}{(2\pi)^3 4} y_N^2 M_\phi^2\left(1-\frac{4m_N^2}{M_\phi^2}\right)^{3/2}e^{-E_1/T}\\ &= \frac{y_N^2}{32\pi^3}M_\phi^2\left(1-\frac{4m_N^2}{M_\phi^2}\right)^{3/2}\int_{M_\phi^2}^{\infty}\sqrt{E_1^2-M_\phi}e^{-E_1/T}dE_1,\end{aligned} \tag{F.17}$$

where we have used the fact that $pdp = EdE$ and $p = \sqrt{E^2 - m^2}$. Now to integrate over the energy we use the identity

$$x\mathcal{K}_1(x) = \int_x^\infty \sqrt{z^2 - x^2} e^{-z} dz, \tag{F.18}$$

and, by changing variables $z = E_1/T$ in Eq. F.17 we finally obtain

$$\text{Num} = \frac{y_N^2}{32\pi^3} T M_\phi^3 \left(1 - \frac{4m_N^2}{M_\phi^2}\right)^{3/2} \mathcal{K}_1\left(\frac{M_\phi}{T}\right). \tag{F.19}$$

Now, we can compute the denominator:

$$n_{\text{eq}}^\phi = \int \frac{d^3p_\phi}{(2\pi)^3} f_{\text{eq}}^\phi = \int \frac{d^3p_\phi}{(2\pi)^3} e^{-E_\phi/T}. \tag{F.20}$$

Going in polar coordinates we find

$$n_{\text{eq}}^\phi = \frac{1}{2\pi^2} \int \sqrt{E_\phi^2 - M_\phi^2} E_\phi e^{-E_\phi/T} dE_\phi. \tag{F.21}$$

This integral can be solved by considering the integral representation of Bessel functions [100]:

$$\mathcal{K}_\nu(z) = \frac{\left(\frac{z}{2}\right)^\nu \Gamma\left(\frac{1}{2}\right)}{\Gamma\left(\nu + \frac{1}{2}\right)} \int_1^\infty e^{-zt} (t^2 - 1)^{\nu - 1/2} dt. \tag{F.22}$$

For $\nu = 2$ we obtain:

$$\mathcal{K}_2(z) = \frac{\left(\frac{z}{2}\right)^2 \Gamma\left(\frac{1}{2}\right)}{\Gamma(2 + \frac{1}{2})} \int_1^\infty e^{-zt} (t^2 - 1)^{3/2} dt, \tag{F.23}$$

by changing coordinates $tz = x$ and by performing an integration by parts we finally find:

$$\mathcal{K}_2(z) = \frac{1}{z^2} \int e^{-x} x \sqrt{x^2 - z^2} dx. \tag{F.24}$$

Therefore Eq. F.21 becomes

$$n_{\text{eq}}^\phi = \frac{T^3}{2\pi^2} \int_{M_\phi/T}^\infty \sqrt{z^2 - \frac{M_\phi^2}{T^2}} z e^{-z} dz = \frac{T M_\phi^2}{2\pi^2} \mathcal{K}_2\left(\frac{M_\phi}{T}\right), \tag{F.25}$$

where we have performed a change of variable $E_\phi/T = z$. From these considerations we conclude that

$$\langle \Gamma_{\phi \to NN} \rangle = M_\phi(T) \left(1 - \frac{4m_N^2}{M_\phi(T)^2}\right)^{3/2} \frac{\mathcal{K}_1(M_\phi(T)/T)}{\mathcal{K}_2(M_\phi(T)/T)}. \tag{F.26}$$

F.2 $2 \to 2$ process

Now we consider the $\phi\phi \to NN$ process. To compute the amplitude we follow the method illustrated in Ref. [101] and we fix a fermion flow in this way: The amplitude of this diagram is given by:

$$i\mathcal{M} = -\frac{\lambda_\phi v_\phi y_N}{2\sqrt{2}} \bar{u}_i \frac{i}{s - M_\phi^2} v_j - i\frac{y_N^2}{8} \bar{u}_i \frac{\not{p}_1 - \not{p}_3 + m_N}{t - m_N^2} v_j + i\frac{y_N^2}{8} \bar{u}_i \frac{(\not{p}_1 - \not{p}_4) + m_N}{u - m_N^2}. \tag{F.27}$$

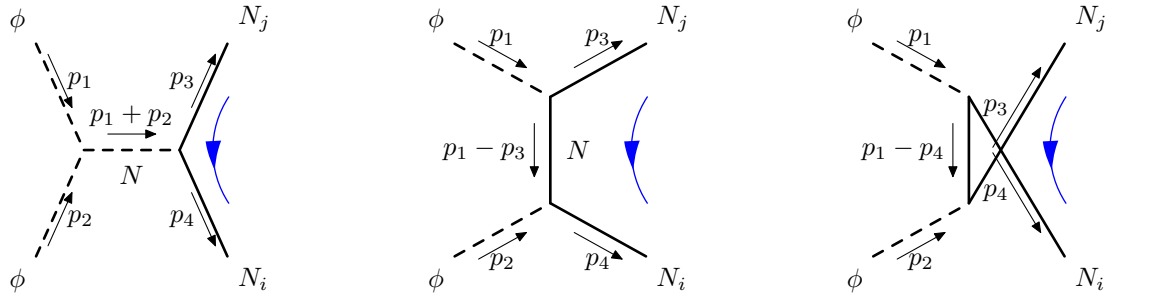

We have chosen the reference order of the external fermions to be (i, j). At this point we can compute the square amplitude. The trace contractions have been computed with the Mathematica package FeynCalc [102–105]. The square amplitude is:

$$|\mathcal{M}|^2 = |\mathcal{M}_1|^2 + |\mathcal{M}_2|^2 - |\mathcal{M}_3|^2 + 2\Re(\mathcal{M}_1^*\mathcal{M}_2) - 2\Re(\mathcal{M}_1^*\mathcal{M}_3) - 2\Re(\mathcal{M}_2^*\mathcal{M}_3) \tag{F.28}$$

and we obtain the following expression[1], which has already been simplified using the identity of Mandelstam variables $s + t + u = 2m_N^2 + 2M_\phi^2$:

$$\begin{aligned}|\mathcal{M}|^2 =& \frac{1}{32} y_N^2 \Bigg(\frac{8\lambda_\phi^2 v_\phi^2 (s-4m^2)}{(M^2-s)^2} - \frac{8\sqrt{2}\lambda_\phi m v_\phi y_N \left(8m^4 - 2m^2(s+4u) + 2su + (t-u)^2\right)}{(m^2-t)(m^2-u)(M^2-s)} \\ &+ \frac{y_N^2(-16m^8 + 4m^6(s+8u) - m^4(8su + 3t^2 - 6tu + 19u^2))}{(m^2-t)^2(m^2-u)^2} \\ &+ \frac{y_N^2(m^2\left(4su^2 - t^3 + 5t^2u - 7tu^2 + 3u^3\right) + (t-u)^2(tu - M^4))}{(m^2-t)^2(m^2-u)^2} \Bigg).\end{aligned} \tag{F.29}$$

To determine the cross section we consider the process in the c.o.m. frame and we assume that the collision axis is parallel to the z axis, therefore

$$p_1 \begin{bmatrix} E_1 \\ 0 \\ 0 \\ p \end{bmatrix}, \qquad p_2 = \begin{bmatrix} E_2 \\ 0 \\ 0 \\ -p \end{bmatrix}, \qquad p_3 = \begin{bmatrix} E_3 \\ 0 \\ p' \sin\theta \\ p' \cos\theta \end{bmatrix}, \qquad p_4 = \begin{bmatrix} E_4 \\ 0 \\ -p' \sin\theta \\ -p' \cos\theta \end{bmatrix}, \tag{F.30}$$

where we assumed $\vec{p}_3$ to be in the yz-plane, and, since $\vec{p}_4 = \vec{p}_1 + \vec{p}_2 - \vec{p}_3$, $\vec{p}_4$ must be in the same plane. We have $p = |\vec{p}_1| = |\vec{p}_2|$, since in the c.o.m. we have $\vec{p}_1 + \vec{p}_2 = \vec{0}$, θ is the scattering angle and $p' = |\vec{p}_3| = |\vec{p}_4|$. To derive the cross section we first derive the differential cross section with the usual formula in the c.o.m. frame:

$$\frac{d\sigma}{d\Omega} = \frac{1}{64\pi^2 s} \frac{p_{fin}}{p_{in}} |\mathcal{M}|^2, \tag{F.31}$$

where $d\Omega = 2\pi d\cos\theta$. From the Mandelstam variables definition we can substitute

$$t = m_1^2 + m_3^2 - 2p_1 \cdot p_3 = M^2 + m^2 - 2(E_1E_3 - pp'\cos\theta); \tag{F.32}$$

$$u = m_1^2 + m_4^2 - 2p_1 \cdot p_4 = M^2 + m^2 - 2(E_1E_4 + pp'\cos\theta); \tag{F.33}$$

and, using the mass-shell relation: $p_1^2 = E_1^2 - p^2$, we get

$$p_{in} = p = \frac{\sqrt{(E^2 - (m_1+m_2)^2)(E^2 - (m_1-m_2)^2)}}{2E}, \tag{F.34}$$

[1] To simplify the notation we will wrtie $m_N = m$ and $M_\phi(T) = M$

and similarly for $p' = p_{fin}$. From this relation, and taking into account the fact that $m_1 = m_2$, $m_3 = m_4$ and that in the c.o.m frame $E_i = E_f = E_{cm}/2 = \sqrt{s}/2$, we finally obtain:

$$p_{in} = \sqrt{\frac{E_{cm}}{2} - M^2} \qquad p_{fin} = \sqrt{\frac{E_{cm}}{2} - m^2}. \tag{F.35}$$

By substituting these relations in Eq. F.31 we obtain the differential cross section, which can be integrated to obtain the final cross section:

$$\sigma = 2\pi \int_{-1}^{1} \frac{d\sigma}{d\Omega} d\cos\theta \tag{F.36}$$

$$\begin{aligned}
\sigma =& \frac{1}{1024\pi} y^2 \sqrt{\frac{(s-4m^2)(s-4M^2)}{s}} \Bigg(\frac{16\lambda^2 v^2 (s-4m^2)}{(M^2-s)^2} \\
&+ \frac{64\sqrt{2}\lambda m v y \left(\frac{4(2m^2-M^2)\coth^{-1}\left(\frac{2(s-2M^2)}{\sqrt{(s-4m^2)(s-4M^2)}}\right)}{\sqrt{(s-4m^2)(s-4M^2)}} - 1 \right)}{s-M^2} \\
&- \frac{1}{(s-2M^2)\sqrt{(s-4m^2)(s-4M^2)}\,(4m^2(s-4M^2)+16M^4-12M^2s+3s^2)} \\
&\times \Bigg(4y^2(-2(2M^2-s)\sqrt{(s-4m^2)(s-4M^2)}(64m^4+m^2(4s-48M^2)+3(8M^4-4M^2s+s^2)) \\
&+ 2\big(16m^4(8M^4-6M^2s+s^2) - 8m^2(28M^6-31M^4s+13M^2s^2-2s^3) \\
&+ 96M^8 - 136M^6s + 82M^4s^2 - 24M^2s^3 + 3s^4\big) \log\Big(-\sqrt{(s-4m^2)(s-4M^2)} - 4M^2 + 2s\Big) \\
&- 2\big(16m^4(8M^4-6M^2s+s^2) - 8m^2(28M^6-31M^4s+13M^2s^2-2s^3) + 96M^8 \\
&- 136M^6s + 82M^4s^2 - 24M^2s^3 + 3s^4\big) \log\Big(\sqrt{(s-4m^2)(s-4M^2)} - 4M^2 + 2s\Big) \Bigg) \Bigg).
\end{aligned} \tag{F.37}$$

To find the thermal averaged cross section, defined as

$$\langle \sigma v_{12} \rangle = \frac{\int d^3p_1 d^3p_2 f_1^{eq} f_2^{eq} \sigma_{12} v_{12}}{\int d^3p_1 d^3p_2 f_1^{eq} f_2^{eq}}, \tag{F.38}$$

we follow Ref. [106] and we cast the numerator in a covariant form:

$$\text{Num} = \int \frac{d^3p_1}{(2\pi)^3 2E_1} \frac{d^3p_2}{(2\pi)^3 2E_2} f_1^{eq} f_2^{eq} W_{12}, \tag{F.39}$$

where we have assumed that the scalar ϕ follows a Maxwell-Boltzmann distribution, thus $f_1^{eq} = e^{-E_1/T}$ and $f_2^{eq} = e^{-E_2/T}$. W_{12} is the unpolarized annihilation rate per unit volume corresponding to the covariant normalization of $2E$ colliding particles per unit volume and is related to the cross section through:

$$W_{12} = 4p_{12}\sqrt{s}\sigma = 4\sigma\sqrt{(p_1 \cdot p_2)^2 - m_1^2 m_2^2} = 4E_1 E_2 \sigma v_{12}, \tag{F.40}$$

where $p_{12} = p$, see Eq. F.34 and v_{12} is the relative velocity, defined as

$$v_{12} = \frac{\sqrt{(p_1 \cdot p_2)^2 - m_1^2 m_2^2}}{E_1 E_2} = \frac{1}{s/2}\sqrt{\frac{s(s-4M^2)}{4}}. \tag{F.41}$$

The integral in Eq. F.39 can be reduced by rewriting the momentum volume element as

$$d^3\vec{p_1}d^3\vec{p_2} = 4\pi|\vec{p_1}|E_1 dE_1 4\pi|\vec{p_2}|E_2 dE_2 \frac{1}{2} d\cos\theta, \tag{F.42}$$

where θ is the angle between $\vec{p_1}$ and $\vec{p_2}$ and the integration region is $E_1 > m_1$, $E_2 > m_2$, $|\cos\theta| < 1$. Now we can change variables by defining:

$$\begin{aligned} E_+ &= E_1 + E_2 \\ E_- &= E_1 - E_2 \\ s &= (p_1 + p_2)^2 = m_1^2 + m_2^2 + 2E_1E_2 - 2|\vec{p_1}||\vec{p_2}|\cos\theta, \end{aligned} \tag{F.43}$$

and the integration region becomes

$$\begin{aligned} & s \geqslant (m_1^2 + m_2^2) \geqslant 4m^2 \\ & E_+ \geqslant \sqrt{s} \\ & |E_- - E_+ \frac{m_2^2 - m_1^2}{s}| \leqslant 2p_{12}\sqrt{\frac{E_+^2 - s}{s}}, \end{aligned} \tag{F.44}$$

Finally, we can find the new integration variables by considering the Jacobian

$$J = det\left(\frac{\partial y_i}{\partial x_j}\right) = -\frac{1}{4|\vec{p_1}||\vec{p_2}|} \tag{F.45}$$

where $y_i = E_+, E_-, s$ and $x_j = E_1, E_2, \cos\theta$. So we have found

$$\frac{d^3\vec{p_1}}{(2\pi)^3 2E_1}\frac{d^3\vec{p_2}}{(2\pi)^3 2E_2} = \frac{1}{8}\frac{1}{(2\pi)^4} dE_+ dE_- ds. \tag{F.46}$$

Now the product of the equilibrium distribution functions depends only on E_+ and not on E_- and the invariant rate W_{12} depends only on s. Therefore, the integral over dE_- is trivial and led to

$$\int dE_- = 4p_{12}\sqrt{\frac{E_+ - s}{s}}. \tag{F.47}$$

The volume element becomes

$$\frac{d^3p_1}{(2\pi)^3 2E_1}\frac{d^3p_2}{(2\pi)^3 2E_2} = \frac{1}{(2\pi)^4}\frac{p_{12}}{2}\sqrt{\frac{E_+^2 - s}{s}} dE_+ ds. \tag{F.48}$$

We can notice that the solution of the integral over dE_+ can be written in terms of the modified Bessel functions of the second kind $\mathcal{K}_1$, i.e.

$$x\mathcal{K}_1(x) = \int_x^\infty \sqrt{z^2 - x^2} e^{-z} dz. \tag{F.49}$$

So the numerator in Eq. F.39 becomes

$$\frac{T}{32\pi^4}\int_{4M^2}^\infty ds W_{12} p_{12} \mathcal{K}_1\left(\frac{\sqrt{s}}{T}\right). \tag{F.50}$$

For what concerns the denominator, we use Eq. F.25. Finally, to obtain the cross section rate $\Gamma_{\phi\phi\to NN} = n_{eq}^{\phi}\langle\sigma v_{12}\rangle$. This expression has been numerically integrated and the results are shown in Fig. 5.4 in Chapt. 5.2.1.

Bibliography

[1] Georges Aad et al. "Observation of a new particle in the search for the Standard Model Higgs boson with the ATLAS detector at the LHC". In: *Phys. Lett. B* 716 (2012), pp. 1–29. DOI: 10.1016/j.physletb.2012.08.020. arXiv: 1207.7214 [hep-ex].

[2] Serguei Chatrchyan et al. "Observation of a New Boson at a Mass of 125 GeV with the CMS Experiment at the LHC". In: *Phys. Lett. B* 716 (2012), pp. 30–61. DOI: 10.1016/j.physletb.2012.08.021. arXiv: 1207.7235 [hep-ex].

[3] Peter J. Mohr, David B. Newell, and Barry N. Taylor. "CODATA recommended values of the fundamental physical constants: 2014". In: *Rev. Mod. Phys.* 88 (3 Sept. 2016), p. 035009. DOI: 10.1103/RevModPhys.88.035009. URL: https://link.aps.org/doi/10.1103/RevModPhys.88.035009.

[4] S. Navas et al. "Review of Particle Physics". In: *Phys. Rev. D* 110 (3 Aug. 2024), p. 030001. DOI: 10.1103/PhysRevD.110.030001. URL: https://link.aps.org/doi/10.1103/PhysRevD.110.030001.

[5] B. Aharmim et al. "Combined analysis of all three phases of solar neutrino data from the Sudbury Neutrino Observatory". In: *Phys. Rev. C* 88 (2 Aug. 2013), p. 025501. DOI: 10.1103/PhysRevC.88.025501. URL: https://link.aps.org/doi/10.1103/PhysRevC.88.025501.

[6] G. Danby et al. "Observation of High-Energy Neutrino Reactions and the Existence of Two Kinds of Neutrinos". In: *Phys. Rev. Lett.* 9 (1 July 1962), pp. 36–44. DOI: 10.1103/PhysRevLett.9.36. URL: https://link.aps.org/doi/10.1103/PhysRevLett.9.36.

[7] K. Kodama et al. "Observation of tau neutrino interactions". In: *Phys. Lett. B* 504 (2001), pp. 218–224. DOI: 10.1016/S0370-2693(01)00307-0. arXiv: hep-ex/0012035.

[8] Y. Fukuda et al. "Evidence for Oscillation of Atmospheric Neutrinos". In: *Phys. Rev. Lett.* 81 (8 Aug. 1998), pp. 1562–1567. DOI: 10.1103/PhysRevLett.81.1562. URL: https://link.aps.org/doi/10.1103/PhysRevLett.81.1562.

[9] Ettore Majorana. "Teoria simmetrica dellelettrone e del positrone". In: *Nuovo Cim.* 14 (1937), pp. 171–184. DOI: 10.1007/BF02961314.

[10] Paul A. M. Dirac. "The quantum theory of the electron". In: *Proc. Roy. Soc. Lond. A* 117 (1928), pp. 610–624. DOI: 10.1098/rspa.1928.0023.

[11] Carl D. Anderson. "The Positive Electron". In: *Phys. Rev.* 43 (6 Mar. 1933), pp. 491–494. DOI: 10.1103/PhysRev.43.491. URL: https://link.aps.org/doi/10.1103/PhysRev.43.491.

[12] A. G. Cohen, A. De Rújula, and S. L. Glashow. "A MatterAntimatter Universe?" In: *The Astrophysical Journal* 495.2 (Mar. 1998), pp. 539–549. ISSN: 1538-4357. DOI: 10.1086/305328. URL: http://dx.doi.org/10.1086/305328.

[13] Murray Gell-Mann, Pierre Ramond, and Richard Slansky. "Complex Spinors and Unified Theories". In: *Conf. Proc. C* 790927 (1979), pp. 315–321. arXiv: 1306.4669 [hep-th].

[14] Osamu Sawada and Akio Sugamoto, eds. *Proceedings: Workshop on the Unified Theories and the Baryon Number in the Universe: Tsukuba, Japan, February 13-14, 1979*. Tsukuba, Japan: Natl.Lab.High Energy Phys., 1979.

[15] Maurice Lévy et al., eds. *QUARKS AND LEPTONS. PROCEEDINGS, SUMMER INSTITUTE, CARGESE, FRANCE, JULY 9-29, 1979*. Vol. 61. NATO Science Series B: Springer, 1980. ISBN: 978-0-306-40560-0, 978-1-4684-7199-1, 978-1-4684-7197-7. DOI: 10.1007/978-1-4684-7197-7.

[16] Rabindra N. Mohapatra and Goran Senjanovi . "Neutrino Mass and Spontaneous Parity Nonconservation". In: *Phys. Rev. Lett.* 44 (14 Apr. 1980), pp. 912–915. DOI: 10.1103/PhysRevLett.44.912. URL: https://link.aps.org/doi/10.1103/PhysRevLett.44.912.

[17] M. Fukugita and T. Yanagida. "Baryogenesis Without Grand Unification". In: *Phys. Lett. B* 174 (1986), pp. 45–47. DOI: 10.1016/0370-2693(86)91126-3.

[18] W. Buchmüller, P. Di Bari, and M. Plümacher. "Leptogenesis for pedestrians". In: *Annals of Physics* 315.2 (Feb. 2005), pp. 305–351. ISSN: 0003-4916. DOI: 10.1016/j.aop.2004.02.003. URL: http://dx.doi.org/10.1016/j.aop.2004.02.003.

[19] Laura Covi, Esteban Roulet, and Francesco Vissani. "CP violating decays in leptogenesis scenarios". In: *Physics Letters B* 384.14 (Sept. 1996), pp. 169–174. ISSN: 0370-2693. DOI: 10.1016/0370-2693(96)00817-9. URL: http://dx.doi.org/10.1016/0370-2693(96)00817-9.

[20] Sacha Davidson, Enrico Nardi, and Yosef Nir. "Leptogenesis". In: *Physics Reports* 466.45 (Sept. 2008), pp. 105–177. ISSN: 0370-1573. DOI: 10.1016/j.physrep.2008.06.002. URL: http://dx.doi.org/10.1016/j.physrep.2008.06.002.

[21] A. D. Sakharov. "Violation of CP Invariance, C asymmetry, and baryon asymmetry of the universe". In: *Pisma Zh. Eksp. Teor. Fiz.* 5 (1967), pp. 32–35. DOI: 10.1070/PU1991v034n05ABEH002497.

[22] V.A. Kuzmin, V.A. Rubakov, and M.E. Shaposhnikov. "On anomalous electroweak baryon-number non-conservation in the early universe". In: *Physics Letters B* 155.1 (1985), pp. 36–42. ISSN: 0370-2693. DOI: https://doi.org/10.1016/0370-2693(85)91028-7. URL: https://www.sciencedirect.com/science/article/pii/0370269385910287.

[23] Sacha Davidson and Alejandro Ibarra. "A lower bound on the right-handed neutrino mass from leptogenesis". In: *Physics Letters B* 535.14 (May 2002), pp. 25–32. ISSN: 0370-2693. DOI: 10.1016/s0370-2693(02)01735-5. URL: http://dx.doi.org/10.1016/S0370-2693(02)01735-5.

[24] Laurent Canetti and Mikhail Shaposhnikov. "Baryon asymmetry of the Universe in the MSM". In: *Journal of Cosmology and Astroparticle Physics* 2010.09 (Sept. 2010), pp. 001–001. ISSN: 1475-7516. DOI: 10.1088/1475-7516/2010/09/001. URL: http://dx.doi.org/10.1088/1475-7516/2010/09/001.

[25] Apostolos Pilaftsis and Thomas E.J. Underwood. "Resonant leptogenesis". In: *Nuclear Physics B* 692.3 (Aug. 2004), pp. 303–345. ISSN: 0550-3213. DOI: 10.1016/j.nuclphysb.2004.05.029. URL: http://dx.doi.org/10.1016/j.nuclphysb.2004.05.029.

[26] Mathias Garny, Alexander Kartavtsev, and Andreas Hohenegger. "Leptogenesis from first principles in the resonant regime". In: *Annals of Physics* 328 (Jan. 2013), pp. 26–63. ISSN: 0003-4916. DOI: 10.1016/j.aop.2012.10.007. URL: http://dx.doi.org/10.1016/j.aop.2012.10.007.

[27] E. Kh. Akhmedov, V. A. Rubakov, and A. Yu. Smirnov. "Baryogenesis via Neutrino Oscillations". In: *Physical Review Letters* 81.7 (Aug. 1998), pp. 1359–1362. ISSN: 1079-7114. DOI: 10.1103/physrevlett.81.1359. URL: http://dx.doi.org/10.1103/PhysRevLett.81.1359.

[28] Takehiko Asaka and Mikhail Shaposhnikov. "The MSM, dark matter and baryon asymmetry of the universe". In: *Physics Letters B* 620.12 (July 2005), pp. 17–26. ISSN: 0370-2693. DOI: 10.1016/j.physletb.2005.06.020. URL: http://dx.doi.org/10.1016/j.physletb.2005.06.020.

[29] M. Drewes et al. "ARS leptogenesis". In: *International Journal of Modern Physics A* 33.05n06 (Feb. 2018), p. 1842002. ISSN: 1793-656X. DOI: 10.1142/s0217751x18420022. URL: http://dx.doi.org/10.1142/S0217751X18420022.

[30] Asli M Abdullahi et al. "The present and future status of heavy neutral leptons". In: *Journal of Physics G: Nuclear and Particle Physics* 50.2 (Jan. 2023), p. 020501. ISSN: 1361-6471. DOI: 10.1088/1361-6471/ac98f9. URL: http://dx.doi.org/10.1088/1361-6471/ac98f9.

[31] C. Antel et al. *Feebly Interacting Particles: FIPs 2022 workshop report*. 2023. arXiv: 2305.01715 [hep-ph]. URL: https://arxiv.org/abs/2305.01715.

[32] Juraj Klaric, Mikhail Shaposhnikov, and Inar Timiryasov. "Reconciling resonant leptogenesis and baryogenesis via neutrino oscillations". In: *Physical Review D* 104.5 (Sept. 2021). ISSN: 2470-0029. DOI: 10.1103/physrevd.104.055010. URL: http://dx.doi.org/10.1103/PhysRevD.104.055010.

[33] Julian Heeck and Daniele Teresi. "Leptogenesis and neutral gauge bosons". In: *Physical Review D* 94.9 (Nov. 2016). ISSN: 2470-0029. DOI: 10.1103/physrevd.94.095024. URL: http://dx.doi.org/10.1103/PhysRevD.94.095024.

[34] Andrea Caputo, Pilar Hernandez, and Nuria Rius. "Leptogenesis from oscillations and dark matter". In: *Eur. Phys. J. C* 79.7 (2019), p. 574. DOI: 10.1140/epjc/s10052-019-7083-y. arXiv: 1807.03309 [hep-ph].

[35] Miguel Escudero and Samuel J. Witte. "The hubble tension as a hint of leptogenesis and neutrino mass generation". In: *The European Physical Journal C* 81.6 (June 2021). ISSN: 1434-6052. DOI: 10.1140/epjc/s10052-021-09276-5. URL: http://dx.doi.org/10.1140/epjc/s10052-021-09276-5.

[36] Chris Quigg. *Gauge Theories of the Strong, Weak, and Electromagnetic Interactions: Second Edition*. USA: Princeton University Press, Sept. 2013. ISBN: 978-0-691-13548-9, 978-1-4008-4822-5. DOI: 10.1515/9781400848225.

[37] Matthew D. Schwartz. *Quantum Field Theory and the Standard Model*. Cambridge University Press, Mar. 2014. ISBN: 978-1-107-03473-0, 978-1-107-03473-0.

[38] Andrea Romanino. "The Standard model of particle physics". In: *9th Baikal Summer School on Physics of Elementary Particles and Astrophysics*. 2009.

[39] A. Ceccucci, Z. Ligeti, and Y. Sakai. "The CKM quark-mixing matrix". In: (2008).

[40] A. Arbey and F. Mahmoudi. "Dark matter and the early Universe: A review". In: *Progress in Particle and Nuclear Physics* 119 (July 2021), p. 103865. ISSN: 0146-6410. DOI: 10.1016/j.ppnp.2021.103865. URL: http://dx.doi.org/10.1016/j.ppnp.2021.103865.

[41] R. Essig et al. *Dark Sectors and New, Light, Weakly-Coupled Particles*. 2013. arXiv: 1311.0029 [hep-ph]. URL: https://arxiv.org/abs/1311.0029.

[42] Jim Alexander et al. *Dark Sectors 2016 Workshop: Community Report*. 2016. arXiv: 1608.08632 [hep-ph]. URL: https://arxiv.org/abs/1608.08632.

[43] Theodota Lagouri. "Review on Higgs hidden-dark sector physics". In: *Phys. Scripta* 97.2 (2022), p. 024001. DOI: 10.1088/1402-4896/ac42a6.

[44] Silvia Pascoli. "Neutrino physics". In: *CERN Yellow Rep. School Proc.* 6 (2019). Ed. by M. Mulders and C. Duhr, pp. 213–259. DOI: 10.23730/CYRSP-2019-006.213.

[45] Carlo Giunti and Chung W. Kim. *Fundamentals of Neutrino Physics and Astrophysics*. 2007. ISBN: 978-0-19-850871-7. DOI: 10.1093/acprof:oso/9780198508717.001.0001.

[46] B. Pontecorvo. "Mesonium and Antimesonium". In: *Sov. Phys. JETP* 6 (1958), pp. 429–431.

[47] Ziro Maki, Masami Nakagawa, and Shoichi Sakata. "Remarks on the unified model of elementary particles". In: *Prog. Theor. Phys.* 28 (1962), pp. 870–880. DOI: 10.1143/PTP.28.870.

[48] J. Schechter and J. W. F. Valle. "Neutrino masses in SU(2) $\bigotimes$ U(1) theories". In: *Phys. Rev. D* 22 (9 Nov. 1980), pp. 2227–2235. DOI: 10.1103/PhysRevD.22.2227. URL: https://link.aps.org/doi/10.1103/PhysRevD.22.2227.

[49] P. I. Krastev and S. T. Petcov. "Resonance Amplification and t Violation Effects in Three Neutrino Oscillations in the Earth". In: *Phys. Lett. B* 205 (1988), pp. 84–92. DOI: 10.1016/0370-2693(88)90404-2.

[50] C. Jarlskog, ed. *CP Violation*. WSP, 1989. ISBN: 978-981-4503-28-0, 978-9971-5-0560-8. DOI: 10.1142/0496.

[51] Ivan Esteban et al. "NuFit-6.0: updated global analysis of three-flavor neutrino oscillations". In: *Journal of High Energy Physics* 2024.12 (2024). ISSN: 1029-8479. DOI: 10.1007/jhep12(2024)216. URL: http://dx.doi.org/10.1007/JHEP12(2024)216.

[52] Steven Weinberg. "Baryon- and Lepton-Nonconserving Processes". In: *Phys. Rev. Lett.* 43 (21 Nov. 1979), pp. 1566–1570. DOI: 10.1103/PhysRevLett.43.1566. URL: https://link.aps.org/doi/10.1103/PhysRevLett.43.1566.

[53] Tsutomu Yanagida. "Horizontal Symmetry and Masses of Neutrinos". In: *Prog. Theor. Phys.* 64 (1980), p. 1103. DOI: 10.1143/PTP.64.1103.

[54] Peter Minkowski. "$\mu \to e\gamma$ at a Rate of One Out of 10^9 Muon Decays?" In: *Phys. Lett. B* 67 (1977), pp. 421–428. DOI: 10.1016/0370-2693(77)90435-X.

[55] Rabindra N. Mohapatra and Goran Senjanovic. "Neutrino Masses and Mixings in Gauge Models with Spontaneous Parity Violation". In: *Phys. Rev. D* 23 (1981), p. 165. DOI: 10.1103/PhysRevD.23.165.

[56] J.A. Casas and A. Ibarra. "Oscillating neutrinos and e,". In: *Nuclear Physics B* 618.12 (Dec. 2001), pp. 171–204. ISSN: 0550-3213. DOI: 10.1016/s0550-3213(01)00475-8. URL: http://dx.doi.org/10.1016/S0550-3213(01)00475-8.

[57] Edward W. Kolb and Michael S. Turner. *The Early Universe*. Vol. 69. 1989. ISBN: 978-0-201-62674-2. DOI: 10.1201/9780429492860.

[58] Fabio Iocco et al. "Primordial nucleosynthesis: From precision cosmology to fundamental physics". In: *Physics Reports* 472.16 (Mar. 2009), pp. 1–76. ISSN: 0370-1573. DOI: 10.1016/j.physrep.2009.02.002. URL: http://dx.doi.org/10.1016/j.physrep.2009.02.002.

[59] Gary Steigman. "Primordial Nucleosynthesis in the Precision Cosmology Era". In: *Ann. Rev. Nucl. Part. Sci.* 57 (2007), pp. 463–491. DOI: 10.1146/annurev.nucl.56.080805.140437. arXiv: 0712.1100 [astro-ph].

[60] K. Nakamura et al. "Review of particle physics". In: *J. Phys. G* 37 (2010), p. 075021. DOI: 10.1088/0954-3899/37/7A/075021.

[61] Wayne Hu and Scott Dodelson. "Cosmic Microwave Background Anisotropies". In: *Annual Review of Astronomy and Astrophysics* 40.1 (Sept. 2002), pp. 171–216. ISSN: 1545-4282. DOI: 10.1146/annurev.astro.40.060401.093926. URL: http://dx.doi.org/10.1146/annurev.astro.40.060401.093926.

[62] Scott Dodelson. *Modern Cosmology*. Amsterdam: Academic Press, 2003. ISBN: 978-0-12-219141-1.

[63] Chee Sheng Fong, Enrico Nardi, and Antonio Riotto. "Leptogenesis in the Universe". In: *Advances in High Energy Physics* 2012 (2012), pp. 1–59. ISSN: 1687-7365. DOI: 10.1155/2012/158303. URL: http://dx.doi.org/10.1155/2012/158303.

[64] Mariano Quiros. *Finite temperature field theory and phase transitions*. 1999. arXiv: hep-ph/9901312 [hep-ph]. URL: https://arxiv.org/abs/hep-ph/9901312.

[65] G. 't Hooft. "Symmetry Breaking through Bell-Jackiw Anomalies". In: *Phys. Rev. Lett.* 37 (1 July 1976), pp. 8–11. DOI: 10.1103/PhysRevLett.37.8. URL: https://link.aps.org/doi/10.1103/PhysRevLett.37.8.

[66] Dietrich Bödeker and Wilfried Buchmüller. "Baryogenesis from the weak scale to the grand unification scale". In: *Reviews of Modern Physics* 93.3 (Aug. 2021). ISSN: 1539-0756. DOI: 10.1103/revmodphys.93.035004. URL: http://dx.doi.org/10.1103/RevModPhys.93.035004.

[67] A. Abada et al. "Flavour Matters in Leptogenesis". In: *JHEP* 09 (2006), p. 010. DOI: 10.1088/1126-6708/2006/09/010. arXiv: hep-ph/0605281.

[68] Edward W. Kolb and Stephen Wolfram. "Baryon Number Generation in the Early Universe". In: *Nucl. Phys. B* 172 (1980). [Erratum: Nucl.Phys.B 195, 542 (1982)], p. 224. DOI: 10.1016/0550-3213(82)90012-8.

[69] W. Buchmuller, P. Di Bari, and M. Plumacher. "Cosmic microwave background, matter - antimatter asymmetry and neutrino masses". In: *Nucl. Phys. B* 643 (2002). [Erratum: Nucl.Phys.B 793, 362 (2008)], pp. 367–390. DOI: 10.1016/S0550-3213(02)00737-X. arXiv: hep-ph/0205349.

[70] Chee Sheng Fong and J Racker. "On fast CP violating interactions in leptogenesis". In: *Journal of Cosmology and Astroparticle Physics* 2010.07 (July 2010), pp. 001–001. ISSN: 1475-7516. DOI: 10.1088/1475-7516/2010/07/001. URL: http://dx.doi.org/10.1088/1475-7516/2010/07/001.

[71] Michael E. Peskin and Daniel V. Schroeder. *An Introduction to quantum field theory*. Reading, USA: Addison-Wesley, 1995. ISBN: 978-0-201-50397-5, 978-0-429-50355-9, 978-0-429-49417-8. DOI: 10.1201/9780429503559.

[72] Björn Garbrecht. "Why is there more matter than antimatter? Calculational methods for leptogenesis and electroweak baryogenesis". In: *Progress in Particle and Nuclear Physics* 110 (Jan. 2020), p. 103727. ISSN: 0146-6410. DOI: 10.1016/j.ppnp.2019.103727. URL: http://dx.doi.org/10.1016/j.ppnp.2019.103727.

[73] Jeffrey A. Harvey and Michael S. Turner. "Cosmological baryon and lepton number in the presence of electroweak fermion number violation". In: *Phys. Rev. D* 42 (1990), pp. 3344–3349. DOI: 10.1103/PhysRevD.42.3344.

[74] Steve Blanchet et al. *Leptogenesis with heavy neutrino flavours: from density matrix to Boltzmann equations*. 2013. arXiv: 1112.4528 [hep-ph]. URL: https://arxiv.org/abs/1112.4528.

[75] Enrico Nardi et al. "The importance of flavor in leptogenesis". In: *Journal of High Energy Physics* 2006.01 (Jan. 2006), pp. 164–164. ISSN: 1029-8479. DOI: 10.1088/1126-6708/2006/01/164. URL: http://dx.doi.org/10.1088/1126-6708/2006/01/164.

[76] Asmaa Abada et al. "Flavor issues in leptogenesis". In: *JCAP* 04 (2006), p. 004. DOI: 10.1088/1475-7516/2006/04/004. arXiv: hep-ph/0601083.

[77] Bruce A. Campbell et al. "On the baryon, lepton-flavour and right-handed electron asymmetries of the universe". In: *Physics Letters B* 297.12 (Dec. 1992), pp. 118–124. ISSN: 0370-2693. DOI: 10.1016/0370-2693(92)91079-o. URL: http://dx.doi.org/10.1016/0370-2693(92)91079-0.

[78] P. Hernández et al. "Testable baryogenesis in seesaw models". In: *Journal of High Energy Physics* 2016.8 (Aug. 2016). ISSN: 1029-8479. DOI: 10.1007/jhep08(2016)157. URL: http://dx.doi.org/10.1007/JHEP08(2016)157.

[79] P. Hernández et al. "Bounds on right-handed neutrino parameters from observable leptogenesis". In: *Journal of High Energy Physics* 2022.12 (Dec. 2022). ISSN: 1029-8479. DOI: 10.1007/jhep12(2022)012. URL: http://dx.doi.org/10.1007/JHEP12(2022)012.

[80] Brian Shuve and Itay Yavin. "Baryogenesis through neutrino oscillations: A unified perspective". In: *Physical Review D* 89.7 (Apr. 2014). ISSN: 1550-2368. DOI: 10.1103/physrevd.89.075014. URL: http://dx.doi.org/10.1103/PhysRevD.89.075014.

[81] G. Sigl and G. Raffelt. "General kinetic description of relativistic mixed neutrinos". In: *Nuclear Physics B* 406.1 (1993), pp. 423–451. ISSN: 0550-3213. DOI: https://doi.org/10.1016/0550-3213(93)90175-O. URL: https://www.sciencedirect.com/science/article/pii/0550321393901750.

[82] Takehiko Asaka, Sintaro Eijima, and Hiroyuki Ishida. "Kinetic equations for baryogenesis via sterile neutrino oscillation". In: *Journal of Cosmology and Astroparticle Physics* 2012.02 (Feb. 2012), pp. 021–021. ISSN: 1475-7516. DOI: 10.1088/1475-7516/2012/02/021. URL: http://dx.doi.org/10.1088/1475-7516/2012/02/021.

[83] I. Ghisoiu and M. Laine. "Right-handed neutrino production rate atTgt; 160 GeV". In: *Journal of Cosmology and Astroparticle Physics* 2014.12 (Dec. 2014), pp. 032–032. ISSN: 1475-7516. DOI: 10.1088/1475-7516/2014/12/032. URL: http://dx.doi.org/10.1088/1475-7516/2014/12/032.

[84] J. Ghiglieri and M. Laine. "GeV-scale hot sterile neutrino oscillations: a derivation of evolution equations". In: *Journal of High Energy Physics* 2017.5 (May 2017). ISSN: 1029-8479. DOI: 10.1007/jhep05(2017)132. URL: http://dx.doi.org/10.1007/JHEP05(2017)132.

[85] Asmaa Abada et al. "Neutrino masses, leptogenesis and dark matter from small lepton number violation?" In: *Journal of Cosmology and Astroparticle Physics* 2017.12 (Dec. 2017), pp. 024–024. ISSN: 1475-7516. DOI: 10.1088/1475-7516/2017/12/024. URL: http://dx.doi.org/10.1088/1475-7516/2017/12/024.

[86] A.D. Dolgov. "Neutrinos in cosmology". In: *Physics Reports* 370.45 (Nov. 2002), pp. 333–535. ISSN: 0370-1573. DOI: 10.1016/s0370-1573(02)00139-4. URL: http://dx.doi.org/10.1016/S0370-1573(02)00139-4.

[87] Paolo Gondolo and Graciela Gelmini. "Cosmic Abundances of Stable Particles: improved analysis". In: *Nuclear Physics B - NUCL PHYS B* 360 (Aug. 1991), pp. 145–179. DOI: 10.1016/0550-3213(91)90438-4.

[88] A. Granelli et al. "ULYSSES: Universal LeptogeneSiS Equation Solver". In: *Computer Physics Communications* 262 (May 2021), p. 107813. ISSN: 0010-4655. DOI: 10.1016/j.cpc.2020.107813. URL: http://dx.doi.org/10.1016/j.cpc.2020.107813.

[89] A. Granelli et al. "ULYSSES, universal LeptogeneSiS equation solver: Version 2". In: *Computer Physics Communications* 291 (Oct. 2023), p. 108834. ISSN: 0010-4655. DOI: 10.1016/j.cpc.2023.108834. URL: http://dx.doi.org/10.1016/j.cpc.2023.108834.

[90] Ivan Esteban et al. "The fate of hints: updated global analysis of three-flavor neutrino oscillations". In: *Journal of High Energy Physics* 2020.9 (Sept. 2020). ISSN: 1029-8479. DOI: 10.1007/jhep09(2020)178. URL: http://dx.doi.org/10.1007/JHEP09(2020)178.

[91] Gustavo C. Branco et al. "A bridge between CP violation at low energies and leptogenesis". In: *Nuclear Physics B* 617.13 (Dec. 2001), pp. 475–492. ISSN: 0550-3213. DOI: 10.1016/s0550-3213(01)00425-4. URL: http://dx.doi.org/10.1016/S0550-3213(01)00425-4.

[92] Elizabeth Jenkins and Aneesh V. Manohar. "Rephasing invariants of quark and lepton mixing matrices". In: *Nuclear Physics B* 792.12 (Mar. 2008), pp. 187–205. ISSN: 0550-3213. DOI: 10.1016/j.nuclphysb.2007.09.031. URL: http://dx.doi.org/10.1016/j.nuclphysb.2007.09.031.

[93] Elizabeth E Jenkins and Aneesh V Manohar. "Algebraic structure of lepton and quark flavor invariants andCPviolation". In: *Journal of High Energy Physics* 2009.10 (Oct. 2009), pp. 094–094. ISSN: 1029-8479. DOI: 10.1088/1126-6708/2009/10/094. URL: http://dx.doi.org/10.1088/1126-6708/2009/10/094.

[94] S. Pascoli, S.T. Petcov, and A. Riotto. "Leptogenesis and low energy CP-violation in neutrino physics". In: *Nuclear Physics B* 774.13 (July 2007), pp. 1–52. ISSN: 0550-3213. DOI: 10.1016/j.nuclphysb.2007.02.019. URL: http://dx.doi.org/10.1016/j.nuclphysb.2007.02.019.

[95] Marco Drewes. *On the Minimal Mixing of Heavy Neutrinos*. 2019. arXiv: 1904.11959 [hep-ph]. URL: https://arxiv.org/abs/1904.11959.

[96] F Hahn-Woernle, M Plümacher, and Y.Y.Y Wong. "Full Boltzmann equations for leptogenesis including scattering". In: *Journal of Cosmology and Astroparticle Physics* 2009.08 (Aug. 2009), pp. 028–028. ISSN: 1475-7516. DOI: 10.1088/1475-7516/2009/08/028. URL: http://dx.doi.org/10.1088/1475-7516/2009/08/028.

[97] J Garayoa et al. "On the full Boltzmann equations for leptogenesis". In: *Journal of Cosmology and Astroparticle Physics* 2009.09 (Sept. 2009), pp. 035–035. ISSN: 1475-7516. DOI: 10.1088/1475-7516/2009/09/035. URL: http://dx.doi.org/10.1088/1475-7516/2009/09/035.

[98] Ashok K. Das. *Finite Temperature Field Theory*. New York: World Scientific, 1997. ISBN: 978-981-02-2856-9, 978-981-4498-23-4.

[99] L. F. Abbott. "Introduction to the Background Field Method". In: *Acta Phys. Polon. B* 13 (1982), p. 33.

[100] I. S. Gradshteyn and I. M. Ryzhik. *Table of integrals, series, and products*. Seventh. Translated from the Russian, Translation edited and with a preface by Alan Jeffrey and Daniel Zwillinger, With one CD-ROM (Windows, Macintosh and UNIX). Elsevier/Academic Press, Amsterdam, 2007, pp. xlviii+1171. ISBN: 978-0-12-373637-6; 0-12-373637-4.

[101] Ansgar Denner et al. "Feynman rules for fermion number violating interactions". In: *Nucl. Phys. B* 387 (1992), pp. 467–481. DOI: 10.1016/0550-3213(92)90169-C.

[102] Vladyslav Shtabovenko, Rolf Mertig, and Frederik Orellana. "New developments in FeynCalc 9.0". In: *Computer Physics Communications* 207 (Oct. 2016), pp. 432–444. ISSN: 0010-4655. DOI: 10.1016/j.cpc.2016.06.008. URL: http://dx.doi.org/10.1016/j.cpc.2016.06.008.

[103] R. Mertig, M. Böhm, and A. Denner. "Feyn Calc - Computer-algebraic calculation of Feynman amplitudes". In: *Computer Physics Communications* 64.3 (1991), pp. 345–359. ISSN: 0010-4655. DOI: https://doi.org/10.1016/0010-4655(91)90130-D. URL: https://www.sciencedirect.com/science/article/pii/001046559190130D.

[104] Vladyslav Shtabovenko, Rolf Mertig, and Frederik Orellana. "FeynCalc 9.3: New features and improvements". In: *Computer Physics Communications* 256 (Nov. 2020), p. 107478. ISSN: 0010-4655. DOI: 10.1016/j.cpc.2020.107478. URL: http://dx.doi.org/10.1016/j.cpc.2020.107478.

[105] Vladyslav Shtabovenko, Rolf Mertig, and Frederik Orellana. "FeynCalc 9.3: New features and improvements". In: *Computer Physics Communications* 256 (Nov. 2020), p. 107478. ISSN: 0010-4655. DOI: 10.1016/j.cpc.2020.107478. URL: http://dx.doi.org/10.1016/j.cpc.2020.107478.

[106] Joakim Edsjö and Paolo Gondolo. "Neutralino relic density including coannihilations". In: *Physical Review D* 56.4 (Aug. 1997), pp. 1879–1894. ISSN: 1089-4918. DOI: 10.1103/physrevd.56.1879. URL: http://dx.doi.org/10.1103/PhysRevD.56.1879.